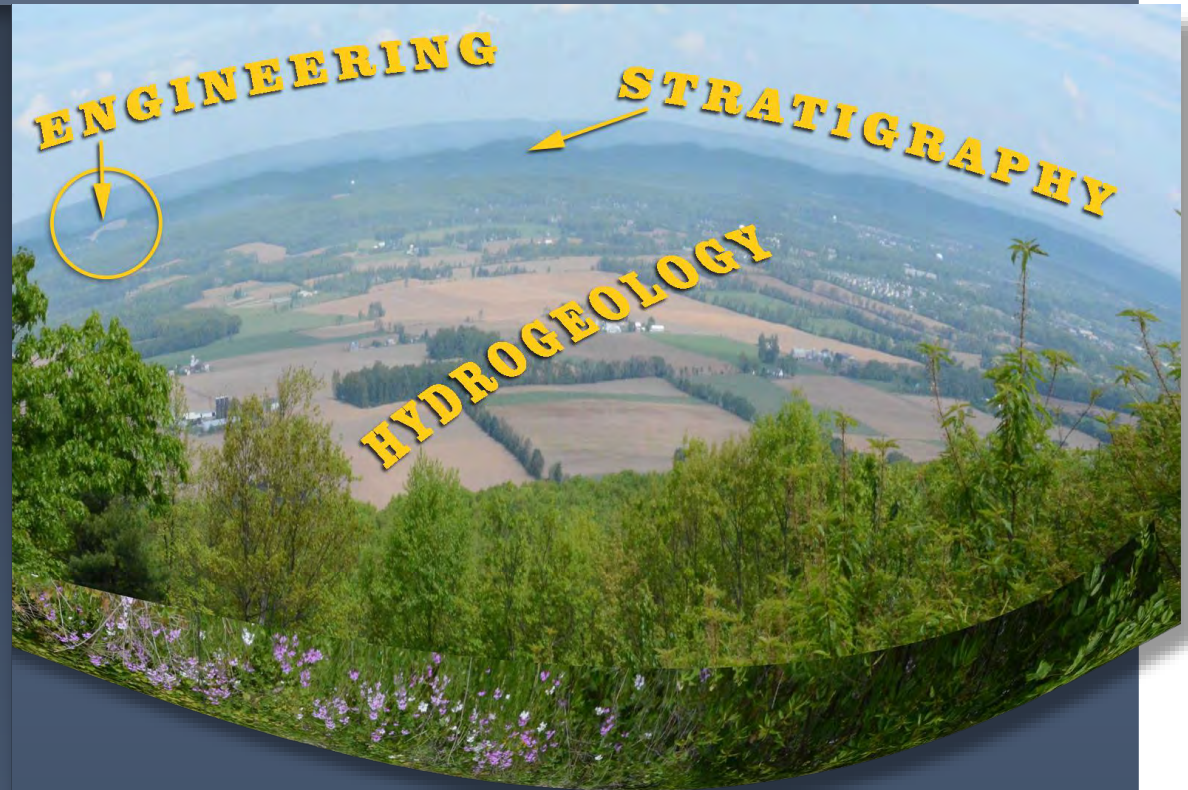


HOSTS:

THE
PENNSYLVANIA
STATE
UNIVERSITY



PA DCNR
BUREAU OF
TOPOGRAPHIC &
GEOLOGIC
SURVEY



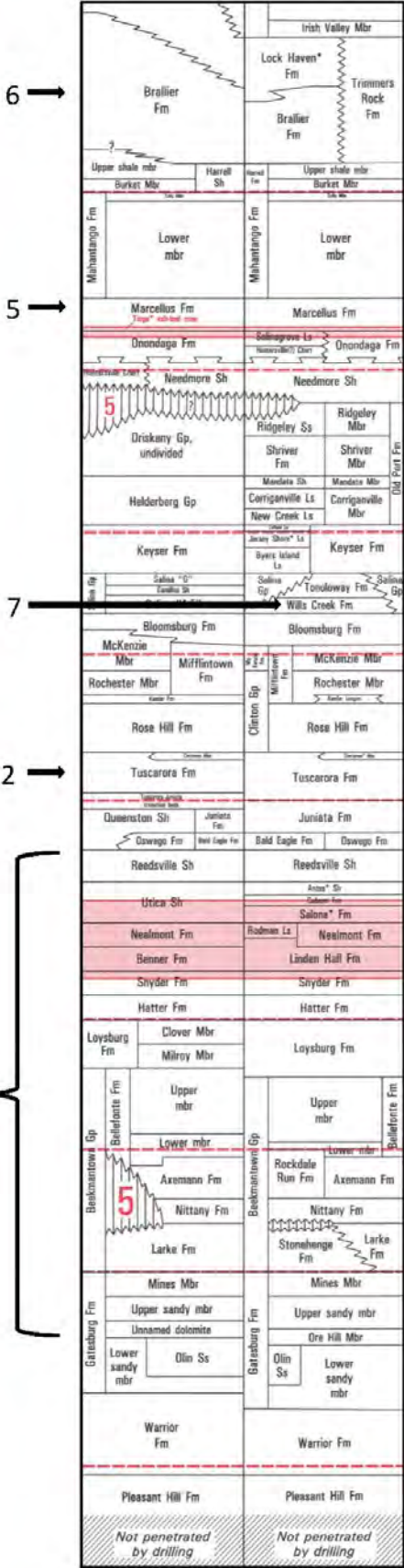
Recent Geologic Studies & Initiatives in Central Pennsylvania

82ND ANNUAL FIELD CONFERENCE
OF PENNSYLVANIA GEOLOGISTS

OCTOBER 5 – 7, 2017

FCOPG STRATIGRAPHIC COLUMN

Devonian	Upper
	Middle
	Lower
Silurian	U
	M
	L
Ordovician	Upper
	M
	L
	Upper
Cambrian	Upper
	M



- Day 1 Stops
- Day 2 Stops
- S → Stratigraphy
- E → Engineering
- H → Hydrology

Cover: View from Jo Hays Vista

**GUIDEBOOK FOR THE
82ND ANNUAL FIELD CONFERENCE OF PENNSYLVANIA GEOLOGISTS**

OCTOBER 5 — 7, 2017

**RECENT GEOLOGIC STUDIES & INITIATIVES IN
CENTRAL PENNSYLVANIA**

STRATIGRAPHY, ENGINEERING AND HYDROGEOLOGY

STATE COLLEGE, PENNSYLVANIA

Editor

Robin Anthony, Pennsylvania Geological Survey, Pittsburgh, PA

Field Trip Organizer

David “Duff” Gold, Emeritus, The Pennsylvania State University

Field Trip Leaders and Guidebook Contributors

David “Duff” Gold, Emeritus, The Pennsylvania State University

Charles Miller

Arnold Doden, GMRE, Inc.

Terry Engelder, Emeritus, The Pennsylvania State University

William White, Emeritus, The Pennsylvania State University

Richard Parizek, Emeritus, The Pennsylvania State University

David Yoxtheimer, The Pennsylvania State University

Ryan Mathur, Juniata College

Roman DiBiase, The Pennsylvania State University

Susan Brantley, The Pennsylvania State University

Joanmarie DeVecchio, The Pennsylvania State University

Ashlee Dere, University of Nebraska

David Eissenstat, The Pennsylvania State University

Li Guo, The Pennsylvania State University

Jason Kaye, The Pennsylvania State University

Henry Lin, The Pennsylvania State University

Gregory Mount, Indiana University of Pennsylvania

Nicole West, Central Michigan University

Jennifer Williams, The Pennsylvania State University

Hubert Barnes, Emeritus, Pennsylvania Geological Survey

Barry Scheetz, The Pennsylvania State University

Hosts

Pennsylvania Geological Survey

The Pennsylvania State University

Headquarters

Ramada Inn, State College, PA

ACKNOWLEDGEMENTS

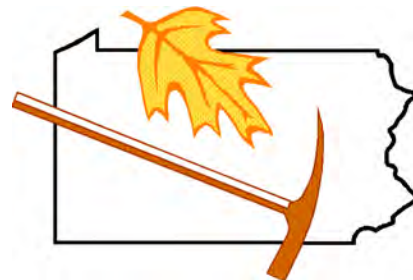
We extend special thanks to FCOPG officers, stop leaders, guidebook contributors, volunteers,

And to:

- 👍 Area Wide Protective for keeping us safe,
- 👍 Fullington Trailways for working with us,
- 👍 all of our trip leaders for working so hard on the road log and articles,
- 👍 our bus leaders, Kurt Freihoff, Frank Pazzaglia, Sean Cornell and Pam Trowbridge
- 👍 Richard Alley for speaking at our banquet
- 👍 Andrew Sicree for assistance in the field
- 👍 Hanson Aggregates Pennsylvania LLC. and their staff at the Oak Hall Quarry for allowing us access to their quarry, access to reports, and help during field work
- 👍 PennDOT for access to outcrops in the I-99 right of way

Special Thanks to:

- 👍 David “Duff” Gold for a lifetime of dedication to the field of geology and bringing this field conference to fruition. And his wife Jackie for letting us have him.



A TRIBUTE TO DAVID P. “DUFF” GOLD

A former Penn State geology colleague said: “Duff’s problem is that he is in love with geology.” His “problem” is our gain. He is a consummate geologist – researcher, teacher, consultant, and mapping geologist. His interests are diverse: diamonds, carbonatites, fulgurites, rogue kimberlites and lamproites, bentonites, fractals, exploration geology, astroblemes, fracture analysis using remote-sensing, tectonic deformation of ore deposits, rare earths, fission-track dating, geologic mapping – to name a few. He has served on Congressional committees including making recommendations on near-earth asteroids and conditions of the lunar surface as it might have affected manned landings, organized professional field trips, analyzed atomic bomb explosions, trained astronauts, and spoken on diamonds to the American Museum of Natural History. While receiving professional recognition for these efforts, Duff is willing to talk with cub scouts and other youth organizations. He comments: “You never know where the next geologist will come from.”



At Penn State, Duff received an award for outstanding teaching. His dedication to teaching is partly reflected in his willingness to purvey geological knowledge with others, in and out of the classroom. There are quite a few of us attending this year’s field conference who have benefited from an association with him. He shares field information with professors of neighboring institutions, often taking them on “one-on-one” field excursions. Several years ago my wife asked: “Why do you go in the field with Duff?” My immediate response was: “Because it’s a free education. I always learn something new.”

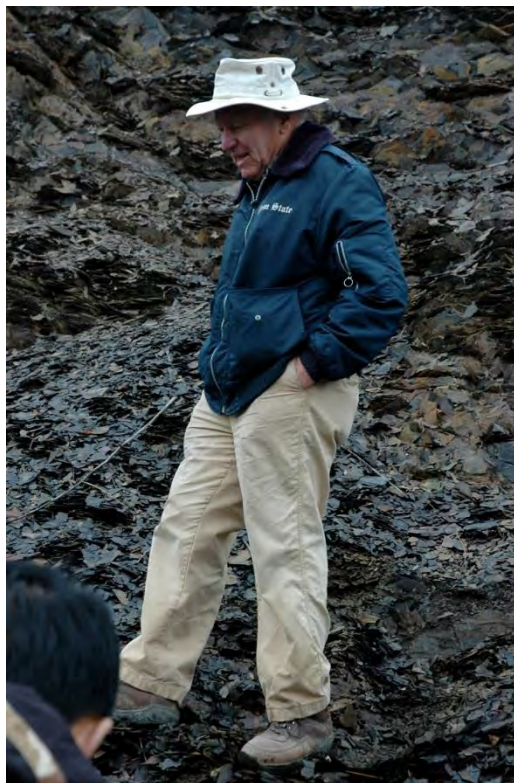
The Field Conference acknowledges Duff’s many contributions. He has been associated for decades: a field trip leader and editor for the 50th, 68th, and this year’s conference. In addition, he was contributor for the 81st conference.

82nd Annual Field Conference of Pennsylvania Geologists

His collaborations with the Pennsylvania Geological Survey have been a mutual admiration society. He has worked with a host of Survey geologists and participates in the STATEMAP program. One of his contributions is the partial training of State Geologist, Gale Blackmer, who was a doctoral student of Duff's.

Since his 1998 retirement as Emeritus Professor of Geology from Penn State, Duff continues his "love of geology," mentoring undergraduate geology students, speaking to classes, meeting with geologists of the Pennsylvania Geological Survey, publishing, meeting with the public on issues such as sinkholes, teaching short courses for the National Well Water Association and PetroChina, attending professional meetings, geological studies at an ancient archaeological site in Southern Egypt, developing courses for a new mining school in Nigeria, consulting, running field trips for Tohoku University, and more. His consulting includes evaluating gravel deposits in Pennsylvania and Maryland, core analyses for Penn DOT, and site evaluations for carbon dioxide sequestrations. In other words, he is not "retired."

Duff writes: "I feel blessed in choosing a career that matched my temperament as an explorer in the physical world, a job that required interaction with young minds, and being at the right place at the right time to participate in interesting programs and initiatives."



This tribute to Duff would be incomplete without a few anecdotes about his geology exploits. His work has been international at times. Early in his career as a doctoral student, his thesis objective was to examine emplacement energy of igneous dikes of the host marble of Oka and St. Hilaire, Quebec. Some initial tests were problematical. He suspected the carbonates were not Grenville Marble but a carbonatite like some he had seen in southern and east Africa. However, this was when students did not question professors. His request for a change in objectives in characterizing the rocks was met with opposition and skepticism. One comment was that the idea of "mantle carbonates" was ridiculous and another was Duff probably also believed in "continental drift." However, three years later, the professor apologized. The site on which Duff worked is now known as the Oka Carbonatite Complex, a 117 Ma old double ring-dike/cone sheet structure that was later mined for niobium and rare earth minerals.

Again working in Canada, Duff was part of a geology field crew. On a particular day, he was the cook. The group had just been resupplied with a backlog of steaks. So, steaks were served. One member of the crew noticed that his steak was somewhat undercooked. He asked Duff if all people from South Africa ate their meat raw. Duff said, tongue-in-cheek, "only when we eat human flesh." For the next two weeks, the guy would not sleep when Duff slept and at the end of the two weeks he shipped out from lack of sleep. He thought Duff was a cannibal.

Charles E. Miller, Jr.

State College, PA

TABLE OF CONTENTS

Stratigraphic Column Central Pennsylvania	inside front cover
Acknowledgements	ii
A Tribute to David P. “Duff” Gold	iii
Table of Contents	v
A Geological Traverse through the Nittany Mountain Syncline	1
Preamble	1
Introduction	1
Stratigraphy	4
Bellefonte	4
Loysburg	4
Hatter Formation	8
Snyder Formation	8
Linden Hall Formation	9
Nealmont Formation	10
Salona Formation	11
Coburn Formation	13
Antes Formation	17
Depositional setting and tectonic implications	18
Cycles	19
Mineralogy	20
Structural geology	21
Primary structural elements	23
Secondary discontinuities/features	24
Secondary (superimposed) structural features	25
References	32
Plate 1: Oak Hall Quarry: Geology and cross-section of strata	34
Lower and Middle Ordovician stratigraphy and structure along the Mt. Nittany Expressway	35
Preamble	35
Introduction	35
Stratigraphy	36
Bellefonte Formation	36

82nd Annual Field Conference of Pennsylvania Geologists

Loysburg Formation	43
Joint Systems.....	49
On shallowing-upward carbonate cycles in the Loysburg (?)	49
Sedimentary flow features.....	50
Paleogeography	52
Depositional environments.....	53
Conclusion.....	53
References	54
Plate 1: Road-bank log of pertinent mesoscopic scale depositional and structural features	56
I-99 roadway construction history and pyrite discovery at Skytop, Central Pennsylvania	57
Introduction	57
Early I-99 development.....	59
Environmental, geological and political challenges	61
The “discovery” of pyrite at Skytop	65
References	66
Geology of the Skytop roadcuts, Centre County, Pennsylvania	67
Introduction	67
Geological setting.....	70
Stratigraphy.....	71
Coburn Formation.....	72
Antes Member	73
Reedsville Formation	73
Bald Eagle Formation	74
Juniata Formation	75
Tuscarora Formation.....	75
Rose Hill Formation.....	77
Structure	77
Lineaments and fracture traces	82
Epigenetic veins: mineralization and chemistry	84
Conclusions	93
Selected References.....	94
Mineralogy of Skytop	97
Introduction	97

Sulfide minerals	99
Pyrite	99
Sphalerite	100
Galena	101
Other sulfide minerals	101
Other secondary minerals	101
Barite/Dolomite	101
Quartz	102
Oxidized iron minerals	102
Phosphate minerals	102
Sulfate minerals	102
Genesis of epigenetic minerals at Skytop	103
References	105
Plate 1: Environmental SEM images of pyrite and other minerals from Skytop	105
Post-excavation mineralogy and acid-rock drainage treatments at Skytop	109
Introduction	109
Skytop time-line	109
Geo-Web cover system	115
Treatment testing	117
Tank experiments	117
Bauxsol™ slurry	118
Lime kiln dust slurry	119
Acid-cure slurry and further testing	120
Alteration processes	122
Efflorescent minerals	124
Legacy	126
References	126
Monitoring environmental impacts of the I-99 construction project at Skytop	127
History and environmental setting	127
Acid rock drainage generation	128
Acid mine drainage treatment	128
ARD at Skytop	128
Environmental impacts	129

82nd Annual Field Conference of Pennsylvania Geologists

Surface water	133
Remediation	133
Remediation of exposed rock cuts.....	133
Remediation of the fill areas.....	135
Remediation of discharges and streams.....	135
ERPA.....	137
ERPA leachate and monitoring well chemistry.....	138
Conclusions	141
References	141
Archeological lithic materials in Centre County, Pennsylvania	143
Roadlog	143
Abstract.....	147
introduction	147
Lithic materials.....	148
Local lithic materials: Bald Eagle (aka Hooverville) Jasper.....	150
Impact origin of jasper	154
Local lithic materials: Early Ordovician carbonate sequence	155
Geological origin of chert with an emphasis on Centre County	156
Chert (including jasper variety).....	157
Textures and structures of cherts.....	157
Occurrences	157
Nodular chert.....	157
Fracture-related jasper	158
Sources of silica.....	158
The replacement process.....	159
Summary of geological origins of chert	160
References cited.....	160
Sinking Valley, Pennsylvania.....	163
Geologic setting	163
Geologic features	164
Sponsors	inside back cover
80st Annual FCOPG attendees	back cover

A GEOLOGICAL TRAVERSE THROUGH THE NITTANY MOUNTAIN SYNCLINE

DAVID (DUFF) GOLD¹, ARNOLD G. DODEN² AND ANDREW A. SICREE³

¹EMERITUS PROFESSOR OF GEOLOGY, DEPARTMENT OF GEOSCIENCES, THE PENNSYLVANIA STATE UNIVERSITY, UNIVERSITY PARK, PA, ²GMRE (GEOLOGIC MAPPING AND RESOURCE EVALUATION), INC., 925 WEST COLLEGE AVE., STATE COLLEGE, PA, ³CONTINUING EDUCATION, THE PENNSYLVANIA STATE UNIVERSITY, UNIVERSITY PARK, PA

Preamble

Construction of the Mt. Nittany Expressway during the 1970's resulted in several deep roadcuts across the axis of the Nittany Mountain Syncline. These fresh outcrops, coupled with exposures of the middle Ordovician limestone units in the Oak Hall Quarry provided an almost complete, continuous section from the upper Bellefonte to the basal Reedsville formations. This paper develops the geological history of the Nittany Syncline from these exposures, and local mapping of the Oak Hall Quarry Property (Gold and Doden, 2015), and regional mapping of the State College Quadrangle (Doden and Gold, 2010, 2011) (Figures 1 & 2). It could not have been written without the cooperation and candor of Hanson Aggregates, operator of Oak Hall Quarry.

Introduction

Nittany Valley is a breached 1st order anticline (the Nittany Arch or Anticlinorium) that preserves a karst valley underlain by Cambrian and Middle to Upper Ordovician carbonates in the Valley and Ridge Physiographic Province. Younger clastic sediments (Upper Ordovician and Silurian age) crop out in the sub-parallel trending ridges to the northwest and southeast, as well as in the 2nd order syncline, appropriately named the Nittany Mountain Syncline (by Butts and Moore, 1936) that preserves Nittany Mountain near the crest of the anticlinorium (Figure 1). Key exposures include the southeast limb of the syncline in Oak Hall

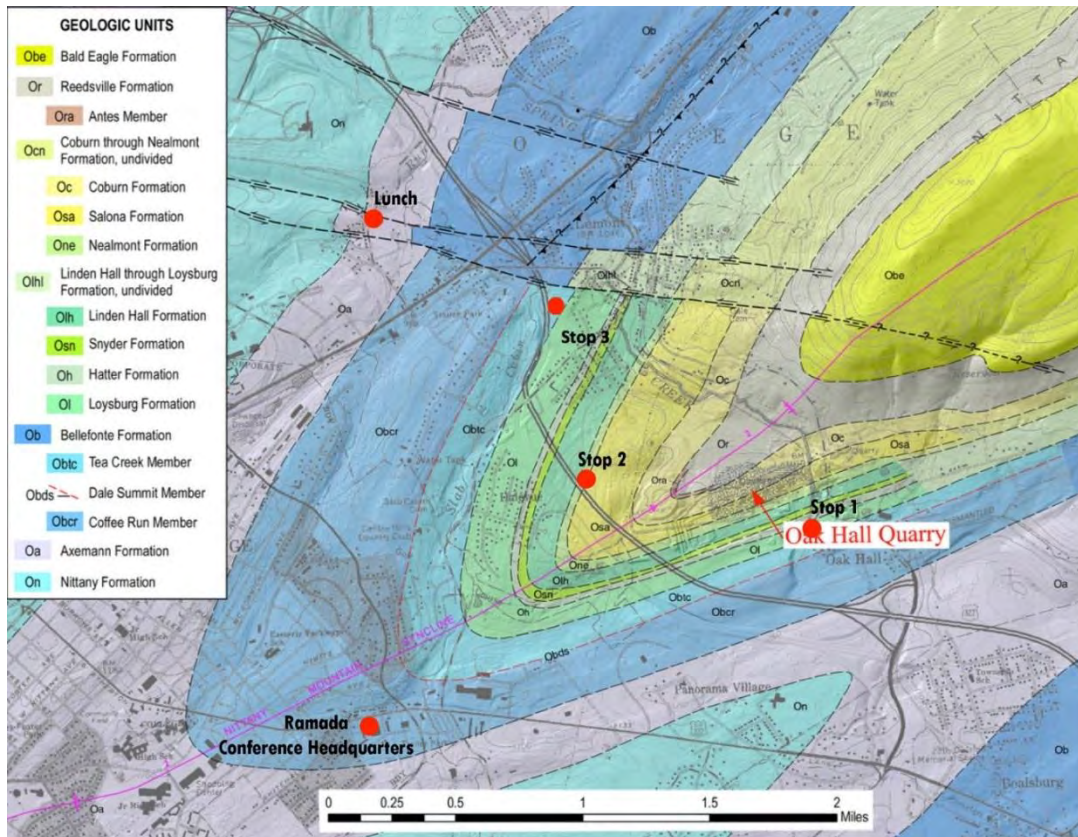


Figure 1. Geological Map of Mt Nittany Syncline and Mt. Nittany Expressway. Red dots with stops mark key exposures.

The setting is a 2nd order syncline plunging 10°/057° with an inclined axial plane striking approximately 055°/70° and a dihedral angle of 114° (Figure 26). A broad hinge zone is apparent in the carbonate units exposed in the Mt. Nittany Expressway roadcuts. Approximately 1200 feet of Middle Ordovician carbonate strata (formations) are exposed in the quarry dipping relatively constantly 54° to the NNW.

At least seven repetitions of silty beds in the upper 190 feet of the Loysburg Formation of are exposed in the southeast corner of the quarry. Some of these beds contain dispersed vugs, typically 4 to 15 cm across, that may contain primary gypsum and secondary calcite and strontianite (Figures 5, and 23). These beds are overlain successively northward by dominantly limestone lithologies of the Clover, Hatter, Snyder, Linden Hall, Nealmont, Salona and Coburn formations, and are capped 1400 feet to the north by pyritic black calcareous carbonaceous shale of the Antes Formation. Two long roadcuts along Mt. Nittany Expressway expose respectively Salona, Nealmont and upper Linden Hall strata in the hinge zone, and lower Loysburg and upper Bellefonte strata on northwest limb of the syncline. The latter is located approximately 290 feet northeast of the bridge is a spectacular 30- to 50- foot deep bank, half-mile-long roadcut, exposing the lower 94 feet of the Loysburg (Milroy Member), 146' 9" of the Tea Creek, 3 feet of the Dale Summit, and 46 feet of the Coffee Run members of the Bellefonte Formation. A number of volcanic ash (strictly metabentonite, but hereafter referred to as bentonite) beds are exposed, and these are tagged with alphanumeric cyphers (B-4 to B-17) in keeping with the system and stratigraphic section established by Berkheiser and Cullen-Lollis (1986), and Laughrey *et al.*, (2004) on Rte. 453 road-cuts near Union Furnace. The bentonites are important, not only as stratigraphic markers, but also as aquicludes. Zircons from the B-5 and B-13 bentonites respectively yield depositional ages of 455 and 451 Ma (Mathur *et al.*, 2011).

Although closure of underlying shale and carbonate formations occurs on the Hanson Quarry Property, only the southeast limb of the syncline plunging 10°/057° (Figure 26) has been exploited to date as a source of aggregate. A quarry was developed in 1917 on the east side of Boalsburg Road in College Township, to extract high-grade limestone for the iron mills in Pittsburgh. A second pit was opened across the road to the west after the 2nd World War to fuel the growth of State College and The Pennsylvania State University. Approximately 500,000 tons of aggregate and crushed stone products are extracted annually from the new quarry, which has a footprint of approximately 3000 feet along strike and 1400 feet across dip in underlying Middle Ordovician formations. Seven benches are developed to a depth of 960 feet above mean sea level. The quarry, now known as Oak Hall Quarry, is owned and operated by Hanson Aggregates Pennsylvania.

The dominant joint sets, J₁ and J₂ correspond, respectively, to the regionally accepted early Alleghenian and post-Alleghenian events. (Orkan and Voight, 1985; Hancock and Engelder, 1999). A hydration front is developed marginal to some of the wide-spaced, shallow, southeast-dipping joints, designated J_x. Any other measurable joint or fracture that appears to be systematic is lumped into the J_x category. The thin, through-going carbonate veins are distinguished from stratabound tension-crack type in the more competent limestone interbeds of the upper Salona and Coburn formations. The former are generally clustered into broad zones. They may represent healed early J₂ joints. Similar mesoscopic-scale *en echelon* veins occur near, and appear to have a mechanical relationship to faults. In contrast, the tension cracks tend to be open, lensoid on a decimeter scale, and exhibit an early

calcite followed by dolomite and rare clear-quartz paragenesis (Figure 13). They share a common orientation with the J₂ joint set and an association with “necked and boudinaged” beds in some rhythmites. Thin (several mm) and through-going calcite veins (selvages) occur on some bedding surfaces and on J₃ joints. These tend to be healed. A late, segmented, steeply-dipping joint, oriented east-northeast is developed in some of the thicker beds. Definition is difficult because they tend to be discontinuous and widely spaced. Engelder identifies them as neotectonic joints (Handcock and Engelder, 1989), a consequence of the current NE-SW direction horizontal compression (ambient stress field). The J₃ joints are best exposed in the roadcut.

Depositional structures include compositional and textural discontinuities and local erosional unconformities. Horizons of dispersed vugs - some preserving gypsum, mudcracks and ripple marks, sponge baffle mounds and large stromatolites (Figure 6) attest to peritidal settings. Secondary structures include (a) stylolites associated with diagenetic (essentially bedding parallel) and tectonic (strike/bedding-normal) and cross-strike sets (b) joints (c) faults, (d) folds, veins, and tension cracks.

Stratigraphy

Bellefonte

Sections of the Bellefonte Formation are exposed in roadcuts along the Mt. Nittany Expressway and the Boalsburg Road through Oak Hall. The Tea Creek Member is projected to underlie the settling pond to the east of the crusher on the Hanson Property. A medium-to coarse-grained, poorly-sorted, matrix-supported dolomitic sandstone bed, eight feet thick (the Dale Summit Member), is exposed the south-bound lane roadcuts on the expressway, 1,200 feet southeast of the Hanson property line. It is only 34 inches thick where it is exposed in the roadcut, 6500 feet to the north, on the NW limb of the syncline.

Loysburg

Some of the lower Loysburg (Milroy Member) is projected to underlie the southeast corner of the property (Figure 3). One hundred and ninety-seven feet of the Tea Creek Member (Upper Bellefonte Fm) and 86 feet the Milroy Member of the Loysburg Formation are exposed in a continuous section in the Mt. Nittany Expressway road cuts approximately 2,500 feet north of the quarry (Figure 4).



Figure 3. Bench 4 in SE corner of Quarry, exposing 195 feet of the Milroy and 18 feet of the overlying Clover members of the Loysburg Formation. (IMG 2030: 9/29/2014).

Table 1. Thickness of stratigraphic units and intervals between bentonite markers, normalized to zero on the B-11 bentonite (lower member of the “twins”).

State College Quadrangle - STATEMAP Program					
Measured Section through Oak Hall Quarry: July-August 2009 Temporal/spatial modifications: October 2015/March 2017					
<i>Station Number</i>	<i>Formation Member</i>	<i>Unit Bentonites</i>	<i>Stratigraphic distance above (+) below (-) B-11</i>	<i>Thick feet, or cm</i>	<i>Interval</i>
From Drill core CB-02 (January 2014)					
	Antes			90 +	
	Antes	<i>Cleavage duplex</i>	566		6' above base of Antes
36	Reedsville	Antes/Coburn contact	560		
	Coleville			147	
		Shale/ash? (contact?)	413		73' above shale marker
	Milesburg	Shale/ash? Marker	340	156	231' above B-15
	Coburn	Coburn/Salona contact	257	303	
		<i>B-16?</i>			
29	Roaring Spring	<i>B-15</i>	109		10 48.5' above B-14
		Ro SP - New En contact	91	107	
28	New Enterprise	<i>B-14</i>	60.5		20 35.5' above B-13
27		<i>B-13</i>	25		20 23' above B-12
26		<i>B-12</i>	2		15 2' above B-11
25		<i>B-11</i>	0		10
24		<i>B-10?</i>	-15		5 15' below B-11
23	Salona	Salona/Rodman	-31	288	
		<i>B-9?</i>	-92		8 to 12 77' below B-10
22	Nealmon	Nealmon/Linden Hall	-92	61	
	Rodman			21	
21		<i>B-8?</i>	-110		8 18' below B-6
			-184	40	
19	Centre Hall	<i>B-6?</i>	-184		10 74' below B-5
	Linden Hall	Linden Hall/Snyder	-248	156	
	Snyder			70 - 80	
	Hatter			70?	
	Loysburg	Clover		30+?	
		Milroy		370?	
Gap: Data cobbled from air rotary holes on Tressler Farm (July 2000) and Mt Nittany Expressway road-cut					
		Shale/ash <i>Bo ?</i>			10?
	Bellefonte				
		Tea Creek		147	
		Dale Summit		4 to 12	
		Coffee Run		1000	



Figure 4. Roadcut on Mt. Nittany Expressway showing dark gray limestone, light gray dolostone, some thin buff-colored silty shale interbeds and rare dark horizons of insoluble residues. The medium gray bed (left center) is a 4-foot thick tiger strip limestone bed at the base of the Milroy Member of the Loysburg Formation. Light-colored dolostone of the Bellefonte are exposed to the left (IMG 0765: 3/20/2010).

A cross-section of the Loysburg strata approximately 200 feet thick was measured in high-walls on benches 2, 3, 4, and 7 (Figure 3) in the southeast corner of the quarry. Strata consist of at least eight repetitions of relatively porous, thin platy and vuggy siltstones, some with stromatolites and sponge baffle mounds spaced 2 -12 m (6-40 feet) apart. Six distinctive “ribbon banded” or “tiger stripe” (Kay 1955) units, characteristic of the Milroy Member are exposed here. Four other tiger stripe beds are exposed in Mt. Nittany Expressway roadcut, southwest of the Elmwood bridge, with no demonstrable overlap. The transition into the biomictites (Chavez, 1969) of the Clover Member has yet to be identified. At least 86 feet of the Lower Milroy Member are exposed in the expressway roadcuts approximately 3,000 feet north of the quarry. Repetition of limestones/dolostones and mega-stylolites (Figure 27) of the Milroy Member are apparent in the, light and dark-gray colored limestone/dolostone interbeds on a 30 cm to 1.5 m scale. (Figure 4). These were interpreted as “meter-scale shallowing upward cycles” Flemings and Grotzinger (1996) in an exercise on sequence stratigraphy.

Milroy strata present a greater variety of lithologies than other formations exposed in the quarry. Individual litho-units vary from a few inches to tens of feet in thickness and in composition from very fine-grained dolomitic laminites to dololutes overlying medium- to dark-gray to off- white

calclutites, capped by rusty thin-bedded, silty, stromatolitic limestones. Also present are thin rip-up-clast beds and dispersed mineralized vugs (calcite and strontianite) up to 30 cm across (Figure 5 and 23), and limey beds with sponge baffle mounds up to 1 m across and 20-30 cm high (Figure 6).



Figure 5. Open and mineralized vugs exposed on a bedding surface in Loysburg (IMG 0203: 1/14/2012).



Figure 6. Sponge baffle mounds in the Clover Member, SW corner of quarry (IMG 718099: 7/18/2007).

Gypsum preserved in some of the vugs is interpreted as primary, deposited in a shallow sabkha environment. Some buff colored platy silty beds preserve salt casts. Mud cracks and intraformational “breccias” attest to an energetic shallow water to tidal-flats setting. Bedding-parallel stylolites are

common, some with a wavelength of decimeters and amplitude of many centimeters. Rare smaller cross-strike stylolites are noted. The tectonic implication of the stylolites have been addressed by Srivastava and Engelder (1990) and the road log accompanying this volume.

The 195-foot section exposed in the quarry represents a stratigraphic thickness of approximately 200 feet of an estimated 128 m (400 feet), inferred, but not well constrained, from drill holes on the Dressler property to the south. This estimate may be high (especially compared to the 230-foot section inferred from mapping along Rte. 453 near Union Furnace (see Gold and Doden map in Laughrey *et al.*, 2004).

The Clover represents the transition from dominantly dolomitic strata in the underlying Milroy Member to the micritic limestones of the Hatter Formation.

Hatter Formation

A complete section, approximately 90 feet thick, of the Hatter Formation can be pieced together from exposures on the 7th, 5th, 4th and 2nd benches along the southern edge of the quarry. Transition from the underlying Milroy strata is abrupt, with a change to massive calcilutites of the Clover and lower Hatter. The basal Grazer Member contains massive calcilutites with a reticulate texture and wavy-bedded argillaceous calcilutites, and grades into the overlying Hostler Member of interbedded bioclastic limestone and micritic limestone on a 10 to 20 cm scale, which marks the top of the formation. A quieter peritidal and agonal setting is inferred. The contact with overlying Snyder is at the abrupt change from interbedded bioclastic and gray micrite into massive (meter-scale), light-gray Mg-calcilutites, ripple-marked and mud-cracked limestone.

Snyder Formation

An uninterrupted section of Snyder lithologies is exposed on bench 7, with segments on benches 5 and 3. It is characterized by a diverse limestone lithology of thick (1-2 m) Mg-limestone beds, calcilutites, weakly-siliceous calcarenite, limestone laminites and diamictites(?) in regular well-defined beds for a thickness of approximately 83 feet. The latter occur in beds up to 20 cm thick of granule to pebble size light gray micrite dispersed (Figure 7) in a dark gray calcarenite matrix. The paucity of sorting is difficult to reconcile with the high degree of rounding.



Figure 7. Well-rounded clasts of light gray micrite (unsupported), unsorted and dispersed in dark gray calcarenite matrix. Snyder Formation. Photograph by Charles Miller.

Mud-cracks, ripple marks (Figure 8), large stromatolites and rip-up clasts conglomerates attest to a peritidal setting. The compositionally well-defined beds of the Snyder grade abruptly into massive micrites of the Linden Hall Formation.



Figure 8. Ripple marks and mud-cracks in Snyder Formation. Old Quarry (IMG 1703: 4/17/2014).

Linden Hall Formation

The approximately 156-foot thick Linden Hall Formation consists mainly of thick-bedded dove-gray weathering, medium-to dark-gray micritic, some lightly burrowed, with a fucoid texture and fine-grained fossiliferous limestones. This remarkable uniformity is exposed in all benches along the long axis of the quarry, extending from the center of the old quarry to where it converges on the southern boundary to the west. A change in dip attitude from 54° north-northwesterly in the quarry, to east to southeasterly gently dipping beds in the road cuts on Mount Nittany Expressway demonstrates the synclinal setting of these formations. The massive dominantly micritic, locally sparry, fenestral calcilutites represent the highest quality of stone (from both its equant breaking properties and grade of limestone). For many years, it has been the backbone of local quarry operations. The Valentine Member, recognized in the quarries near Center Hall, appears to have shoaled out and is not evident in the Oak Hall Quarry. Other subdivisions recognized are an Upper Oak Hall Member, a Middle Valley View Member, and a basal Stover Member consisting mainly of massive sparry limestone, some with a reticulated pattern.

The Oak Hall Member, intersected in drill hole CB-03, consists mainly of massive, medium dark-gray (N4) micrite (calcilutites), in beds ranging from 1 to 10 cm (average \pm 5 cm) thick separated by “wispy” irregular partings. Some interbeds are grayish-black (N2) argillaceous limestone on a 1 to 5 mm scale. The massive limestones exhibit a dove to light-gray color (N7 to N8) on a cut surface. Fossils are scarce except in darker interbeds.

A 10-cm thick meta-bentonite bed, tentatively identified as B-4, occurs 52 feet up in the Stover Member and is composed mainly of massive reticulated calcilutites. Another meta-bentonite (B-5) is exposed 97 feet up in the Valley View Member, approximately 22 feet below the B-6 meta-bentonite in the overlying Nealmont Formation. The B-5 meta-bentonite bed is taken as the base of the overlying Nealmont Formation, and appears to be deposited on an unconformity.

Nealmont Formation

A complete section of the upper (Rodman Member) and lower (Centre Hall Member) is exposed in the road-cut on Mt. Nittany Expressway. Dark-gray massive micrites with discontinuous bioclastic and wackestone lenses characterize it. In drill hole CB-03, the transition from the underlying Oak Hall Member of the Linden Hall Formation is marked at massive (1-2 m) beds of gray Mg-calcilutites with thin wavy interbeds of dark-gray argillaceous limestone. Some of the latter contain gastropods and crinoid fragments. The distinctive, flaser-textured, nodular calcarenites of the Rodman Member (Figure 9) comprise the upper 15 - 20 feet. The pinch and swell morphology of the nodules is attributed to differential compaction. Smith et al., (1986) also evoked pressure solution, and/or patchy sea-floor cementation. This formation represents a 63-foot transitional sequence from massive micrite deposition to cyclical conditions with a marked increase in argillaceous and biological components as well as an increase of volcanic events (B-6 to B-10) upwards.



Figure 9. Nodular beds of Upper Nealmont (Rodman Member), exposed in Mt. Nittany Expressway roadcut (IMG 1339: 9/24/2014).

Oak Hall Member

The Oak Hall Member consists dominantly of medium-gray (N-5) calcilutite (with a light-gray (N-8) streak on a cut surface), and thin (1-5 mm) wavy interbeds (some wispy) of dark grayish black (N-2) argillaceous limestone. Apart from scattered worm tubes (3 – 6 mm across) dispersed in some thicker micrite beds, there is a paucity of fossils. Some beds exhibit a reticulated texture. Calcite veins

tend to be open and cross-strike in attitude. A few bedding-parallel stylolites are noted. Appearance of calcarenite interbeds marks a transition from massive micrite, typical of the Centre Hall Member, into the overlying nodular calcarenites of the Rodman Member.

Rodman Member

The Rodman Member is characterized as a matrix-supported, flaser-textured limestone in which “nodules” (Figure 9) dominantly of calcarenite, are sheathed in wavy beds of dark-gray, argillaceous calcilutites, some of which are fossiliferous. Fossils in the matrix include crinoids, brachiopods, bryozoans, and gastropods. Nodules, ranging from 3 to 10 cm across, consist of medium-gray (N-5) calcarenite in a matrix of darker (N-3) argillaceous limestone, and exhibit a light-gray color (N-7) on a cut surface. Bioturbation is apparent in reticulated textures and relict worm tubes (3 – 5 mm across).

Only one of four bentonite horizons known to exist in the Nealmont is exposed in the Oak Hall quarry. The Salona Formation, overlies the top of the nodular calcarenite beds (in places the B-10 bentonite), heralding a change to rhythmite cycles, with a marked increase in siliciclastic interbeds and sympathetic decrease in abundance of fossils.

Salona Formation (rhythmites)

The Salona strata are characterized as asymmetric rhythmites in which the dominant medium- to dark-gray (micritic) limestone beds that range from 10-50 cm are 1-5 times thicker than the interbedded, very dark-gray to black, argillaceous limestone and lime mudstones, or “dirty” greenish gray, very fine-grained limestones. Truncated and undulose bases of many limestone beds suggest an interrupted sedimentation regime. Bioclastic material (brachiopods, crinoids, ostracods and trilobites) generally occurs in the clay-rich layers. A pattern of competency and fissility is apparent in the “argillaceous” beds on a 15- to 50- foot scale with a change to more shaley components in the upper Salona and Coburn rhythmites.

Approximately 288 feet of Salona rhythmites containing at least eight bentonite horizons have been identified from the B-10 to a Black Shale marker (B-17?). The lower five ash beds (B-10 to B-14) (Figure 10) in the New Enterprise strata signify both vigorous and active subduction during the Taconic orogeny. Two distinct bentonites 36 to 42 inches apart serve as the important stratigraphic marker known as the “twins” (Figure 11). These are designated as the B-11 and B-12 bentonites (Berkheiser and Cullen-Lollis, 1986). The B-12 has been identified as the Deicke; the B-14, approximately 57 feet above, is the Millbrig. This pair of bentonites has an intercontinental distribution (Berkheiser and Cullen-Lollis, 1986; Cullen-Lollis and Huff, 1986; Kolata *et al.*, 1996; Mathur *et al.*, 2011). Their distinctive fissile texture and light gray (ashen) color, so apparent in the fresh exposures of B-10 to B-15 in the high-wall on bench 7 (see Plate 6-A, K) is less easy to distinguish in the weathered outcrops along Mt. Nittany Expressway. B-15 and B-16 bentonites occur in the Roaring Springs strata.

The top of the Salona Formation is set arbitrarily on a black shale horizon (the Black Shale Marker) and/or a coquina (Thompson, 1963), above which tempestites are common. These criteria are not easy to follow in the field. Two members are recognized. The stratigraphic thicknesses for the lower, New Enterprise Member (thicker interbeds; fewer black shales and more “sandy” grainstone beds), and the upper, Roaring Spring Member (thinner interbeds), are projected from drill hole CB-04 to be of the order of 106 feet and 200 feet thick respectively.



Figure 10. Bentonite beds B-12, B-13, B-14, and B-15 in high wall of 3rd bench (IMG 2038; 9/30/2014).



Figure 11. Bentonite B-11 and B-12 (the twins approximately 27 inches apart) occur above and below the rusty zone. The prominent dip slope on the right in the footwall of B-13. (IMG 1796; 5/8/2014).

New Enterprise Member

In drill hole CB-03, the lower New Enterprise stratigraphy consists of asymmetric rhythmites on a decimeter scale, dominated by medium dark-gray (N-4) calcilutite (micritic limestone). These micrites, exhibiting a dove-gray (N-7) surface streak or weathered surface, are interbedded with thinner (cm-scale) “dirty” olive-gray (5GY3/2) micritic limestone and grayish-black to black (N-2 to N-1) argillaceous, carbonaceous limestone (commonly fossiliferous with bivalve shells and algal filaments).

A rhythmic sequence is apparent in the basal section and becomes more distinctive upwards. Dispersed fossils (tentatively identified crinoids, bryozoans, brachiopods and gastropods) on a millimeter to centimeter scale occur in the darker argillaceous limestone. A Black Shale bed overlying light- to olive-gray, clay-rich beds, is identified as the B-13 meta-bentonite. The “dirty” limestones tend to be thicker and more abundant near the base. Calcite veins tend to be open and cross-strike in attitude.

Roaring Spring Member

The Roaring Spring strata are characterized by alternating interbeds of micritic limestone, argillaceous lime mudstones and calcareous shale. Most of the limestone occurs as thin- to medium bedded planar and cross-laminated recrystallized lime mudstones (Slupik, 1999). There is an upward trend in these rhythmites towards more black shale and fewer “sandy” grainstone beds. The top of the Roaring Springs Member is placed above an abrupt change in from med to thick bedded cohesive section in to thin-to medium bedded recessive section at approximately 105 feet above the top of the Rodman. This transition is apparent in the Mt Nittany Expressway road-cut.

The lower section of the Roaring Spring Member cored in drill hole CB-04 layers (10 to 40 cm scale) of “clean” dark-gray (N3 to N4), or greenish-gray to dusky-green (5G 3/2) (“dirty” micritic) limestones occurs intercalated with cm-scale beds of dark-gray to grayish-black (N2) argillaceous, limestone that commonly hosts fossils. A very fine-grained granular pyrite occurs within some fossil shells.

The Upper Roaring Spring stratigraphy in CB-04 is an asymmetric rhythmite, dominated by thicker beds of a dark-gray (N3-N4) to grayish-blue (5PB 5/2) micritic (calcilutites) limestone, that appear dove gray (5B 6/2 to 5PB 7/2) on a weathered or cut surface (designated as “clean” limestone). A darker olive-gray (5GY 3/2) variant occurs locally in beds typically 10 - 20 cm thick, intercalated with dark greenish-gray (5G 4/1) or black (N2 to N3) argillaceous limestone, or more rarely with a black calcareous, carboniferous shale. Dispersed fossils (tentatively identified as crinoids, bryozoans, brachiopods and gastropods) on a millimeter to centimeter scale occur in the darker argillaceous beds. A few thin (cm scale) coquinas, and some rare fine-grained grainstone beds (1 to 3 cm thick) occur mainly in the lower 100 feet. Very fine-grained pyrite occurs locally, generally within relict fossils. Light to olive-gray, clay-rich beds, 5 to 15 cm thick (B-15? bentonite horizon), occur approximately 20 feet above the contact. The “dirty” limestones tend to be thicker and more abundant down section.

Coburn Formation

No distinctive marker horizon was recognized defining the Salona/Coburn contact except for an increase grain-size and bioskeletal clasts along bedding plane surfaces. The bioclastic lags rest on an

erosion base and grade upward into sparry lime mudstones and argillaceous lime mudstones and/or calcareous shale (Slupik, 1999). These are interpreted to be tempestite deposits on a distal ramp margin (Hoover, 1995). The limestones commonly preserve planar and cross laminations and fossils are common. There is an increasing trend to calcareous carbonaceous shale upward.

A coquina bed is taken as the transition between the more shaley rhythmites of the upper units (Coleville Member) and the relatively more “limy” beds of the lower units (Milesburg Member). A stratigraphic thickness of 147 feet and 156 feet respectively is inferred from segments stitched together in the quarry (Doden and Gold, 2010). A longer-range cycle is apparent in the rhythmic variation in centimeter to decimeter scale interbed thicknesses. These changes have been measured in the drill cores, but not processed.

Milesburg Member

At other localities, the Milesburg Member is a thin to medium bedded, quartz-rich lime mudstone interbedded with thin argillaceous lime mudstone (Slupik 1999). Convolute laminae and flame structures are present locally and bioskeletal lags are common grading upward into packstones to grainstones to mudstones (Slupik, 1999).

A rhythmic sequence is apparent in core from drill CB-02. Dark-gray calcilutite (dove gray streak on a rough-cut surface) in discrete as well as boudinaged beds, centimeters to decimeters thick, with thinner interbeds of either an olive-gray “dirty” argillaceous limestone or a dark greenish-gray to black calcareous, carbonaceous shale. Fossil shells and algal matre (?) filament are dispersed in some of the argillaceous beds. An incipient spaced (5 to 10 mm) cleavage is apparent, at a high angle to bedding, in some of the argillaceous beds. A “graphitic” glei fracture surface is present in some of the carbonaceous shale beds. The rare cross-strike veins of cream to white carbonate veins in the drill core are seen to be associated with fault zones in the quarry benches. Open carbonate veins are well exposed, particularly in the northeast high-walls, where stratabound tension cracks (Figure 12) are apparent. These lensoid cracks

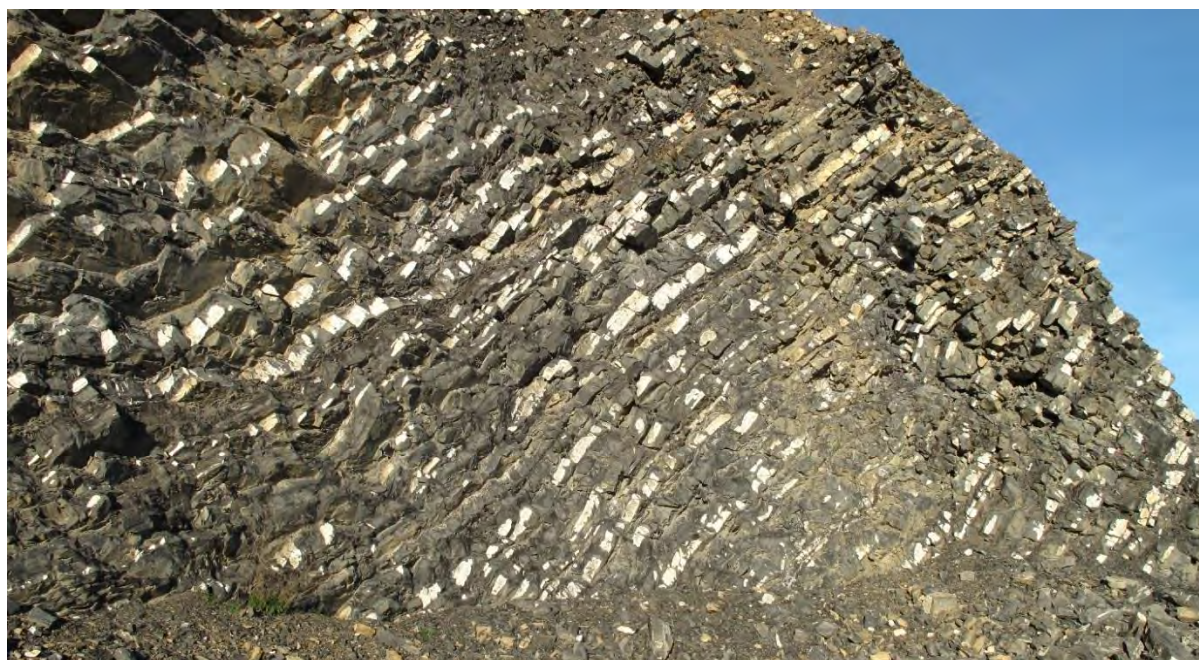


Figure 12. Stratabound tension cracks in Coburn Formation – NE wall of Quarry (IMG 1473: 11/10/2014).

show a paragenetic sequence of early calcite followed by dolomite and rare late clear quartz (Figure 13) or fluorite. Mesoscopic-scale folds, apparent in drill core from the change in core angle, are interpreted as slump features rather than drag folds associated with the Nittany Mountain Syncline (Figure 14).



Figure 13. Tension Crack showing paragenesis of early calcite (white), followed by dolomite (pink) and quartz (clear crystal) in the center (IMG 3742: 11/8/2014). Quartz crystal is 12 mm long.



Figure 14. Mesoscopic scale concentric folds (probably slump) in Coburn rhythmites exposed on 3rd bench, north side of Quarry (IMG 100 0770: 7/20/2009).

Coleville Member top CB-02

The Coleville Member has been characterized regionally as a “thin-bedded, dark gray planar and locally cross-bedded, quartz-rich lime mudstones interbedded with argillaceous lime mudstone and shale” (Slupik, 1999). In the quarry a marked difference in stiffness (competency) is apparent in the recesses nature of the exposed “argillaceous” beds, and the presence of stratiform tension cracks in the limestones beds. The latter typically are filled with calcite and dolomite.

The top section of drill hole B-02 intersected alternating beds of a dark gray N6 to 5B 6/2 micritic (calclutite) limestone (dove-gray streak on a cut surface). They occur as discrete and in places as boudinaged interbeds of “clean limestone” centimeters to decimeters thick within thinner interbeds of either an olive-gray (N3 to dark olive-gray 5GY 3/2) “dirty” argillaceous limestone, or a dark greenish-gray (5G 4/1) to black (N2) calcareous, carbonaceous shale. A rhythmic sequence is apparent. Fossiliferous horizons range from bioclastic (coquinas) beds many centimeters thick to dispersed fossil shells (mainly crinoids and brachiopods) and algal matte filaments (1 mm to 1 cm scale) common in some of the more argillaceous interbeds. A fossil hash layer (coquina) at the base of some of the micritic limestone beds is interpreted as a “tempestite” (below normal and into storm wave base events). The asymmetric ratio of thicker (centimeters to several decimeters) calcilutite beds to the more argillaceous lithologies (that range from millimeter scale partings to decimeter thick beds) reverses near the top. The contact with the Antes is placed at the first thick (2-3 feet) bed of black, carbonaceous pyritic shale (Figure 15). It marks a change to a dominantly clastic lithology of meter-scale calcareous argillites and black carbonaceous shales (Figure 16).



Figure 15. Black Shales of the Antes Formation on northern perimeter road of the Quarry (IMG 1475: 6/7/2014).



Figure 16. *Interbedded Black Shale and limy argillite in road cut on northern perimeter road of the Quarry. Slaty cleavage dips 70° to the left; a fracture cleavage (rusty surface) is developed in the more competent, limy argillite beds (IMG 1000794: 7/20/2009).*

Antes Formation

For a long time, the limy back shales, overlying the limestone/shale rhythmites of the Coburn Formation were considered to be the Antes Member and informally (Wagner, 1966) were referred to as the Anter Member. Along the nose of Nittany Mountain it is exposed on the upper bench wall on the north side of the quarry, and beneath a culvert on Boalsburg Road to the north. At least 90 feet of calcareous argillite and compact black shale was in drill site on the road berm. (Gold, 2015). The Antes Formation is mainly a black (dark-gray to grayish-black N2 to N4), carbonaceous, calcareous shale with lighter color (olive gray 5Y 3/2 to grayish olive green 5GY 3/2) calcareous interbeds on a millimeter to decimeter scale. Pyrite is present locally as very fine grains commonly clustered to form blebs (3 - 10 mm across) as well as in thin stringers or beds. The blebs probably represent replaced fossils. A slaty cleavage is developed in the black shales (Figure 15).

An incipient cleavage 3 - 5 mm spaced is apparent in the drill core of some of the lighter-colored more competent limy interbeds, dipping in opposite sense (antithetic) to the beds. This antithetic cleavage/bedding attitude has created decimeter long cleavage mullions on scree slopes near outcrops. Fine clayey light-gray bed, 25 cm thick, (Figure 16) was near this contact in the quarry wall

was originally mapped as volcanic ash, were not cored in the nearby CB-02 drill hole. These have been reinterpreted as gouge and sulfurization products on bedding shears.

In the quarry walls the Black Shale is easy to discern by its characterized rusty stain (Figure 13) and the local presence of efflorescent minerals [calcite (CaCO_3), gypsum [$\text{CaSO}_4 \cdot 2\text{H}_2\text{O}$], melanterite [$\text{FeSO}_4 \cdot 7\text{H}_2\text{O}$], halotrichite [$\text{Fe}^{2+}\text{Al}_2(\text{SO}_4)_4 \cdot 22\text{H}_2\text{O}$] and copiapite [$\text{Fe}^{2+}\text{Fe}^{3+}_4(\text{SO}_4)_6(\text{OH})_2 \cdot 20\text{H}_2\text{O}$].



Figure 17. Slaty cleavage and cleavage/bedding lithons in road cut on northern perimeter road of the Quarry (IMG 1173: 9/24/2014). Top to right.

Depositional Setting and Tectonic Implications

The shallow peritidal with extensive mudflats and lagoons of the Loysburg, and shallow subtidal limestones of the Linden Hall and Nealmont formations, were abruptly overlain by hemipelagic deposits (Salona) and mid-ramp tempestites of the Coburn (Hoover, 1995). The Antes is interpreted as a clastic wedge in the emerging foreland basin.

Slupik (1999) deduced an overall upward deepening progression from change in dominant lithotypes of “floatstones and wackestones in the upper Nealmont to the argillaceous lime mudstones of the lower and middle Salona, to the laminated, quartz-rich lime mudstones and bioskeletal lags of the upper Salona and lower Coburn formation. These settings reflect a transition from platform to a prograding storm dominated ramp in a foreland basin, progressively interfingering with siliclastic sediments from the rising Taconic highlands to the east. Antes and Reedsville shales represent a prograding clastic wedge, a precursor to the Queenston Delta.

This sequence records the history of plate collision during the late Ordovician, the demise of the Great American Bank (Hardie, 1989) that covered most of North America and the birth of the Taconic orogeny. Overall, they reflect the transition from a passive to an active margin of the Great American Bank (Hardie, 1989).

Cycles

Cycles on a decimeters scale, as well as 5-15 m scale (Hoover, 1995), are apparent. The former are medium to thinly bedded limestone rhythmically intercalated with thinner beds of argillaceous limestone and/or calcareous shale. These represent interfingering of carbonate (platform) sediments with siliciclastic influx off a rising origin in a foreland basin. In the Salona, these tend to be sharp-based laminated micritic limestones with bioturbated tops capped by limy shale (Hoover, 1995) from a distal shelf setting. In contrast the Coburn rhythmites exhibit sharp erosive based calcarenites and skeletal grainstones, fining upwards to bioturbated tops capped by shale or argillaceous limestone (Hoover, 1995). In the decimeter-scale couplets the limestones are “periods of rapid sedimentation separated by miniature condensed of shale/argillaceous limestone” (Hoover, 1995).

In the road-cut, a change in color, dominant bed thickness and cohesiveness of the shaley interbeds is apparent on a 10-50 foot scale (Figure 18). On a weathered surface the more shaley interbeds have weathered back into a recessed pattern, whereas the more limy interbeds have maintained their cohesiveness (coherent in the accompanying table). Not only do the latter tend to be thicker but they also break across bedding surfaces to yield a more competent aggregate. Hoover (1995) concluded that in the longer-term cycles, calcareous tempestites are driven by events, such as storms, while a shale/argillaceous limestone assemblage is a manifestation of a slow background sedimentation in a hemipelagic setting. He concludes they represent deep- to mid- ramp parasequences with bentonites accumulating on some flooding surfaces. A possible forcing mechanism is eustatic sea level cycles.



Figure 18. Variation in the limestone bed thicknesses and weathering pattern in the Salona strata exposed in the west-bound roadcut on Mt. Nittany Expressway

Centimeter-scale cycles are apparent in the composition and grain-size alternations in the “tiger-stripe” limestone beds in the Loysburg. These change from a micrite to a more granular limy

dolostone, with varying degree of bioturbation yielding a range of ichnofabrics. We hypothesize periodic weather/climate related events in a restricted tidal mud-flat basin or lagoon (see companion article in this volume by Miller and Gold).

Mineralogy

Some unusual minerals have been found in the Lemont and Oak Hall Quarry. They included:

- *Lemont Diamonds* that have been picked up in the soil by generations in inhabitants in Lemont. These are clear and milky white, doubly terminated quartz crystals weathered out of the tension crack veins in the Coburn Formation (Figures 19, 20 and 13).
- *Nodules of very fine-grained pyrite* that weather out of the bentonites, mainly B-12, B-13 and B-14 (Figures 21 and 22). These range in size from 2 to 10 cm across, and clearly are authigenic in origin.
- *Secondary strontianite* is present in some of the 5-20 cm vugs in the Milroy silty beds (Figure 4). There are white needle-like, spherical clusters (Figure 23).
- *Efflorescent minerals* associated with Antes outcrops include calcite [CaCO₃], gypsum [CaSO₄•2H₂O], melanterite [FeSO₄•7H₂O], halotrichite [Fe²⁺Al₂(SO₄)₄•22H₂O] and copiapite [Fe²⁺ Fe³⁺₄(SO₄)₆(OH)₂•20H₂O].



Figure 19. Lemont Diamonds. Clear, Cloudy doubly terminated quartz crystals. Courtesy Stuart Bingham 2015.



Figure 20. Cloudy doubly terminated quartz crystals. Courtesy Stuart Bingham 2015.



Figure 21. Pyrite nodule in B-12 bentonite (IMG 1897: 3/19/2014).



Figure 22. Pyrite nodules weathered out of B-12, B-13 and B-14 bentonite (IMG 3777: 11/8/2014).



Figure 23. Acicular stromantianite crystals in vug. Loysburg Formation (IMG 2032: 9/29/2014).

Structural Geology

The Oak Hall quarry is developed on the southeast limb of the 2nd order Nittany Mountain Syncline in the Valley and Ridge Physiographic Province. The trace of this syncline is located on the Hanson property, approximately 200 feet north of northwestern benches. The hinge-zone of this fold is shown in the cross-section (Plate 1), as an open (dihedral angle 70°-120°) fold, based on a quasi-circular inflection inferred from the bedding attitudes along the Mt. Nittany Expressway. A kink-fold model (Engelder, 2000) would project a much deeper trough. However, the trough, yet to be exposed in the workings, is constrained by two drill holes respectively in the southeast dipping Salona and Coburn formations. Outcrops in the west-bound lane of the expressway reflect the presence of the northwest limb. An axial planar cleavage is developed in the shaly interbeds in the Coburn and in the overlying Antes Shale near the hinge zone. Mesoscopic-scale flexures occur locally within the quarry (Figure 12), and along the expressway, where their association with ramp faults is apparent (Figure



Figure 24. Ramp fault in Lower Salona rhythmites. Mt Nittany Expressway roadcut (IMG 1798: 5/8/2014). The staff is 5 feet long.

24) in the Nealmont and lower Salona strata. Other, essentially concentric mesoscopic-scale folds, are exposed along the 3rd, 4th and 5th north-side benches (Figure 13) in thinly bedded Coburn rhythmites. Although these appear to be co-axial with the Nittany Mountain Syncline, they do not exhibit the form and sense of associated drag folds. Most exhibit an S-sense asymmetry. Both the ramps and incompatible folds are interpreted as “layer parallel shortening” phenomena.

Bedding faults are common. Most contain slickensides of slivers of carbonate gouge on a platy jogged surface. A reverse sense of motion from the jogs and a relatively constant pitch of 78° to the west for the slickenlines suggests a flexural-slip mechanism perpendicular to the axis of the Nittany Mountain Syncline. In contrast, transverse faults are relatively rare (Figure 25).



Figure 25. Cross-strike fault (138°/80° cutting Snyder beds (243°/57°) in south wall of Quarry (Stn 1448: IMG 1793: 5/8/2014).

The presence of transverse faults (Figure 1) is inferred from juxtaposition of stratigraphic units. The traces of two macroscopic faults mapped in the State College Quadrangle (Hoskins and Root, 1976; Doden and Gold, 2011) have been projected to extend onto Nittany Mountain from linear trends on LIDAR image of the area (Figure 39). A fault striking 140°, was mapped for at least 500 feet exposed in the quarry. Displacement increases southeastward, from zero in the Coburn to an estimated 20 feet in the Snyder strata 350 feet to the southeast.

From a projection of the axes (30°/265°) of dragfolds (decimeter scale) shale beds in the Coburn rhythmites adjacent to this fault in the northwest corner of bench 7 suggest a right lateral, essentially strike-slip motion of a 10/15 cm. The slip vector is estimated to plunge 10°/38°.

Primary Structural Elements

Structural data are summarized in orientations diagrams (Figures 26 to 32).

Bedding

Bedding attitudes are remarkably uniform, and the bimodal distribution in the orientation plot (Figure 2: π diagram of bedding attitudes) reflects the opposing limbs of the Nittany Mountain Syncline, plunging $10^\circ/057^\circ$, about an axial plane oriented $055^\circ/70^\circ$.

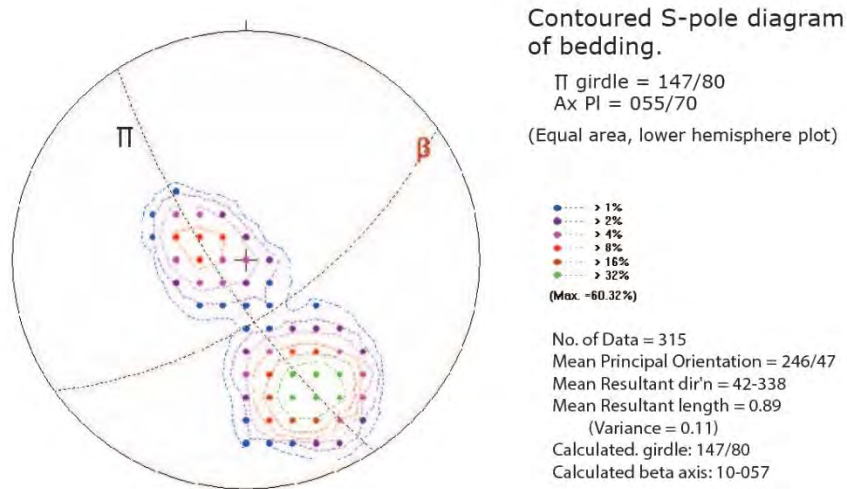


Figure 26. Orientation diagram showing strong bimodal distribution of bedding planes, a well-defined π girdle, axial plane and axial line (β).

Bedding is apparent as changes in composition, and/or grain size, some with ripple marks, mud cracks and trace fossil tracks, an alignment of “evaporate vugs, algal mats, stromatolite horizons and local intra-formational conglomerates. Penecontemporaneous slump features are preserved in some beds. Rip-up-clasts are common in the Loysburg and Snyder strata. There is a cyclical order on a different scale in the stratigraphy. Rhythmites occur in decimeter-scale alternations of limestone and argillaceous limestone or calcareous shale of the Salona and Coburn formations (Figure 18), and centimeter-scale alternations, known as “tiger stripes” occur as meter-thick beds in the Loysburg Formation. Meter-scale repetitions are apparent in the Loysburg, Snyder and Nealmont formations. Other bedding features include mud-cracks, ripple marks trace fossil tracks and salt casts and sponge baffle mounds (Figure 6). They were noted only in the Loysburg and Snyder formations.

Unconformities

Although most of the formational boundaries are either unconformable or disconformable, none of these were apparent in the Oak Hall Quarry. However, local diastems exist in the form of hard grounds and in local, minor truncations of some footwall beds (e.g., of bench 3 ramp, north side). However, the latter could be difficult to distinguish from mesoscopic scale ramp faults.

Secondary Discontinuities/Features

Dissolution features: stylolites and cavities (caves and vugs)

Apart from scalloped solution surfaces exposed in upper benches near the sub-outcrop pinnacles, no open conduits were noted. A Br tracer test (Schmotzer *et al.*, 1973) confirmed the existence of a conduit linking the swallow hole in the floor of the old quarry to the spring near the asphalt plant. Diagenetic and tectonic dissolution is apparent in the common bedding stylolites (Figure 27).



Figure 27. Mega-stylolite subparallel to bedding exposed in Mt. Nittany roadcut. Up to 15 mm of truncation of beds with insoluble residue in the cusped dissolution interface (IMG 1997: 9/24/2014).

Cusps on the mega-stylolites have a lower aspect ratio than the millimeter-scale stylolites and transgress bedding (Figure 27 & 28). Amplitudes of up to 10 cm were noted. Insoluble residues consist mainly of clay minerals and kerogen with minor amounts of quartz and pyrite. A slightly elevated iridium content was detected in some stylolite residues.



Figure 28. Insoluble residue (black) on cusped mega-stylolite interface (IMG 2060: 10/5/2014).

A study of fluid inclusion in veins [bedding (BPV), strike (SV) and cross-fold (CFV)], and associated crack-seal veins in stylolites in the Tea Creek and Milroy strata exposed in the road cut, half a mile north of the quarry, yields initial trapping conditions of lithostatic pressure [$P \leq 180$ MPa (1.8 Kb)], temperature $\leq 267^\circ\text{C}$ and salinity of 23.4 % NaCl (Srivastava and Engelder, 1990). The strike and cross-fold sets presumably equate to J_1 and J_2 respectively, and the lithostatic load to a 5.4 km depth of burial. They conclude that the growth and development of Nittany Mountain Syncline can be tracked to the late CFV stryolitic veins (Figure 29) with trapping conditions of 20.5 % NaCl, $P \leq$ to 116 MPa, and $T \leq 179^\circ\text{C}$.

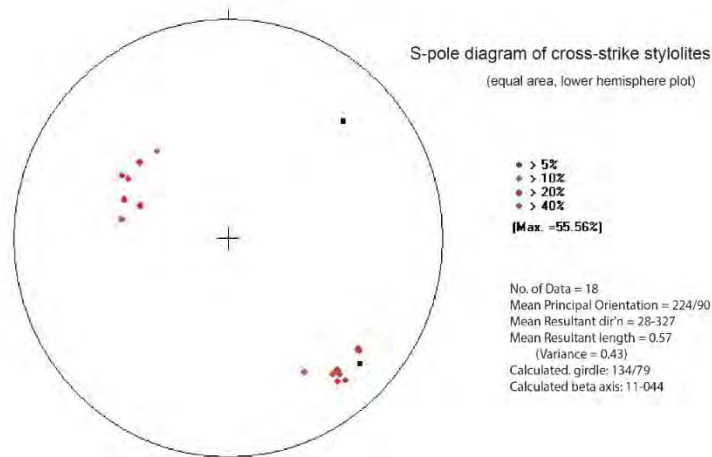


Figure 29. Orientation diagram of cross-strike stylolites

Secondary (superimposed) structural features:

These include joints and veins, faults (bedding, ramp and transverse), mesoscopic-scale folds and associated axial-plane cleavage. The joints are interpreted as mode 1 fractures, and these have been sorted by attitude into *strike joints* (J_1), *cross-strike or dip-plane joints* (J_2), and *other cross-strike joints* (J_x) regardless of age.

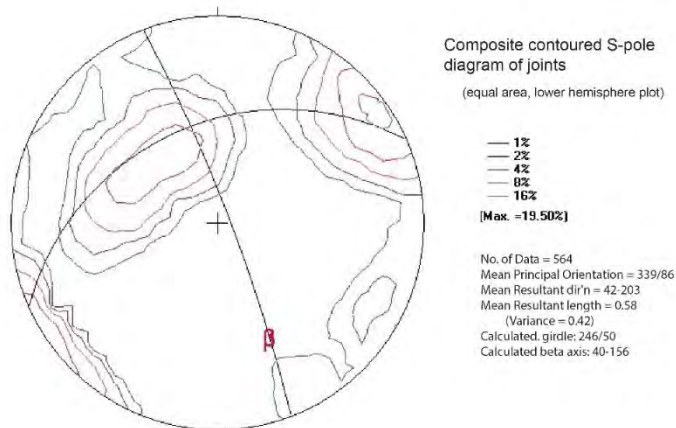


Figure 30. Orientation diagram showing distribution of all joints measured. The two girdles reflect the dominant strike directions of J_1 (065°) and J_2 sets (339°)

1. *Strike joints* are designated “J₁”. They form approximately perpendicular to bedding, and tend to be more widely spaced in the thicker beds. Typical separations are 12 – 30 inches in the rhythmites and 24 – 40 inches in more massive limestones. Strike joints impart a blocky aspect to many beds. Many of the surfaces are plumose and a few are decorated with insoluble residues. The dominant maximum (Figure 31) reflects a sampling bias for the dominantly NNW dipping beds exposed in the quarry on the SE limb of the Nittany Mountain Syncline. The secondary maximum represents less sampled-beds on the opposite limb, and the few outliers reflect the synclinal closure along the Mt. Nittany Expressway. The π girdle implies rotation of the J₁ planes and their development prior to the main folding episode. They are interpreted as early Alleghenian, with a hydraulic fracturing component.

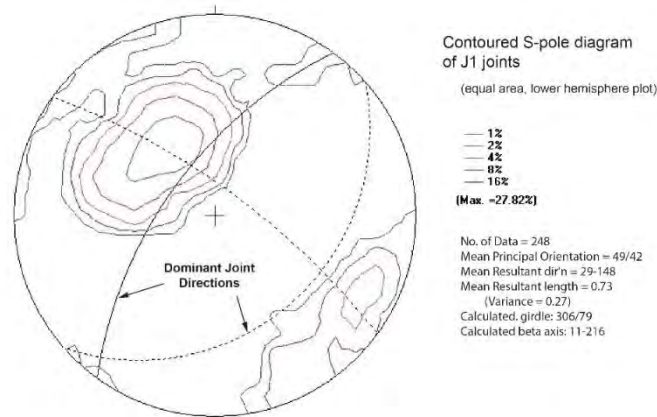


Figure 31. The bimodal distribution of J₁ joints in the orientation diagram reflects the pre-folding nature of the J₁ joints. Their mean orientation on the SE limb is 245°/52°, and on the NW limb 040°/70°.

2. *Cross-strike joints* “J₂” represent a steeply dipping, through-going master set, with a southwesterly strike (Figure 32). Spacing is typically 1-2 meters apart, but locally some more tightly spaced (centimeter) clusters were mapped. Plumose fracture patterns are preserved on some J₂ surfaces. All are tight; many are healed with secondary calcite. They are part of a regional system of joints that fans with the Appalachian orocline, formed during the late Alleghenian orogeny (Orkan and Voight, 1985).

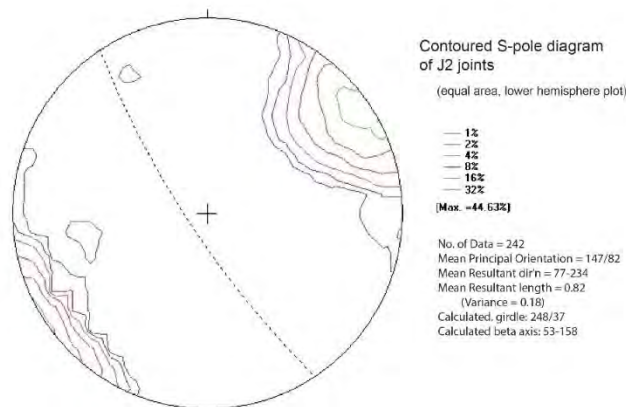


Figure 32. Orientation diagram of J₂ joints showing a strongly preferred attitude of 145°/82°.

3. Other *cross-strike joints* are broadly categorized as “ J_x ” (see Figure 33). They represent penetrative, but more random sets of *cross-strike joints*, whose regional significance are not understood. They are best seen in the long dip-slope exposures along the southern highwalls as a widely spaced (3-5 meters) set marked by the leached and/or stained halos marginal to the fracture. Many of this category J_x joints are decorated with secondary calcite, and a few have stylolite sutures. They are considered as late fracture phenomena.

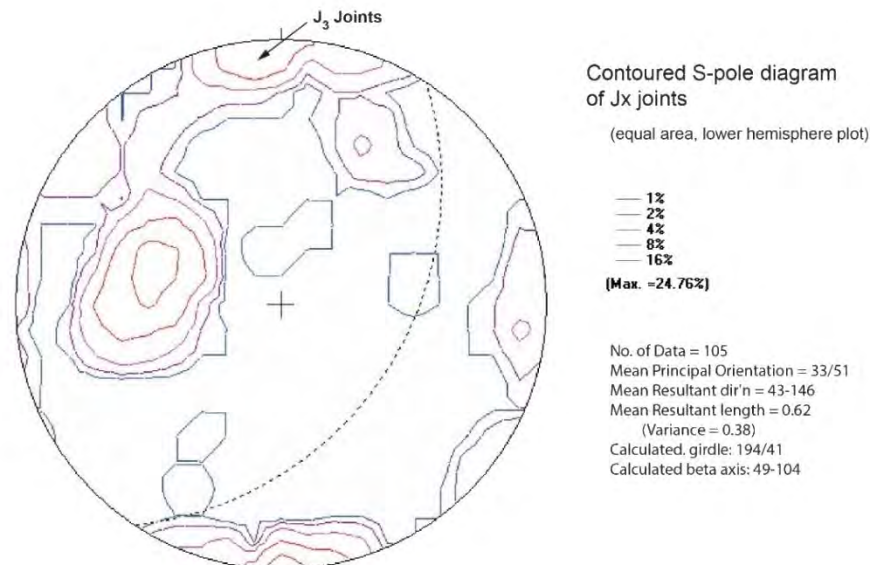


Figure 33. Orientation diagram of J_x joints with a preferred attitude of $020^\circ/40^\circ$.

4. *Neotectonic joints*. A relatively rare but distinct set of joints striking 080° (J_3 in Figure 33) is more apparent in the “seasoned” outcrops on the expressway than in the fresh cuts in the quarry. They are widely-spaced, steeply dipping, single or double fractures, and may be restricted in lateral and vertical continuity in the near surface regime. They tend to occur in the more massive carbonate strata, independent of the strike of bedding. These late-formed joints are classified as “neotectonic” (Hancock and Engelder, 1989; Srivastava and Engelder, 1990) because they propagate sub-parallel to the contemporary tectonic stress field.

Other secondary structural features include:

- a) *Stratabound Tension cracks* are common (Figure 34), particularly in the rhythmite, but their distribution is not uniform (Figure 12). Their lensoid shape, decimeter-scale length, steep dip in a strongly-preferred southeasterly attitude, open nature and distinctive-filling paragenesis (Figure 13) distinguish them from the through-going carbonate veins. The tension cracks are characteristically stratabound to the limestone interbeds in the rhythmite units, and have a geometric relationship to J_2 joints (cf., Figures 32 and 35). Well-formed white calcite crystals line walls of the cracks. Most exhibit overgrowths of pearl- to buff-colored “saddle” dolomite crystals and, in a few, doubly-terminated clear quartz crystals up to 2 cm long have grown in the center (Figures 13 and 19). Despite obvious fluid inclusions, no systematic study has been done on quarry samples. However, fluid inclusion studies from samples collected in the State College area (Orkan, 1985) yielded a range of trapping temperatures from $70^\circ - 227^\circ\text{C}$ (peaking at $100^\circ - 150^\circ\text{C}$). These are considered low, when compared to the regional values of $200^\circ - 205^\circ\text{C}$ and a burial depth of 6 - 9.5 km (LaCazette, 1991) for crack-seal veins in the Bald Eagle Formation. However, they are

consistent with a 150° – 225°C range for homogenization of methane-CO₂-rich inclusions in hydrothermal veins at Skytop (Mutti, 2006). They are inferred to be late Alleghenian in age. Some non-stratabound tension cracks are developed in a conjugate pattern around faults.

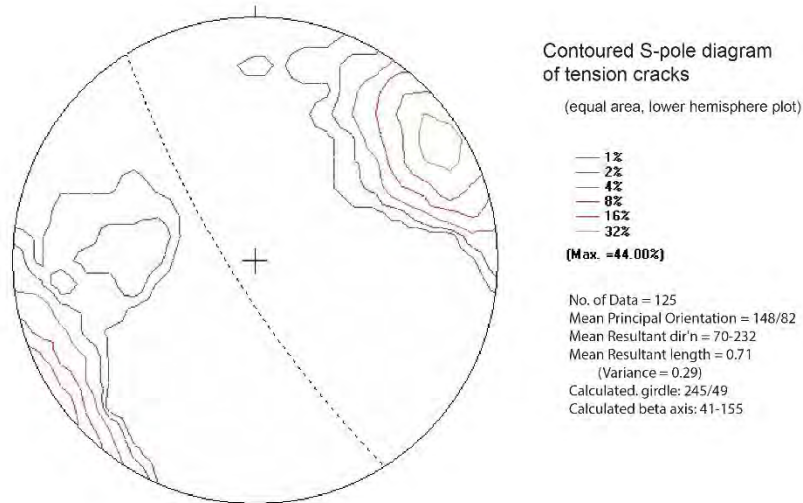


Figure 34. Orientation diagram of tension cracks. Their strongly preferred southeasterly orientation suggests a link to the formation of J₂ joints.

- b) The *carbonate veins* likewise, are steeply dipping and directional (Figure 35). They typically are thin (millimeters to centimeters) and through-going, and have a strong geometric relationship to J₂ joints (cf. Figures 31 and 36). A few carbonate veins are mapped parallel to bedding, and some in J₁ joints. Some may be associated with faults and most are inferred to be healed J₂ joints.

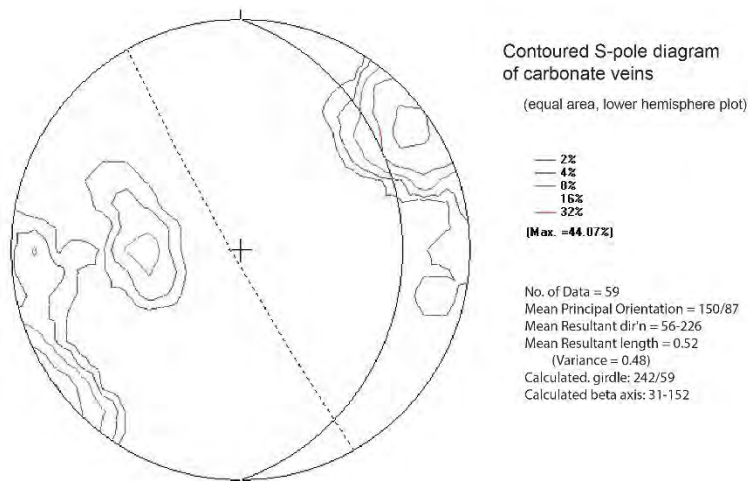


Figure 35. Orientation diagram of carbonate veins. Most are associated with south-southeast trending faults.

- c) *Boudins* were noted in some of the thinner (10 cm scale) limestone interbeds in the Upper Coburn Formation, particularly where adjacent argillaceous beds are approximately the same thickness. Necking is apparent co-linearly with J_2 joints and tension cracks. These boudins differ in shape, composition and distribution from the calcarenites and bioclastic nodules in the more massive limestone beds of the Rodman Member in the Nealmont Formation.
- d) *Faults*. Most bedding planes in thicker limestone strata exhibit jogged slickensided surfaces of secondary calcite. A reverse sense, indicated from the jogs, and slickenlines pitching approximately 78° to the west, suggests a flexural-slip origin for these *bedding faults*. These are apparent as the northeasterly striking planes on the orientation plot.

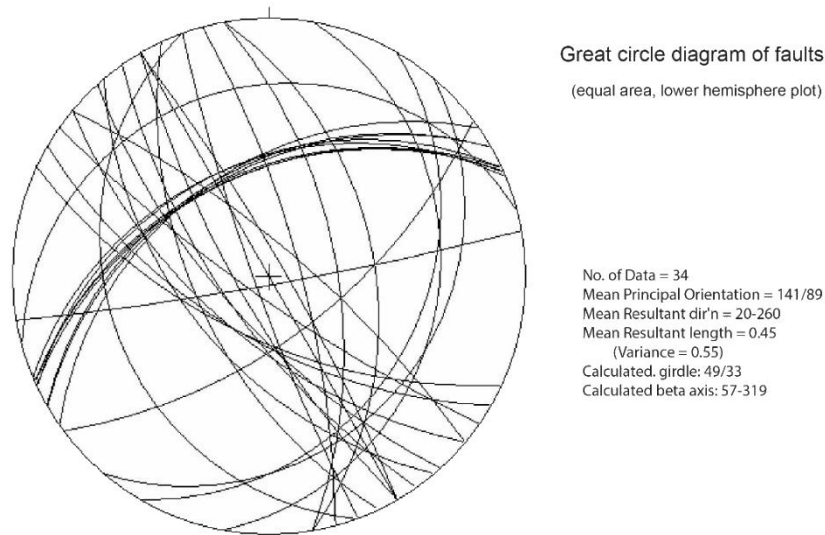


Figure 36. Orientation diagram of faults. The east-northeast trending group is flexural-slip bedding.

In contrast the *cross-strike faults* are relatively rare, exhibit a range of dips, and strike generally southeastward (Figure 35). Most of these occur in the Salona and Coburn rhythmites as meter-scale breaks with a left-lateral strike-slip component and a displacement of only tens of centimeters.

Only 4 mesoscopic-scale (tens to hundreds of meters) faults have been mapped. They tend to be healed with secondary calcite, dip steeply and strike to the south-southeast (see Figure 37). The best exposed of these is a fault that can be traced 500 feet across the quarry from the 7th-bench highwall in the Coburn rhythmites southeastwards to the 6th-bench southern highwall in the Snyder tidalites (Figure 25). A right lateral strike slip sense is inferred from warped shale interbeds at its distal end in the Coburn and an increasing juxtaposition of beds southeastward approximately 5 m into the Snyder. A right lateral displacement that increases southeastward from a few cm in the Coburn to up to 5 m in the Snyder is apparent. It is considered to be essentially a strike-slip fault.

Two mesoscopic-scale *ramp faults* are well exposed in the south-bound road-cut of Mt. Nittany Expressway, respectively 250 and 150 feet southeast of the Route 26 road sign. Both are located stratigraphically in Lower Salona rhythmites between the B-12 and B-14 bentonites, in the hinge

zone northwest of the Nittany Mountain Syncline axis. A north-northwesterly thrust motion is inferred, (Figure 24), with a ramp climb on the order of 2 meters. A number of low angle oblique slip reverse faults mapped in the pit probably represent more of these “layer parallel shortening” ramp faults.

- e) *Conjugate tension cracks and joints sets* (Figure 36) were recognized locally, mainly in the Coburn rhythmites. Their association with mapped cross-strike faults presents an opportunity for a kinematic interpretation, assuming that the perpendicular to the acute bisector is the direction of the maximum principal stress, at the time of the main cross-fault generation.

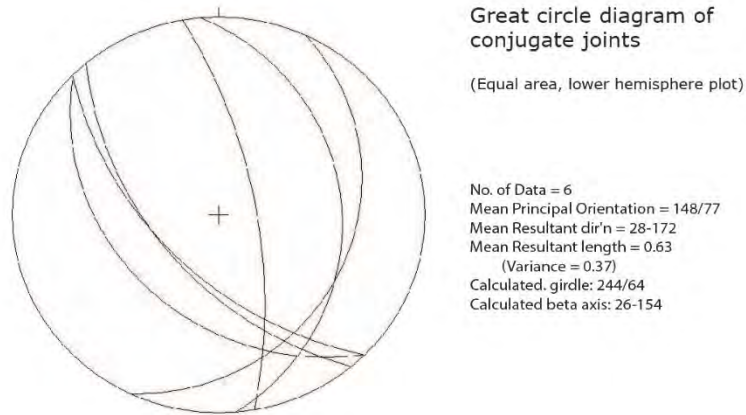


Figure 37. Orientation diagram of conjugate sets of joints/tension cracks. A plunge of approximately 60°/340° is inferred for the maximum principal stress axis σ_1 , at the time of the main cross-fault generation.

- f) *Cleavage*. A cleavage is developed in the argillaceous bed of the Upper Coburn rhythmites and in the carbonaceous shales of the Antes Formation.

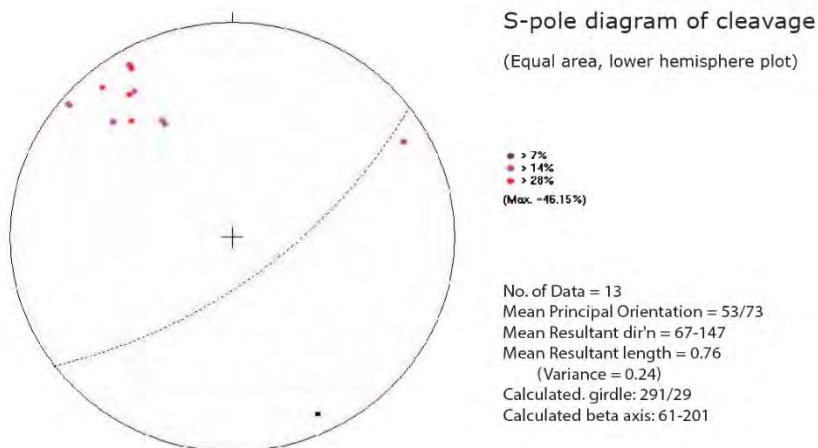


Figure 38. Orientation diagram of cleavage.

References

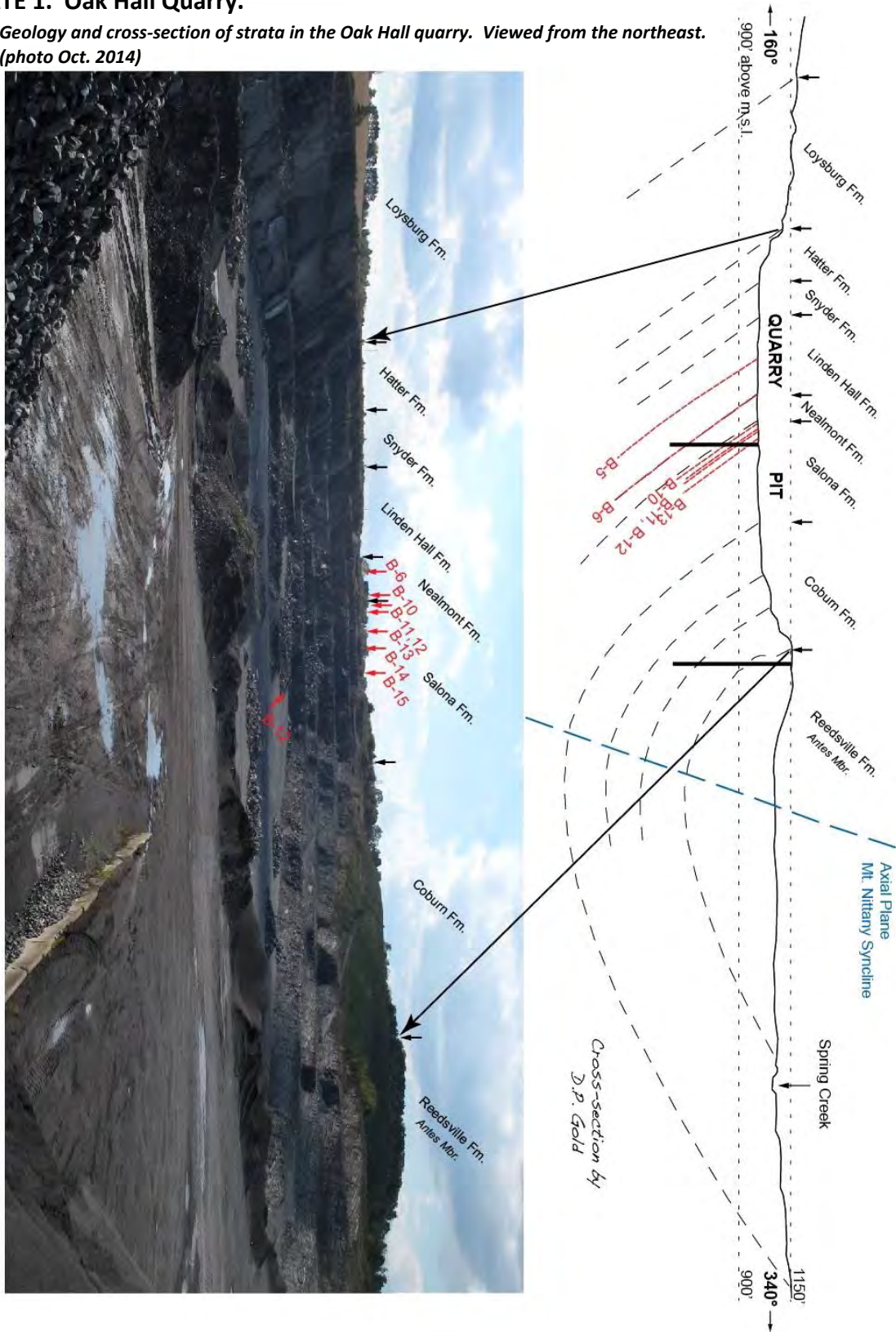
- Berkheiser, S.W., and Cullen-Lollis, J., 1986. Stop 1. Union Furnace Section: Stratigraphy and sedimentology: in Sevon, W.D, ed., Selected geology of Bedford and Huntingdon Counties. Guidebook, 51st Annual Field Conference of Pennsylvania Geologists, Huntingdon, PA. p. 111-119.
- Bezilla, M., and Rudnicki, J., 2007. Rails to Penn State; the story of the Bellefonte Central. Stackpole Books Pub., 310 p.
- Butts, C. and Moore, E.S., 1936. Geology and Mineral Resources of the Bellefonte Quadrangle, Pennsylvania. U.S. Geological Survey Bulletin 855, 111 p.
- THE CAVES OF CENTRE COUNTY, PA. 1979. Bull 11 of Mid- Appalachian Region of the National Speleological Society. Compiled and edited by G.C. Dayton and W.B. White, 126 p.
- Chafetz, H.S., 1969. Carbonates of the Lower and Middle Ordovician in central Pennsylvania: Pennsylvania Geological Survey Bulletin G58, 39 p.
- Clark, J.H., 1965. The Geology of the Ordovician Carbonate Formations in State College Area, Pennsylvania, and their relationship its relationship to the general occurrence and movement of ground water. Unpub. M.S. Thesis, Penn State University, 114 p.
- Cullen-Lollis, J., and Huff, W.D., 1986. Correlation of Champlainian (Middle Ordovician) K-bentonite beds in central Pennsylvania based on chemical fingerprinting. Jour. Geol., v. 94, p. 865-874.
- Doden, A.G., Gold, D.P., Mathur, R., and Jensen, L.A., 2010, Bedrock Geologic Map of the State College Quadrangle, Centre County, Pennsylvania. Open-File Report. 1:24,000 scale map.
- Doden, A.G., Gold, D.P., Mathur, R., and Jensen, L.A., 2011 and in progress. Bedrock Geology of the State College Quadrangle, Centre County, Pennsylvania. DCNR, Open File Report.
- Engelder, T., and Geiser, P., 1980. On the use of regional joint sets as trajectories of paleostress fields during the development of the Appalachian Plateau, New York. Jour. Geophysical Res., v.85, p 6319-6341.
- Engelder, T., 2000. Geology Field Trips and Laboratory Exercises: an Introduction to the Geology of the Nittany Valley. G.Sc 20 Manual, Department of Geosciences. The Pennsylvania State University, 124 p.
- Flemings, P.B., and Grotzinger, J.P., 1996. STRATA: Freeware for analyzing classic stratigraphic problems. GSA Today, v. 6, No 12, p. 1-7.
- Folk, R.F., 1946. Composition of the Insoluble Residues from the limestones at Oak Hall Quarry, p. 10-12 in Guidebook for 12th Annual Field Conference of Pennsylvania Geologists, From the Cambrian to the Silurian near State College and Tyrone, Ed. P.D. Krynine. Pa. Geol. Survey.
- Gardiner-Kuserk, M.A.1989. Cyclic Sedimentation Patterns in the Middle Ordovician Trenton Group of Central Pennsylvania. Chapter 5, P 55-76, in THE TRENTON GROUP (UPPER ORDOVICIAN SERIES) OF EASTERN NORTH AMERICA; Ed. B.D. Keith. Amer. Assoc. Petrol. Geol. Series in Geology, #29.
- Geiser, P., and Engelder, T., 1983. The distribution of layer parallel shortening fabrics in the Appalachian foreland of New York and Pennsylvania: Evidence for two non-coaxial phases of the Allegheny orogeny. In Contributions to the Tectonics and Geophysics of Mountain Chains, Geol. Soc. America, Memoir 158, p. 161-176.
- Gold, D.P., Alexander, S.S., and Parizek, R.R., 1973. Application of Remote Sensing to Natural Resources and Environmental Problems in Pennsylvania. Earth & Mineral Sciences Bulletin, Pennsylvania State University, v. 43, No 7, p. 49-53.
- Gold, D.P., and Doden. 2015. Geology of the Oak Hall Quarry Property, Centre County, Pennsylvania. Permit Application Report for Hanson Aggregates, LLC., to PADEP 118 p.
- Handcock, P.L., and Engelder, T., 1989. Geological Society of America, Bull. V. 102, p. 116-128.
- Horowitz, D.H., 1965. Petrology of the Upper Ordovician and Lower Silurian rocks in the central Appalachians. Ph.D. Thesis. Penn State University, 221 p.
- Hoskins, D.M., and Root, S.I., (1976), State College Quadrangle, (p.536) in the Atlas of Preliminary Geologic Quadrangle Maps of Pennsylvania. Map 61, 1981. Eds. Berg, T.M., and Dodge, C.M., Pennsylvania Geological Survey.
- Hunter, P.M., 1977. The environmental geology of the Pine Grove Mills-Stormstown area, central Pennsylvania, with emphasis on the bedrock geology and ground water resources. Unpub. M.S. thesis, Penn State University.
- Kolata, D.R., Huff, W.D., and Bergstrom, S.M., 1996. Ordovician K-bentonites of Eastern North America. Geological Society of America, Special Paper # 313.
- LaCazette, A.J., 1991. Natural hydraulic fracturing in the Bald Eagle Sandstone in central Pennsylvania and the Ithaca Siltstone at Watkins Glen, New York. Unpub. Ph.D. Thesis, Penn State University, 225 p.
- Landon, R.A., 1961. Geology of the Gatesburg Formation in the Bellefonte quadrangle, Pennsylvania, and its relationship to the general occurrence and movement of ground water. Unpub. M.S. Thesis, Penn State University, 88 p.

- Laughrey, C.D., Kostelnik, J., Gold, D.P., Doden, A.G., and Harper, J.A., 2004. Trenton and Black River Carbonates in the Union Furnace Area of Blair and Huntingdon Counties, Pennsylvania. Field Trip Guidebook, Pittsburgh Assoc. Petroleum Geologists. Pub. Pa. Geol. Surv. 81 p.
- Lesley, J.P., and d'Inwilliers, 1883. Geological Map of Centre County. 2nd Geological Survey of Pennsylvania.
- Mathur, R., Gold, D.P., and Doden, A.G., 2011. U-Pb ages from zircons in the Middle Ordovician bentonite and bentonite-like horizons in central Pennsylvania. Abstract, Northeastern and North-central section meeting of Geological Society of America, v. 43, no.1, p.?
- Meiser, E.W., Jr., 1971. The geology and water resources of the Bellefonte-Mingoville area, Pennsylvania. Unpub. M.S. thesis, Penn State University.
- Meiser & Earl, Inc. 2005. Ground-Water Elevation Contour Map of University Park Campus and State College Borough Area. Scale 1:12,000.
- Myers, D., 1979. CE 36 Oak Hall Cave; in THE CAVES OF CENTRE COUNTY, PA. Bull 11 of Mid-Appalachian Region of the National Speleological Society. Compiled and edited by G.C. Dayton and W.B. White, 126 p.
- Mutti, L.J., 2006, (p. 100-102) in Sulfide occurrences in central Pennsylvania. Field Trip Guidebook, 41st Annual Meeting of Northeast Section of Geological Society of America, A.P. de Wet, ed. 128 p.
- Nickelsen, R.P., 1963. In Cate, A., ed., p. 13-29; Tectonics and Cambrian-Ordovician Stratigraphy, Central Pennsylvania. Guidebook Pittsburg Geol. Soc. /Appalachian Geol. Soc. Sept., 1963, 129 p.
- Orkan, N.I., and Voight, B., 1985. Regional joint evolution in the Valley and Ridge Province of Pennsylvania in relation to the Allegheny orogeny. Guidebook, 50th Annual Field Conference of Pennsylvania Geologists. PA Geol. Survey, Harrisburg, p. 144-163.
- Orkan, N.I., 1986. Regional joint evolution and paleothermometry-barometry from fluid inclusions in the Valley and Ridge Province of Pennsylvania in relation to the Allegheny orogeny. Unpub. M.S. Thesis, Penn State University, 192 p.
- Parizek, R.R., and Filley, T.H., 1982. Centre Region Aquifer Study, Part I (Abstract and Maps from Definitions of Aquifers and Confining Beds within the Centre Region, Centre County, Pennsylvania). Centre Regional Planning Commission.
- Parizek, R.R., White, W.B., and Langmuir, D., 1971. Hydrogeology and geochemistry of folded and faulted rocks of the central Appalachian type and related land use problems. Penn State University: Earth and Mineral Sciences Experiment Station, Circular 82, 181 p.
- Parizek, R.R., White, W.B., 1985. Application of Quaternary and Tertiary Geological Factors to Environmental Problems in Central Pennsylvania. Field Trip # 3, Guidebook, 50th Annual Field Conference of Pennsylvania Geologists. PA Geol. Survey, Harrisburg, p. 63- 119.
- Parizek, R.R., and Gold, D.P., 2014. Fracture Traces and Lineaments: Examples and Applications. For Fracture Traces and Lineaments Short Course. National Ground Water Association. 105 p.
- Parizek, R.R., and Gold, D.P., 2014. Exercise 4, on Nittany Valley, Central Pennsylvania, in the Manual for Short Course, "Fracture Traces and Lineaments Analysis". National Ground Water Association, 754 p.
- Rauch, H.W., and White, W.B., 1970. Lithologic controls on the development of solution porosity in carbonate aquifers. Water Resources Research, v. 6, No. 4 p. 1175-1192.
- Rones, M., 1969. A lithostratigraphic, petrographic, and chemical investigation of the Lower Middle Ordovician carbonate rocks in central Pennsylvania. PA Geol. Survey Bulletin G53, 224 p.
- Schmotzer, J.E., Jester, W.A., and Parizek, R.R., 1973. Groundwater Tracing with Post Sampling Activation Analysis. Jour. of Hydrology, v. 20, p. 217-236.
- Sicree, A.A., Gold, D.P., and Doden, A.G., 2011. Diverse origins for economic minerals in central Pennsylvania. Abstract, Northeastern and North-central section meeting of Geological Society of America, v. 43, no.1, p.?
- Srivastava, D.C., and Engelder, T., 1990. Crack-propagation sequence and pore-fluid conditions during fault-bend folding in the Appalachian Valley and Ridge, central Pennsylvania. Geological Society of America, Bull. V. 102, p. 116-128.
- Taber, T.T., 1987. Railroads of Pennsylvania: Encyclopedia and Atlas. Type written script, 507 p.
- Taylor, L.E., 1997. Water Budget for Spring Creek Basin. Publication No. 184, for Centre Regional Planning Agency. Text and Water table Map
- Turner, F.J., and Weiss, L. E., 1963. Structural Analysis of Metamorphic Tectonites. McGraw-Hill Book Co., New York, 545 p.
- Thompson, A.M., 1999. Ordovician. Chapter 5 in GEOLOGY OF PENNSYLVANIA. C.H. Schultz, Ed. Pennsylvania Geological Survey, Special Publication # 1.
- Thompson, R.R., 1963. Lithostratigraphy of the Middle Ordovician Salona and Coburn Formations in Central Pennsylvania. General Geology Report G 38. Pa Geol. Surv. 154 p.

Wagner, W.R., 1966. Stratigraphy of the Cambrian to Middle Ordovician Rocks of Central and Western Pennsylvania. General Geology Report G 49. Pa Geol. Surv. 156 p.
 Wilson, J.L., 1952. Upper Cambrian Stratigraphy in the Central Appalachians. Bull. Geol. Soc. Amer. v. 63, pp. 265-322.

PLATE 1. Oak Hall Quarry.

*Geology and cross-section of strata in the Oak Hall quarry. Viewed from the northeast.
 (photo Oct. 2014)*



LOWER AND MIDDLE ORDOVICIAN STRATIGRAPHY AND STRUCTURE ALONG THE MT. NITTANY EXPRESSWAY AT STATE COLLEGE, PENNSYLVANIA

CHARLES E. MILLER, JR.¹ AND DAVID (DUFF) GOLD²

D.ED., RETIRED, STATE COLLEGE, PA (CH.TRIASSIC@GMAIL.COM) EMERITUS PROFESSOR OF GEOLOGY, DEPARTMENT OF GEOSCIENCES, PENN STATE UNIVERSITY, UNIVERSITY PARK, PA (GOLD@EMS.PSU.EDU)

Preamble

Construction on the Mt. Nittany Expressway began in the mid-1970s. The roadbed was laid in 1985 and this section opened in 1986. More than three decades of weathering of fresh bedrock outcrop in the roadcut has accentuated not only color differences but also subtle internal bedforms and fossils. This paper focuses on sections of Loysburg and upper Bellefonte formations exposed in the roadcuts.



Figure 1. Roadcut along Mt Nittany Expressway exposes multiple layers of limestone (dark) and dolostone (light) in the lowermost Milroy member of the Loysburg. Do they represent shallowing upward carbonate cycles? Visit stations DD – FF to discuss.

Introduction

The setting is on the 2nd order Nittany Mountain Syncline in a breached 1st order anticlinorium in the Ridge and Valley Physiographic Province. Mt. Nittany Expressway traverses across this inclined syncline (Figure 2), exposing Lower Ordovician carbonates on both limbs, and Middle Ordovician carbonates of the Salona, Nealmont and Linden Hall formations in the hinge zone. The syncline is characterized as essentially concentric and open, plunging 10°/057° and an inclined axial plane (055°/70°). The Expressway skirts around the village of Oak Hall and west of a large quarry (Figure 2), with the same name, operated by Hanson Aggregates Pennsylvania LLC. The trace of the axial plane lies on the Hanson Property. The southeast limb of the syncline is exposed in the Oak Hall Quarry, where approximately 1200 feet of Middle Ordovician units from the Loysburg to the Coburn have been excavated for aggregate.

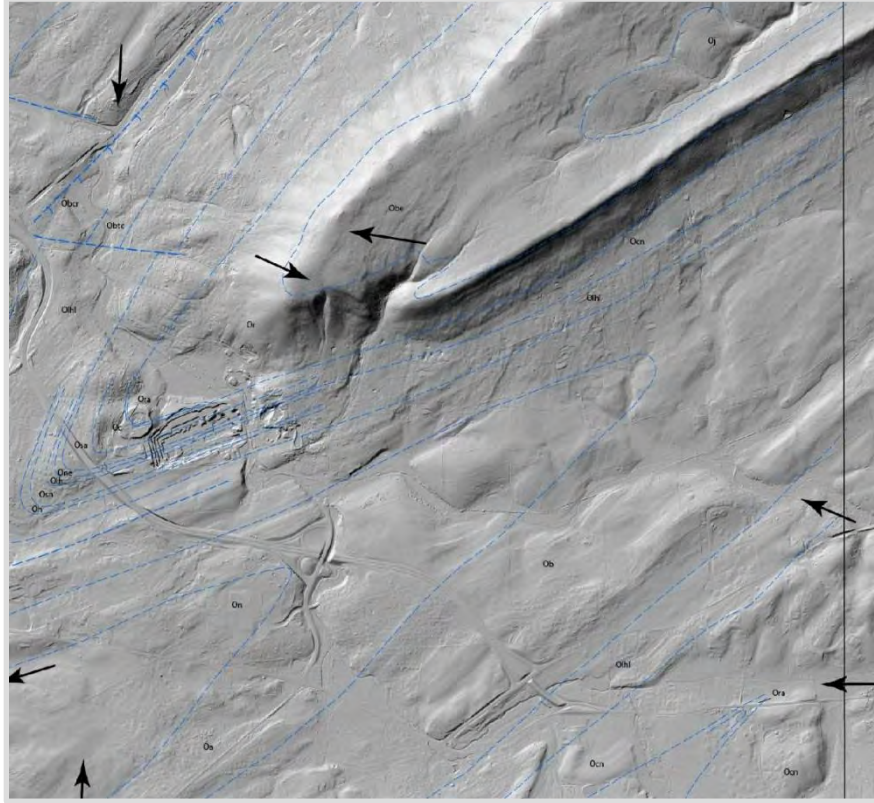


Figure 2. Lidar Image of Nittany Syncline and Mt. Nittany Expressway

The lower Loysburg has 94.4 feet of section exposed in the Nittany expressway roadcuts (Tabulated in the Roadlog – Stop 3, Day 2). A traverse across bench 4 in Oak Hall Quarry during the summer 2014 records the upper 220 feet of the Loysburg lithologies and includes approximately 30 feet of the Clover Member. This measured section produced a stratigraphic column shown in Figure 3. A total thickness for the Loysburg is estimated as 400 feet from a regional cross-section (Gold and Doden, 2015). The Tea Creek, Dale Summit, and upper Coffee Run members of the Bellefonte are well-exposed in the northwestern limb of Nittany Mountain Syncline. A continuous section that includes the Dale Summit and Coffee Run members, exposed in the roadcut along the southern end of the Expressway was not included in this study.

Stratigraphy

Bellefonte Formation

Initially, the uppermost formation of the Beekmantown Group was assigned to the “Bellefonte Dolomite.” At the type section in Bellefonte (Butts and Moore, 1936), it was 2231 feet thick. Rones (in Swartz, 1955) modified this to exclude the upper limestone-bearing section of approximately 300 feet currently known as the Loysburg Formation (Wagner, 1966). The roadcut near the Elmwood Street overpass (stop 3 in road log) exposes the upper 194 feet of the Bellefonte Formation. Lithology is predominantly dololomite with shale interbeds, non-algal laminites, a six-foot sandstone layer, chert nodules, and bedded, commonly discontinuous, chert layers. Some shale interbeds are up to 4-6 inches thick.

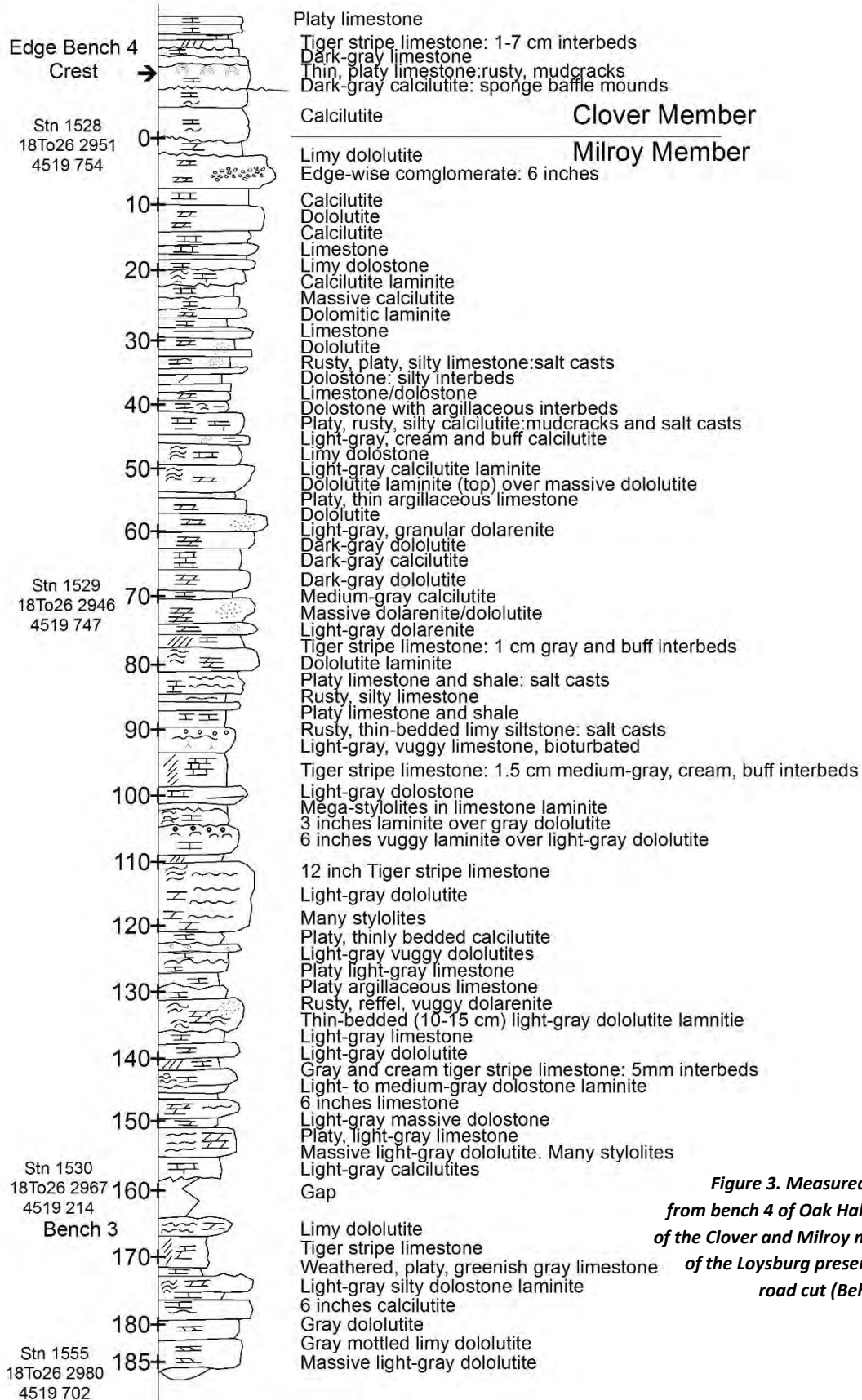


Figure 3. Measured section from bench 4 of Oak Hall Quarry of the Clover and Milroy members of the Loysburg present in this road cut (Behr, 2017)

Variants of the dolostones include: dololomite, doloarenite, and dololomite laminate. Symmetrical and asymmetrical stylolites are common, including mega-stylolites (inches high amplitude, and feet long wave-length). Open vugs, up to 11.8 inches across length, appear throughout this exposure although most are in the upper half. Some other sedimentological features include mudcracks, hardgrounds, cross stratification, erosion channels, soft-sediment deformation features, clastic dikes and sills, intraformational deposits, bioturbation casts, and oxidized pyrite nodules. Fossil diversity at this stop is low. A few stromatolites are the only macrofossils.

Dololomites are the predominant lithology. These fine-grained dolomitic muds reflect low-energy, quiet water such as in a tidal-flat or shallow subtidal depositional setting. Storms occasionally punctuated this quiet setting, depositing quartz sand and mud. The former produced doloarenites or quartz sand lenses, as in the Dale Summit Member. Mud was deposited as shale, shaly interbeds, and argillaceous limestone. At other times, the depositional setting was subjected to subtle changes in environmental condition that affected the chemistry of the sediments deposited.

Coffee Run Member

Forty-two feet of the Coffee Run are exposed here. This lowest member is like the Tea Creek in that both are predominantly dolostone. The Coffee Run Member contains fine- to very fine-textured dololomites interbedded with medium- to coarse-crystalline doloarenites. This member is, on the average, more thinly bedded than the Tea Creek. In addition, black chert in this member further distinguishes it from the Tea Creek (Wagner, 1966). Stratabound vugs (up to six inches) are present, but less abundant than in the Tea Creek. Fossil diversity is low. The only macrofossils are rare and dispersed stromatolites. A range of bedding-parallel stylolites are present, and these include symmetrical and asymmetrical types. The mega-stylolites are conspicuous, with amplitudes of up to four inches. Other sedimentological features include insoluble residues, arenaceous lenses, cross-stratification, drainage channels, clastic sills and dikes, mudcracks, intraformational clasts, and imbricate flow fabric.

Dale Summit Member

The Dale Summit is a relatively thin, gritty sandy dolostone to quartz sandstone unit separating the lower and upper dolostone members. It was referred to as the Sandstone Member of the Bellefonte Dolomite (Butts and Moore, 1936) and as the Bellefonte Sandstone (Krynine, 1941). In the Mt. Nittany Expressway road-cuts, the Dale Summit ranges from three feet on the northwest limb to eight feet on the southeast limb of the Nittany Mountain Syncline. Krynine (1946) reports a thickness of 14 feet at other Central Pennsylvania locations, and as much as 50 feet on the ridge northwest of the Mountain View Country Club and south of Linden Hall (Doden and Gold, 2011).

This sandstone is a significant lithologic break in the Bellefonte – and, therefore, in the approximate 7000 feet of Cambro-Ordovician carbonates of Central Pennsylvania. Where deposited, this influx of sand was prodigious enough to temporarily stop local carbonate deposition. It consists of rounded pure quartz, and sub-angular gravel of dolomite and chert pebbles, cemented with siliceous (secondary quartz) and dolomite cement (Butts and Moore, 1936; Krynine, 1946). Krynine and Tuttle (1941) interpret the Dale Summit as a tectonic sandstone, derived from the upper sandy member of the Gatesburg exposed near present-day Lake Erie or in southwest Ontario (Wagner,

1966). Tracing Dale Summit sands to those in the Gatesburg is based on petrographic observations such as similarities in type and percentage of tourmaline. Heterogeneity of composition, abrupt lithologic changes, and angularity of dolomite pebbles in the Dale Summit suggest a relatively short transport distance, of the order of 50-100 miles (Krynine, 1946; Krynine, 1960). Alternatively, the Dale Summit may represent sand weathered from the southern edge of the Canadian Shield and washed out into the shallow carbonate sea down into Pennsylvania.

Tea Creek Member

The complete section measuring 145 feet of the Tea Creek is exposed in the roadcut. It is a microcrystalline to very fine-textured dolostone, locally lithographic or sublithographic, with conchoidal fracture, and rare thin, calcarenite (grainstone) layers and laminites. It differs from the Coffee Run in the absence of chert, and abundance of macro vugs and mega-stylolites (symmetrical and asymmetrical). Other sedimentological and structural features include vugs, stylolites, plumose fractures, hardgrounds, bioturbation fabric, intraformational clasts, and pyrite nodules. The top of this member is taken as the black shale bed 21 inches below the thick “tiger stripe” limestone bed near the base of the Loysburg (Figure 4), at Station FF in the Road Log.

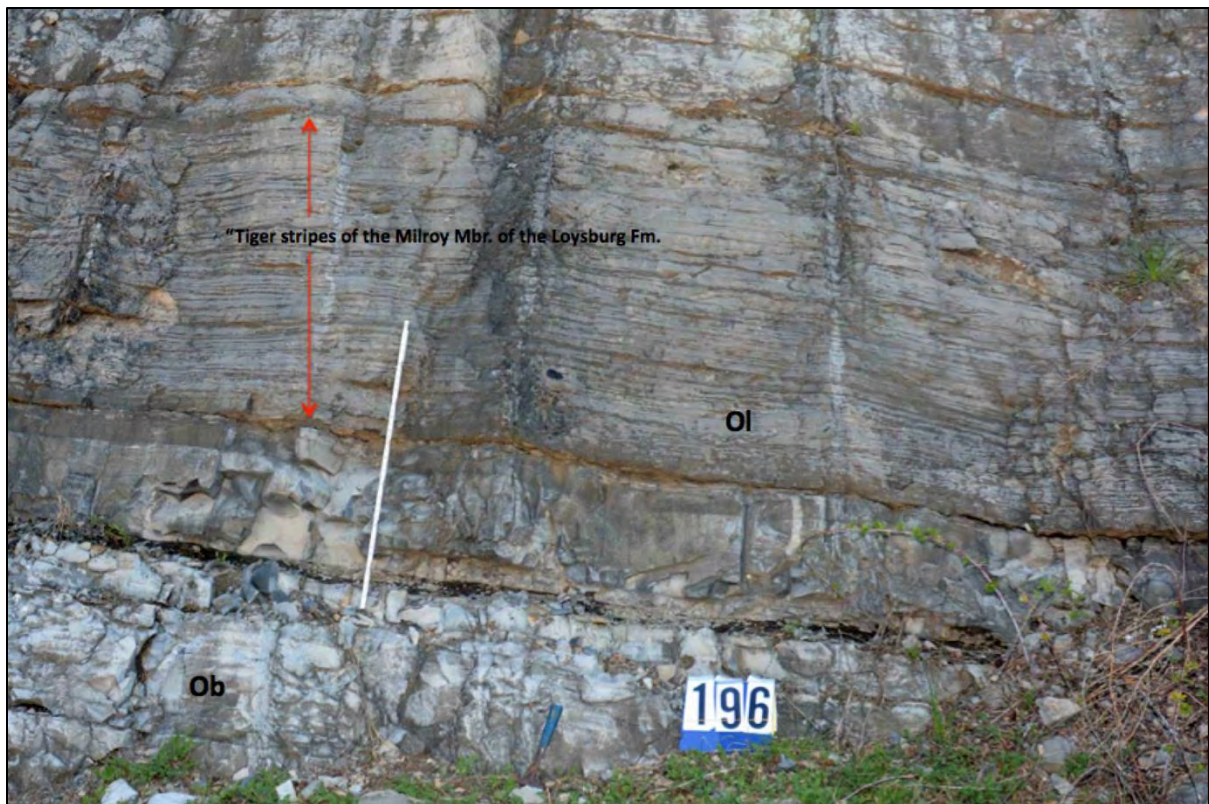


Figure 4. Contact of the Bellefonte Dolomite and Loysburg Formation at Station FF of the Road Log. A distinguishing lithological feature of the lowermost Loysburg is the presence of “tiger stripes” (Kay, 1944). These are marker beds for this stratigraphic interval.

Hardgrounds

A hardground is a syn-sedimentarily lithified seafloor, formed as carbonate cement precipitates in situ in primary pore spaces. Many are formed subaqueously at or near the sediment-water interface and form under low sedimentation rates (Bathurst, 1971). They are hard substrates in a soft-sediment sea bottom (Brett and Liddell, 1978). The hard surfaces become substrates for encrusting marine organisms, such as bryozoans, echinoderms, and sponges. The diverse fossils provide paleoecological information of a localized depositional setting. Other characterizing features include borings of organisms and discoloration from iron oxide or other minerals. Figures 5 and 6 show hardgrounds at Station OO in the Tea Creek Member of the Bellefonte.



Figure 5. Hardgrounds in Tea Creek Member of the Bellefonte. (1) Hardground surfaces. (2) Infauna burrows. Station OO.

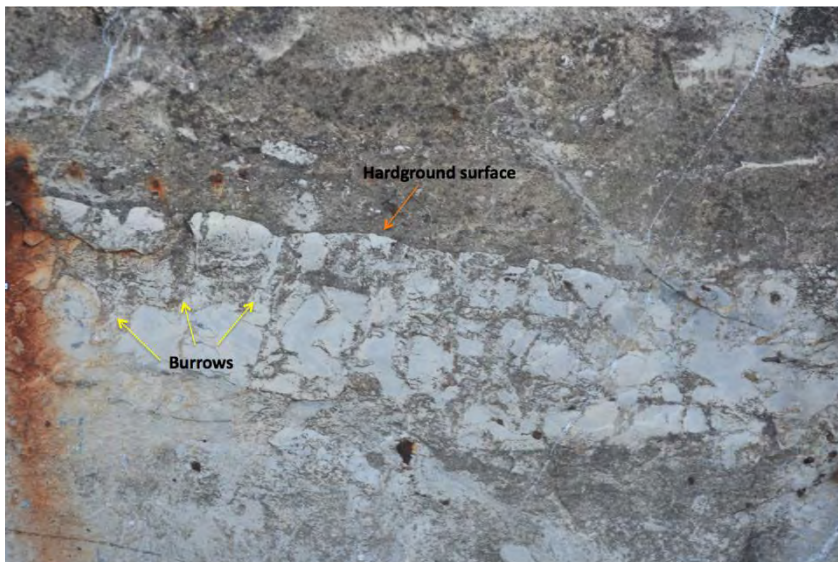


Figure 6. Hardgrounds in the Tea Creek Member of the Bellefonte. These are located 1-2 feet to the right of roadcut section shown in Figure 5. Orange arrow = hardground surface. Yellow arrows = infauna burrows. Note rusty stain from weathered pyrite. Station OO.

Drainage Channels

Several erosion troughs (Figure 7, Station PP of the Road Log) and (Figure 8, Station RR of Road Log) are identified in the Bellefonte at this stop. Tidal flats are commonly replete with stream or drainage run-off channels, usually of an ephemeral nature.



Figure 7. Erosion trough in the Bellefonte Dolomite at Station PP.



Figure 8. Erosion trough in the Bellefonte Dolomite at Station RR.

Clastic Dikes and Sills

Presence of clastic dikes and sills on a cm-scale were observed in some beds. These are interpreted as rearrangement and escape conduits in zones of trapped pore fluids.

Figure 9 (Station UU of Road Log) shows a breccia zone with numerous clastic dikes and sills in dololomite of the Coffee Run. There are many synonyms for these clastic features such as clastic

intrusion, sandstone dike, and soft-sediment deformation. The largest dike (Figure 9) is 4.3 inches tall and 0.75 inches wide. It is composed of sandy granular doloarenite, distinguishing it from the surrounding, lighter-colored dololutite. The limited range of these clastic dikes and absence of bedding contortions suggests a relatively low pore pressure regime. Folk (1952) describes contorted beds/soft-sediment deformation in the Bellefonte.



Figure 9. Clastic dikes and sills in a high pore-pressure layer. Coffee Run Member of the Bellefonte. (1) Clastic dike 4.3 inches tall and 0.75 inches wide. (2) Dololutite. (3) Black chert. (4) Doloarenite. (5) Clastic sills. (6) Vug. The pen is 5.5 inches in length. Station UU.



Figure 10. Faulted black chert in the Coffee Run Member of the Bellefonte Dolomite. Length of portion of pen is 1.8 inches. Station TT.

Loysburg Formation

Overlying the Bellefonte is the Loysburg Formation, sub-divided into the Milroy (lower) and Clover (upper) members (Figure 3). The former is approximately 300 feet thick at Bellefonte (Rones, 1955; 1969) but only the bottom 93 feet crops out in this roadcut. The Milroy consists mostly of alternating and intercalating limestone and dolostone, transitioning into dominantly limestone in the Clover (exposed in the quarry). The dominant lithofacies at this stop is dololutite. Variants include: dololutite laminites, argillaceous dololutite, and doloarenite (dolostone grainstone). Other lithofacies include: limestone, shale, silty shale, and calcarenite. There is a greater range in bed thickness and variety of lithologies in the Loysburg than in the Bellefonte.

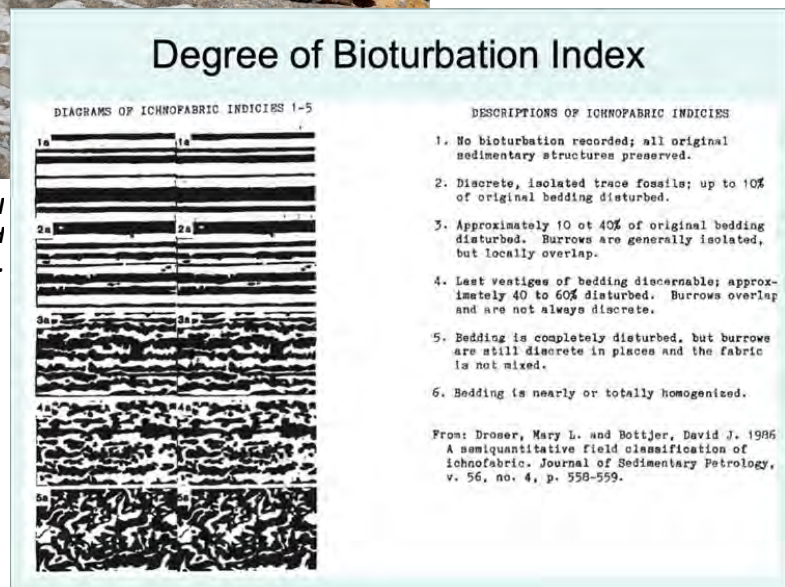
Fossil diversity is low. Hemispherical (SH) stromatolites (Logan *et al.*, 1964) are the only macrofossils. Some other stratigraphic features include stylolites with insoluble residues, intraformational/rip-up clasts, stratabound vugs, mudcracks, plumose fractures, disconformities, and an unusual “ribbon rock” referred to as a “tiger stripe”. Stylolites are common. They are distinguished by attitude as bedding-parallel (load compaction), dip normal, and cross-strike (tectonic) structures. The former are well developed and conspicuous, suggesting their dissolution of mainly limestone beds. These features are discussed in more detail in later sections.

Tiger Stripe beds



A distinctive lithofacies in the Milroy are the “Tiger Stripes” beds (Kay, 1944). These consist of alternating thin beds of medium-gray (N5), micritic limestone and pale-yellow brown (10YR 6/2) granular, dolomitic limestone (Figures 4, 11, and 12). They are

Figure 11. Rearrangement fabric in basal tiger stripe bed at Station FF (top): compared to “Degree of Bioturbation Index” (right). The pen is 6.5 inches long. sufficiently characteristic for the Milroy to be referred to as the “Tiger-striped Member” (Chafetz, 1969). Some exhibit a “picket fence” habit with bioturbation ichnofabric patterns (Figure 11). In many “tiger stripes,” only the last vestiges of



bedding are discernible while a few, often incomplete burrows are recognizable. For some “tiger stripes,” bioturbation is nearly ubiquitous. When compared to the “Degree of Bioturbation Index” of Droser and Bottjer (1986; Figure 11), indices of four and five are identified.

In a typical sample (TS-2, Figure 12 and Table 1) from the basal Tiger Stripe bed (# 64 in Appendix 1), the striped pattern consists of alternating thin beds of medium light gray (N6) to light, olive gray (5Y 6/1) and interbedded thin limestone and Mg-limestone (dolostone) on a 0.4-0.8-inch scale. These layers weather differentially to stand out in relief in a distinctive buff/yellow and olive-gray banded pattern that appears to be controlled by grain size and chemistry. Another sample (TS-1, Figure 12 and Table 1) from higher in the section has three components in thinner interbeds on a 0.8- to 3.9-inch scale. They are a dove-gray micritic limestone, a medium light-gray bioclastic limestone, and a cream-colored argillaceous Mg-enriched limy mudstone.



Figure 12. Typical sample of the “Tiger Stripes” in the lowermost Milroy Member. Cut specimen is on the left and a typical unweathered surface is on the right. Circles represent samples for analyses.

Table 1. Tiger strip rock, composition of layers

TABLE X. Tiger stripe rock, composition of layers																
Sam	Layer/date	CaO	MgO	K2O	SiO2	Al2O3	FeO	TiO2	S	SUM	CaO/MgO	Mg/Ca	Color	Color	Lithology	Texture/Comments
T-S 1 7/16/16																
	dark	60.9	1.49	0.38	3.44	0.73	0.13	0.025	2.02	69.08	40.8	max	N6	5Y 6/1	Limestone plus gypsum?	Dense, micritic and stands out in relief
	light	40.5	6.48	1.64	21.7	5.34	0.7	0.190	1.69	78.30	6.3	0.13	5Y 8/1	5Y 7/2	Argillaceous Mg-limestone	Coarser grained; weathers back
	coarse	59	2.36	0.35	8.90	0.98	0.17	0.088	0.76	72.60	25.0	0.03	N6	N5	Low fossiliferous Mg-limestone	Bioclastic grainstone
T-S 2 2/17/17																
	dark 1	63.2	1.84	0.11	1.79	<LOD	0.029	0.030	0.091	67.07	34.3	0.02	N6	N5	Nearly pure limestone	Dense, micritic and stands out in relief
	dark 2	59.5	<LOD	0.12	1.58	<LOD	0.032	0.114	0.130	61.49			N6	N5	Nearly pure limestone	Dense, micritic and stands out in relief
	dark 3	56.5	1.75	0.13	1.93	<LOD	0.023	0.006	0.094	60.40	32.3	0.03	N6	N5	Nearly pure limestone	Dense, micritic and stands out in relief
	light a	42.2	13.3	0.10	1.29	<LOD	0.107	<LOD	0.238	57.23	3.2	0.27	10YR 7/4	10YR 6/2	Limy dolostone	Coarser grained, more porous; weathers back
	light b	41.5	6.38	0.83	1.22	<LOD	0.093	<LOD	0.066	50.04	6.5	0.13	10YR 8/2	10YR 6/2	Limy dolostone	Coarser grained, more porous; weathers back
	light c	40.9	15.8	0.65	0.94	<LOD	0.116	<LOD	0.171	58.55	2.6	0.33	10YR 7/4	10YR 6/2	Limy dolostone	Coarser grained, more porous; weathers back
Carbonate Chemistry:																
Dolomite in weight percent is (21.9% MgO + 30.4% CaO + 47.7% CO2)											1.38	1	Stoichiometric dolomite			
The Equivalent Mole weight for Calcite is (56% CaO + 44% CO2)																

Stromatolites

Stromatolites are usually mounded structures formed by blue-green algae (cyanobacteria) (Figure 13, Station B of Road Log). They form when calcium carbonate deposits on a mucilaginous algal surface, preserving the organism as a fossil. Stromatolites are one of the oldest fossils, ranging back 3.5 billion years (Taylor and Taylor, 1993). They are credited for producing much of Earth’s early oxygen, eventually enabling aerobic organisms to evolve (Holland *et al.*, 1994; Kasting and Siefert, 2002).

Stromatolite morphologies reflect their distribution on modern tidal flats (Figure 13; Logan *et al.*, 1964; Anstey and Chase, 1974). Supratidal forms consist of laterally-linked hemispheroids with continuous laminae (LLH). Intertidal stromatolites develop larger, more distinct domes or hemispheroids forming columns or club-like “cabbage heads” (SH, LLK-SH). Subtidal forms (SS) are diminutive in comparison, consisting of discrete spheroids.



Figure 13. Intertidal stromatolite at Station B in the Milroy Member of the Loysburg.

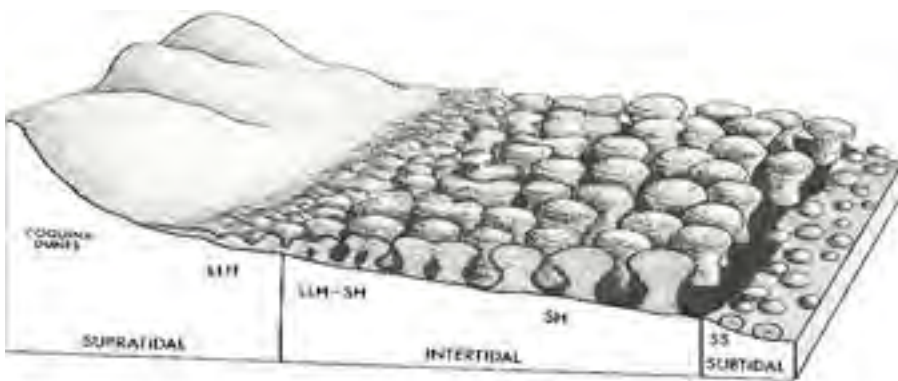


Figure 14. Block diagram of stromatolite distribution on carbonate tidal flats. (Anstey and Chase, 1974; use with permission)

The stromatolite, above, is interpreted as intertidal, based on morphology and sedimentary observations in the Loysburg

See diagram in Figure 14, on the left.

Stylolites

Stylolites are secondary diagenetic structures resulting from differential pressure solution perpendicular to the prevailing principal stress direction. Most stylolites are bedding-parallel (Figure 15), reflecting weight of the overburden. Less common are those antithetic to the bedding, and cross-strike (Figure 16). The latter types reflect a change in the principal stress direction and are considered to be tectonic in origin. A pre-Taconic (middle to late Ordovician) age is deduced for the bedding-parallel stylolites. The varying attitude of the other stylolites records changes in the local stress field from structural compression during the Taconic and Appalachian Orogenies and later NE-SW (contemporary) compression (Srivastava and Engelder, 1990).



Figure 15. High-amplitude (mega), symmetrical stylolite in the Milroy Member of the Loysburg. The hammer is 11 inches long. Station BB.

Confined dissolution preferentially removes the more soluble bedrock, leaving the insoluble residues as stylolites. Insoluble residues consist of clay, silt, silica, mica, pyrite, oxides of iron and manganese, and organic carbonaceous residues (hydrocarbons). The volume of dissolution, estimated to be as much as 40-50 percent (Shaub, 1939), is based on the volume of insoluble residue in the stylolite assuming a similar tenor in the adjacent bedrock. Railsback, (2003) discusses the limitations of these types of estimates. Bathurst (1971) uses the amplitude of stylolite sutures to indicate the minimum thickness of the dissolved material.

Limestones tend to be the more soluble component in these interbedded carbonate sediments. Porosity is another factor that influences water/rock interactions. This is a concern for the petroleum industry where the percent of porosity is important in a potential producing zone.

The unusually large stylolites exposed in the roadcut appear to be typical of the Loysburg and upper Bellefonte in Central Pennsylvania (Doden and Gold, 2011). They used the name of mega-stylolite for those with amplitudes on the centimeter-scale and wavelengths on a decimeter-scale to describe bedding parallel stylolites with thick accumulations of insoluble residue up to several cm thick. In contrast, the millimeter- to centimeter-scale stylolites tend to be tectonic (Gold and Doden, this volume).

Most of the mega-stylolites exhibit bi-directional cusps (sutures) on both top and bottom (Figure 15). These are symmetrical with a similar geometry to a fold train. Some have only an upper or lower cusped surface, and are considered asymmetrical. These are associated with shale beds or other lithic barriers and tend to be unidirectional upward (Figure 17).



Figure 16. Sub-vertical, cross-strike “tectonic” stylolite. Milroy Member Loysburg Formation. The pen is 6.5



Figure 17. Asymmetrical stylolite in the Tea Creek Member of the Bellefonte. Note the flat bottom and cusped top of black shaly bed. Rusty stains are from weathered pyrite. Station OO.

Disconformities

Several disconformities are exposed in the Milroy, one of which is shown in Figure 18 (Station E in Road Log). These are local unconformities or diastems, not attaining regional status. Subaerial exposure, as in a supratidal or intertidal setting, is suggested, or possibly a diagenetic effect enhanced long after initial deposition.



Figure 18. Disconformity at Station E in the Milroy Member of the Loysburg Formation. The geology hammer is 11 inches long.

Vugs

Vugs vary in size and filling material. They may have multiple origins. Presence of barite and gypsum in some suggests those are due, in part, to growth of evaporite minerals. Others may be due to solution and/or decay of algae, leaving voids. While most are small (1-2 inches in diameter), others are quite large – up to 12 inches in length. The mentioned origins of the vugs are consistent with a carbonate tidal-flat depositional setting.

Bioturbation

Bioturbation textures are evident as “tiger stripes” beds (Figure 11).

Joint Systems

Only 195 feet of stratigraphy are exposed in the nearly half mile of roadcut, a consequence of the small divergence in bedding attitude (strike 060° and dip 15-20°) and road-bed orientation. Fractures in the Bellefonte Dolomite and Axemann limestone in the Nittany Anticlinorium include five distinct types (Srivastava and Engelder, 1989). These are identified based on their orientation, filling, size, and present aperture as bedding-parallel veins, strike veins, cross-fold veins, cross-fold joints, and late-formed vertical joints (Srivastava and Engelder, 1990). Strike veins are, in many cases, normal and restricted to the bed regardless of its dip. Two sets of cross-fold joints are present, with one open and the other filled. Both cut and, hence, postdate the strike veins (Srivastava and Engelder, 1989). Presence of more than one cross-fold joint set is common in the Valley and Ridge as well as in the Appalachian Plateau. As the beds of the Nittany Syncline rotated about their fold axis, the cross-fold joints were tilted, depending on location of the bed relative to the nose.

Dating of fractures is based on cross-cutting relationships. The strike veins are found in the elastically stiffer beds, which in the case of the Loysburg, are dolostone. The strike veins are characterized by a plumose morphology indicating an initial propagation as a joint later coated with an insoluble residue and then filled. Cross-fold veins cut strike veins, indicating that the cross-fold veins formed later. The last joint to develop is vertical and independent of the bedding strike. These late-formed joints are classified as “neotectonic” as they propagate parallel to the contemporary tectonic stress field.

Neotectonic joints are the most recent joint systems to form within a region subject to uplift and erosion. Relative to other joints in the Appalachians, these are shallow (within 0.5 km of the surface), late-formed joints. Initiation and propagation is due to unloading of overburden and by fluid pressure (Hancock and Engelder, 1989). These are referred to as J₃ joints.

On Shallowing-Upward Carbonate Cycles in the Loysburg (?)

Carbonates, including those in Central Pennsylvania, commonly show sedimentary cycles (Gardiner-Kuserk, 1988). Krynine (1946) describes 53 cycles in the Gatesburg Formation near Birmingham and other cycles in the Warrior Formation. Lees (1972) and Doden *et al.*, 2011 describe cycles in the Axemann and Bellefonte Formations, respectively. These cycles are inferred from repetition of strata, such as alternating limestones and dolostones in a predictive sequence in carbonate sediments. The cycles suggest periodic flooding of platforms through transgressions (Tucker and Wright, 1990). However, these may also be due to slight changes in seawater chemistry, climate/weather, sediment, groundwater/pore chemistry, and diagenesis (Roger Cuffey, personal communication). This is a departure from the classic clastic-tidal-sequence model.

The Milroy Member in the roadcut shows conspicuous color variations and repetition of the “tiger-stripes” limestone that are difficult to reconcile in shallowing-upward carbonate cycles/sequences (Figures 1 and 19). Subtle chemical changes affect growth conditions for algae/stromatolites, groundwater/pore water, and early diagenetic changes (stylolites). Stylolization may be the critical factor in our attempt to deduce a cyclical forcing mechanism.



Figure 19. Alternating layers of limestone (dark) and dolostone (light) in the lowermost Milroy Member of the Loysburg. Do these represent cycles? Stations DD-FF.

Sedimentary Flow Features

Several different sedimentary features with hydrodynamic implications are exposed in the roadcut. These include: intraformational breccias/rip-up clasts, small erosion channels, directionally imbricated clasts, and draping sediment. The breccias originated as mudcracks in the supratidal/upper intertidal zones. Probably due to storms, the mudcracks were eroded, transported, and redeposited. Angularity of these allochthonous clasts attest to a relatively short transport distance, as from the supratidal and upper intertidal zones to lower intertidal to subtidal zones of a tidal flat. Most or all of the current indicators depicted in Figure 20 are from right to left (west to east). This assessment is based upon the asymmetry of the large pebble (#1) – probably due to water transport, an erosion scour on the stoss side of the pebble, sediment draping (right to left) over the pebble, and imbricated clasts (located two feet to the left of the view in Figure 20, in the same layer).



Figure 20. Sedimentological features at Station DD of the Road Log. (1) Asymmetrical pebble showing a sloping stoss side that includes an erosion scour in contrast to a steep lee side. (2) Sediment draping over the pebble in (1), indicating flow from right to left. Red arrows point to numerous small erosion channels or scours. The white arrow points to hydrodynamically oriented intraformational clasts. Two feet to the right of this image, in the same layer, are imbricated clasts indicating flow direction from right to left.

Paleogeography

Central Pennsylvania Cambro-Ordovician carbonates were deposited as a shallow sea transgressed westward and northward across Laurentia. In Pennsylvania, the transgression extended to its western border. At this time, Pennsylvania was located at or near 25 degrees south latitude, placing it in the tropics (Laughery *et al.*, 2004). Carbonates were deposited in shallow, warm, clear water super-saturated with calcium carbonate. Maximum water depth was approximately 90 feet (Laughery *et al.*, 2004) but most of it was at or near sea level (< 10 m) (Demico and Mitchell, 1982).

The paleogeography of Bellefonte deposition in Pennsylvania reflects shallower and more restricted conditions to the northwest. Presence of desiccation cracks, dolomite, and low fossil diversity support this observation. In Pennsylvania, the Bellefonte covers an area from approximately 60 miles east of State College westward to the state border (Wagner, 1966). This formation is dolomitic to the northwest and equivalents are calcitic to the southeast. Dolomite deposition occurs in restricted depositional settings of greater salinity; lime deposition is mostly in less restricted, more open-water environments (Folk, 1952). Local uplifts or marine withdrawals may have produced barriers or low islands, creating restricted settings and tidal flats (Wagner, 1966). These restricted settings, in combination with tropical temperatures, are marked with an increase in salinity.

The Loysburg reflects transitioning paleogeographic conditions in Pennsylvania during the earliest Middle Ordovician. Massive dolomites of the Bellefonte transition into limestones of the Hatter Formation. Shallow water, restricted settings of the Bellefonte are replaced with less restricted,

shallow, lagoon or subtidal sediments of the Hatter (Laughrey *et al.*, 2004). Lithological changes (bottom to top) within the Loysburg reflect the transition. The Milroy Member consists of alternating limestone and dolomites deposited in a tidal-flat depositional environment. In contrast, the overlying Clover Run Member is dominantly limestone of a lagoon or shallow subtidal setting. These transitioning paleogeographic conditions can also be seen laterally across the State. The Loysburg correlates with the New Market Limestone of the St. Paul Group in the southern Great Valley of Pennsylvania and Maryland (Folk, 1952; Berg *et al.*, 1983). The New Market is predominantly limestone, with only sparse dolomites, like the upper Loysburg. The Loysburg of central Pennsylvania represents tidal-flat and lagoon deposits while its more easterly equivalent – the New Market Limestone – reflects more open-water, less restricted settings.

Depositional environments

Any interpretation on depositional environments involving limestones and dolostones raises issues on the origin of the latter. In past decades, it was suggested that dolomite forms as either primary or secondary deposits. There is now consensus that primary dolomite is very rare and that most dolostone in the geologic record is of replacement origin (Tucker and Wright, 1990). Machel (2003) gives a good summary of dolomitization models. An enduring debate in geology is the origin of massive dolomites, such as the Bellefonte, approximately 2000 feet thick. Massive dolomites are problematic because there are no modern analogs for comparisons and because dolomite is difficult to study in the laboratory. Massive dolomitization takes place when seawater or modified seawater (by evaporation and/or mixing with meteoric water) flows through porous and permeable lime sediments (Land, 1985).

Presence of dominantly dolostones in the Bellefonte and a mixed assemblage of dolostones and limestones in the Loysburg require some special conditions. Generally, dolomite deposition occurs in restricted settings of greater salinity; lime deposition is mostly in less restricted, more open-water environments (Folk, 1952). During the Cambro-Ordovician transgression, as carbonate sediment built toward sea level, depositional environments, at times, became progressively more restricted and, increasingly, more saline. Wagner (1966) references Early Ordovician rocks in central Pennsylvania as examples. Low fossil diversities, algal mats (Wagner, 1966), mudcracks, dolomite deposition, elevated salinities, and evaporites characterize upper zones in restricted settings.

A likely scenario for Bellefonte dolomitization (Roger Cuffey, personal communication) involves meteoric water mixing with magnesium-rich water in an arid tidal flat. Some algae concentrate magnesium in their tissues. Decay of algal mats added magnesium to the meteoric groundwater that, in turn, replaced calcite in preexisting lime sediment (Davies, Bubela, and Ferguson, 1974; Folk, 1952; Gebelein and Hoffman, 1973; Mitchell and Horton, 1995; Shinn, 1983; van Tuyl, 1914). The great thickness of the Bellefonte attests to a long-duration process.

An extensive, low-relief tidal flat not much above low tide is interpreted. Subtidal areas probably had maximum water depths of only a few feet, based on comparisons at Andros Island (Roger Cuffey, personal communication). Major storms, especially hurricanes, would have transported copious amounts of terrigenous mud. In such shallow water, there is virtually no deeper depths and in-flowing mud disperses throughout, eventually consolidating into shale. The sediment thicknesses deposited

from hurricanes can be prodigious. Following Hurricane Agnes in 1972, sand deposits 12 feet thick along Spring Creek in State College were observed (Roger Cuffey, personal communication). Presence of shale layers in the Bellefonte and not in the Loysburg may reflect a difference in climate-induced storm frequency and not necessarily a difference in depositional environment.

Lithologic and paleontological observations for both formations suggest deposition on tidal-flats (Chafetz, 1969; Berkheiser and Cullen-Lollis, 1986; Gardiner-Kuserk, 1988; Laughrey *et al.*, 2004; and Roger Cuffey (personal communication). These tidal flats are the semi-isolated basins separated by ridges of Chafetz (1969). Some vugs in both formations contain gypsum and barite. Presence of these minerals as well as secondary strontianite and calcite suggest an arid setting. The only macrofossils in either formation are stromatolites. This low fossil diversity reflects increased salinity, a harsh environment of periodic subaerial exposure in an intertidal-supratidal setting, and the effect of dolomitization. At Station A in the lower Milroy, stromatolites are exposed and are interpreted as being intertidal. Intraformational breccias/rip-up clasts attest to storm erosion and deposition. Angularity of the clasts indicates short transport distances. Mudcracks indicate desiccation due to subaerial exposure. Thinly bedded (cm-scale) argillaceous dololomite with a mounded appearance are interpreted as mud mounds, suggesting a carbonate tidal flat. Dolomite deposition is consistent with a tidal-flat setting.

A characteristic feature of the Loysburg are the “tiger-stripe” beds (Figures 1 and 19). The “tiger stripes” are alternating layers of dolomitic limestones and limey dolostones, accentuated by color and grain size. Composition variations may be due to slight changes in salinity (Roger Cuffey, personal communication) in a shallow-water setting. Salinity is sensitive to short-term environmental factors such as rainfall and climate.

A source of the magnesium is likely to be algal, an important factor, coupled with salinity, in the precipitation of dolomitic carbonates. An example is the fluctuation on the Great Bahama Bank where salinity can fluctuate from 40 ppt during the dry season to 20 ppt during the wet season and down to 15 ppt during hurricanes (Roger Cuffey, personal communication). These suggest a shallow-water depositional environment. A likely scenario would be a broad, low relief tidal flat/flat-sheltered lagoon, nearing equilibrium to promote dolomite deposition. Seasonal variation in rainfall can cause rapid and significant changes in salinity effectively controlling fluctuations back and forth between carbonate muds lithifying into dolomitic limestone versus limey dolomite.

Conclusion

Approximately 7000 feet of carbonates - limestones and dolostones - are exposed in central Pennsylvania, ranging from the Upper Cambrian to Middle Ordovician, spanning approximately 100 million years (Demicco and Mitchell, 1982). This Cambro-Ordovician sequence was deposited on a carbonate platform - the Great American Bank (GAB) (Ginsburg, 1982; Hardie, 1981) or the Great American Carbonate Bank (GACB) (Derby, et al, 2013) – developed on the passive margin of the paleocontinent Laurentia; then covered by a warm, shallow sea that slowly transgressed across that paleocontinental edge. The nearly continuous succession of carbonates implies an extremely long period of local tectonic quiescence. No major orogeny affected central Pennsylvania during the transgression until the Taconic Orogeny began in the later Middle Ordovician. Cessation of local

Cambro-Ordovician carbonates was initiated with alternating limestone and shale in the Salona/Coburn Formation, then with mud and sand (flysch) deposits of the Antes and Reedsville Shales, precursors to the Taconic Wedge or Queenston Delta.

References

- Anstey, R., and Chase, T., 1974, *Environments Through Time*: Minneapolis, Burgess Publishing Company, p. 80.
- Bathurst, R. 1971. *Carbonate Sediments and Their Diagenesis*: Amsterdam, Elsevier, 620 p.
- Berg, T.M., McInerney, M.K., Way, J.H., and MacLachlan, D.B., 1983, *Stratigraphic Correlation Chart of Pennsylvania*, General Geology Report 75.
- Berkheiser, S.W. and Cullen-Lollis, J., 1986, Stop 1. Union Furnace section: Stratigraphy and sedimentology, in Sevon, W.D., ed. *Selected geology of Bedford and Huntingdon Counties*. Guidebook, 51st Annual Field Conference of Pennsylvania Geologists, Huntingdon, PA, p. 111-119.
- Brett, C. and Liddell, W., 1978, Preservation and paleoecology of a Middle Ordovician hardground community: *Paleobiology*, v. 4, no. 3, p. 329-348.
- Butts, C. and Moore, E., 1936, *Geology and Mineral Resources of the Bellefonte Quadrangle, Pennsylvania*. USGS Bull. 855, 111 p.
- Chafetz, H., 1969, Carbonates of the Lower and Middle Ordovician in Central Pennsylvania, PA Topographic and Geologic Survey, Gen. Geol. Rept. G58, 4th Series, p. 1-34.
- Davies, P.J., Bubela, B., and Fergusson, D., 1974, Dolomite and organic material, Bureau of Mineral Resources, Geology and Geophysics, Canberra, p. 1-5.
- Demicco, R.V. and Mitchell, R.W., 1982, Facies of the Great American Bank in the Central Appalachians, in Lyttle, P.J., ed., *Central Appalachian geology*: American Geological Institute, Falls Church, p. 171-266.
- Derby, J.R., Fritz, R.D., Longacre, S.A., Morgan, W.A., and Sternbach, C.A., (eds), 2012, *The Great American Carbonate Banks: The Geology and Economic Resources of the Cambrian-Ordovician Sauk megasequence of Laurentia*. American Association of Petroleum Geologists Memoir 98, 528 p.
- Doden, A.G., Gold, D.P., Mathur, R., and Jensen, L.A., 2011 in progress. *Bedrock Geology of the State College Quadrangle, Centre County, Pennsylvania*. DCNR, Open File Report.
- Droser, M.L. and Bottjer, D.J., 1986, A semiquantitative field classification of ichnofabric, *J. of Sed. Pet.*, v. 56, no. 4, p. 558-559.
- Flemings, P.B. and Grotzinger, J.P., 1996, STRATA: Freeware for analyzing classic stratigraphic problems, *GSA Today*, v. 6, No. 12, p. 1-7.
- Folk, 1952, *Petrography and Petrology of the Lower Ordovician Beekmantown Carbonate Rocks in the Vicinity of State College, Pennsylvania*. PSU Ph.D. dissertation, University Park, PA, p. 60-61.
- Gardiner-Kuserk, M.A., 1988, Cyclic sedimentation patterns in the Middle and Upper Ordovician Trenton Group of Central Pennsylvania. In: Keith, B.D. (ed.) *The Trenton Group (Upper Ordovician Series) of Eastern North America*, AAPG Studies in Geology #29, p. 59-75.
- Gebelein, C.D. and Hoffman, P., 1973, Algal origin of dolomitic laminations in stromatolitic limestone, *Journal of Sed. Petrology*, v. 43, p. 603-613.
- Ginsberg, R.N., 1982, Actualistic depositional models for the Great American Bank (Cambro-Ordovician), Congress on Sedimentology, Ontario, International Association of Sedimentologists, abs., p. 114.
- Gold, D.P. and Doden, A.G., 2015, *Geology of the Hanson Property and the Oak Hall Quarry*. Permit Application Report to PaDEP, 118 p.
- Hancock, P. and Engelder, T., 1989, Neotectonic joints: *Geological Society of America Bulletin*, v. 101, p. 1197-1208.
- Hardie, L.A., Demicco, R.V., and Mitchell, R.W., 1981, The Great Cambro-Ordovician Bank of the central Appalachians: (abstract) *Northeastern Section, GSA Abstracts with Programs*, v. 13, no. 3, p. 136.
- Holland, H.D., 1994, Early Proterozoic atmospheric change, in Bengtson, S., *et al*, *Early Life on Earth*, New York, Columbia University Press, p. 237-244.

- Kasting, J.F., and Siefert, J.L., 2002, Life and the evolution of Earth's atmosphere, *Science*, v. 296, p. 1066-1068.
- Kay, M., 1944, Middle Ordovician of central Pennsylvania: *Journal of Geology*, v. 52, no. 2, p. 97-116.
- Krynine, P.D., 1946, From the Cambrian to the Silurian, Twelfth Annual Field Conference of Pennsylvania Geologists, State College, PA, May 30-31, June 1-2, p. 1-32.
- Krynine, P.D., 1960, Sedimentation near University Park (State College), central Pennsylvania, NSF Summer Conference on Stratigraphy and Structure of the Appalachians, June 16-17, 29 p.
- Krynine, P.D. and Tuttle, O.F., 1941, Bellefonte sandstone-an example of tectonic sedimentation, *Geological Society of America Bulletin with Abstracts*, v. 52, p. 1918.
- Land, L.S., 1985, The origin of massive dolomite: *Journal of Geological Education*, v. 33, p. 112-125.
- Laughrey, C. D., Kostelnik, J., Gold, D. P., Doden, A. G., and Harper, J. A., 2004, Trenton and Black River Carbonates of the Union Furnace Area of Blair and Huntingdon counties, Pennsylvania: Pittsburgh Association of Petroleum Geologists, Field Trip Guidebook, 81 p.
- Logan, B. W., Rezak, R., and Ginsburg, R. N., 1964, Classification and environmental significance of algal stromatolites: *Journal of Geology*, v. 72, p. 68-83.
- Machel, H.G., 2003, Dolomites and dolomitization, *in*: Middleton, G., et al, eds., *Encyclopedia of Sediments and Sedimentary Rocks*: Boston, Kluwer Academic Publishers, p. 234-242.
- Mitchell, S.W. and Horton, Jr., R.A., 1995, Dolomitization of modern subtidal sediments, New Providence Island, Bahamas, *in* Curran, H.A. and White, B., *Terrestrial and Shallow Marine Geology of the Bahamas and Bermuda*, GSA Special Paper 300, p. 201-222.
- Railsback, L.B., 2003, Stylolites, *in* Middleton, G.V., ed., *Encyclopedia of Sediments and Sedimentary Rocks*, Boston, Kluwer Academic Publishers, pp.
- Rones, M., 1955, A litho-stratigraphic, petrographic and chemical investigation of the lower Middle Ordovician carbonate rocks in central Pennsylvania. Unpub. Ph.D. dissertation, The Pennsylvania State University, 345 p.
- Rones, M., 1969, A lithostratigraphic, petrographic, and chemical investigation of the lower Middle Ordovician carbonate rocks in central Pennsylvania, PA Geol. Survey, 4th ser., Bull. G 53, 224 p.
- Schinn, E.A., 1983, Tidal flat environment, *in* Scholle, P.A., Bebout, D.G., Moore, C.H. (eds.), *Carbonate Depositional Environments*, AAPG Memoir, p. 173-210.
- Shaub, B.M., 1939, The origin of stylolites: *Journal of Sedimentary Petrology*, v. 9, p. 47-61.
- Srivastava, D. and Engelder, T., 1990, Crack-propagation sequence and pore-fluid conditions during fault-bend folding in the Appalachian Valley and Ridge, central Pennsylvania: *Geological Society of America Bulletin*, v. 102, no. 1, p. 116-128.
- Swartz, F.M., Rones, M., Donaldson, A.C., and Hea, J.P., 1955, Stratigraphy of Ordovician limestones and dolomites of Nittany Valley in area from Bellefonte to Pleasant Gap, Pennsylvania, Guidebook, 21st Field Conf. of PA. Geologists, p. F1-F25.
- Taylor, T.N. and Taylor, E.L. 1993, *The Biology and Evolution of Fossil Plants*: Englewood Cliffs, Prentice Hall, 982 p.
- Tucker, M.E. and Wright, V.P., 1990, Dolomites and dolomitization models: *Carbonate Sedimentology*: Oxford, Blackwell Scientific Publications, p. 365.
- Van Tuyl, F.M., 1914, The origin of dolomite, Iowa Geological Survey Annual Report, v. 25, p. 252-422.
- Wagner, W.R., 1963, Cambro-Ordovician stratigraphy of central and south-central Pennsylvania: Guidebook, Tectonics and Cambro-Ordovician Stratigraphy in central Appalachians of Pennsylvania, Pittsburgh and Appalachian Geological Societies, 129 p.
- Wagner, W.R., 1966, Stratigraphy of the Cambrian to Middle Ordovician Rocks of Central and Western Pennsylvania, Pennsylvania Geological Survey, 4th Series, General Geology Report G49, p. 1-10.

82nd Annual Field Conference of Pennsylvania Geologists

PLATE 1. Road-bank log of pertinent mesoscopic scale depositional and structural features

Road bed	Flag	bed #	Feature/structure	Comment	Attitude		
					Joint 1	Joint 2	Joint 3
Blue		White					
2400		95		Start of traverse			
2352	A	94	Large stromatolite on J1		J1 180/77		
2324			Plumose pattern stylolite and joint J2		St 240/60	J2 128/90	
2300		92	3 joint sets: blocky	gf-blocky; small vugs.	J1 190/80	J2 130/90	J3 080/73
2225		87/86	Channel	Disconformity			
2100		86/84	Mega-stylolite (symmetrical); conglomerate	Rip-up-clast cong., 2 ft above marker			
2085		84t	Mega-stylolites; vugs	27" dololulite with vugs			
1985		84b	Neotectonic joint	Massive dololulite	J3 092/90		
1916		84b	Neotectonic joint	Massive dololulite	J3 092/90		
1895		84b	Vugs: neotectonic joint	Massive dololulite	J3 080/90		
1852	B	83	Mound; 6 ft along base	Thin platy silty dololulite			
1838		83	Early and neotectonic joints		J1 200/81	J3 090/85	
1767		84	Low mound; tectonic stylolite	Massive, over platy silty dolostone	St 230/69		
1750		80	Tectonic stylolite		St 230/68		
1706	83	83/	Small mud mound				
1690		82	Mud mound in silty layers				
1606	Road sign	80	5-ft thick bed; tectonic stylolite	5 ft thin laminae dololulites	St 220/68		
1537		80	6-ft thick bed; tectonic stylolite	5 ft thin laminae dololulites	St 223/73		
1385		80/79	Mega-stylolite in bed 79				
1342	IV	78	2 tectonic stylolites in overlying bed	Tiger stripe limestone	St 232/68		
1296		78	Neotectonic joint	Tiger stripe limestone	J3 080.86		
1234		78/77	Neotectonic joint	Tiger stripe limestone	J3 084/88		
1191	G	77	Tectonic stylolite		St 220/69		
1180	Road sign						
1137	III	76/75		12 " thick tiger stripe limestone	J3 080/90		
1086		73	Mega-stylolite				
1082	C						
1050	N		Mega-stylolite		J245/75		
992	II	70	Stromatolites/vugs in limestone	48" tiger stripe (algal?) vuggy			
955	G2	70/69	Shale; mega-stylolite; conglomerate	Rip-up-clast cong., calcite veins	J1 200/83	J2 130/90	cv 310/85
							cv 150/75
900			Rusty stain from stylolite	Pyrite; insoluble residue			
816	I	64/63/62	Shale \dolostone\limestone	Tiger stripe bioturbated	J1 200/68	J2 133/90	St 232/72
				Bellefonte Fm. Tea Creek Mbr			
743			Mega-stylolite (symmetrical); vugs	Massive dololulite			
650		57/56	Mega-stylolite (symmetrical); vugs	Large (10-30 cm) vugs			
500		49					
400					J1 200/75	J2 130/90	J 105/90
388		43			J1 190/78		J 110/90
381			Stromatolite in loose boulder				
300		42					
200		37			J 110/60		
				Tea Creek Mbr	J 295/71		
150	E	32	Shale.Hardgrounds.Dolarenite; qtz grs.	Dale Summit Mbr (32 " thick)	cv 184/75	cv 200/81	
			5-10 cm shale below asymmetrical stylolite	Rusty stain; pyrite blebs			
125	F	31	Channel; base of Dale Summit sandstone	Vugs at ground level: Coffee Run Mbr	B020/20	J 180/85	J 200/75
100		27/26	Thin symmetrical mega-stylolite				
64	D	21	Channel				
60	K	20	Thin stringers of bedded black chert				
57	J	19	Black chert nodules cut by joint		B030/27	J 110/90	J 198/60
30	I	13/12	Cm -scale clastic dikes	High pore-pressure interval			
0		1, 2, 3		End of traverse			

I-99 ROADWAY CONSTRUCTION HISTORY AND PYRITE DISCOVERY AT SKYTOP, CENTRAL PENNSYLVANIA

ARNOLD G. DODEN¹ AND DAVID (DUFF) GOLD²

¹ GMRE, Inc., 925 West College Ave., State College, Pa 16801. ² Emeritus, Department of Geosciences, Penn State University, University Park, PA

Introduction

The construction of roadways in Pennsylvania has many geologic challenges, but one that has come into focus in recent years is that of acid rock drainage (ARD), specifically, the alteration of pyrite and other sulfide minerals to produce sulfuric acid runoff. A well-known consequence of the coal mining industry, ARD³ can also adversely affect highway construction. A definitive example of this problem is the construction of Interstate Highway I-99 through Skytop wind gap in Centre County, Pennsylvania. During excavation of Bald Eagle Mountain, a machine operator spotted something “shiny and metallic” in a rubble pile. The work was halted, albeit too late: more than 1,000,000 tons of the Bald Eagle Formation, some of which contained in excess of 5 wt. % pyrite, had been excavated and dumped into nearby waste piles (Arbogast, Siebert, and Skytop). A substantial amount of this same pyritic rock was used as fill and dressing aggregate along an eight-mile highway section. Often referred to as a “disaster” (see local newspaper reports), the Skytop pyrite exposure was indeed a disaster if one considers not only the immediate environmental contamination, but also the immense financial obligation imposed on Pennsylvania to remediate the problem. The negative publicity was an additional burden for Penn DOT⁴.

However, the pyrite problem at Skytop was fortuitous in some respects. The deep excavation through much of the wind gap, followed by remedial geologic mapping and related work, provided a better understanding of the nature of the Skytop pyrite and how it formed. Prior to the I-99 work, many non-specialists believed pyrite occurrences were like those that occur in coals (“bedded” pyrite). The remedial geological investigation, however, demonstrated this was not the case at Skytop. Although sulfide minerals had been documented at Skytop years earlier (Smith, 1977), no one recognized the mineralization extent. The dense concentration and widespread network of pyrite veins was surprising. Also, mineralogical investigations revealed the presence of “whisker” pyrite, a rare and highly reactive form that was also unexpected. Furthermore, bedrock exposures afforded an exceptional view of the stratigraphy and structure in Bald Eagle Ridge, thereby facilitating the remedial geology work. Geologists and engineers could now better understand the complex

¹ GMRE, Inc., 925 West College Ave., State College, PA 16801

² Emeritus, Department of Geosciences, Penn State University, University Park, PA

³ ARD is an older term associated with the mining industry, but this concept is also referred to as *acid mine drainage* or *acid and metals drainage* (AMD).

⁴ This paper does not intend to assign blame on any individual or organization. The sequence of events of any road construction project is complex and many subcontractor companies and individuals are typically involved. It has been a learning experience for all. Ultimately the Skytop ARD problem was largely resolved (ongoing remediation techniques are still in effect).

structural relationships in this part of the Valley and Ridge Province. A more in-depth understanding of the scientific concepts also better prepares us for future ARD encounters.

The story of Skytop begins with the history of road building and the geologic setting, the latter not only influencing the former, but dictating many aspects of the whole process. The geologic setting of Pennsylvania provides many natural obstacles for transportation, whether one uses trails, railways, or modern roadways. The most obvious of these challenges are high mountains that dominate many parts of the state, including the Valley and Ridge Province. Large water gaps through the mountains provided, perhaps, the easiest access routes for early travelers. Game trails commonly followed rivers through water gaps and were likely some of the earliest pathways for travel by foot and horseback. If navigable, larger streams and rivers offered an alternate means of transportation. However, the long mountain ridges of Central Pennsylvania stretch for hundreds of miles and broad water gaps are not always conveniently located (see Figure 1). Travelers needed to find other pathways over the long ridges, and wind gaps logically offered the easiest access. Wind gaps are shallow “notches” in a ridge from which small streams typically flow and where game trails are abundant.

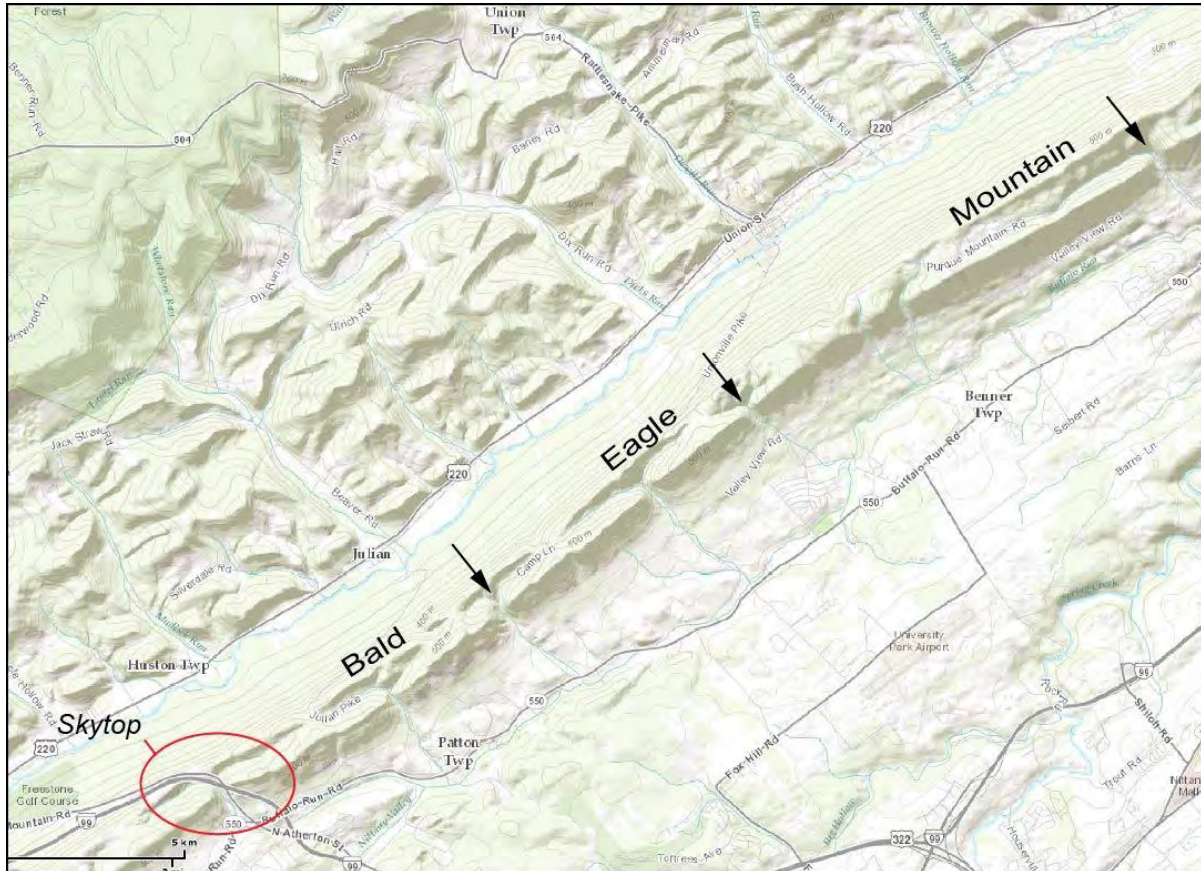


Figure 1. Topographic map of a portion of Bald Eagle Mountain in central Pennsylvania. Wind gaps occur every few kilometers along this ridge, typical of many mountains in the region. The Skytop wind gap through which S.R. 322 and I-99 cross the mountain is circled in red. Note the difference in topography between the SE corner of the map (largely Cambro-Ordovician carbonates of the Valley and Ridge Province) vs. that of the NW corner (gently dipping Silurian-Devonian clastic sediments of the Appalachian Plateau).

Wind gaps are commonly spaced a few kilometers apart (Figure 1) and undoubtedly helped early travelers avoid the steepest slopes and boulder-choked areas. A wind gap in Bald Eagle Mountain (BEM) approximately 10 miles (15 km) west of State College is locally known as Skytop. Modern roadway construction takes advantage of these same wind and water gaps, using the latest technology and machinery for efficiently cutting and filling to produce paved highways. High-speed, four-lane highways (including those of the U.S. Interstate System), however, require relatively gentle grades, which in some cases demand deeper cuts through gaps than those made many years ago for local highways. Modern excavating capabilities allow the removal of as much of a mountain as is needed, but in doing so increases the potential to reveal reducing conditions below the ground water table. The exposure of vein-type pyrite and associated ARD at Skytop is a prime example of such a major problem.

Bald Eagle Mountain is a prominent ridge trending approximately SW to NE, extending from South-central Pennsylvania and curving to the northeast. It is also significant in that it represents the westernmost mountain in the Valley and Ridge province of Central Pennsylvania. Bald Eagle Mountain borders the Allegheny Front structural boundary and to the west of this lies the Allegheny Plateau. The Valley and Ridge geologic structures and stratigraphy differ significantly from those of the Allegheny Plateau. For many years, Skytop wind gap has provided access across Bald Eagle Mountain via State Route 322 and is the primary transportation route between Nittany Valley on the east and Bald Eagle Valley to the west.

Interstate Highway 99 (I-99) has a southern terminus at the Pennsylvania Turnpike (I-70/I-76) north of Bedford, PA. From there I-99 extends north/northeastward, passing near the city of Altoona through Bald Eagle Valley, overlaying the pre-existing U.S. Route 220. Farther north I-99 climbs Bald Eagle Mountain and crosses through Skytop wind gap, then passes the north side of State College and ends at Interstate 80 near the town of Bellefonte. Thus, I-99 provides an important high-speed route connecting the two major east-west throughways of Pennsylvania with population centers in the middle of the state. Long-term plans call for further extensions of I-99. One would extend southward from Bedford, continuing along the Route 220 corridor to an interchange with I-68 in Cumberland, Maryland. Another extension of I-99 would go northward from Bellefonte making use of the pre-existing US 220 and US 15 corridors, eventually terminating at an interchange with I-86 west of Corning, New York.

How the I-99 roadway came to exist is an interesting and complex story, involving politics, environmental issues, and geology. Few people could have anticipated how the geology would impact road construction across Skytop.

Early I-99 Development

Interstate Highway 99 retraces much of the original “Corridor O” route, first planned in 1925 as part of the Appalachian Development Highway System. I-99 would extend from Cumberland, Maryland to Bellefonte, PA sharing the existing route US 220. From there it would continue to Lock Haven, through Williamsport, and then follow the U.S. 15 freeway north to the New York state line (Appalachian Regional Commission report, 2009). Early work concentrated on converting the existing Route 220 to a four-lane freeway with high-speed ramps and interchanges.

The initial construction of I-99 in Pennsylvania finally began in the late 1960's with a short segment starting at the Turnpike (I70/76) at Bedford and ending at PA Route 56 near Cessna. A larger part of the freeway development occurred in the 1970's. During this era two long sections were built: a southern part from PA 56 north to modern exit 15 in Blair County, and a more northerly second part extending from Charlottesville (exit 45) to the village of Bald Eagle. The portion between modern exit 15 and Altoona (exit 33) was finished in the 1980's whereas the segment between modern exits 33 and 45 was opened by 1997 (Pennsylvania Official Transportation Map, 1989; Appalachian Regional Commission Report, 2009). Interstate 99 between the Pennsylvania Turnpike and Bald Eagle, along the U.S. 220 freeway, was first posted with signs designating it as I-99 in 1995.

The next section of U.S. 220 freeway was opened between State College and Interstate 80 on November 25, 2002, and this was followed by the part between Bald Eagle and Skytop, which opened December 17, 2007. The freeway between Skytop and State College finally opened on November 17, 2008, following a major delay caused by the pyrite discovery.

Undoubtedly the Skytop wind gap (as well as others) provided a relatively easy way for early inhabitants of the area to cross Bald Eagle Mountain, first by footpath and later by primitive roads. Vintage PennDOT highway maps show that roadways have exploited the Skytop wind gap for many years; the first two-lane concrete version of Route 322 was built in the 1930's.

Route 322 and other local highways provided sufficient access to Nittany Valley for years. But rapid growth in the area, particularly in State College, made it apparent by the 1950's that an expanded highway system was needed. In 1960 the concept of a detour around State College was first discussed (Dooms, 2015). Named the Mount Nittany Expressway, the new highway system would divert substantial traffic flow from the old Route 322 that passed through downtown State College out to the new "bypass" as it was known locally. The first section of the Expressway opened in 1969 in Patton Township, and the southern section in Harris Township was completed by 1972. The bypass was not finished until 1985 due to controversies involving the locations of interchanges, number of lanes, and other issues (Dooms, 2015). The Mount Nittany Expressway would provide the initial track for future I-99 freeway segments, which were completed by 2002 and ultimately connected the State College bypass to the Bellefonte area and I-80.

A report prepared for the Federal Highway Administration (FHA) report (Louis Berger Group, *et al.*, 2003) described some practical reasons for constructing a high-speed, limited access, four-lane roadway that would connect the southern part of the state with Interstate 80, the major east-west route through central/northern PA. In addition to rapid access for private transportation needs, there are potential benefits for local industry:

Direct, short haul distances for transportation of goods and materials, raw materials and finished products, both to and from State College. The city is the general economic hub of the region encompassing substantial industry and a major university.

Reduced commuting distances. Penn State University is the Nittany Valley's largest employer and traditionally many employees have driven long distances to their jobs, in many cases from well outside Centre County. Per the FHA report (2003), select industries will be able to reside farther from I-99

itself. Consequently, those industries located along the main highway spine will be able to draw from a greater labor pool due to side corridor accessibility.

Decreased travel times for general business travel. Fast, convenient routes to large commercial centers to the east and west will greatly facilitate general business travel. Executive staff, clients, and skilled employees will be more willing to re-locate to and visit the region if the trip is quick and direct (FHA report, 2003).

More direct travel for tourist traffic. Tourist traffic is likely to be impacted due to easier and quicker access for day trips, more pass through overnight traffic, and easier access to more remote areas for those traveling from outside the region. This is also true for special university events (e.g., football games, concerts) that require high-traffic volumes moving over short time spans.

Although the general concept of a high-speed freeway linking the immediate State College area to the outside world seemed agreeable, a big question loomed: where would it be built? The existing freeway coming from the southern part of Pennsylvania ended in Bald Eagle Valley, near Bald Eagle (Figure 2). The logical place to cross Bald Eagle Mountain was through a wind gap and the obvious choice among gaps was that of Skytop, which already accommodated S.R. 322 and opened into Nittany Valley toward State College. But before reaching the crest of Bald Eagle Mountain a choice had to be made in routing I-99: would the roadway pass primarily through Bald Eagle Valley and use a minimal footprint on the western side of Bald Eagle Mountain, or would the roadway avoid the valley bottom as much as possible and be situated on the mountain slope for most of this section? Advantages and disadvantages for the environment were evident for both options, as well as for effects on local population centers and privately-owned land.

Environmental, Geological, and Political Challenges

Originally the Corridor “O” vision saw a freeway extending northeastward up Bald Eagle Valley to connect directly with Interstate 80. The general concept of a north-south, high-speed roadway connecting the Pennsylvania Turnpike in Southern PA with I-80 seemed logical, but developing a routing plan that pleased everyone was another matter entirely.

In the early stages of planning for I-99, Penn DOT recognized that 90% of cars and trucks on Routes 322 and 220 were driving to State College (Joseph, 2004). Consequently, Penn DOT decided to divert I-99 out of Bald Eagle Valley and cross over Bald Eagle Mountain to reach Nittany Valley. The natural depth of the Skytop wind gap had been sufficient (presumably with some modifications) years earlier to allow the existing Route 322 roadway to cross the mountain. But Penn DOT engineers also understood that for a limited access, high-speed highway to cross through the gap a significant amount of excavation was necessary to deepen the gap enough to meet grade requirements.

Before this could become a reality, however, alternative routes had to be examined for passing the new road through Bald Eagle Valley and across Bald Eagle Mountain. What impacts would such a high-speed, four-lane highway have on the environment and nearby population centers? Some consequences would depend on the route chosen: should the highway be routed, as much as possible, along the valley floor or high on the mountainside? In either case, it was inevitable that the roadway would cross Bald Eagle Mountain for this segment of I-99 to link State College with I-80. Preliminary

studies of the geologic and environmental setting, including the west side of Bald Eagle Mountain, quickly identified challenges with constructing a four-lane highway. Potential environmental problems existed in the valley bottom, the west slope of Bald Eagle Mountain, and the ridge crest.

That plans for building a four-lane highway conflicted with environmental concerns is not surprising. Pennsylvania is home to a broad, diverse range of flora and fauna and much of the Commonwealth is covered with forests, farmlands, and wetlands. Bald Eagle Mountain, one of the major geologic features through which the roadway would pass, contains a variety of habitats, including “mature forests, late successional stage fields, perennial and intermittent streams, and hillside seeps” (DCNR website). Individuals and organizations dedicated to preserving the wildlife have helped establish designated areas to protect certain species. For example, the Audubon Society has designated large parts of Bald Eagle Mountain as Important Bird Areas (IBA’s) and within this domain site #1140 is listed as “D3”, indicating certain species exist in a rare and/or unique habitat (see netapp.audubon.org/iba/site/1140). The Audubon Society counts among the protected birds on Bald Eagle Mountain the Broad-Winged Hawk, Cerulean Warbler, and the Wild Turkey.

In addition, the Indiana bat is a well-known protected species and exists in an Important Mammal Area (IMA) on Bald Eagle Mountain (pawildlife.org/imap.htm). The bats in particular received attention during public discussion prior to I-99 construction in the 1990’s, including from sources out of state (e.g., Deseret News, 1998; Kinney, 1999). Several hundred of the Indiana species of bat were known to winter over in an old limestone mine in Blair County, some 20 miles from Skytop. The U.S. Fish and Wildlife Service decided in 1994 that the cave was too far away to affect the I-99 plan, but pressure from local citizens and environmental groups, including a court battle won by environmentalists over the endangered species, forced the Fish and Wildlife Service (FWS) to continue their search for bats that could be affected by logging and development (Kinney, 1999). The FWS was also concerned about the mountainside’s wildlife habitat in general, including isolated wetlands. The FWS preferred I-99 to pass through the valley and avoid Bald Eagle Mountain as much as possible.

But a valley route for I-99 offered plenty of challenges for PennDOT, including the presence of Bald Eagle Creek (designated a Cold-Water Fishes/Migratory Fishes stream), wetlands, small towns, and numerous private properties. Some of these, indeed, were encountered during construction of the final route, part of which had to traverse northeastward up the valley from Bald Eagle.

The western slope of Bald Eagle Mountain posed significant engineering challenges. One obvious problem was the boulder field exposed at the surface – primarily talus consisting of rocks that range from fist-size to more than 2 m in length. Sandstones resistant to erosion typically cap mountain ridges in Central Pennsylvania. Double-ridged mountains, such as Bald Eagle Mountain, are common. The Bald Eagle and Tuscarora Formations cap those ridges. The slopes beneath each ridge are covered by the respective formation’s talus.

Talus and other colluvium combine to form a thick cover on the western slope of Bald Eagle Mountain. Test drilling demonstrated that colluvium low on the slope was more than 100 feet thick in places. Mountain slopes in central Pennsylvania typically have a colluvial mantle that thickens from slope top to bottom. Colluvium can have variable but usually thick concentrations of talus boulders on top of it, making it heterogeneous in fragment size, rock type, soil type and thickness, and overall

thickness. Particularly on steeper slopes the colluvium is unstable and is subject to downhill creep. For I-99 roadway construction, talus and other colluvium had to be removed and a road base built on a relatively solid bedrock foundation. Large boulders, of course, are subject to downhill movement, ranging from slow creep to rock fall rates. Talus boulders probably constitute the most obvious threat to roadways and drivers.



Figure 2. Geologic map of the Port Matilda area in Bald Eagle Valley. The double ridge crest of Bald Eagle Mountain (BEM) is composed primarily of the Bald Eagle (Obe), Juniata (Oj), and Tuscarora (St) formations and is shaded in gray. Highway 220 lies along the valley floor, sub-parallel to Bald Eagle Creek, west of the mountain. Near the top of this map (1976 vintage) Route 322 splits from Route 220 and ascends the west side of BEM to Skytop. The approximate path of I-99 is shown as the thick blue line. I-99 uses a much longer path than Route 220 to climb BEM in order to maintain a relatively low grade. Both routes cross a thick mantle of colluvium and talus that overlies Devonian age carbonates, siltstones, and shales. (Highways 220 and 322 now share the I-99 path, according to the latest PennDOT highway map for Centre County.) Nittany Valley lies to the east of BEM and hosts Cambro-Ordovician units comprising mostly carbonates and sandstones. Note the presence of cross-strike faults in Nittany Valley, including two that cross the mountain in wind gaps east and south/southwest of Port Matilda. Base map adapted from Hoskins (1981).

Another source of potential slope instability on Bald Eagle Mountain was the bedrock underlying the roadway path. The upper part of Bald Eagle Mountain's northwest slope consists of clastic sediments whose bedding dips range from steeply overturned at the ridge crest, changing down slope northwestward to beds dipping moderately to the northwest. Closer to the valley floor the bedrock is a mix of gently-dipping clastic and carbonate sedimentary rocks. For example, soft fissile shales of the Rose Hill Formation support the upper, western slope of BEM and their overturned beds with steep dips contribute further to instability. Farther downslope, thinly-bedded, argillaceous limestones of the Tonoloway Formation afford a base of only marginal strength. Karst solution is an additional problem affecting limestones in the local stratigraphic section. Small sinkholes were, in fact, noted while mapping the west side of Bald Eagle Mountain (Doden *et al.*, 2009). The combination of colluvium/talus, sedimentary bedrock, and structures lends itself to potential mass movements.

Interstate 99, also known as the Appalachian Thruway and the Bud Shuster Byway, received its designation in an unusual, if not controversial, sequence of events. Most Interstate Highway numbers are assigned by the American Association of State Highway and Transportation Officials (AASHTO) to fit into an established east-west and north-south grid system of numbering (AASHTO report, 1998). Under this orderly system, the lowest numbers are on the U.S. West Coast and the highest numbers are on the East Coast. Several north-south routes, including Interstates 81, 83, 87, 89, 91, 93, 95, and 97 all lie east of I-99. The number "99" conflicts with the standard numbering convention associated with Interstate highways. Per numbering guidelines, I-99 should be near the Atlantic coast, not in central Pennsylvania. I-99, however, received special consideration by Bud Shuster, Congressional Representative of the district through which the highway passes. It was written into Section 332 of the National Highway Designation Act of 1995 by Shuster, who at the time was also chair of the U.S. House Committee on Transportation and Infrastructure. This was the first Interstate Highway number to be written into law rather than to be assigned by AASHTO (AASHTO report, 1998). Representative Shuster said that the standard numbering was not "catchy", and so designated the new route as I-99 after a street car Number 99, that took people from Shuster's hometown of Glassport to McKeesport (Hamill, 2008).

Congress approved the I-99 designation as part of the National Highway System Designation Act, signed into law by President Clinton on November 28, 1995 (GPO report, 1995). Three years later, on November 6, 1998, the part of I-99 between Bedford and Bald Eagle was approved by AASHTO's Route Numbering Subcommittee. The freeway north of Bald Eagle, yet to be built, remained undesignated at the time.

Four years later work began to extend I-99 northeast from Bald Eagle through Port Matilda to State College. However, unlike earlier parts of I-99, the path of this latest extension was highly controversial. Environmentalists wanted I-99 to be constructed in Bald Eagle Valley, whereas PennDOT and some valley residents advocated a route that took the freeway above the valley and along the side of the ridge. Following considerable debate among community members and state government representatives (Gibb, 2002; Bock, 2007; Hamill, 2008), the final roadway configuration (see Figure 2) resulted in I-99 passing through Bald Eagle Valley, diverting west around the village of

Port Matilda, then crossing back over the valley floor and continuing up the west side of Bald Eagle Mountain.

The “Discovery” of Pyrite at Skytop

I-99 diverts from Route 220 and follows Route 322 up the west side of Bald Eagle Ridge, where it crosses through the Skytop wind gap. Acid-producing rocks were exposed at Skytop during deep excavations there in 2002. This should not have been a surprise because since the 1950’s (Smith, 1977) generations of geology students from Penn State University visited the gossan exposed on a road cut on old Route 322. However, the true nature and abundance of these deposits was not understood prior to 2002.

The largest cut at Skytop was made through the eastern and highest ridge of the mountain, primarily in the Bald Eagle Formation, and secondarily in Reedsville and Juniata units. This major cut, as well as other excavations on Skytop, accounted for over 1 million cubic yards of bedrock removed. The ultimate depth of this cut depended, in part, on the configuration of roadways and bridges. The relatively narrow wind gap could not accommodate both roadways (I-99 and the existing Route 322) side-by-side through the entire gap and, consequently, one had to cross over the other. A critical decision, apparently, was made concerning the routing of the existing Route 322 roadway with that of the new I-99: PennDOT chose to route the two-lane S.R. 322 *over* the four-lane I-99, allowing use of a smaller bridge for local traffic on 322 and maintaining the lowest grade possible for I-99. This configuration avoided construction of a much larger bridge(s) for I-99, probably a cost-effective decision regarding bridges. However, the large cut had to be made sufficiently deep to accommodate the wide four-lane I-99 roadway. This deep excavation penetrated well into the pyrite-bearing bedrock, probably deeper with a wider cut than would have been needed for only a two-lane roadway.

Work began on the Skytop segment of I-99 in 2002 and the deep cut through Bald Eagle Mountain advanced quickly. But in 2003 an excavator operator noticed some “unusual shiny minerals” among the rock fragments (personal communication to the authors). PennDOT halted further excavation until the problem could be dealt with properly. The sequence of events regarding who amongst PennDOT, Department of Environmental Protection (DEP), and various contractors first recognized and reported the pyrite occurrence is not clear (e.g., Centre Daily Times report of 15 Feb. 2004). But in any case, the pyrite discovery came *after* some 1,000,000 cubic yards had already been excavated and distributed as cut and fill material. The work required to remediate the pyrite and associated acid runoff problems was neither simple nor easy. Details of the Skytop ARD remediation are discussed in other papers of this guidebook.

The pyrite problems were more or less under control four years later, so construction resumed on the portion of the freeway south of Skytop Mountain. The I-99 section from Bald Eagle to Port Matilda was opened to traffic on December 17, 2007, whereas the remaining part between Port Matilda and the west end of the Mount Nittany Expressway near State College was finally opened by November 17, 2008. In all, the Bald Eagle–State College section of I-99 cost \$631 million to construct (Hamill, 2008). The pyrite mitigation alone cost approximately \$120 million. Following completion of the Bald Eagle-to-State College-segment I-99 was extended via the pre-existing Mount Nittany Expressway to meet I-80 northeast of Bellefonte.

References

- Appalachian Regional Commission Report, 2009, Status of the Appalachian Development Highway System as of September 30, 2009 (PDF).
- AASHTO report, 1998, "Report of the Special Committee on U.S. Route Numbering to the Standing Committee on Highways" American Association of State Highway and Transportation Officials.
- AASHTO web site: <http://www.transportation.org/Pages/Default.aspx> "Report of the Special Committee on U.S. Route Numbering to the Standing Committee on Highways", American Association of State Highway and Transportation Officials. May 31, 2003.
- Bock, Greg, 2007, "Long-awaited I-99 stretch opens", (December 18, 2007). Altoona Mirror.
- Joseph, Mike, 2004, "An environmental challenge", (February 15, 2004) Centre Daily Times newspaper archives, article #220, State College, PA www.centredaily.com.
- Kinney, David, 1999, "Endangered bat stalls road project", Los Angeles Times, (September 26, 1999).
- Department of Conservation and Natural Resources (DCNR) website: www.dcnr.state.pa.us
- Doden, Arnold G., and Gold, David P., 2009, Bedrock Geologic Map of the Julian Quadrangle, Centre County, Pennsylvania. Pennsylvania Geological Survey Open-File Report. 1:24,000 scale map.
- Dooms, T.M., 2015, 50 Years of Town & Gown: Controversies shape the growth – and nongrowth – of Happy Valley. June edition of Town & Gown Magazine, p. 28-34.
- Gibb, Tom (December 7, 2002). "I-99 segment gets environmental OK". Pittsburgh Post-Gazette.
- Government Printing Office (GPO), 1995, National Highway System Designation Act of 1995, <http://www.gpo.gov/fdsys/pkg/PLAW-104publ59/html/PLAW-104publ59.htm>
- Hamill, Sean D. (December 27, 2008). "Road Stirs Up Debate, Even on Its Name". The New York Times.
- Louis Berger Group *et al.*, 2003 for the Federal Highway Administration (FHA), U.S. Dept. of Transportation, Pennsylvania I-99 Summary Report, 2003, www.fhwa.dot.gov/planning/economic_development/technical_and_analytical/i99pa.cfm.
- [Netapp.audubon.org/iba/site/1140](http://netapp.audubon.org/iba/site/1140).
- Pennsylvania Official Transportation Map (PDF). Pennsylvania Department of Transportation. 1989.
- Smith, R.C., 1977. Zinc and lead occurrences in Pennsylvania. Pennsylvania Geological Survey, 4th ser., Mineral Resources Report 72, 318 p.
- <http://thomas.loc.gov/cgi-bin/bdquery/z?d102:HR02950>, Bill Text H.R.2950"
- www.pawildlife.org/imap.htm

GEOLOGY OF THE SKYTOP ROADCUTS CENTRE COUNTY, PENNSYLVANIA

DAVID (DUFF) GOLD¹ AND ARNOLD G. DODEN²

WITH CONTRIBUTION FROM ANDREW SICREE³ AND RYAN MATHUR⁴

¹ EMERITUS PROFESSOR OF GEOLOGY, DEPARTMENT OF GEOSCIENCES, THE PENNSYLVANIA STATE UNIVERSITY, UNIVERSITY PARK, PA, ² GMRE (GEOLOGIC MAPPING AND RESOURCE EVALUATION), INC., 925 WEST COLLEGE AVE., STATE COLLEGE, PA, ³ CONTINUING EDUCATION, THE PENNSYLVANIA STATE UNIVERSITY, UNIVERSITY PARK, PA, ⁴ DEPARTMENT OF GEOLOGY, JUNIATA COLLEGE, HUNTINGDON, PA

Introduction

This version of the geology of Skytop could not have been developed without the deep excavations associated with the construction of an interstate highway. These provided fresh exposures of bedrock in an area of few outcrops, as well as the interface between oxidized and reduced conditions in the same strata. This interface zone coincided with a fluctuating groundwater table and set the stage for efflorescent mineral precipitation on the deeper slopes. The Skytop story is one of relatively rapid geological changes in response to construction operations, and blends inherent condition with anthropogenic operations.

Skytop is the name given to a wind-gap in the Bald Eagle Ridge, approximately 5 miles (8 km) west of State College, in central Pennsylvania (Figure 1). This wind gap has long been used as a transportation route between Nittany Valley to the east and Bald Eagle Valley to the west. State highway Route 322 and Interstate 99 cross the ridge through this saddle. In addition to Skytop being the westernmost ridge of the Ridge and Valley Physiographic Province it also forms the boundary between two structural domains. The C-12 section in Figure 1 coincides with mesoscopic scale

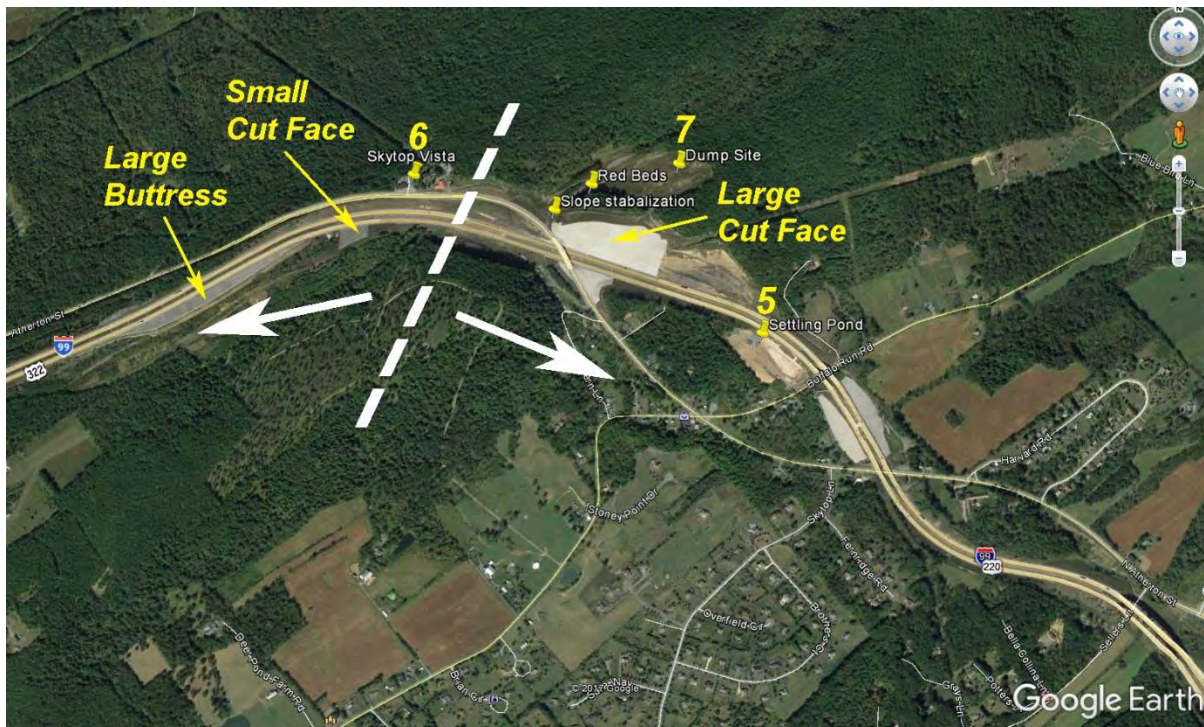


Figure 1. Skytop area. State College is 5 miles to the ESE. The white dashed line is the divide in the windgap and separates contract sectors C-12 from A-12, as well as structural domains.

chevron folds, and the A-12 section with a steeply-dipping structural domain characterized by monoclinical terrain.

The unusual and unexpected geology provided a challenge to highway construction. Because these conditions are site specific, it is convenient to consider the problems encountered by locality. Fortuitously, the engineering Section C-12 corresponds to a geologic terrane in which the bedrock structure is dominated by sharply hinged (chevron) folds, whereas the A-12 section is characterized by uniformly steeply dipping strata. The section C-12, west of the ridge crest (Figure 1), is slightly oblique to the strike of chevron folds, whereas section A-12 between Skytop and Buffalo Run curves through the bedrock lithology in a deep cut, well below oxidized near-surface rocks and into a drained groundwater regime.

The deep roadcuts, well below the water table introduces an added REDOX parameter to geologic mapping that is rarely encountered except around sulfide ore deposits. An irregular zone between weathered (oxidized) and fresh (reduced) regimes that approximate the fluctuating ground water table, is referred to as a REDOX front. This interface may be highly pinnacled, especially in well-jointed rocks.

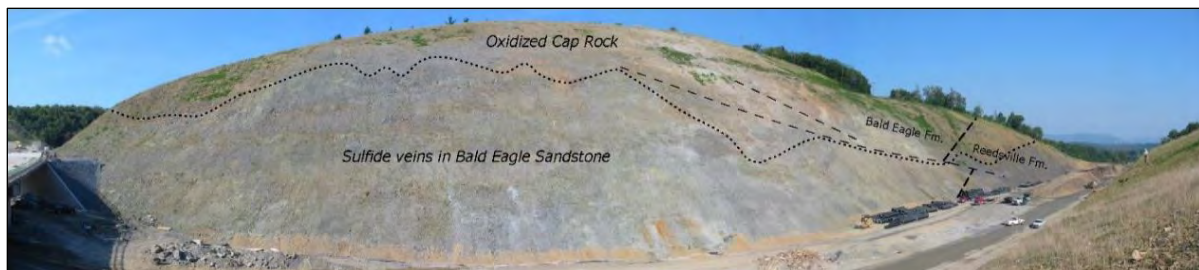


Figure 2. Panoramic view of Large Cut Face (LCF) showing sulfide-bearing rock beneath oxidized cap rocks. Growth of efflorescent minerals on the former resulted in weather sensitive color changes of the slope.

Several unusual geologic conditions contribute to the location of the ridge as well as the position of the wind gap. These include an overturned sequence of competent (and erosionally resistant) sandstone units and less competent limestone and shale units beneath a major thrust fault, a set of mesoscopic⁵ to macroscopic⁶ scale low-angle faults, striking generally 110° (see Figure 1), with a left lateral strike-slip component, and a late vein system trending generally 160° through the competent rocks. A gossan zone on Route 322 was visited periodically on geology class field trips, but the magnitude of this pyrite-bearing vein system was unexpected. The presence of chevron folds in the Silurian beds underlying the western slope of the ridge was another unexpected condition conducive to the development of landslides. This paper attempts to record the pertinent geological features now buried beneath the remedial cover as well as landscaped slopes.

Pyrite-bearing veins, well developed in the Bald Eagle sandstone, were exposed in the “Large Cut Face” (LCF) road-cut over approximately 1000 feet. A visual estimate of 4 to 5% pyrite by volume is

⁵ Mesoscopic refers to “features” ranging from 1 cm to several meters in size.

⁶ Macroscopic refers to “features” ranging from several meters to 10 kilometers in size

Supergene minerals, such as limonite, hematite and jarosite have locally precipitated locally onto joints in OCR over vein networks (Figure 5). To the locals, these are the “rainbow rocks”, highly sought after as ornamental pieces.



P7280032



106-0622-3



106-0671



106-0646

Figure 5. “Rainbow Rock”. Gossan stain in OCR over sulfide veins.

Geological Setting

Central Pennsylvania is characterized by contrasting topography, with relatively flatland of the Appalachian Plateau Physiographic Province to the northwest, and sinuous ridges with broader intervening valleys of the Ridge and Valley Physiographic Province to the east. Skytop is set at this boundary (Figure 1), overlooking the Allegheny Front to the northwest, separating major structural domains. Figure 6 is a terrain map which graphically illustrates the contrasting topography between provinces.

On the northwest side of Skytop Upper Silurian and Devonian age rocks underlie most of Bald Eagle Valley, and extend upwards into Mississippian and Pennsylvanian aged rocks on the Appalachian Plateau. The thickness of these units is estimated to be 2000+ feet for the Silurian strata (Laughrey, 1999), 8000 feet for the Devonian strata (Harper, 1999), and 1280 feet for the Mississippian strata up to the Pocono Formation (Berg, 1999). Thus, there is a stratigraphic discordance of 14,000 feet (4375 m) between the Tuscarora Formation in the crest of Bald Eagle Ridge and rocks at equivalent altitude

on the Plateau (Pocono Formation). These accordant summits represent the Schooley peneplain, an early Tertiary erosion surface (Williams and Slingerland, 1985), with an estimated 15,000 feet (4573 m) of denudation at the Allegheny escarpment since the Permian (Paxton, 1983).



Figure 6. Lidar terrain and geologic map graphically illustrates the boundary between the Appalachian Plateau Physiographic Province to the northwest and the Ridge and Valley Physiographic Province to the east. The Skytop Roadlog stops are indicated by the yellow dots. ERPA is the Engineered Rock Placement Area for sequestering toxic waste rock, to the southwest of Skytop, also indicated by a yellow dot.

Cultural and agricultural development likewise is influenced by topography and geology. The valleys between the more resistant sandstone ridges are eroded into carbonate rocks, over which are developed thick soils suitable for arable agriculture. Communication between the early settled valley bottoms was mainly through the wind and water gaps that occur at irregular intervals through the ridges. Modern transportation routes tend to follow the early road networks, but with an enhanced scale of excavation.

Stratigraphy

The dominant lithologies along I-99 between Bald Eagle Valley and State College increase in age from Devonian to Cambrian. The pertinent section at Skytop is shown in Table 1. Subdivisions of these formations recognized elsewhere in central Pennsylvania were not mapped at Skytop, except for the Antes Member of the Reedsville Formation.

Table 1. Abridged stratigraphic section for Centre County

Silurian		
Rose Hill Formation	600-800 ft?	Dominantly shale and siltstone
Tuscarora Formation	400 ft	Quartzose sandstone (quartzite) and minor shale
Ordovician		
Juniata Formation	600 ft	Red shales, siltstones and sandstones
Bald Eagle Formation	700 ft	Green impure sandstones, with minor siltstones and shales
Reedsville Formation	600-700 ft	Dominantly shales, minor siltstones and coquinas
Antes Member	70-80 ft	Black carbonaceous, calcareous shale
Coburn Formation		Interbedded limestone and calcareous shale

These units represent a succession of transgressions and regressions, progressing upwards from marine shelf carbonates and shales to clastic “red beds” and the beach sand deposits of the Tuscarora Formation.

A reduction of thickness for all formations exposed along I-99 through Skytop is apparent when compared to the typical regional thicknesses for these units. The greatest reductions are in the shaley units. The upper member of the Juniata Formation appears to be missing.

Coburn Formation

The upper part of the Coburn Formation is exposed in the eastern part of the southbound lane at the LCF (Lower Cut Face), at engineering station 902+00 and in the northbound road cut bank at station 901+00. Here the beds strike 060°, dip steeply southeast and are overturned, with tops to the northwest. The contact with the overlying Reedsville Formation coincides with the break in slope leading up to Bald Eagle Ridge. The topography from here to Buffalo Run is characterized by gentle swales, a paucity of surface drainage, and sinkholes (near the settling ponds). This under-drained system reflects a carbonate bedrock.

The Coburn Formation typically consists of interbeds of dark gray to black calcareous shale and dark bluish gray limestone. The beds range in thickness from 20 to 50 cm, with a shale to limestone ratio of approximately 1:2. The limestone beds are very fine-grained to micritic with relatively rare fossils. These interbeds are considered to be rhythmites, deposited below storm wave base in a shelf/slope environment. A spaced cleavage (097°/40°) with a sigmoidal shape is developed in the shale beds and appears to be refracted into the limestone beds. Although this cleavage is compatible with an overturned limb of an anticline, the shallow angle suggests it was formed before the limb was rotated to its current overturned attitude: probably before the development of the Birmingham thrust system.

The general attitude of the beds is 060°/80° with tops to the northwest (i.e., overturned). Some 4th order folds occur locally. Their S configuration and shallow plunge suggest they are drag folds

associated with the Nittany anticlinorium. Well-developed joints (Plate 1-2, c) are preserved locally, and some of these host thin (< 1 mm) veinlets of pyrite. The general attitude for these fractures is 160°/90°, and they are interpreted to be the Late Alleghanian J₂ joint set (Srivastava and Engelder, 1990).

Several faults striking 090° to 120°, and dipping 30°-50° north, are apparent in the northbound LCF as the break-away surfaces of small landslides (Figure 14). Although these faults are spoon-shaped and irregular on a meter scale, their surfaces are smooth. These faults are classified as left oblique-slip normal, with a transport direction of 30°/285°. The development of land-slip scarplets where the faults were “daylighted” on the northbound road-cut slopes, prompted PennDOT to lay these slopes back to 2H: 1V. Another fault (strike 120°, dip steeply northeast) displaces the Reedsville/Bald Eagle contact in the north side road-cut approximately 120 feet up from station 889+00 to 891+00 (Figure 2). Rotation of the adjacent beds into the fault plane and sense of displacement for stratigraphic juxtaposition suggest this fault has a high dextral strike-slip component.

The transition into the overlying Bald Eagle Formation is marked by an increasing number of sandstone interbeds over an interval of 20-30 feet. The contact is placed at the first persistent sandstone bed. It is a muddy sandstone, generally devoid of any internal structure and highly bioturbated.

Antes Member

The Antes Member of the Reedsville Formation is exposed as a 70-80 feet thick section of black carbonaceous calcareous shale. It is exposed in the road cuts as a fissile shale (Plate 1-1, c & d). Springs and seeps occur along the contact with the underlying Coburn limestone. A non-cohesive mud near the base is the source of some road-bed instability. The occurrence of syngenetic pyrite and the high organic content in these shales suggests anoxic depositional conditions.

Reedsville Formation

The calcareous shales of the Antes Member grade upward into olive gray shales and buff/tan siltstones of the main Reedsville Formation. Towards the eastern end of the southbound road cut (LCF), the shale is weathered to a buff/brown color to a depth of 50 feet. Shale is the dominant lithology in the lower part of the formation with minor siltstone interbeds 10 to 50 cm thick towards the middle. Rare coquinas (fossil hash) that locally are ferruginous and sideritic (Clinton-type iron ore) are more common near the top of the formation, where they are seen as rusty weathering zones, up to 1-m thick, in the road cut.

The general attitude of the beds is 060°/80° with tops to the northwest (i.e., overturned). Some 4th order folds occur locally. Their S configuration and shallow plunge suggest they are drag folds associated with the Nittany anticlinorium. Well-developed joints are preserved locally, and some of these host thin (< 1 mm) veinlets of pyrite. The general attitude for these fractures is 160°/90°, and they are interpreted to be the Late Alleghanian J₂ joint set (Srivastava and Engelder, 1990).

Several faults striking 090° to 120°, and dipping 30°-50° north, are apparent in the northbound lane road cut as the break-away surfaces of small landslides (Figure 15). Although these faults are spoon-shaped and irregular on a meter scale, their surfaces are smooth. These faults are classified as left oblique-slip normal, with a transport direction of 30°/285°. The development of land-slip scarplets

where the faults were “daylighted” on the northbound road-cut slopes, prompted PennDOT to lay these slopes back to 2H: 1V. Another fault (strike 120°, dip steeply northeast) displaces the Reedsville/Bald Eagle contact in the north side road-cut approximately 120 feet up from station 889+00 to 891+00 (Figure 2). Rotation of the adjacent beds into the fault plane and sense of displacement for stratigraphic juxtaposition suggest this fault has a high dextral strike-slip component.

The transition into the overlying Bald Eagle Formation is marked by an increasing number of sandstone interbeds over an interval of 20-30 feet. The contact is placed at the first persistent sandstone bed. It is a muddy sandstone, generally devoid of any internal structure and highly bioturbated.

Bald Eagle Formation

The Bald Eagle Formation consists mainly of greenish-gray impure sandstone (low rank graywackes) in beds typically 1 m thick. Rip-up-clasts (Figures 2, 5 and 7), up to 20 cm across, occur at the base of many of the beds, which grade upward through poorly sorted cross-bedded sandstone into planar bedded shale and siltstone 3-10 cm thick. The bedding cycle is repeated in a coarsening upward sequence. Despite the deep excavation in Bald Eagle strata at Skytop, the degree of alteration from the emplacement and weathering of sulfide veins renders these rocks poor candidates for developing a stratigraphic section. The imprint of sulfide mineralization is sufficient to alter the nature of the host, where the sandstones have been reduced in color and competence to a drab green/gray color friable “funky” sandstone, some of which have an oily green hue (Figure 7). Two distinct colored zones are apparent in the LCF above the southbound lane. The lower zone has a drab green/gray color that takes on whitish yellow overtones during dry periods, whereas the light rusty brown to buff colored upper section, near the skyline, is part of the “oxidized cap rock” gossan.



Figure 7. Pyrite veins in reduced Bald Eagle sandstone. Note rip-up-clasts on bedding surface (IMG 106 082: 4/19/1004).

The Bald Eagle sandstones are low rank graywackes are composed mainly of quartz and minor feldspar set in a matrix of chlorite and illite (Thompson, 1970a, 1970b). The rocks exhibit a granular “sugary” texture, with subangular to subrounded quartz grains that vary in size from coarse to fine. Accessory minerals include magnetite, xenotime, and zircon (Horowitz, 1970). The diagenetic history

has been complex, and it is apparent that the green-gray color is not primary, but represents a later regional episode of aqueous reduction and dissolution (Thompson, 1970a). These reducing “fluids” were neither pervasive nor stratabound. A deep-maroon colored sandstone was exposed at station 888+00 approximately 40 feet above the base, and at the new Route 322 Bridge over I-99, red sandstone beds change along strike into green beds. At this latter site, red beds (Figure 3) of the Bald Eagle Formation, with similar morphology and composition (rip-up-clasts, cross-bedded sandstone and overlying siltstone and shale) owe their color to ferruginous clays and hematite (Horowitz, 1970). It is apparent that reduction diagenesis converted the clay minerals to chlorite and the hematite to magnetite (Thompson, 1970a). Pyrite that occurs as the matrix, cementing quartz grains in small knots of 1-3 mm across, is believed to be part of this reduction process. A likely cause is the late Alleghanian gas drive, recognized by Engelder (2004) and Lacazette (1991) as the hydrofracturing medium for the regional J₂ joints.

The contact with the overlying Juniata Formation is an enigma, because a commonly held criterion based on color is invalid. Unfortunately, the convenient stratigraphic marker of the Lost Run Conglomerate (present elsewhere in the state) is not developed locally. The Lost Run Conglomerate marks the transition from a coarsening upward to a fining upward depositional condition for the Juniata Formation; a sequence increasingly dominated by red shale. Thus, the rocks assigned to the Bald Eagle Formation should be restricted to those deposited in the regressional cycle, and those of the Juniata Formation to the next transgressional cycle.

Juniata Formation

The basal sandstones of the Juniata Formation resemble those of the Bald Eagle Formation with shale rip-up-clasts in coarse-to fine-grained, cross-bedded sandstones on a meter scale, with thin interbedded shales and siltstones. The shale beds become thicker and more dominant upwards. They are characterized by a deep reddish-brown to maroon color and the pervasiveness of ferruginous clays (dominantly illite) and hematite in the matrix. At Skytop, the formation is projected to be approximately 600 feet thick, with part of the Middle (Plummer Hollow Member) and Upper Juniata (Run Gap Member) strata missing.

Pale green to cream-colored reduction zones are apparent in these vividly colored rocks. The REDOX fronts either are stratabound (usually sub-parallel to some sandy bed), or are transgressive to bedding (associated with fractures and/or sulfide-bearing veins).

The contact with the overlying Tuscarora Formation is marked by the presence of a very light gray to white, clean, well-sorted sandstone (quartzite) interbedded with vari-colored cream, pink and buff-colored shale and siltstone over a stratigraphic interval of 10-15 feet.

Tuscarora Formation

The Tuscarora Formation typically is made up of beds 20 cm to 2 m thick of a hard, clean, whitish cross-bedded, quartzose sandstone with thin shale interbeds. The sandstones are composed dominantly of well-sorted quartz grains cemented with quartz to form a tough, hard, competent rock with minimum porosity. Most of the quartz grains are subrounded, and vary in size from coarse to fine in well-defined cross-beds. The rock is referred to as quartzite because a siliceous cement bonds adjacent grains.

These rocks are exposed along the crest of the western (highest) ridge and underlie parts of the upper northwest slope. At Skytop they crop out behind the microwave antenna and in the road cut to the southwest along old Route 322. In contrast to the steeply overturned attitude of the underlying Juniata Red beds, these quartzite beds dip 20°-40° to the southeast and appear to be overturned.

Mesoscopic scale asymmetric chevron folds (Figure 8, right) were exposed during construction of the C-12 section of I-99 between stations 813+00 to 861+00 (see Figure 3 geologic map and closeup of the C-12 section below, in Figure 9). These were seen to have long (30-50 m) southeast limbs dipping 30°-50° NW and shorter northwest limbs (10-15 m) dipping 20°-40° SE.

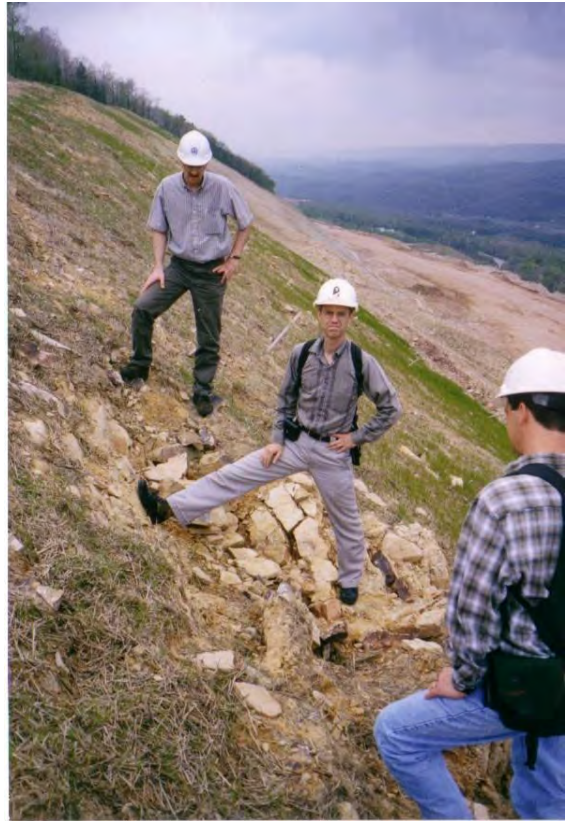


Figure 8. Chevron fold on slope above Big Buttriss, in C-12 sector (domain). Paul Zell (middle) with each leg perpendicular to bedding plain.

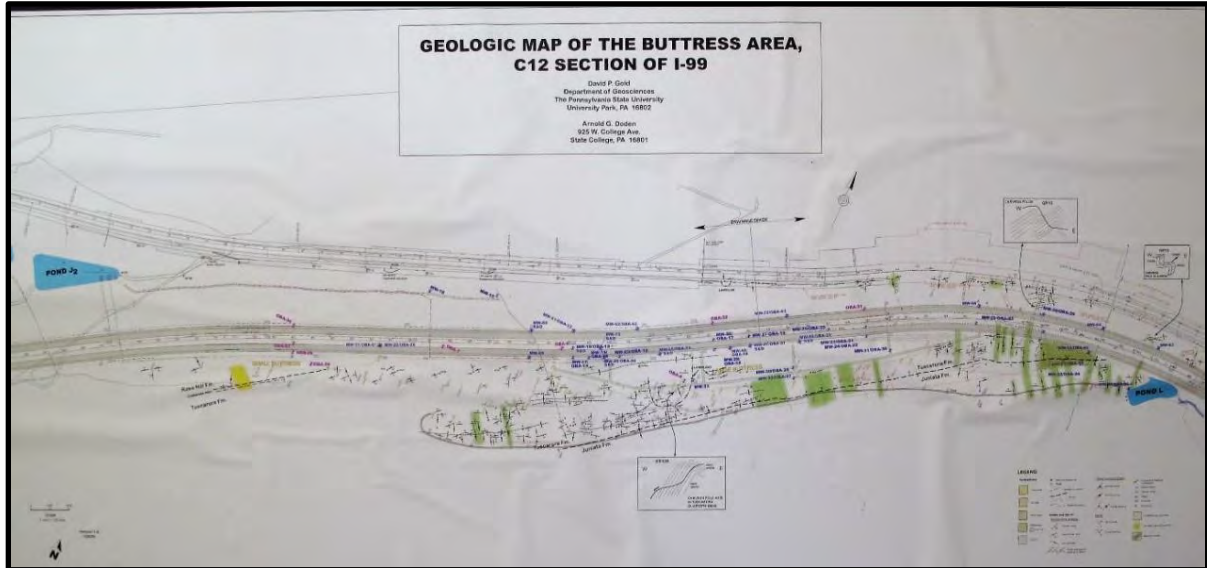


Figure 9. Geological Map of roadcut in section (domain) C-12; slope above Big Buttriss, showing mesoscopic scale chevron folds.

Favorable conditions for slope failure (landslides) were developed when and where construction cut slopes exceeded the bedding dip (refer to Figure 16c in the Structure section of this article). Because of close match in scale between natural (chevron folds) and anthropogenic (road cut) slopes many small landslides developed on both sides of the road cut (Figure 10). To stabilize these slopes, those adjacent to the northbound lane were cut back from 1H: 2V slope to 2H: 1V slope gradient. In

addition, as a preventative measure, the toe on the northbound road bed was raised up to 17 feet between stations 833+00 and 855+00 (bifurcation zone).

Joints are well developed in the Tuscarora Formation. Three sets occur pervasively with regular spacing from 30 cm to 1 m. The earliest is J_1 , a strike joint dipping approximately perpendicular to bedding. Later cross-strike joints J_2 are nearly vertical joints, developed in the dip plane of the beds. The third set are bedding joints. In many places along Bald Eagle Ridge these joints are stained with iron oxyhydroxide (gossan) minerals (Figure 5). These are part of an oxidized cap rock, widely diffused beyond the limits of any underlying sulfide-bearing veins, along the J_1 joints. Steeply dipping sulfide- and sulfate-bearing veins are exposed locally in the road cuts. They have a general strike of 160° , and locally form vein networks (stations 858+00 to 861+00) (Figure 7). Phosphate minerals of the wavellite group have been found in some of the J_2 joints.



Figure 10. Tension gashes in headwall of rock slide. Slope above Big Buttress, C-12 sector (domain). Paul Zell for scale.

The tendency for the resistant quartzite beds to break out (also by frost heave) into rectangular blocks, led to their use as foundation stones in many of the early settlement buildings, and as refractory brick (ganister) in iron ore and ceramic furnaces. Frost heaved Tuscarora float occurs locally in open scree (talus) patches along the upper northwest slopes of Bald Eagle Ridge, and these were exploited as a source of ganister during the late 19th Century and early years of the 20th Century.

Rose Hill Formation

The overlying Rose Hill Formation is exposed locally in the road cut near the southwest end of the bifurcation zone (stations 813+00 to 817+00). The beds near station 813+00 dip southeast and appear to be overturned (045° - $055^\circ/40^\circ$ - 45°), but this may be anomalous due to the presence of kink band chevron folds on thrust faults. Vari-colored shales and siltstones occur at the base in a gradational contact with the interbedded shales and sandstones of the Tuscarora Formation. The Rose Hill Formation consists mainly of buff/brown to khaki-colored shales with minor silt interbeds. The high illite content in the shales enhances the slaking properties of these shales and their conversion into sticky mud.

Structure

Two distinct and separate structural domains are apparent on the mesoscopic scale. Fortunately, these two domains coincide with the construction sections designated C-12 for the western slopes of Bald Eagle Ridge and A-12 for the eastern slopes (Bedding attitudes range from 30° NE to 30° SW on the west facing slope (C-12 section), to steeply dipping overturned in the main A-12 road-cut. The general attitude for the Juniata and Bald Eagle strata is $070^\circ/80^\circ$ (overturned), and the relatively tight cluster (Figure 11) is consistent with steeply dipping beds in a relatively uniform monoclinial setting. In contrast, bedding attitudes for the C-12 domain define two maxima (Figure 12) with S-poles distributed along a steeply dipping great circle (a π girdle), whose pole, β ($5^\circ/060^\circ$) defines a fold axis.

This is the domain of the chevron folds with an interlimb (dihedral) angle of 84° . These settings are depicted in conceptual structural models in Figure 13, where the structural discordance of the Tuscarora Formation beds is accommodated in a kink band splay thrust setting. These models reflect a pre- and a post I-99 excavation knowledge base. The former, an “overturned fold model” presumed the Tuscarora beds exposed in the Rte. 322 road cut was overturned and detached from the underlying Juniata strata. The latter invokes a series of lystric thrust slices in an “imbricate thrust model” to account for the mesoscopic scale chevron folds in the Tuscarora beds.

A-12 Section Bedding

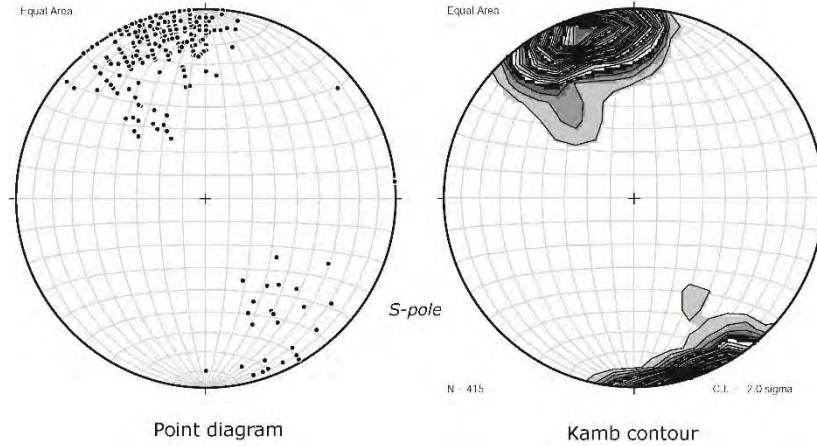


Figure 11. Orientation diagram of bedding in A-12 domain. The single maximum is consistent with steeply dipping monoclonal beds striking 060° .

C-12 section (Bifurcation) bedding

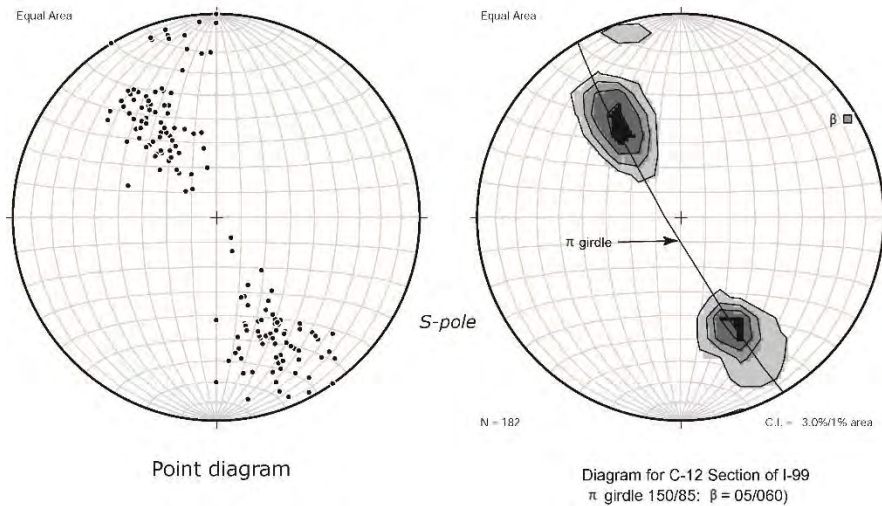


Figure 12. Orientation diagram of bedding in C-12 domain. The two maxima are consistent with vertical folds with sharp hinges, plunging $7^\circ/050^\circ$.

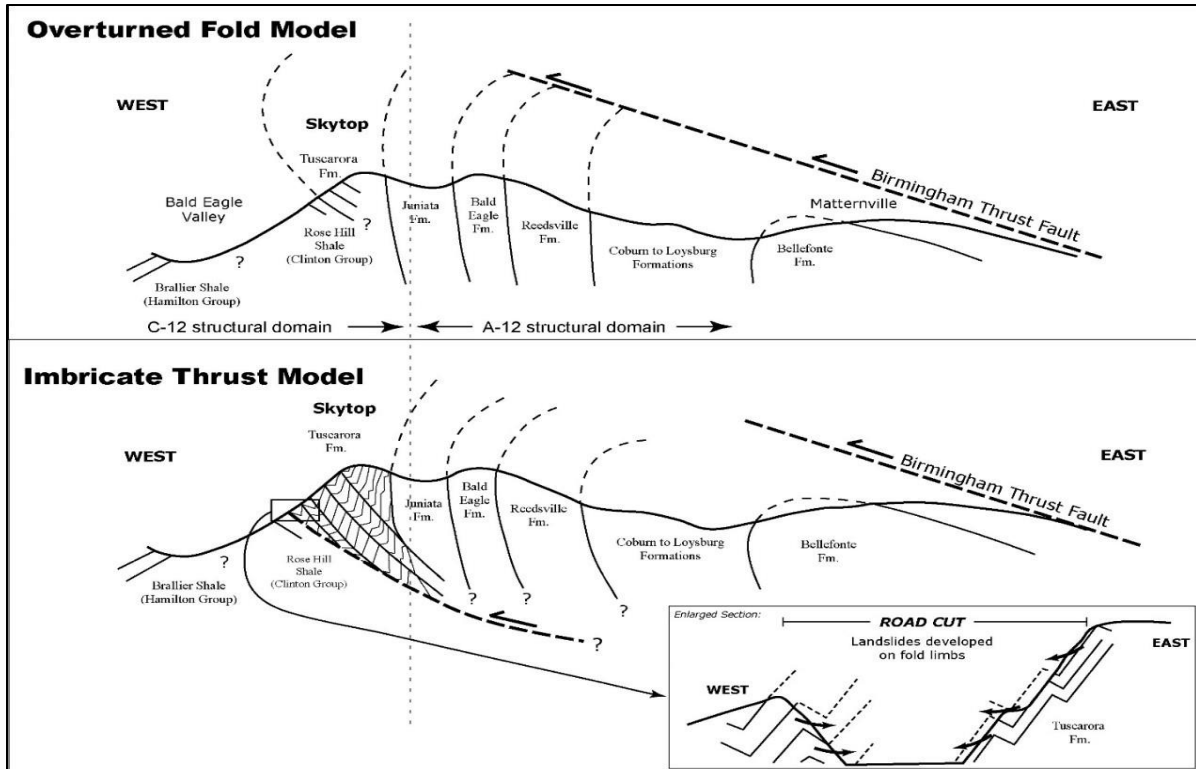


Figure 13. Conceptual models of Skytop structures from pre-and post-construction eras.

Structural anomalies noted during the excavation stage (April to August, 2002) still need to be reconciled. These include a mesoscopic scale fold (plunging 0° - $5^{\circ}/237^{\circ}$), exposed (August, 2002) above the present road bed locality near 863+50, in Juniata “red beds” (Figure 14). The counter-clockwise sense of this fold, indicating an east verging, anticlinal fold to the northwest is incompatible with the overall structural setting. A similar relationship was noted during the excavation stage (April, 2002) above and to the east of Station 838+00, where bedding ($223^{\circ}/75^{\circ}$) and cleavage ($225^{\circ}/45^{\circ}$) indicate a synclinal axis beneath Bald Eagle Ridge in an east verging fold. Potential rotation in the landslide block that was mapped in this area is insufficient to account for the reversal in cleavage attitude: kink band rotation on a duplex is a more likely explanation.



Figure 14. Mesoscopic scale fold in Juniata red beds. The counter-clockwise sense of this fold, indicating an east verging, anticlinal fold to the northwest is incompatible with the overall structural setting. (August 2002).

Mesoscopic scale faults are ubiquitous and their attitudes appear somewhat random until commonalities in type and setting are considered. Most of the bedding faults, so common in the Bald Eagle beds, have down dip slickenlines (dip-slip movement) that are consistent with a flexural slip mechanism during the folding of these beds in the Nittany Anticlinorium. However, some of these bedding faults have a dominant strike-slip component. These show up as the densest cluster of great circles (Figure 15) oriented ENE and dipping steeply SSE.

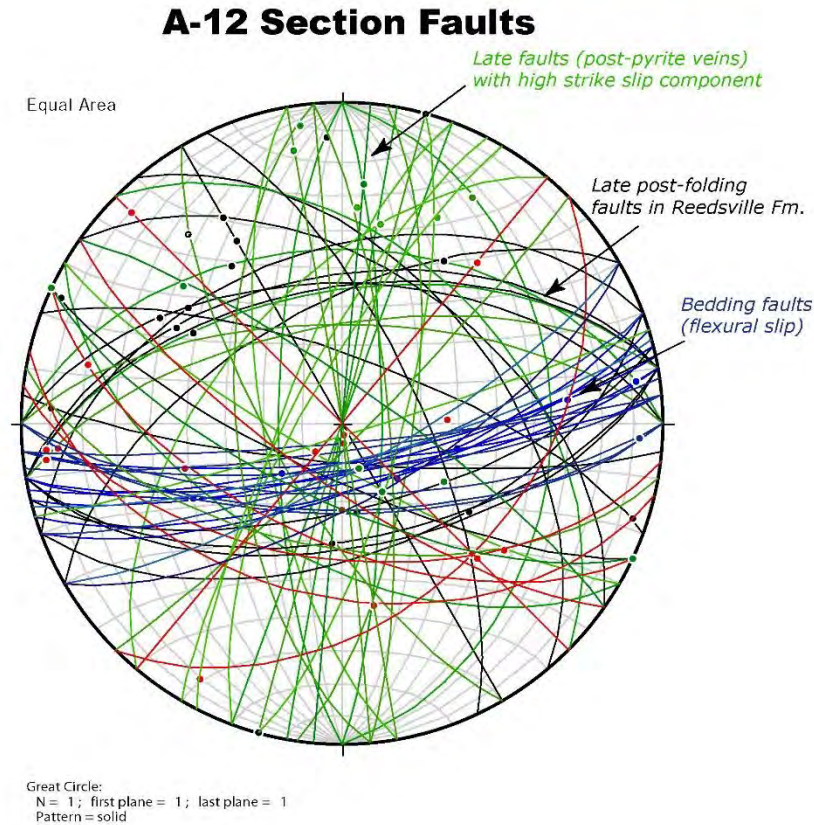


Figure 15. Great circle diagram of mesoscopic faults in A-12 domain.

At least a dozen mesoscopic scale, low angle, oblique-slip faults were mapped in the Reedsville Shale, particularly in the north-facing road-cut in the A-12 section. They have a general ENE strike and dip less than 45° north. Although these faults have smooth surfaces on a mm scale, they are scalloped and grooved on a mesoscopic scale, with a left oblique-slip normal component plunging 30°/290°. However, the extent of mapping on these was limited to individual beds; although no magnitude of displacement could be determined, it was judged to be small. Extension cracks and scarplets developed locally where the cut slopes intersected less steep fault planes.

Another group of faults trend ESE and dip steeply to the southwest. The trace of one can be seen in the LCF, approximately 100 feet up-slope from Station 888+00 where it displaces marker beds approximately 100 feet (30 m) in a right lateral sense. The trace of another fault (140°/57°) is apparent in the northbound lane road cut near station 887+60 (Figure 3). This group most likely is associated with the fault mapped across Nittany Valley to the east.

Several high angle reverse faults were mapped in the shale outcrops along Old Route 322. They have a general ENE strike and a 65° northerly dip. The steeply dipping, northerly trending faults appear to be later than the rest. One of these faults (207°/77° SE) was exposed 375 feet east of the Route 322 bridge abutment in the southbound road cut, near Station 885+70. Three sets of slickenlines are apparent on a highly-polished surface (mirror finish), indicating it has a high strike-slip component (Figure 16d). The significance of this fault is that it cuts and displaces a vein network of pyrite.



Figure 16. Collage of faults: (a) Large Cut Face; (b) east bound lane, LCF area; (c) small landslide in Reedsville shale, east bound lane, LCF area; (d) fault with two slip directions (wooden sticks) cutting massive pyrite veins in LCF. Andrew Sicree for scale. Summer, 2008.

A macroscopic scale fault is inferred to extend through the gully near Pond M (Figure 3) and across the divide west of Station 868+00. Five hundred feet to the west, near station 861+00, another fault trending 175° is inferred from the juxtaposition of Juniata “red-beds” against Tuscarora “quartzites”.

Three dominant joint sets in the Skytop rocks are identified as J_1 (strike joints), J_2 (cross-strike joints), and bedding joints. J_1 joints are nearly horizontal, with shallow northerly to northwesterly dips (Figure 16). They are strike joints perpendicular to bedding, and probably developed before the strata were folded during Alleghanian deformation. In the A-12 section they appear as the flat dipping joints (Figure 17). In the C-12 section, the orientation pattern is more complex, with two distinct groupings;

one dipping northwest at approximately 30° and the other southeast at 40° (Figure 18). These two populations reflect the attitudes of strike joints perpendicular to bedding in the limbs of the chevron folds.

A-12 Section Joints

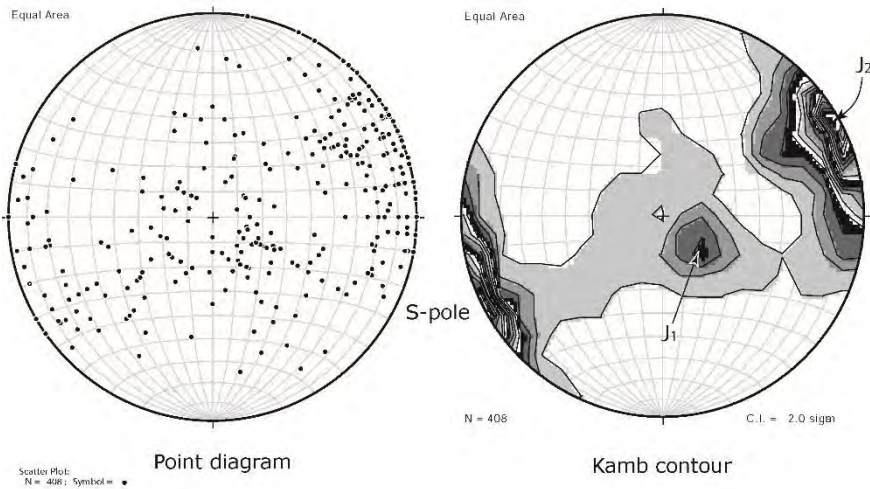


Figure 17. Orientation diagrams of joints in A-12 domain.

C-12 Section (Bifurcation) Joints

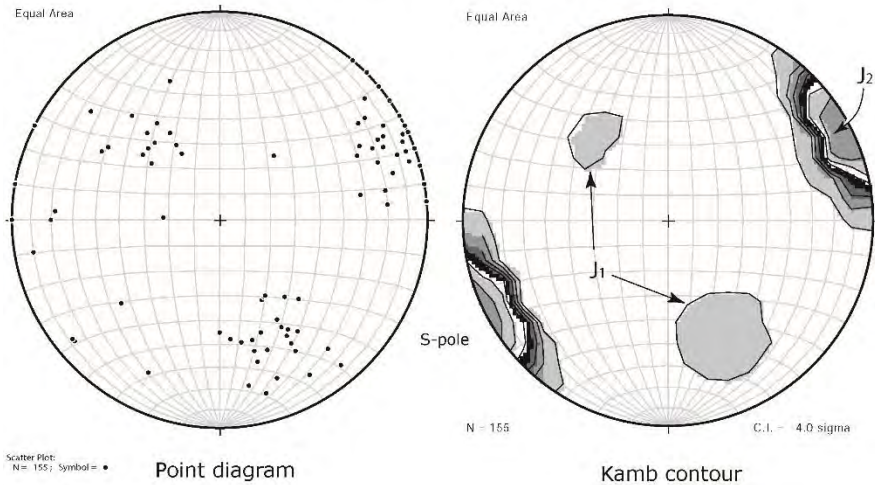


Figure 18. Orientation diagrams of joints in C-12 domain.

The J₂ joints have a preferred SSE orientation ((Figure 17 & 18) and steep dip. These have been attributed to a hydrofracturing event during a late Alleghanian gas drive (Srivastava and Engelder, 1990; Lacazette, 1991; Engelder, 1996, 2004) after the formation of the Nittany Anticlinorium.

Lineaments and Fracture Traces

An examination of small-scale topographic maps and aerial photographs shows that wind gaps, as well as more prominent water gaps, are spaced typically at 1-3 kilometer intervals along many of the major ridges in central Pennsylvania. The position of the Skytop wind gap is controlled by the

presence of faults (discernible as a lineament⁷, see below), which has important implications for sulfide deposits. Standard mapping techniques were used to update the local State College and Julian quadrangle bedrock maps (Doden and Gold, 2009; 2010), but newer methods of analyzing the geology have been helpful in revealing previously unrecognized features. Lidar data acquired as part of the DCNR’s PaMap program (2008) were combined with a digital elevation model (DEM) to create a composite hillshade image covering the Julian and State College quadrangles and several miles beyond (Figure 19). This map forms the basis for detecting linear or sub-linear features in a subjective selection process resembling that traditionally performed with stereo-pairs of aerial photos. The hillshade images reveal many details of faults and geologic contacts not visible in the field or on conventional aerial photographs. Figure 19 shows lineaments in the Julian and State College quadrangles, only a few of which can be detected visually on the ground or on the traditional geologic map.

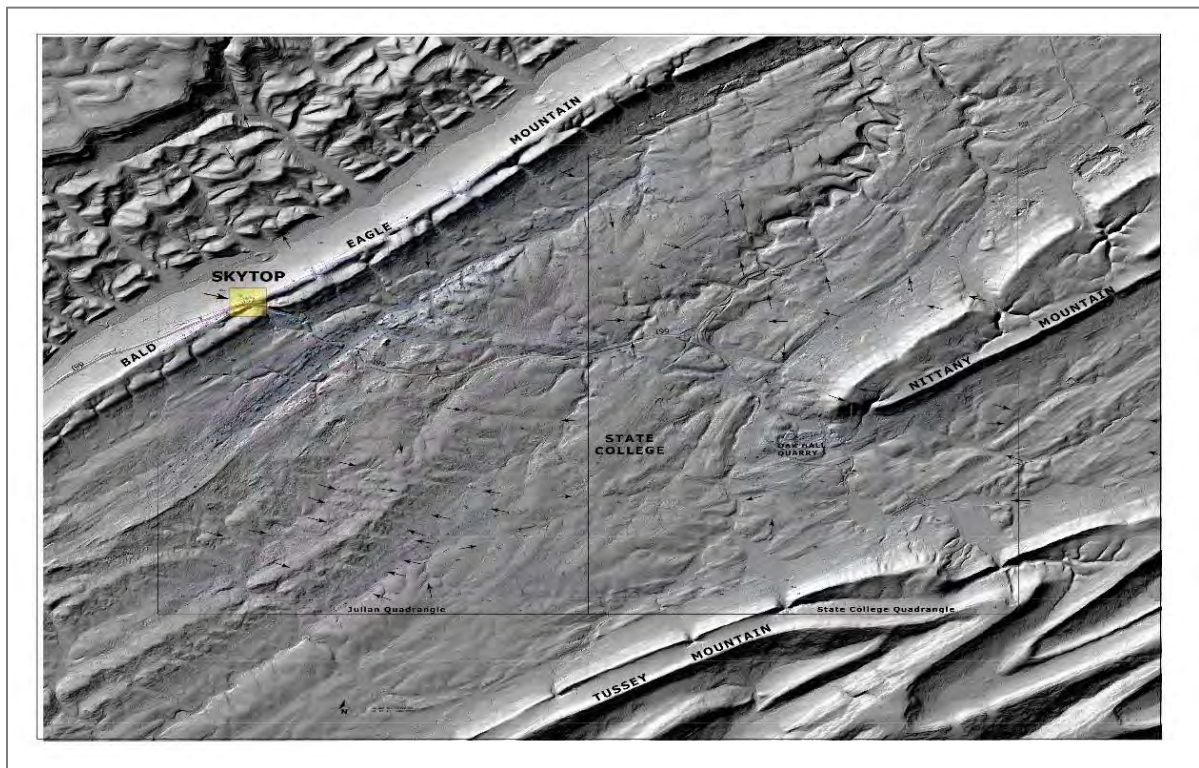


Figure 19. Lidar image of Skytop and State College showing fracture traces and lineaments.

A major linear feature apparent on the Lidar image follows an azimuth of approximately 100° from Skytop in the Julian quadrangle 18 km to Nittany Mountain in the State College quadrangle (Figure 19). Geologic mapping shows that faults offsetting uppermost Cambrian through lower Ordovician

⁷ A “lineament” is defined as a linear feature that is an expression of an underlying geological structure such as a fault. The word “linear” is commonly used for features that also are linear but do not necessarily represent geological structures. For simplification, the terms will be used interchangeably in this discussion.

units comprise part of this lineament. Faults offsetting Lower Ordovician carbonate units northwest of Nittany Mountain comprise a substantial part of the 18 km Skytop-Nittany Mountain lineament, as do faults mapped through the western end of Skytop. A cluster of sinkholes in the Hatter through Coburn formations (Middle Ordovician limestones) also lies along this lineament near Nittany Mountain.

Epigenetic Veins: Mineralization and Chemistry

(further information in Mineralogy of Skytop article – this Guidebook)

Skytop had long been known as a location for sulfide veins. Pyrite veins were noted by D.P. Gold, (circa 1998) in core drilled by G.O. Hawbaker, Inc., in the old ganister workings along the ridge to the west of Skytop, as well as steeply dipping gossan one (9-feet thick) exposed in a road cut along Old Route 322. The latter site was visited by many generations of Penn State geology students. This gossan was located in the western abutment of the new Route 322 Bridge (near station 882+00). The I-99 roadcuts have exposed two sulfide vein-systems that are portrayed in a modified block diagram (Figure 20), as viewed from the south.

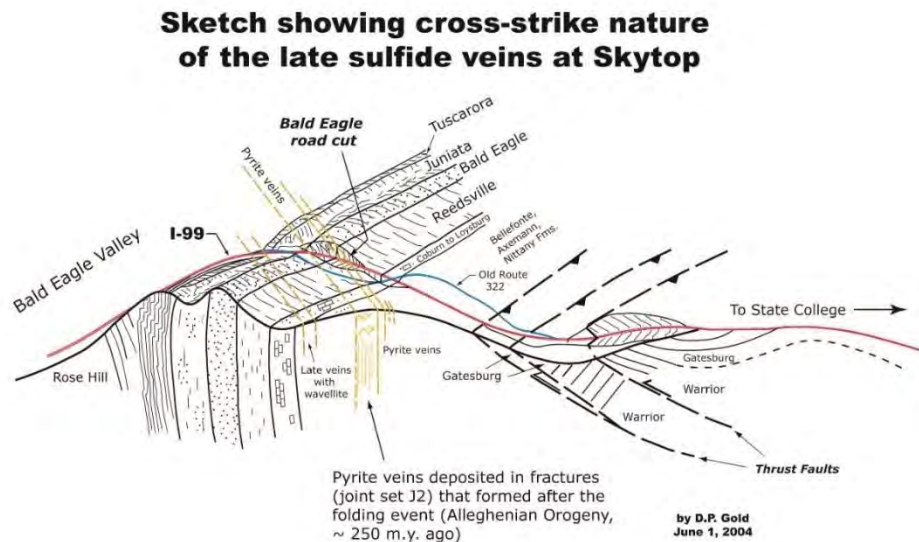


Figure 20. Conceptual isometric view (from the south) of Skytop geology and vein systems.

Although veins that transgress bedding are exposed in all the road cuts, most are concentrated in the Bald Eagle sandstones, and to a lesser extent in the Tuscarora quartzites and Juniata sandstones. These “cross-strike” veins are far less common in the over- and underlying shaley formations. The preferential development of veins in the more competent strata is attributed to the well-developed J₂ joint system in these units. Although the orientation of the veins is relatively constant, different types are distinguished by composition, thickness and alteration halos. Sulfide-bearing veins are by far the most abundant and occur as steeply dipping, cross-strike sets oriented generally SSE, essentially coincidental with the preferred orientation of the J₂ joint set (Figure 21; compare with Figures 17 & 18). The slightly geometrical obliquity suggests there may have been two different hydrofracturing events; an early one to form the J₂ joint set and a later vein forming event.

A-12 Pyrite-bearing Veins

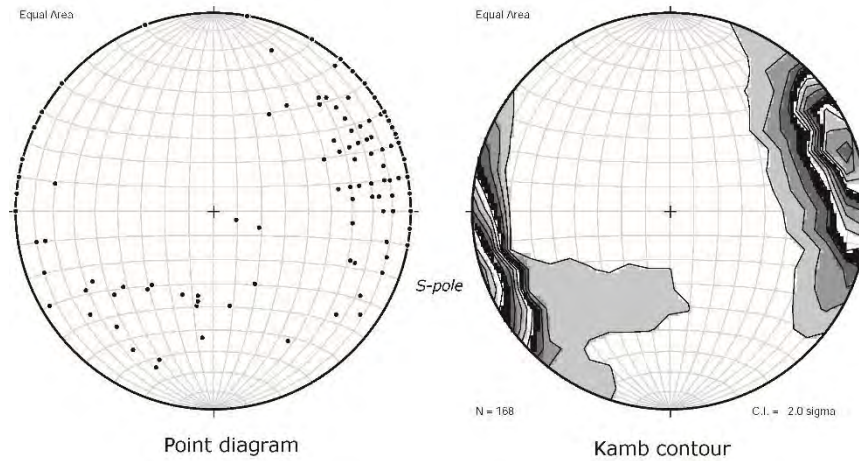


Figure 21. Orientation diagram summarizing attitudes of sulfide veins.

Quartz and calcite veins occur marginal to the high concentration of sulfide veins exposed in the road cut through the Bald Eagle Formation. A few thin veins of early quartz covered by later pyrite have been found near the contact of the Bald Eagle and Juniata formations. One vein with barite as a major constituent is exposed in the Juniata red beds in the western road cut near station 867+60. Wavellite was identified in a sample of Tuscarora quartzite float picked up during construction near station 840+00. The veins host mineral assemblages interpreted as hydrothermal in origin. The minerals tentatively identified and suspected are listed in Table 2.

Table 2. Tentative list of minerals identified in the epigene vein system at Skytop.

SULFIDES			
	Pyrite	FeS ₂	cubic
	Marcasite	FeS ₂	ortho
	Pyrrhotite – 4C	Fe _{1-x} S	mono
	Pyrrhotite – 7C	Fe _{1-x} S	hex
	Chalcopyrite	CuFeS ₂	tetra
	Tennantite?	(Cu,Fe) ₁₂ As ₄ S ₁₃	cubic
	Sphalerite	ZnS	cubic
	Wurtzite?		
PHOSPHATES			
	Wavellite	Al ₃ (PO ₄) ₂ (OH,F) ₃ · 5H ₂ O	ortho
	Variscite	AlPO ₄ · 5H ₂ O	ortho
	Woodhouseite	CaAl ₃ (PO ₄)(SO ₄)(OH) ₆	trig
	Xenotime	Y PO ₄	tetra
OXIDES AND OXY-HYDROXIDES			
	Quartz	SiO ₂	hex
	Rutile	TiO ₂	tetra
	Zircon	Zr SiO ₄	tetra
	Hematite	Fe ₂ O ₃	trig
	Limonite/Goethite	Fe ³⁺ O(OH)	ortho
	Lepidocrocite?		
	Jarosite	K2Fe ³⁺ ₆ (SO ₄) ₄ (OH) ₁₂	hex

Table 2., continued ...

EFFLORESCENT MINERALS			
	Alunogen	$\text{Al}_2(\text{SO}_4)_3 \cdot 17 \text{H}_2\text{O}$	trig
	Copaipite	$\text{Fe}^{2+}\text{Fe}^{3+}4(\text{SO}_4)_6(\text{OH})_2 \cdot 20 \text{H}_2\text{O}$	trig
	Halotrichite	$\text{Fe}^{2+}\text{Al}_2(\text{SO}_4)_4 \cdot 22 \text{H}_2\text{O}$	mono
	Gypsum	$\text{CaSO}_4 \cdot 2 \text{H}_2\text{O}$	mono
	Melanterite	$\text{FeSO}_4 \cdot 7 \text{H}_2\text{O}$	mono
	Rozenite	$\text{FeSO}_4 \cdot 4 \text{H}_2\text{O}$	mono
OTHER SUSPECTED PHASES			
	Barite	BaSO_4	ortho
	Ankerite	$\text{Ca}(\text{Fe},\text{Mg},\text{Mn})(\text{CO}_2)_2$	trig
TRACE ELEMENTS			
	Cd, As, Sb, Au, Ag, Hg	probably epigenic in pyrite	

The majority of veins are composed of sulfides. These are best developed in the Bald Eagle sandstone strata exposed in the A-12 section LCF road cuts between stations 881+00 and 888+00 (Figure 2). Locally veins of pyrite, up to 2 cm thick, generally on the order of 1 cm or less, occur with a spaced interval of 50 cm to 1 m. The strike of these steeply dipping veins ranges from 130° to 190°, (Figure 21) and overlaps spatially with the regional J₂ joints (Figures 17 & 18). Cross-linking veins locally form vein networks that vary from fine (centimeter scale) to open (decimeter scale).

The distribution of vein and vein networks is not uniform and an average grade of 4-5% sulfides in the LCF road cut is based on integrated visual estimations made in traverses at 50 feet intervals across the slopes of the road cut (Figure 3).

A more rigorous estimate of pyrite content was attempted by Ed Meiser and Arthur Rose (Meiser, 2004), who sampled the northern LCF road cut at 3-foot intervals. These samples were composited into 30-foot units (10 adjacent samples) and analyzed for major and minor chemical element contents (Table 3). Sulfur contents ranged from 0.66% to 4.69% to yield an average grade of 2.27% S, or 4.25% pyrite. Samples of aggregate from the 2RC aggregate piles had a range of sulfur content from 1.13 to 1.46% with an average of 1.25% S. Higher sulfur values, reflecting a pyrite content from 4.5 to 24 %, were obtained from selected samples from the southbound side (LCF) road cut and the northbound lane beneath the bridge. Samples from the fault zone near Station 880+00 consist mainly of pyrite, yielding a sulfur content of 32.10%.

Table 3. Partial chemical analyses of samples of Bald Eagle Sandstone from the Large Cut Face (LCF) in section A-12 between stations 882+00 to 888+50.

Station Feet	Sulfur %	Zinc ppm	Lead ppm	Arsenic ppm
0-30	1.25			
33-80	0.94	26	20	2.7
63-90	1.73			
93-120	2.79	34	40	7.9
123-150	0.82			
153-180	0.66	66	15	3.5
183-210	2.09			
213-240	3.65	57	63	11.3
234-270	2.99			
273-300	3.60	15	45	11.8
303-330	1.47			
333-360	2.78	67	63	6.0
363-390	4.69			
393-420	4.13	294	68	8.2
423-450	2.14			
453-480	1.49	125	71	6.0
483-510	1.35			
Average	2.27	<i>for heavily veined section of Bald Eagle Sandstone</i>		
513-540	0.44			
543-570	0.71			
573-600	0.38			
603-630	0.39			
633-660	0.37			
Average	1.86	<i>for all Bald Eagle Formation exposed east of the bridge</i>		

Samples were collected every 3 feet and composited every 30 feet.

Station numbers represent distance eastward in feet from the Rte. 322 bridge abutment.

Samples collected by Art Rose and Ed Meiser (10/1/04) and Art Rose and Tom Cawthem (10/4/04). Sulfur analyses by Geochemical Testing Inc., (Somerset, PA); trace elements by ACTLABS, (Ancaster, Ontario, Canada).

Sources of data are Meiser (2004), and Rose (personal communication, 2004).

Veins in the Reedsville shales are rare and are unlikely to exceed 0.5% by volume of rock at any place. Calcite and quartz veins tend to occur in the lower Reedsville, with pyrite veins more common towards the top of the formation. Except for their transgressive orientation (160°), the pyrite veins differ markedly in thickness (< 1 mm) and habit (coating on J₂ joint surfaces) from those in the Bald Eagle sandstone.

Because of a common association of gold with hydrothermal vein systems, six samples pristine veined sandstone were selected for a detailed major and trace element analysis at the ACTLAB facility in Ontario. The results are shown in Table 4. The gold content in low ppb was disappointing.

**Table 4. Chemical Analyses of Skytop Rocks:
Major and trace element content for six samples of veined bedrock.**

SAMPLE		#1 S-532	#2 S-412	#3 S-370	#4 S-220	#5 N-00+80	#6 Bifurcation
Road Station		887+45	886+20	885+78	884+30	881+90	859+10
SiO ₂	%	82.08	60.69	39.56	68.05	76.03	68.29
Al ₂ O ₃	%	6.77	3.42	2.16	2.64	5.04	4.87
Fe ₂ O ₃	%	3.57	21.36	37.16	17.15	8.84	14.85
MnO	%	0.023	0.003	0.008	0.006	0.005	0.004
MgO	%	1.39	0.27	0.18	0.31	0.36	0.41
CaO	%	0.03	0.09	0.08	0.04	0.01	0.03
Na ₂ O	%	0.23	0.15	0.10	0.03	0.03	0.04
K ₂ O	%	1.71	1.38	0.46	1.02	1.73	1.86
TiO ₂	%	0.588	0.303	0.182	0.174	0.559	0.289
P ₂ O ₅	%	0.02	0.06	0.04	0.05	0.03	0.02
LOI	%	3.67	12.30	20.10	9.37	6.19	8.54
TOTAL	%	100.07	99.99	100.04	98.85	98.83	99.19
<i>Note: The Fe₂O₃ for the standards is Total Fe₂O₃ and has not been adjusted for the FeO</i>							
S	%	0.39	16.76	25.38	13.69	7.19	12.03
Ba	ppm	198	84	68	77	115	136
Sr	ppm	24	15	14	10	15	15
Y	ppm	18	12	6	6	13	7
Sc	ppm	5	6	-2	3	5	4
Zr	ppm	315	195	154	63	210	94
Be	ppm	1	-3	-2	-1	1	1
V	ppm	44	24	-5	10	38	19
Ag	ppm	-0.3	1.1	1.3	-0.3	0.4	-0.3
Cd	ppm	-0.3	1.2	2.0	1.3	-0.3	0.8
Cu	ppm	9	28	50	9	8	21
Mo	ppm	1	1	-1	-1	3	2
Ni	ppm	25	15	29	32	23	18
Pb	ppm	7	298	430	63	45	25
Zn	ppm	40	46	160	753	19	7
Bi	ppm	-2	-2	-2	-2	-2	-2
Co	ppm	10	11	12	28	9	11
Au	ppb	-2	11	7	-2	-2	4
As	ppm	1.0	8.8	46.4	6.0	9.2	9.6
Br	ppm	0.9	1.5	1.2	1.3	1.2	-0.5
Co	ppm	6	7	7	18	6	7
Cr	ppm	18	15	11	11	20	16
Cs	ppm	1	-1	-1	-1	1	2
Hf	ppm	7	4	3	2	6	2
Ir	ppb	-5	-5	-5	-5	5	-5
Mo	ppm	8	16	14	9	10	-1
Rb	ppm	42	29	-15	-15	45	63
Sb	ppm	0.2	1.6	4.8	0.6	0.3	1.2
Se	ppm	-3	-3	-3	-3	-3	-3
Ta	ppm	-0.5	-0.5	-0.5	-0.5	-0.5	-0.5
Th	ppm	4.5	2.6	1.4	1.8	3.9	3.4
U	ppm	2.0	1.0	-0.5	0.9	2.0	1.2
W	ppm	-1	-1	-1	-1	-1	-1

Table 4., cont.

SAMPLE		#1 S-532	#2 S-412	#3 S-370	#4 S-220	#5 N-00+80	#6 Bifurcation
Road Station		887+45	886+20	885+78	884+30	881+90	859+10
La	ppm	15.7	7.8	5.6	6.2	12.5	12.4
Ce	ppm	27	21	14	16	30	26
Nd	ppm	17	11	-5	8	11	11
Sm	ppm	1.2	1.2	1.0	0.8	0.8	1.0
Eu	ppm	0.8	0.5	-0.2	0.3	0.6	0.3
Tb	ppm	-0.5	-0.5	-0.5	-0.5	-0.5	-0.5
Yb	ppm	1.9	1.0	0.6	0.7	1.6	0.9
Lu	ppm	0.26	0.18	0.10	0.11	0.22	0.13
V	ppm	44	25	17	22	37	26
Ga	ppm	9	14	19	4	16	8
Ge	ppm	1.8	7.8	56.4	2.8	3.7	2.0
Rb	ppm	47	30	18	26	48	48
Sr	ppm	24	13	14	10	15	14
Y	ppm	17.8	11.2	7.0	6.4	13.0	7.1
Zr	ppm	330	202	153	67	211	94
Nb	ppm	8.0	5.1	5.5	2.7	6.6	5.1
Mo	ppm	-2	-2	-2	-2	-2	-2
In	ppm	-0.1	-0.1	-0.1	-0.1	-0.1	-0.1
Sn	ppm	-1	-1	-1	-1	1	1
Cs	ppm	1.5	1.1	0.8	0.9	1.7	1.9
Ba	ppm	198	85	70	75	116	131
La	ppm	20.0	11.5	9.39	8.74	16.6	16.4
Ce	ppm	44.2	25.4	20.2	19.1	35.7	35.4
Pr	ppm	4.71	2.82	2.28	2.07	3.86	3.67
Nd	ppm	17.9	11.2	9.23	8.27	14.9	13.5
Sm	ppm	3.74	2.80	1.91	1.59	2.72	2.20
Eu	ppm	0.714	0.518	0.377	0.332	0.512	0.367
Gd	ppm	3.06	2.25	1.51	1.21	2.06	1.39
Tb	ppm	0.57	0.43	0.26	0.20	0.38	0.21
Dy	ppm	2.97	2.26	1.35	1.03	2.00	1.15
Ho	ppm	0.56	0.42	0.28	0.21	0.42	0.25
Er	ppm	1.98	1.41	0.98	0.72	1.54	0.90
Tm	ppm	0.304	0.206	0.140	0.109	0.250	0.141
Yb	ppm	1.84	1.26	0.86	0.70	1.56	0.96
Lu	ppm	0.259	0.182	0.125	0.101	0.223	0.139
Hf	ppm	7.6	5.5	4.2	1.8	6.1	2.4
Ta	ppm	0.55	0.27	0.18	0.18	0.45	0.36
W	ppm	1.7	-0.5	1.5	-0.5	0.7	0.6
Tl	ppm	0.64	0.97	4.47	2.03	0.84	0.48
Bi	ppm	0.6	2.4	0.6	0.5	1.4	1.0
Th	ppm	5.82	3.64	2.25	1.97	4.80	4.11
U	ppm	1.42	1.24	1.12	0.59	1.40	0.94

Analyses by Activation Laboratories Ltd., December 8, 2004

Sample 1. Sandstone with rare veins from southbound lane in Section A-12.

Sample 2. Fine pyritic vein network in sandstone from southbound lane in Section A-12.

Sample 3. Fault breccia: sandstone fragments in pyritic matrix, southbound lane in Section A-12.

Sample 4. Bright vein pyrite in sandstone, southbound lane in Section A-12.

Sample 5. Thin pyrite vein in sandstone, northbound lane under bridge in Section A-12.

Sample 6. Pyrite veins in Tuscarora quartzite, northbound lane in bifurcation area in Section C-12

Veins in the “red beds” of the Bald Eagle and Juniata formations are much less common than in the more competent, green Bald Eagle beds, but are more easily discerned because of the green REDOX halo surrounding them (Figure 22). In addition to sulfides (mainly pyrite), sulfate (barite) is present in one vein near station 876+50. The reduced zones contain many fine veins that are seen to cluster around a fault with an irregular surface. Undoubtedly the fault and the veins were the conduits for reducing fluids; reduction zones vary from 10’s to 100’s feet thick, and locally follow stratigraphic horizons (usually more porous sandy beds).



Figure 22. Transgressive REDOX zone in red Juniata shales and siltstones.

Likewise veins in the Tuscarora quartzites are less common and thinner than in the Bald Eagle Formation. The veins exposed during excavation of the C-12 road bed were seen to contain pyrite beneath an oxidized cap rock with vari-colored stains from iron oxyhydroxide minerals, not only on the J_2 joints but also the J_1 and bedding joint planes. Although the J_2 joints appear to be the favorable host for vein fill materials to deposit, subsequent oxidation and reduction allowed for the supergene minerals to disperse in the other well-developed joint sets.

At station 856+00 in the eastern road cut of the C-12 section Tuscarora beds dip 30° SE and are overlain by Juniata beds higher up the slope. The attitude of these beds in an extensive pyrite vein network, exposed between stations 858+00 and 861+00, is not known in detail (Figure 23). This has developed into an acid leach zone since the completion of construction, and is discernable as a slope area on which seeded vegetation has not taken root.



Figure 23. Small Cut Face with temporary PVC cover over transgressive vein system 300 feet wide.

A characteristic of epigenetic vein deposits is the surface development of gossan; a term applied to the alteration products of sulfide minerals from oxidization and hydration above the water table. A REDOX front is the interface between the reduced “pyritic” rock (usually drab green and gray) and the “oxidized cap-rock” (rusty browns and reds) from iron oxyhydroxide mineral encrustations (commonly referred to as gossan). The gossan represents the weathering and alteration products of sulfide minerals in the oxidized and hydrated cap-rock, and as such is essentially devoid of any sulfide minerals. The secondary mineral deposits in the gossan are referred to as supergene. The distribution of the oxidized cap-rock is shown in the panoramic view of the LCF (Figure 2) and by a special pattern in the accompanying geological map (Figure 3).

A second form of REDOX occurs when sediments deposited in an oxidizing environment (usually red in color due to the presence of hematite, the high oxidation state for iron) are altered by reduced fluids with the conversion of hematite to magnetite (a lower oxidation state for iron) and an attendant color change to drab greens and grays. Transgressive veins that carried reducing fluids through the “redbeds” are easy to spot by the abrupt color change (green/gray) at the REDOX front (Figure 4).

Rocks representing both these processes are exposed at Skytop. Their combined effects are apparent where sulfide-bearing veins (reducing environment) in the Juniata “red beds” pass into the “oxidized cap rock” (Figure 2). However, this is not the full story of REDOX events at Skytop. There is evidence of a regional gas (dominantly methane) migration (drive) during the late Alleghanian Orogeny (Lacazette, 1991; Engelder, 1996, 2004) that reduced much of the Bald Eagle Formation. The legacy of this event are small knots (1-2 mm across) of pyrite-cemented quartz grains disseminated in some Bald Eagle sandstone beds.

In addition to the supergene minerals, such as hematite, limonite/goethite and jarosite (Table 2) that formed in the gossan over time as the surface weathered down, there are a host of secondary efflorescent minerals currently growing in response to solution and evaporation of vadose ground water. Several efflorescent minerals have been identified (see Table 2). Amongst these, the iron sulfate salts such as alunogen, copiapite (Figure 24), halotrichite, melanterite and rozenite grew in moist seeps as saturated ground water evaporated at the surface to form cauliflower head-like blooms. These salts are extremely soluble in water and do not survive the next rain. Their dissolution results in an immediate increase in sulfate ions in the runoff.



Figure 24. Copiapite growing beneath new Rte. 322 Bridge. Note sulfide veins (top right) and gossan on joint (center right).

Regional fluid inclusion (Orkan and Voight, 1985; Lacazette, 1991) and fission track (Blackmer, 1994) studies suggest host rock temperatures ranging from 150° to 250°C, and a depth of 5-8 km at the time of sulfide fluid migration. More recent fluid inclusion studies (Detrie *et al.*, 2005) on co-genetic vein quartz at Skytop increases this range to 140° – 375°C, with most between 180° – 350°C, and salinities from as little as 9.2% to as much as 25%. Pyrite occurs in a wide range of morphologies, from cuboctahedral crystals to massive blocks, laths, matchsticks and fine needles (Sicree, 2005; Sicree and Barnes, in this guidebook). Sicree (2005) concludes that (a) early striated pyrite followed by smooth-faced cubic crystals reflects a change from low-supersaturation, higher temperature (> 250°C) to moderate-supersaturation, lower temperature conditions, and (b) that the needle-like forms indicate a continued shift to lower temperature (<250°C), low-supersaturation as the main stage of mineralization ceased.

The number of stages and age(s) of mineralization has yet to be determined. A tentative Os/Re age of 18.9 Ma (Mathur, personal communication, 2010) needs to be refined and verified. Clearly, the variety and distribution of “cross-strike” veins in all the road cuts attests to a complex geological history at Skytop.

Real time responses of the toxic bed rock in rock-cuts, waste fill and waste dumps will be treated in a companion paper covering remediation options. This includes the remediation procedures adopted to treat (a) the pyrite-veined road-cuts, (b) already paved toxic fill, and (c) the sequestration of movable toxic waste into an Engineered Rock Placement Area.

Conclusions

- A reduction of thickness is apparent in the stratigraphic units exposed at Skytop, and the Lost Run Conglomerates unit in the Bald Eagle Formation, as well as part of the Middle and Upper Juniata Formation appear to be missing.
- The sulfide minerals exposed at Skytop represent an epigenetic vein system transgressive to bedding in a zone approximately 900 feet wide.
- Although the veins are best developed in the more competent sandstone units, the Bald Eagle sandstones appear to be the preferred site for deposition.
- The sulfide veins at Skytop are coincident with the regional cross strike J₂ joints that were formed by hydraulic fracturing during the late Alleghanian deformation.
- Vein minerals include pyrite, pyrrhotite and marcasite, with minor sphalerite and galena and traces of chalcopyrite and greenockite.
- Different morphologies of pyrite are consistent with a wide temperature range (140°-375°C) and saturation of the hydrothermal fluids, and suggest multiple stages of deposition.
- A depth of vein (and sulfide) emplacement of 5-10 km, inferred from fluid inclusion studies on quartz in the veins, is consistent with fission track and coal vitrinite reflectance estimates of 5-8 km of unroofing at the Allegheny Front.
- The timing for emplacement is post Alleghanian: the setting is in a deep-seated fracture zone that probably is related to other SSE trending lineaments in the Ridge and Valley Physiographic Province: these lineaments are manifest in the alignment of wind- and water-gaps.

- Three distinct REDOX events are apparent: the first is a late Alleghanian gas/fluid drive that reduced most of the “red bed” units in the Bald Eagle Formation, and locally segregated pyrite as small knots in the sandstone matrix. The second involved reducing sulfide-bearing solutions that likewise caused transgressive bleached green zones to develop in the “red beds”. Current weathering has developed an oxidized cap rock above the groundwater table and gossan over the sulfide veins.
- Excavations below the groundwater table in similar geological settings should anticipate the exposure of toxic sulfide minerals.
- Efforts are needed to suppress the development of efflorescent minerals in the large exposed cut faces.

Selected References

- Barnes, J.H., and Sevon, W.D., 1996, **The Geological Story of Pennsylvania**. Dept. of Conservation and Natural Resources. PA. Geol. Surv., Educ. Series # 4, 44 p.
- Berg, T.M., 1999, Devonian–Mississippian Transition, Chapter 8, pp. 128-137, in **The Geology of Pennsylvania**, Ed. C.H. Schultz, Special Pub. # 1, Pennsylvania Geol. Surv., and Pittsburgh Geol. Soc., 888 p.
- Blackmer, G.C., Omar, G.I., and Gold, D.P., 1994, Post-Alleghanian Unroofing History of the Appalachian Basin, Pennsylvania, from Apatite Fission Track Analysis and Thermal Models. *Tectonics*, v. 13, # 5r, pp. 1259-1276.
- Canich, M.R., and Gold, D. P., 1985, Structural Features in the Tyrone - Mt. Union Lineament, across the Nittany Anticlinorium in Central Pennsylvania. *In* Gold, D.P. and others, eds., **Central Pennsylvania Geology Revisited**, Guidebook, 50th Annual Field Conf. of Pennsylvania Geologists, Guidebook, pp. 120-137.
- Detrie, T.A., Mutti, L.J., and Mathur, R., 2005, Quartz Sulfide Mineralization of the Bald Eagle Formation of Skytop Mountain, near State College, Pennsylvania. *Abst. NE- Section Meeting, Geol. Soc. Amer., Saratoga, V.37, # 2, p. 61.*
- Doden, A.G, Gold, D.P., and Van Horn, K., 2003, Geology and Economic Resources of the Osterburg Area, Bedford County, Pennsylvania. pp. 117-126, in **Geology on the Edge**, Eds., G.M. Fleeger, D.P. Gold and J.H. Way, Guidebook for 68th Field Conference of Pennsylvania Geologists, 240 p.
- Engelder, T., 1979, Mechanisms for strain within the Upper Devonian clastic sequence of the Appalachian Plateau, western New York. *Amer. Jour. Science.*, v. 297, pp. 527-542.
- Engelder, T., 2004, Differences in joint rupture velocity as indicated by dissimilarities in the surface morphology of joints in the Appalachian Valley and Ridge, Virginia: Implications for timing of hydrocarbon generation in the southeastern portion of the Appalachian Basin. *Abst. NE-SE Section Meeting, Geol. Soc. Amer., Tysons Corner, V.36, # 2, p. 119.*
- Engelder, T., 2004, Tectonic implications drawn from differences in the surface morphology on two joint sets in the Appalachian Valley and Ridge, Virginia. *Geology*, v. 20. No. 5, pp. 413-416.
- Engelder, T., and Geiser, P., 1980, On the use of regional joint sets as trajectories of paleostress fields during the development of the Appalachian Plateau, New York. *Jour. of Geophys. Res.* V. 85, pp. 6319-6341.
- Gold, D.P., 1985, Field Guide - Cross-Strike and Strike-Parallel Deformation Zones in Central Pennsylvania. *Field Trip # 4, 50th Annual Field Conf. of Pennsylvania Geologists*, pp. 165-203.

- Gold, D.P., 1999, Lineaments and their Interregional Relationships, Chapter 22, pp. 307-313, in **The Geology of Pennsylvania**, Ed. C.H. Schultz, Special Pub. # 1, Pennsylvania Geol. Surv., and Pittsburgh Geol. Soc., 888 p.
- Gold, D.P., Alexander, S.S., and Parizek, R.R., 1974, Application of remote sensing to natural resources and environmental problems in Pennsylvania. *Earth and Mineral Sciences Bulletin*, v. 43, # 7, pp. 49-53.
- Gold, D.P., Doden, A.G., Lowrey, T., and Van Horn, K., 2003, **Roaring Spring Quarry, Appendix C**, pp. 211-223, in **Geology on the Edge**, Eds. G.M. Fleeger, D.P. Gold and J.H. Way, Guidebook for 68th Field Conference of Pennsylvania Geologists, 240 p.
- Gold, D.P., Doden, A.G., Altamura, R.J., and Sicree, A., 2005, The Nature and Significance of Sulfide Mineralization in Bald Eagle Ridge at Skytop, near State College, Pennsylvania. *Abst. NE- Section Meeting, Geol. Soc. Amer., Saratoga Springs, V.37, # 2, p. 64.*
- Gold, D.P., and Parizek, R.R., 1976, Field Guide to lineaments and fractures in central Pennsylvania. 2nd Intern. Conf. on Basement Tectonics (Univ. of Delaware, Newark), 75 p.
- Gold, D.P., and Pohn, H.A., 1985, The nature of cross-strike and strike-parallel structures in central Pennsylvania. *In* Gold, D.P. and others, eds., **Central Pennsylvania Geology Revisited**, Guidebook, 50th Annual Field Conference of Pennsylvania Geologists, State College, PA, p. 138-143.
- Hammarstrom, J.M., Brady, K., and Cravotta, C.A., 2005, Mineralogical Controls on Acid-Rock Drainage at Skytop, Centre County, PA. *Abst. NE- Section Meeting, Geol. Soc. Amer., Saratoga, V.37, # 2, p. 64.*
- Harper, J.A., 1999. Devonian, Chapter 7 pp. 108-127, in **The Geology of Pennsylvania**, Ed. C.H. Schultz, Special Pub. # 1, Pennsylvania Geol. Surv., and Pittsburgh Geol. Soc., 888 p.
- Horowitz, D.H., 1966, Evidence for deltaic origin of an Upper Ordovician sequence in the central Appalachians. Chapter in **Deltas and their Geologic Framework**, edited by M.L. Shirley, and J.A. Ragsdale, Houston Geol. Soc., p. 159-169.
- Hsu, Fu-Tzu, 1973, Geochemical Exploration in the Nittany Valley Area, Centre County, Pennsylvania. Unpub. M.S. Thesis, Department of Geosciences, The Pennsylvania State University, University Park. 108 p.
- Kowalik, W.S., and Gold, D.P., 1976, The Use of LANDSAT-1 imagery in mapping lineaments in Pennsylvania. *Proc. 1st Intern. Conf. on the New Basement Tectonics (Utah Geol. Assoc.), # 5, pp. 236-249.*
- Krohn, M.D., 1976, Relation of Lineaments to Sulfide Deposits and Fracture Zones along Bald Eagle Mountain: Centre, Blair, and Huntingdon Counties, Pennsylvania. Unpub. M.S. Thesis, Department of Geosciences, The Pennsylvania State University, University Park. 104 p.
- Lacazette, A. 1991, Natural hydraulic fracturing in the Bald Eagle Sandstone in Central Pennsylvania and the Ithaca Siltstone at Watkins Glen, New York. Unpub. Ph.D. Thesis, Department of Geosciences, The Pennsylvania State University, University Park. 225 p.
- Laughrey, C.D., 1999, Silurian and Transition to Devonian, Chapter 6 pp. 90-107, in **The Geology of Pennsylvania**, Ed. C.H. Schultz, Special Pub. # 1, Pennsylvania Geol. Surv., and Pittsburgh Geol. Soc., 888 p.
- Laughrey, C.D., Kostelnik, J., Gold, D.P., Doden, A.G., and Harper, J.A., 2003, **Trenton and Black River Carbonates in the Union Furnace Area of Blair and Huntingdon Counties, Pennsylvania**, Ed. J.A. Harper. Field Trip Guidebook for the AAPG-SPE Eastern Regional Meeting, Pittsburgh, September 2003. 80 p.
- Meiser, E.W., 2004, Sampling of Pyritic Sandstone from I-99 Skytop Cut and Alkaline Coal Ash from Seward Generating Plant Station and Development of Leaching Test Procedures for Mixtures of Ash and Sandstone. Report to Robindale Energy Services, Inc, Armagh, PA.

82nd Annual Field Conference of Pennsylvania Geologists

- Miller, B.L., 1924, Lead and zinc ores of Pennsylvania. Pennsylvania Geological Survey, 4th ser., Mineral Resources Report 5, 91 p.
- Nickelsen, R.P., 1974, Early jointing and cumulative fracture patterns. Proc First Int. Conf. New Basement Tectonics; Utah Geol. Assoc. Pub. # 5, pp. 193-199.
- Nickelsen, R.P., 1979, Sequence of structural stages of the Alleghany Orogeny, at Bear Valley strip mine, Shamokin, Pennsylvania. Amer. Jour. Science, v. 279, pp. 225-271.
- Nickelsen, R.P., 1983, Ambient temperatures during the Alleghany Orogeny. In Nickelsen, R.P., and Cotter, E., eds. **Silurian Depositional History and Alleghanian Deformation in the Pennsylvania Valley and Ridge**, Guidebook, 48th Annual Field Conference of Pennsylvania Geologists, Danville, PA, pp. 64-66.
- Nickelsen, R.P., and Hough, V.N.D., 1967, Jointing in the Appalachian Plateau of Pennsylvania. Geol. Soc. Amer. Bull., v. 78, pp. 609-629.
- Orkan, N., and Voight, B., 1985, Regional joint evolution in the Valley and Ridge Province of Pennsylvania in relation to the Alleghany Orogeny. In Gold, D.P. and others, eds., **Central Pennsylvania Geology Revisited**, Guidebook, 50th Annual Field Conference of Pennsylvania Geologists, State College, PA, p. 144-163.
- Paxton, S.T., 1983, Relationship between Pennsylvanian-age lithic sandstones and mudrock diagenesis and coal rank in the central Appalachians. Ph.D. Thesis, Dept. of Geosciences, The Pennsylvania State University, University Park. 340 p.
- Rose, A.W., 1999, Metallic Mineral Deposits – Zinc-Lead-Silver. Chap. 40D in **The Geology of Pennsylvania**, ed. C.H Shultz, Pennsylvania Geological Survey/Pittsburgh Geological Society, Special Publication #1, pp. 583-587.
- Rose, A.W., 1970, Atlas of Pennsylvania Mineral Resources – Part 3, Metal Mines and occurrences in Pennsylvania. Pennsylvania Geological Survey, 4th ser., Mineral Resources Report 50, pt. 3, 14 p.
- Sicree, A.A., 2005, Morphology and Paragenesis of Sulfide Mineralization on Bald Eagle Ridge, Centre Co., Pennsylvania. Abst. NE- Section Meeting, Geol. Soc. Amer., Saratoga, V.37, # 2, p. 64.
- Smith, R.C., 1977, Zinc and lead occurrences in Pennsylvania. Pennsylvania Geological Survey, 4th ser., Mineral Resources Report 72, 318 p.
- Smith, R.C., 2003, Lead and Zinc in Central Pennsylvania. Pennsylvania Geology, v. 33, # 4, pp. 2-8.
- Srivastava, D.C., and Engelder, T., 1990, Crack-propagation sequence and pore-fluid conditions during fault-bend folding in the Appalachian Valley and Ridge, central Pennsylvania. Geol. Soc. Amer., Bull., v 102, 0. 116-128.
- Thompson, A.M. 1970a, Geochemistry of Color Genesis in Red-Bed Sequence, Juniata and Bald Eagle Formations, Pennsylvania. Jour. Sedimentary Petrology, v. 40, # 2, p. 599-615.
- Thompson, A.M. 1970b, Sedimentology and origin of Upper Ordovician clastic rocks, central Pennsylvania. Society of Economic Paleontologists and Mineralogists, Eastern Section Guidebook, 88 p.
- Williams, E.G., and Slingerland, R., 1985. Field Guide – Catskill Sedimentation in Central Pennsylvania. In Gold, D.P. and others, eds., **Central Pennsylvania Geology Revisited**, Guidebook, 50th Annual Field Conference of Pennsylvania Geologists, State College, PA, p. 45-60.

pyrite, sphalerite, smithsonite, cerussite, jordanite, anglesite and hydrozincite, some of which occur only in trace amounts (Smith, 1977; Faill *et al.*, 1989).

Sulfide deposits also occur elsewhere in the general vicinity of Skytop, such as at Milesburg, 12 miles northeast along Bald Eagle Mountain. Butts and Moore (1936) mapped the 15' Bellefonte quadrangle (including Milesburg) and reported only one occurrence of sulfides, a 6-inch-wide vein in an old ganister quarry (Tuscarora quartzite) in Milesburg Gap. The vein "cuts diagonally across bedding and contains galena, pyromorphite, ruby sphalerite, barite, pyrite, and a little silver in some unidentified form, no doubt enclosed in galena". Less confidence can be assigned to reports of some other sulfide deposits in the area, however, such as one in Lamb's Gap, 17 miles northeast of Skytop along Bald Eagle Ridge and another on Nittany Mountain above the village of Zion, approximately 17 miles east/northeast of Skytop. Deposits such as these have yet to be carefully documented and Smith (1977) pointed out that some localities are based on questionable old verbal accounts.

Despite local media announcements of "pyrite discovered at Skytop" the presence of sulfide minerals was known there long before Interstate 99 construction began, at least as far back as the 1950's. For example, Illsley (1955) identified anomalous concentrations of heavy metals in local streams east of Skytop, a clue to nearby sulfide deposits (for further discussion see Smith (1977) and references therein). The existence of gossan at Skytop was direct evidence for sulfides in the immediate area, a site visited for years by Penn State University geology and mineral exploration field trips.

Although the *existence* of sulfide minerals at Skytop has long been known, major excavations in 2004 for the Interstate 99 roadway project revealed the true extent of mineralization: major veins up to 2 cm thick contained mostly pyrite with minor amounts of galena and other minerals. Significant amounts of iron sulfide minerals and minor amounts of sphalerite and galena occurred in a cross-strike vein network. The Large Cut Face excavation provided a deep trench perpendicular through most of the stratigraphy at Skytop and revealed that the greatest concentrations of pyrite are in the Bald Eagle Sandstone, although it exists throughout the Reedsville-to-Tuscarora sequence in lesser concentrations. Later the Large Cut Face and other slopes were covered with remediation materials so the largest pyrite exposures are no longer accessible.

Important sulfide minerals at Skytop include pyrite, sphalerite, galena, marcasite, pyrrhotite, and chalcopyrite. Hammarstrom *et al.* (2004) reported that mineralized sandstones from the cut contain as much as 34 wt. % Fe, 28 wt. % S, 3.5 wt. % Zn, 1% wt. Pb, 88 ppm As, and 32 ppm Cd. Trace metal concentrations in the rock and in associated secondary minerals and seepage were attributed to inclusions (<10 μm) of CdS and Ni-Co-As minerals in pyrite and minor amounts of Cd in sphalerite (0.1 wt. % or less).

Quartz crystals are found lining joint surfaces. Barite, dolomite, and trace amounts of malachite occur in veins in the Juniata formation. Phosphate minerals such as wavellite and variscite have been found in the Tuscarora Sandstone. The principal weathering products of the pyrite are iron oxide minerals such as goethite (or "limonite") and hematite which occur as bright red, orange, or yellow crusts on joint faces (see paper by Doden *et al.*, this guidebook). During dry weather, water-soluble weathering-product minerals such as copiapite and halotrichite form as yellow and white "flowers" on

rock surfaces, but they are rapidly dissolved by rainwater. A compilation of secondary minerals is given in Table 1 of the Doden et al. paper and details for the most abundant minerals are described below.

Sulfide Minerals

The minerals of interest here are generally considered “secondary” in the sense they formed well after the primary minerals that comprise the sedimentary rocks at Skytop. The latter include common minerals such as quartz, feldspar, and clays of the various sandstones and shales of Bald Eagle Mountain. This paper focuses on epigenetic veins that contain some combination of sulfides, quartz, barite, and dolomite. However, other forms of secondary, non-vein minerals occur at Skytop, including iron oxides as small “clots” in the Bald Eagle and Juniata formations, an occurrence that is abundant and common in central Pennsylvania. Also, other pyrite exists at Skytop in *syngenetic* form in the Antes Black Shale, a sulfide that is common but one that formed by sedimentary processes different from that of vein (epigenetic) pyrite.

Pyrite

Pyrite is common at Skytop, although its concentration and habit are dependent on host lithology and other factors. It occurs primarily within the Bald Eagle Formation, although minor amounts have also been observed in the Reedsville, Juniata, and Tuscarora formations. Within the gray-green colored greywackes of the Bald Eagle Formation iron sulfide minerals are typically found on joint surfaces rather than on bedding planes, and some well-formed pyrite crystals have been found where the joints widen. Some faults also cut the sandstones. In one locality, pyrite makes up 50-80% of the material in a fault-brecciated zone that is up to a meter wide. This pyrite is present mostly as very small pyrite grains forming green-gray to black masses interspersed among fragments of gray sandstone. Filiform pyrite of highly unusual morphologies also occurs in open pockets within the fault zone. Fault slickensides occur in the massive pyrite and polished, grooved surfaces are found in the fault plane. The slickensides indicate a nearly horizontal direction of fault motion.

In the large Skytop roadcut through the Bald Eagle Formation (“Large Cut Face”), an oxidized zone (the gossan cap rock) and a reduced sulfide zone were exposed. Rocks in the latter commonly display joint surfaces which are covered with pyrite crystals. On most of these joint surfaces the crystals are small (< 0.5 mm), but concentrations on the sandstone joint surfaces impart a gray-green or bright brassy-white sheen. Many of the joint surfaces are covered with pyrite, and larger (greater than 5 mm thickness) veins occur as well (Figure 2). The larger veins appear to be randomly spaced but there is typically at least one



Figure 2. Thick sulfide veins along J2 joint direction (projecting out of the photograph). Steeply dipping bedding lies in the plane of the photograph (approximately parallel to the knife).

larger vein every 1 to 2 meters. These veins may range up to a meter in thickness (in the brecciated zone associated with the fault described above), but most are less than 15 mm in thickness.

Pyrite appears in at least two types of veins: the “dull” veins with gray-green pyrite and the “bright” veins in which the pyrite is bright brassy-white when freshly exposed. The difference between these two appearances may well be due to weathering and grain size: the duller veins may be composed of many very small, grain-like pyrite crystals with intergranular porosity permitting more rapid weathering, while the bright veins are composed of larger, more tightly intergrown crystals with little intergranular porosity (Sicree, 2005). The bright pyrite veins may have open spaces which can include euhedral pyrite crystals (up to 5 mm) with cubic habits and light striations. Smaller pyrite crystals (less than 2 mm) displaying both cubic and octahedral faces also occur. Most of these crystals have faces which are smooth and bright, and some are shiny metallic white rather than brassy in color.

Pyrites with highly unusual morphologies also occur within the Bald Eagle Formation at Skytop. Regarded as filiform or, more informally, as “whisker” or “needle” pyrites, their crystals are quite small (typically less than 1 mm in length) but they have length-to-width ratios of 10:1 up to 50:1 (see Plate 1). The filiform nomenclature is preferred for several reasons. First, the crystals are not curved lengthwise nor round in cross-section – most of these pyrite crystals have perfectly straight sides which meet at right angles. Under the microscope they more closely resemble a pile of matchsticks. In addition, there are lath-shapes, panel-shapes, irregular shapes with right-angled sides (appearing somewhat like angle-irons), and some pyrite cubes are skewered by “matchsticks”. Other filiform pyrites display intricate re-entrants and complex end terminations, but most have flat ends. Some of the stick-forms are suspected to be pyrrhotite or marcasite (Sicree, 2005). The filiform pyrite habits are associated with both “dull” and “bright” pyrite veins in the Bald Eagle Formation.

Pyrite hosted by the Reedsville Formation is typically disseminated throughout the shales and siltstones rather than distributed on joint surfaces, although some minor, thin veins of pyrite occur in southeast-trending joints. The greatest concentration of pyrite at Skytop outside of the Bald Eagle epigenetic veins is that hosted by the Antes, lowest member of the Reedsville Formation. This unit contains fine-grained sulfides, typical of Black Shales (carbonaceous and calcareous rocks) elsewhere in the region. Although the morphologies and compositions of the Antes sulfides have not been examined in detail, most this sulfide appears to be cubo-octahedral pyrite that formed syngenetically.

In the Tuscarora Formation, pyrite occurs sparsely as small (less than 1mm) bright euhedral crystals on joint faces, typically in association with sprays of variscite ($\text{AlPO}_4 \cdot 2\text{H}_2\text{O}$).

Sphalerite

Sphalerite is the second most common sulfide mineral at Skytop, although it is much less abundant than pyrite. Sphalerite occurs both as dark reddish-black masses and as reddish-black euhedral crystals. Massive sphalerite occurs in the Large Cut Face fault zone described above, intergrown with massive pyrite, typically as small (2-4 mm) blebs, although one specimen of massive sphalerite was found with a seam of sphalerite at least 20 mm wide. Discrete sphalerite crystals are typically less than 2 mm, although some slightly larger crystals occur. Under the microscope, these crystals appear as cone-shapes with flat bases. Some cones have a cratered end rather than a pointed top.

Galena

Galena (Figure 3) is less common than sphalerite and occurs in Skytop rocks as small (2 mm or less) cuboctahedrons, some of which may be heavily etched. The crystals typically have a dull metallic gray color and occur in open space on joint faces, in association with pyrite and sphalerite. Although lead isotopes in Skytop galena were not analyzed, other lead isotopes from central Pennsylvania are notably non-radiogenic. For example, galena from nearby Schad prospect in Milesburg had average values of $Pb^{206}/Pb^{204} = 18.539$, $Pb^{208}/Pb^{204} = 15.617$, $Pb^{208}/Pb^{204} = 38.582$ (Kesler et al., 1994).

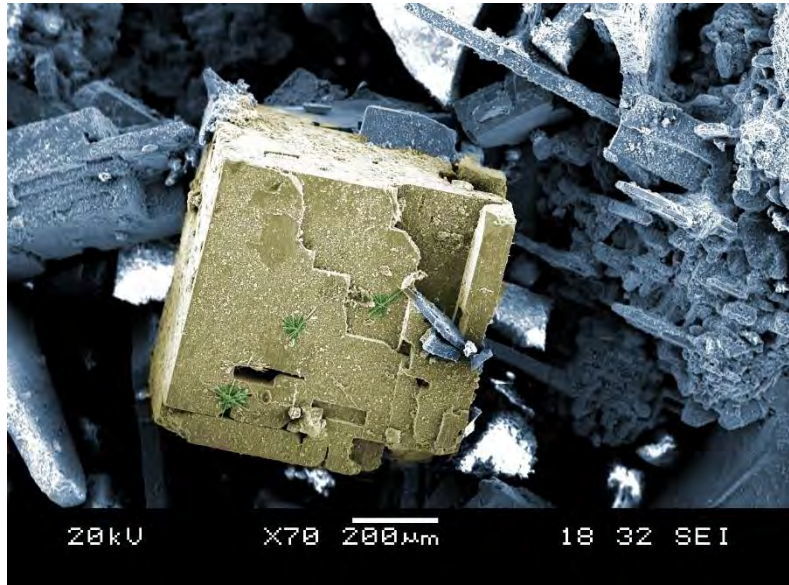


Figure 3. SEM image of plate-like pyrite crystals (gray) on and adjacent to a cube of galena (light tan). Image from R. Mathur, Juniata College.

Other Sulfide Minerals

Traces of pyrrhotite in the Bald Eagle Formation have been confirmed by x-ray powder diffraction. Marcasite may also occur but the relative amounts and distributions of the various minor iron sulfides are, yet, still undetermined.

Rare chalcopyrite occurs as brassy euhedral crystals (up to 5 mm) in the barite/dolomite veins in the Juniata Formation. Locally, these chalcopyrites are weathered, with a bright green (malachite) coating.

Some sprays of phosphate minerals (typically variscite) have at their cores small (3-4 mm) single crystals of a copper sulfide mineral, possibly chalcopyrite or bornite.

Other Secondary Minerals

Barite/Dolomite

A zone of veins containing both barite and dolomite occurs in the Juniata Formation at Skytop. These veins and associated brecciated zones are both concordant and cross-cutting. They are filled with a mass of white minerals which is an intergrown mixture of massive barite and massive dolomite. Veins range from very thin stringers < 1 mm up to about 1 cm thick and the brecciated zones are up to 5 to 10 cm across. As an associated halo around these veins, the reddish-brown siltstones/shales of the Juniata Formation have been altered to a light greenish-gray color. This color change suggests that the emplacement of the barite or dolomite was accompanied by a reducing fluid which, flowing through the joints and fractures, altered the oxidized reddish brown host rocks to a more reduced pale green/gray. Based on the available exposures, the barite/dolomite zone appears not to be in contact with the pyrite-rich zones discussed above.

Quartz

Small quartz crystals occur in the pyrite veins, typically forming a layer between the pyrite and the sandstone country rock. Most of these crystals display pyramidal faces about 1 mm across, although some 2-mm size doubly-terminated clear quartz crystals were also observed. The existence of quartz between the pyrite and sandstone host rock indicates that the quartz was deposited before the pyrite.

Oxidized Iron Minerals

Iron oxide minerals such as goethite and hematite occur in the near-surface oxidized rocks of the Bald Eagle Fm. forming a "gossan". This gossan is particularly well exposed in the remnants of the original road-cut located along old U.S. Rte. 322. The rocks of this oxidized cap are bleached white sandstones whose joint surfaces are covered with a mixture of iron oxide minerals. These surfaces are variously colored dull brown to shiny black to bright red, bright orange, or yellow. Mineralogically, these coatings are hematite, goethite, and other iron oxide minerals which are underlain by a thin layer of small (less than 1 mm) quartz crystals. Layers of iron oxides are typically less than 3 mm thick but can exceed 20 mm in thickness. Typically, the iron oxide minerals coat a layer of quartz crystals similar to the way pyrite coats a layer of quartz crystals in the reduced or sulfide zone.

Phosphate Minerals

The Tuscarora Formation crops out on the southwestern side of Skytop. Road excavations on this part of Bald Eagle Ridge exposed limited amounts of bedrock and little of this exhibited any sulfides. Pyrite was observed on some loose blocks of quartzite talus, although it was much less plentiful than in the Bald Eagle Sandstone. More unusual was the existence of variscite $[\text{AlPO}_4 \cdot 2\text{H}_2\text{O}]$ as apple-green mammillary masses (up to 3 mm thick) of fine radiating sprays of green crystals with white roots. These masses were initially regarded as wavellite $[\text{Al}_3(\text{PO}_4)_2(\text{OH}, \text{F})_3 \cdot 5\text{H}_2\text{O}]$ but later x-ray analyses confirmed their classification as variscite. In close spatial association with the variscite is bonafide wavellite, which appears as white to cream-colored radiating sprays up to 2 mm thick and with individual crystals up to 15 mm long. A single boulder of Tuscarora quartzite yielded both green crusts of variscite and cream-colored sprays of wavellite. Also found in this boulder was a highly-unusual 10 cm pod filled with a tan-colored material. The pod contained brown, 8 mm diameter spheres with white cores approximately 7 mm in diameter. Initial analyses of the pod indicate it comprises a mixture of quartz and minor mica, along with the phosphate minerals variscite, crandallite $[\text{CaAl}_3(\text{PO}_4)(\text{PO}_3\text{OH})(\text{OH})_6]$ and possibly minor amounts of Woodhouseite $[\text{CaAl}_3(\text{SO}_4)(\text{PO}_4)(\text{OH})_6]$ and metavariscite.

Sulfate Minerals

Sulfide-bearing rocks in the outcrops and the spoil piles weather rapidly. White and yellow weathering product minerals have been observed as efflorescent crusts. At least some of the yellow crusts are copiapite, whereas the white crusts are halotrichite. Other sulfate minerals probably occur there as well. Gypsum, however, is rare in the Bald Eagle road cut because of the lack of a source of calcium within the sandstones and shales (although gypsum is probably being formed within the spoil piles because limestone rock was added to these piles to control acid drainage). The copiapite/halotrichite crusts are water-soluble and disappear during rain storms and then reappear as the rocks dry out. These water-soluble sulfate minerals act as a readily-available reservoir of sulfate

ions. During a rain storm, they dissolve rapidly and contribute to an upward "spike" in the total sulfate concentration of run-off waters. Further discussion of efflorescent minerals at Skytop is given in Doden et al., this guidebook.

Genesis of Epigenetic Minerals at Skytop

In many central Pennsylvania localities, the emplacement of sulfide deposits, including those of Skytop, appears to be strongly influenced by local structures, ranging from macroscopic to mesoscopic scales. Faill *et al.* (1989), for example, described sulfide veins in Sinking Valley as semi-planar and having a trend of northwest-southeast, commonly within or sub-parallel to sub-vertical faults. As discussed in the Gold et al. paper of this guidebook, a significant lineament/fault system intersects Bald Eagle Mountain and appears to have had two effects: One is the faulted zone was relatively weak and enhanced erosional processes through the double ridge of the mountain, ultimately forming the Skytop wind gap. Secondly, this fault system provided a complex pathway for movement of sulfide-bearing fluids and local ground waters. The association of sulfide deposits and lineaments (regional-scale structures) in central Pennsylvania was recognized years ago (Hsu, 1973; Krohn, 1976; Howe, 1988). Figure 1 shows the generalized localities of known or suspected sulfide deposits in central Pennsylvania along with an interpretation of regional lineaments based primarily on LandSat images. More recent imagery available from Lidar-based mapping shows a substantial lineament that extends westward from Nittany Mountain to Skytop (Gold et al. paper of this guidebook). Multiple faults have been mapped along the eastern part of the lineament and faults at Skytop comprise its western end.

Another contributing factor to sulfide emplacement at Skytop was the nature of the host sediments. The Bald Eagle Formation has lithologic characteristics amenable to vein emplacement. Through-going fractures developed in this brittle, sandstone-dominated unit more readily than in rocks of the adjacent Reedsville and Juniata formations. The latter have a greater proportion of interbedded softer shales and are therefore presumably less susceptible to brittle fracture. This resembles the mechanism proposed by Smith (in Faill *et al.*, 1989) as the cause for formation of sulfide and gangue minerals in brittle dolostones near in Sinking Valley, near the village of Culp.

In the Large Cut Face roadcut, one may observe both the oxidized cap rock (the "gossan") and unoxidized (reduced) sulfide zone – features characteristic of many near-surface ore bodies (Rose and Burt, 1979). It is possible to find excavated blocks of Bald Eagle sandstone with both iron oxide and iron sulfide coatings, suggesting that they were at the oxide-sulfide (oxidized iron-reduced iron) geochemical boundary. Typically, the iron oxide minerals coat a layer of quartz crystals similar to the way pyrite coats a layer of quartz crystals in the reduced or sulfide zone. This indicates that, upon oxidation of iron sulfide minerals to iron oxide minerals, much of the iron probably did not move, although the sulfur was carried away as dilute sulfuric acid (sulfate ions in solution).

Observations of vein relationships and pyrite morphologies permit us to establish a tentative paragenetic sequence. The existence of quartz coatings between the pyrite and sandstone host rock indicates that the quartz was deposited before the pyrite. Fluid inclusion formation temperatures for quartz from the Bald Eagle Formation cover a wide range, from 150-250°C, suggesting that the quartz was precipitated from hydrothermal fluids at a depth of 5-8 km (Barnes, 2015). Precipitation of different morphologies of pyrite from hydrothermal fluids has been observed experimentally at

various temperatures and degrees of supersaturation (cf. Murowchick and Barnes, 1987). Thus, it is possible to correlate pyrite morphology paragenesis with changing conditions of deposition.

Early, striated cubic pyrite crystals are followed by smooth-faced cubic crystals. The change from early, lightly-striated pyrite to smooth-faced cubic crystals is indicative of a progression from low-supersaturation, higher-temperature (above 250°C) conditions to moderate-supersaturation, lower-temperature conditions. Filiform pyrites appear to be a third, possibly much later stage of pyrite deposition or recrystallization. Later filiform pyrite may indicate a subsequent shift to low-temperature (below 250°C), low-supersaturation conditions. It is also possible that filiform pyrites are the result of a later remobilization of the pyrite.

In their mapping near Milesburg, Butts and Moore (1936) observed sulfide deposits and noted that the gangue minerals consist of clay and barite, and the “deposit has the appearance of having been concentrated by meteoric waters percolating through the sandstone and collecting the metals in a fissure and along the bedding planes of the sandstone.” Their description hints at an epigenetic origin from hydrothermal fluids. This and eight other localities discovered since then near Milesburg are discussed by Smith (1977). The general mineral assemblages at these sulfide localities include pyrite, sphalerite, galena, and barite. The Skytop sulfide mineralization resembles in some respects other sulfide deposits in central Pennsylvania, such as the Fort Roberdeau lead mines east of Altoona, the Keystone zinc mine east of Tyrone, and the Schad zinc-lead prospect between Bellefonte and Milesburg.

Given the morphologies, abundances, and structural geological conditions of the host rocks, it is concluded that most of the pyrite occurring on joint faces in the sandstones of the Bald Eagle Formation at Skytop must have been emplaced from hydrothermal fluids, long after lithification of the host sediments.

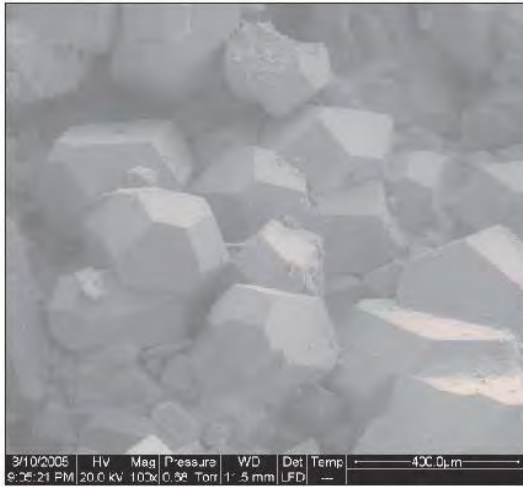


References

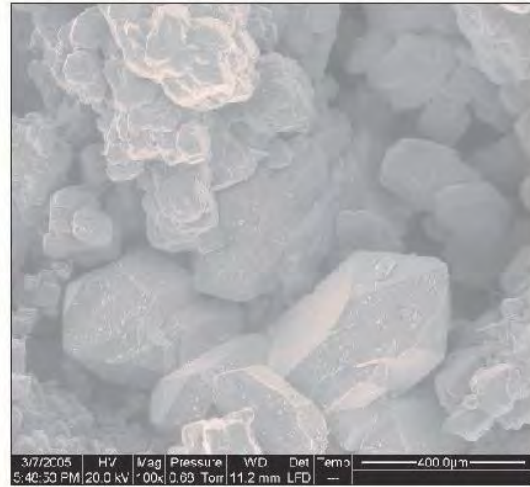
- Barnes, H.L., 2015, Hydrothermal processes, *Geochemical Perspectives* 4, 28-31.
- Butts, Charles, and Moore, E.S., 1936, Geology and mineral resources of the Bellefonte quadrangle, Pennsylvania. U.S.G.S. Bulletin 855, 111 p.
- Fail, R.T., Glover, A.D., and Way, J.H., 1989, Geology and mineral resources of the Blandburg, Tipton, Altoona, and Bedford Quadrangles, Blair, Cambria, Clearfield, and Centre Counties, Pennsylvania. Pa. Geol. Survey, 4th Series, Atlas 86, 209 p.
- Gold, D.P., 1999. Lineaments and their Interregional Relationships, Chapter 22, pp. 307-313, in *The Geology of Pennsylvania*, Ed. C.H. Schultz, Special Pub. # 1, Pennsylvania Geol. Surv., and Pittsburgh Geol. Soc., 888 p.
- Hammarstrom, J.M. Brady, K.B.C., and Cravotta III, C. A., 2004, Acid-rock drainage at Skytop, Centre County, Pennsylvania, USGS Open-File Report 2005-1148.
- Howe, S. S., 1988, Locations and descriptions of mineralized rock samples from Mississippi Valley-type lead-zinc occurrences in central Pennsylvania, Menlo Park, California, U. S. Geological Survey Open File Report 88-250, 37 p.
- Hsu, Fu-Tzu, 1973. *Geochemical Exploration in the Nittany Valley Area, Centre County, Pennsylvania*. Unpub. M.S. Thesis, Department of Geosciences, The Pennsylvania State University, University Park. 108 p.
- Illsley, C.T., 1955, An investigation of geochemical prospecting by testing stream waters. Unpub. M.S. thesis, Pennsylvania State University, University Park.
- Kesler, S. E., Appold, M. S., Cumming, G. L., and Krstic, D. (1994). Lead isotope geochemistry of Mississippi Valley-type mineralization in the central Appalachians. *Economic Geology*, 89 (7), 1492-1500.
- Krohn, M.D., 1976, Relation of Lineaments to sulfide Deposits and Fracture Zones along Bald Eagle Mountain: Centre, Blair, and Huntingdon Counties, Pennsylvania. Unpub. M.S. Thesis, Department of Geosciences, The Pennsylvania State University, University Park. 104 p.
- Miller, B.L., 1924, Lead and zinc ores of Pennsylvania. Penn. Geol. Survey, 4th Series, Mineral Resource Report #5.
- Murowchick, J.B. and Barnes, H.L., 1987, Effects of temperature and degree of supersaturation on pyrite morphology, *Am. Min.* 72, 1241-1250.
- Rose, A.M. and Burt, D.M., 1979, Hydrothermal alteration, in Barnes, H.L., Ed., *Geochemistry of Hydrothermal Ore Deposits*, Second Edition, Wiley-Interscience, New York, Chap. 5, 173-235.
- Sicree, A.A., 2005. Morphology and Paragenesis of Sulfide Mineralization on Bald Eagle Ridge, Centre Co., Pennsylvania. Abst. NE- Section Meeting, Geol. Soc. Amer., Saratoga, V.37, # 2, p. 64.
- Smith, R.C., 1977. Zinc and lead occurrences in Pennsylvania. Pennsylvania Geological Survey, 4th ser., Mineral Resources Report 72, 318 p.
- Smith, R.C., 2003. Lead and Zinc in Central Pennsylvania. *Pennsylvania Geology*, v. 33, # 4, pp. 2-8.

Plate 1. Environmental Scanning Electron Microscope (SEM) images (not gold coated) of pyrite and other minerals from Skytop.

- a. Cubo-octahedral crystals of pyrite (largest is about 0.4 mm across) from Skytop.
- b. Euhedral quartz crystals (largest is about 0.5 mm in length) coated with irregular grains of pyrite.
- c. Quartz crystal with spray of gypsum crystals on pyramidal face, surrounded by lath- and stick-like filiform (“whisker”) pyrite crystals.
- d. Spray of gypsum crystals – possibly recent in origin.
- e. “The Johnstown Flood” pyrite displaying a wide variety of lath-like, stick-like, and board-like crystal habits. Note reentrants on some laths.
- f. Higher magnification view of image in (e) showing details of panel-shaped forms – some of which have grown on the end of filiform pyrite crystals. Note flat end of stick-like crystal on left.
- g. Pyrite plate and matchstick morphologies with right-angle edges and inset corners. Note complicated structures and multiple reentrants.
- h. “The Sword in the Stone” cubo-octahedral pyrite “skewered” by the later out-growth of a matchstick-like pyrite crystal. Note that end terminations are complex, not flat.
- i. Surface of modified cubic crystal of pyrite with multiple epitaxial overgrowths of complex pyrite crystals. Note reentrants.
- j. Highly complex pyrite crystals with multiple complex reentrants. Note similarities between reentrants on different crystals. Note that reentrants display discrete crystal faces lining interiors of reentrants – these are likely growth features rather than dissolution pits (?).
- k. Skeletal pore patterns in pyrite crystals. Note stepped reentrants penetrating interiors but not edges of skeletal pyrite – these are likely growth features rather than dissolution pits (?).
- l. Close-up view of striated faces on cubo-octahedral pyrite crystal.



a.



b.



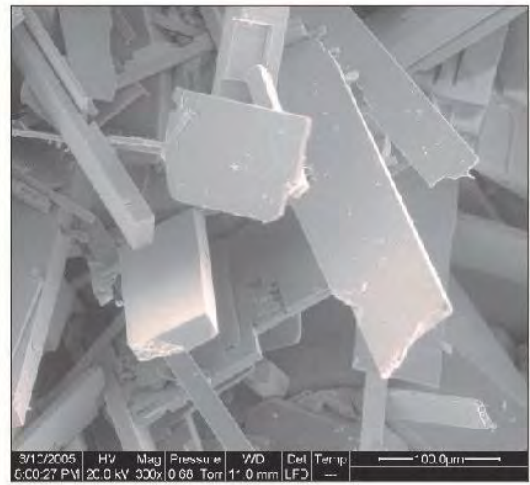
c.



d.



e.



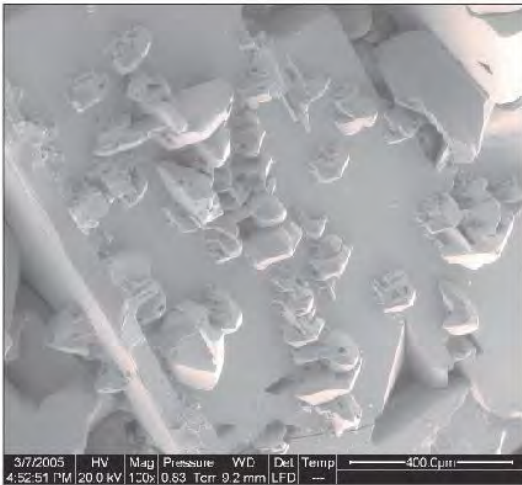
f.



g.



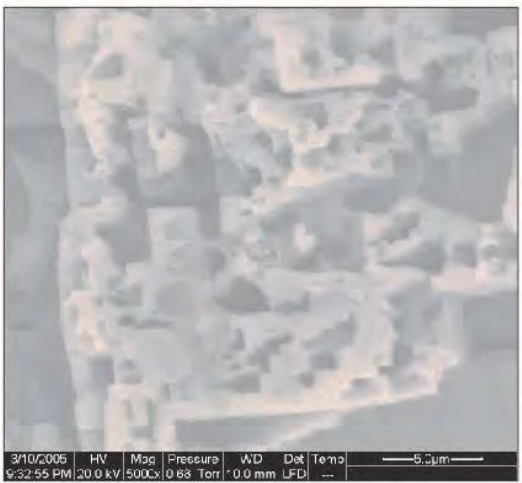
h.



i.



j.



k.



l.

POST-EXCAVATION MINERALOGY AND ACID-ROCK DRAINAGE TREATMENTS AT SKYTOP

ARNOLD G. DODEN¹, DAVID (DUFF) GOLD² AND HUBERT L. BARNES³

¹ GMRE, Inc., 925 West College Ave., State College, Pa 16801. ² Emeritus, Department of Geosciences, Penn State University, University Park, PA. ³ Emeritus Distinguished Professor of Geochemistry, Department of Geosciences, The Pennsylvania State University, University Park, PA 16802

Introduction

PennDOT did not anticipate the unexpected consequences of rock chemistry when the route for I-99 was chosen through Skytop wind-gap. Acid rock drainage (ARD) at Skytop resulted from the exposure and subsequent oxidation of an extensive network of sulfide veins (see accompanying papers in this guidebook). The magnitude and scope of the problem was not fully appreciated until after pyritic rock in deep cuts was used as fill on other sections and as buttress ballast on cuts threatened by slope failure. PennDOT and its subcontractors were faced with the challenge of mitigating significant amounts of ARD that, among other problems, contaminated the high-quality Buffalo Run stream and local water wells. At the time of pyrite discovery (2003) a number of physical, chemical, and biological methods existed by which ARD potentially could be mitigated, only the most important of which are discussed here. This report addresses the post-excavation sequestration and acid rock drainage issues, the real time geological processes and some of the treatment options. But for the sequencing of construction events a “perfect storm” scenario might have been averted.

In the preparation of this discussion, we acknowledge valuable reviews of earlier drafts by Andrew Sicree <sicree@verizon.net> and Antonio Lasaga (<aclasaga314@gmail.com>).

Skytop Time-Line

The deep cuts in the C-12 section (west-northwest of Skytop), and A-12 section (southeast of Skytop) were well advanced by the summer of 2002 (Figure 1). Hill slope creep of up to 10 feet in a 24-hour period developed in the former, requiring not only a change in the slope angle (from 1H:2V to 2H:1V), raising the eastbound roadbed 17 feet, but also loading of the toe with two buttresses. Meanwhile, the cut in the A-12 section, later named the Large Cut Face (LCF), had mined through approximately 1000 feet of Bald Eagle and Juniata sandstones harboring a system of sulfide-bearing veins. The veining had not been recognized and a substantial amount was in the fill and buttresses in the C-12 section. The rest was dumped in the unlined Siebert, Arbogast and Skytop waste sites as well as 97 other places where road bed fill and berm material were needed. It was not until a year later (September, 2003) when Michael Smith noticed rusty-red fluid draining from a 97,000 ton stockpile of aggregate that the gravity of the situation was realized. A substantial amount of

¹ Emeritus, Department of Geosciences, Penn State University, University Park, PA

² GMRE, Inc., 925 West College Ave., State College, PA 16801

³ Emeritus Distinguished Professor of Geochemistry, Department of Geosciences, The Pennsylvania State University, University Park, PA 16802.

sandstone had been crushed and screened for construction material, only to be rejected by PennDOT's petrographic lab for use in concrete.



Figure 1. Skytop sites

Environmental concerns prompted an investigation by the U.S. Geological Survey (Hammarstrom et al., 2004) and state agencies, and for PennDOT to sponsor detailed geological studies by GMRE, Inc., of State College (April, 2004; Gold and Doden, 2005). A special session of the Nittany Mineralogical Society Symposium (June 6/12-14/2004) was dedicated to Skytop issues. The findings of several geological and geophysical studies were presented at the Skytop Acid Rock Conference, sponsored by the Department of Geosciences, Penn State University, and the Clearwater Conservancy, December 19-20, 2004. It was apparent from these meetings that more insight was needed on the chemistry of (a) oxidizing and hydrating sulfide veins, (b) the sulfurization processes in the active REDOX zone, (c) the complex interactions of the pyritic waste rock with the various remediation additives (limestone, baghouse lime (BHL), a.k.a. lime kiln dust (LKD), Pennsuppress, Bauxsol™, and *Acid-Cure* Slurry) and (d) the expansive properties of the alteration products.

A temporary measure of covering waste dumps and fill area with black polyvinyl chloride tarps weighted down with bags of sand (Figure 2) was effective in greatly reducing the volume of ARD. The tarps outlasted their expected life of 1 year by a factor of three. However, concern over acid containment in powdered limestone-hosted fill, as in the S.R. 3042 embankment (Figure 3), spurred a search for other neutralizing agents. Three additional neutralizing agents were tested: slurry mixes of Bauxsol™ powder, magnesium oxide powder, and powdered limestone. Four large concrete septic tanks (~159 cubic feet) were set up on site and filled with waste pyritic rock (Figure 11). During June and July, 2005, the three different neutralizing agents were added periodically at set concentrations, along with daily application of local well water of known temperature, specific conductance and pH to test the effectiveness of each slurry. Further discussion is provided below.



Figure 2. a). above: Weighting of plastic sheeting by plastic bags on three sites.

b). below: Distribution of plastic bags to hold plastic sheeting in place.



In other Skytop evaluations of ARD neutralizing agents, several separate areas in the C-12 section were set aside for pilot-scale test operations to evaluate delivery systems, application volume, and effectiveness. The largest of these was an experiment to apply Bauxsol™, red clay alumina extraction residues from bauxite ores plus patented additives in a spray irrigation system over an area approximately 400 feet wide (Figure 4). This test area incorporates part of the large buttress on the west side of the drainage divide at the road bed. Problems with particle size, slurry mixing, maintaining a uniform slurry viscosity, and the spray delivery system severely limited the effectiveness of the system, and thus compromised an evaluation of the chemical effectiveness of the Bauxsol™ slurry.



Figure 3. A point source acid break-out in a powdered limestone-hosted fill on the S.R. 3042 embankment. Reactions were inhibited by armoring of gypsum.



Figure 4. Test site on the large buttress for spray application of Bauxsol™ across drainage divide in Section C-12.

Other slurry mixes of limestone, magnesium oxide, and *Acid-Cure* Slurry were applied to approximately 100-foot wide test areas east of the Large Buttress, and to a 50-foot test area west of the small buttress (see Figure 1 and 16). Details of these experiments are discussed below.

PennDOT had decided on a removal strategy for waste rock to a permitted site. To do this, the legal remediation mandate of removing all excavated toxic rock had to be revised to “accessible”, because a substantial amount of waste had already been used as roadbed fill, as well as in two buttresses and scores of berm sites. The plan was to move “accessible waste” from road-fill sites S.R. 3042 and Sellers Lane, as well as the seven dump sites identified as Arbogast Wedge, Arbogast Driveway, A-12 Structure 300/301 and the crushed rock pile, Skytop, Trumbull Batch Plant and Siebert. Approximately 48% of the 1,178,464 cu yds of movable material had been pre-treated with lime kiln dust (LKD).

The nearest of these brown-field sites was located near Indiana, Pennsylvania, and the other in Utah. A green-field site was located in Bald Eagle Valley, one mile east of Post Matilda. Clearly, the latter was the best option, and the necessary permitting was expedited and drilling at the site was completed by the end of November, 2005. This site, later to be known as ERPA (Engineered Rock Placement Area), could be accessed from the unopen I-99 highway, less than 4 miles from Skytop. Site preparation for a repository with a 27-acre footprint began during the fall of 2007 (Figure 5) with construction of two lined cells (Figures 6 and 7) to standard specifications, and a planned capacity of 435,000 cu yds of waste rock and 55,000 cu yds of baghouse lime in cell A (I-99 Newsletter, No. 7, November-December, 2007). The objective was to create a “dry tomb” in which pyrite could be sequestered and contained, and any acid produced could be collected in a sump and treated. Baghouse lime (BHL) was chosen to be the neutralizing/sequestration agent because it was readily available and had a proven history in the coalfields of western Pennsylvania. The presence of portlandite (CaOH_2) in the norm could mean a high pH (13.2), with the potential to dissolve silica and alumina, but also increase its effectiveness in neutralizing any sulfuric acid (for details on the mixing ratios see article by Farmerie and Smith, this volume).



Figure 5. Initial construction of the Engineered Rock Placement Area.

The ancillary waste rock contamination sites were mapped during the summer of 2006 over a stretch of 15 miles of I-99 and subsidiary roads. Treatment/remediation strategies have been outlined in a report (Gold and Doden, 2008). Several these issues and the control measures instituted are discussed in more detail below. There were sealing covers installed over areas where pyritic rocks remained in place.



Figure 6. The eastern cell of the ERPA repository.



Figure 7. The western cell of the ERPA repository.

GeoWeb Cover System

Large parts of slopes at Skytop were remediated by use of a GeoWeb system, including the Large Cut Face, Small Cut Face, and Large Buttress (see Figure 8, recent Google Earth image showing coverage). The main part of this system consists of a strong, interwoven network of steel cable-reinforced plastic webbing filled with limestone gravel. To install this system contractors first removed loose rock and debris from the slope to be treated, providing a relatively stable and clean surface. The first layer covering bare rock was a Class 4 geotextile, which in turn was covered by a 40 mm thick textured HDPE liner. This in turn was followed by a second layer of Class 4 geotextile. The top layer consisted of the GeoWeb material (see Figure 9), unrolled from the top of the slope downward, covering the slope in large strips.

The GeoWeb strips were attached to the top of the slopes with stainless steel cables and posts, and cables extend down the entire slopes with attachment points and rebar stakes distributed along the lengths of the GeoWeb strips to hold them in place. The final step was to fill the GeoWeb cavities with limestone gravel, using enough excess gravel to ensure the GeoWeb material was completely buried.

No specific details regarding the GeoWeb system’s condition are available, but visual inspection (Figure 10) shows many parts of the Web are now partially exposed due to downward creep of the aggregate.



Figure 8. Google Earth view of Skytop showing important sites, including GeoWeb installations (light gray areas).



Figure 9. *GeoWeb textile held in place by stainless steel cables. The fill/cover of limestone aggregate has yet to be added.*



Figure 10. *Slumping of limestone aggregate on GeoWeb remediation system, exposing its textile webbing.*

Treatment Testing

There had been general recognition by the Pennsylvania Department of Transportation of the common association of ARD with highway construction. Consequently, when that became a major problem during building at Skytop, there was heightened interest in identifying the optimum means of preventing or treating ARD. Several potential cures were investigated taking advantage of the excavated pyritic waste for testing. Summarized here are the tests conducted and their results.

Tank Experiments

The efficiency of three slurries was tested in several tanks for treating of acidity caused by pyrite weathering. Slurries of Bauxsol™, powdered limestone, and brucite [Mg(OH)₂] were sprayed onto 10-ton masses of pyritic aggregate contained in septic tanks, and the acidity and sulfate concentrations of outflows were monitored for 21.5 months (Figure 11). Each cell contained 159 cubic feet of unscreened broken toxic rock, packed to a porosity of 20%. Five batches of slurry (4 and 8% mixes) were added periodically. A manometer system on the tanks was used to monitor porosity, and fluid throughput was measured after each cycle. After 56 cycles of daily infusions, the cisterns were drained. However, their contents were not exposed and analyzed for travel paths and reaction fronts until March, 2007 (Barnes and Gold, 2008). An additional test was staged in a fourth tank, containing an approximately 10-ton sample of concentrated pyrite veins from road station 885+75. A total of 3270 lbs of Bauxsol™ and 26.4 lbs of MgO were added incrementally as a slurry using recycled effluent to test its effectiveness in neutralizing acid. This experiment was terminated after 232 days (April 26, 2006) of acid production.



Figure 11. *Septic tanks with white sampling valve and a small, near vertical plastic tube that serves as a manometer to indicate water level in each tank. Additives tested were Bauxsol™ in the right tank, MgO in the center tank and limestone in the left tank (from Barnes and Gold, 2008).*

After addition in identical procedures, neutralization of the outflow to a pH of above 6 was achieved by Bauxsol™ for about 1 day, by limestone for 4 days, and by Mg(OH)₂ for the 652 days of the testing. Limestone control of pH was limited by armoring of the CaCO₃ by gypsum [CaSO₄·2H₂O] and by restricting of water flow to channels so that most of this slurry remained unreacted. Channels were not evident in the Mg(OH)₂-treated aggregate. With the limestone and Mg(OH)₂ slurries, sulfate concentrations were controlled by crystallization of gypsum, or at higher concentration of sulfate by hexahydrate [MgSO₄·6H₂O]. The limestone slurry limited sulfate concentrations to approximately 25 percent less than that occurring with the Mg(OH)₂ slurry.

These experiments revealed that (a) mixing is critical but difficult to achieve, (b) only a portion of the limestone reacted due to gypsum armoring, and (c) the flooding delivery systems did not work. An ideal slurry might include Mg(OH)₂ for neutralization, limestone for limiting sulfate concentration, and other components to alter rheological behavior. Thixotropic behavior that favors initial dispersion of the slurry solids yet reduces loss in outwash and limits channelization of water flow is best. Further details of the tank experiments are discussed in Barnes and Gold (2008).

Bauxsol™ Slurry

One test directed by PennDOT involved the application of Bauxsol™ to an area on the Large Buttress of Skytop. Bauxsol™ is a product made of bauxite refinery residues (“red mud”; McConchie et al., 1999) and is developed and marketed by Virotec, Ltd. The precise composition of Bauxsol™ varies according to source, but its composition in Table 1 is that used in the tank experiments and is probably representative of that applied to the Large Buttress.

Table 1. Composition of Bauxsol™ (in wt%) determined by XRD analysis (N. Wonderling, Pennsylvania State University, 2005).

Mineral	Wt.%
Hematite	30.8
Gibbsite	19.3
Sodalite	14.0
Goethite	11.1
Rutile	8.3
Anatase	5.4
Halite	4.1
Calcite	3.8
Quartz	1.7
Boehmite	1.4

Under the supervision of Virotec, Ltd. representatives, Bauxsol™ was mixed with water on site and applied by pumps and a dense network of sprinkler pipes to a test plot of approximately 1000 m²

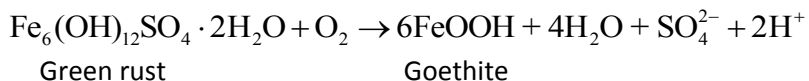
on the Large Buttrass of Skytop (Figure 4). Following application and 60 days to allow penetration by the Bauxsol™ slurry, five trenches were cut by excavator into the layer of rubble covering the slope, well below the zone treated by Bauxsol™ (Figure 12). The bright orange-red color of the slurry permitted easy visual inspection of its three-dimensional distribution within the underlying rubble, a mixture of fine to coarse rock fragments. The Bauxsol™ penetration was limited to approximately 1-2 feet. Where used on pyritic waste on a buttrass at Skytop, it managed to control the pH up to only 4.



Figure 12. View of Bauxsol™ treated area at Skytop. Orange colored Bauxsol™ coated rubble remains on left side of image. Also shown are sprinkler pipes used to distribute the Bauxsol™ slurry over the surface. A trench dug through the rubble is on the right side and foreground in this photograph. As shown here, Bauxsol™ penetration depths into rubble were limited to less than 2 feet.

Lime Kiln Dust Slurry

Preliminary treatments were tried using Bauxsol™ and LKD (lime kiln dust of 56.9 wt% CaO) by applying each to the buttrass (<1 wt% pyrite) on the south berm of I-99 at Skytop. The buttrass test area consisted of alternating layers of LKD and waste rock. Bauxsol™ is seawater-washed waste from bauxite refineries of variable composition and little buffering capacity that after 80 days application to about 6 in, multiple sections showed a layer typically up to 1 ft thick colored by green rust alteration. As soon as that mineral was exposed to air, within minutes it vividly altered, losing its green color to form mostly goethite.



Both treatments failed but for different reasons. Bauxsol™ lowered the acidity of the ARD slightly to remain at moderately acidic pH's, usually of 2 - 4 from pyrite weathering. In contrast, the lime caused caustic outflow, with very alkaline drainage at pH's as high as 12.3 due to buffering by dissolved Ca(OH)₂.



Figure 13. About 1 foot of green rust under less than 1 inch of red Bauxsol™ surface coating.



Figure 14. A mixed layer at pick level with minor green rust above and patches below of black LKD.

Acid-Cure Slurry and Further Testing

Runoff from the pyritic excavations along the south berm of Route I-99 at Skytop was certain to cause acidic pollution from the typical Centre County rainfall of 45 in/yr (Gold et al., 2007; 2008). There, to control the expected ARD, three different, potentially useful slurries were tested. Each was applied in 2006 and the results have been monitored since then. The slurries were applied to the rock slopes from a hydroseeder truck by spraying up to 120 feet up the 23° slope (Figure 15).

Of the sections excavated, three contained about 2 wt% near-surface pyrite and were treated to prevent pollution by runoff. The inorganic slurries used were mixes of fine (325-mesh) powders with solids concentrations adjusted for best viscosities. They were distributed by spraying as shown with Figure 15. Section 1 (0.19 acres), was coated with 1.5 inches of the Penn State **Acid-Cure** slurry, Section 2 (0.22 acres) with 0.5 inches of MgO, and Section 3 (0.19 acres) with 1.5 inches of powdered CaCO₃ (Figure 16). **Acid-Cure** is a thixotropic (paint-like) fluid mix of fine CaCO₃ plus MgO and clay, here with 60 wt% solids fixing its viscosity at about 1350 centipoise for both effective spraying and negligible runoff for that slope. Particularly effective for viscosity control is Georgia clay (>95 wt% kaolinite) which also lowers common ARD pollutants by adsorbing As, Cr, Pb, Co, Mn, Cu, and others. Its virtues are listed in Table 2.



Figure 15. Spraying of a slurry at Skytop.



Figure 16 Looking south at the treated sections.

On, or close to, the surface in the three test sections, a rigid coating of caliche (CaCO₃), up to about 1 in-thick, formed in patches generally less than a foot wide. It is apparently very stable at the acidities of the treated sections. The pH of the three sections has been monitored since the application of the treatments with the results in the following Table 3.

The acidity of the three sections was apparently effectively controlled by the three different slurries at the low pyrite concentrations on these slopes. Where no slurry treatment was applied, the runoff was acidic at 3.7 – 5.8, probably reflecting the local pyrite concentrations. The acidity decreased with time as the pyrite became more weathered. The treatment with powdered limestone on Section 3 was initially nearly as effective as the other slurries, but the limestone's buffering capacity was known to decrease in time due to the reaction of CaCO_3 to become coated with gypsum ($\text{CaSO}_4 \cdot 2\text{H}_2\text{O}$). Buffering by magnesia on Section 2 was about as effective as that on Section 1 but the cost of that component was much higher than the mix for **Acid-Cure**. Note that buffering in these slopes by the **Acid-Cure** on Section 1 has remained effective for over a decade. There, by maintaining weakly alkaline conditions around the pyritic surfaces in these slopes, the pyrite reacts to become armored by multiple oxyhydroxide sulfates which reduce further reactions. Consequently, after a decade with developing armoring, it is probable that the treatment will be permanent with no further additions of **Acid-Cure** required. That treatment is efficient because its Mg content kinetically blocks the reaction of its CaCO_3 with the sulfate of the ARD so that all the carbonate content of the slurry remains an active acid buffer.

TABLE 2: Characteristics of the Acid-Cure Slurry

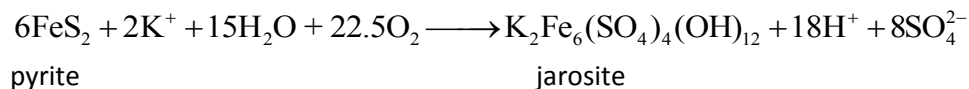
- Components are hazard-free, ingestible compounds.
- Components are common, low cost materials often locally available.
- Slurry viscosity is adjusted with solids concentration for treatment on slopes.
- Slurry quantity needed is set for the pyrite content of the rock volume to be treated; a cost-saving single application is sufficient forever.
- Applicable as a slurry or as a powder if water supplies are limited and later rainwater can redistribute the powder.
- Buffers acidity to near neutral, pH 6-9, never too caustic regardless of amount applied.
- Beneficially reduces concentrations in ARD of polluting As, Cr, Pb, Zn, Cu, Co, Mn, Ti, Fe, etc.
- Controls permanent neutralization of ARD without losing component activity to armoring reactions.
- Rheological behavior favors a thixotropic coating on pyrite that catalyzes armoring to inhibit further pyrite oxidation.

TABLE 3. pH Data from Skytop: Multiple Measurements at Each Date

Date	Section 1	Section 2	Section 3
Surface Runoff			
10-20-2006	8.17	7.90	7.13
11-1-2006	7.54	7.14	6.82
11-20-2006	7.51	8.11	-
3-27-2007	8.28	8.49	8.24
5-2-2007	7.33	7.22	6.97
5-9-2007	7.17	6.67	-
4-15-2016	7.52, 7.53		
5-9-2016	7.06, 7.22, 7.91	7.61, 7.95	
Untreated Area East of Section 1			
1-15-2006	3.74, 5.73, 5.76		
8-5-2016	5.34, 5.80, 5.84		

Alteration Processes

With or without treatment, there are various alteration minerals that form during the weathering of pyrite, examples of which are listed in Table 4. That alteration during growth commonly causes expansion when pyrite is converted to secondary minerals, a process that may disrupt and open the rock matrix catalyzing further weathering. The resulting volume change can be evaluated, first by writing a stoichiometrically balanced reaction from pyrite to the overcoating mineral. Second, by calculating the difference between the molar volumes of the two minerals from Table 4 in proportion to their stoichiometric ratio. For example, pyrite is often replaced by jarosite:



and the change in the molar volume product is $160 - 6 \times 23.94 = 16.36$ cc/mole or $\Delta \bar{V}_R = +2.73$ volume%. Except for producing the simple oxides of goethite or lepidocrocite, most alteration of pyrite causes an increased mineral volume. However, such volume changes can provide lower permeability and form armoring on pyrite surfaces, thereby stalling further alteration. That is a worthy objective of any chemical treatment of ARD, especially where the volume changes are small, as for the above example of jarosite after pyrite. Some efflorescent minerals may form quickly on, or

close to, exposed pyrite surfaces. Examples of such minerals from Skytop are listed in Table 5 and their distributions illustrated in Figures 17 and 18.

TABLE 4. List of Secondary Alteration and Efflorescent Minerals Identified at Skytop

Bauxsol™:

- primary: [Hematite] Fe_2O_3 , [Quartz] SiO_2 , [Gibbsite] $\text{Al}(\text{OH})_3$, [Albite] $\text{Na}(\text{Si}_3\text{Al})\text{O}_8$
- secondary? [Thermonatrite] $\text{Na}_2\text{CO}_3 \cdot \text{H}_2\text{O}$, [Halite] NaCl , [Nepheline] $\text{KNa}_3\text{Al}_4\text{Si}_4\text{O}_{16}$,
 [Sodalite] $\text{Na}_{7.6}(\text{Al}_6\text{Si}_6\text{O}_{24}(\text{CO}_3)_{0.93}(\text{H}_2\text{O})_{2.98})$, [Anhydrite] CaSO_4 , [Arcanite] K_2SO_4 ,
 [Trona] $\text{Na}_3\text{H}(\text{CO}_3)_2(\text{H}_2\text{O})_2$, [Oxammite] $(\text{NH}_4)_2(\text{CO}_2)(\text{H}_2\text{O})$,
 [Manganotychite] $\text{Na}_6\text{Mn}_2(\text{CO}_3)_4(\text{SO}_4)$,
 [Soda-alumina-silicate nitrate] $\text{Na}_8(\text{AlSiO}_4)_6(\text{NO}_2)_2$

Bauxsol™ treated areas:

- [Gypsum] $\text{CaSO}_4 \cdot 2\text{H}_2\text{O}$, [Epsomite] $\text{MgSO}_4 \cdot 7\text{H}_2\text{O}$, [Wattevilleite] $\text{Na}_2\text{Ca}(\text{SO}_4)_2 \cdot 4\text{H}_2\text{O}$,
 [Thenardite] Na_2SO_4 , [Burkeite] $\text{Na}_6(\text{CO}_3)(\text{SO}_4)_2$, [Diaspore] $\text{AlO}(\text{OH})$, [Hexahydrate] $\text{MgSO}_4 \cdot 2\text{H}_2\text{O}$,
 [Whitlockite] $\text{Ca}_{2.993}\text{H}_{0.014}(\text{PO}_4)_2$, [Konyaite] $\text{Na}_2\text{Mg}(\text{SO}_4)_2 \cdot 5\text{H}_2\text{O}$, [Blodite] $\text{Na}_2\text{Mg}(\text{SO}_4)_2 \cdot 4\text{H}_2\text{O}$,
 [Anhydrite] CaSO_4

Untreated area:

- [Hexahydrate] $\text{MgSO}_4 \cdot 6\text{H}_2\text{O}$, [Alungen] $\text{Al}(\text{H}_2\text{O})_6(\text{SO}_4)_3(\text{H}_2\text{O})_{4.4}$
 [Melanterite] $\text{Fe}^{2+}\text{SO}_4 \cdot 7\text{H}_2\text{O}$, [Pickeringite] $(\text{MgO}_{0.93}\text{MnO}_{0.07})\text{Al}_2(\text{SO}_4)_4(\text{H}_2\text{O})_{22}$
 [Epsomite] $\text{MgSO}_4 \cdot 7\text{H}_2\text{O}$, [Alunogen] $\text{Al}_2(\text{SO}_4)_3 \cdot 17\text{H}_2\text{O}$



Figure 17. White efflorescent minerals on veins and gravel fill.



Figure 18. White efflorescent coatings on pyrite in the Siebert waste area.

Efflorescent Minerals

Another consequence of ARD is the growth of efflorescent minerals. In the absence of obvious sulfide minerals or “yellow boy”, efflorescent mineral blooms often provide a clue to concealed ARD sources (Gold et al., 2008). At Skytop, however, the efflorescent minerals were abundant and represented substantially more than merely a clue to the underlying problem.

Efflorescent minerals precipitate or grow on substrates under conditions of super saturation by evaporation from both groundwater seeps and waste rock drainage ponds. The addition of neutralizing agents in some of the waste dumps generated some unconventional species (see Table 4). Common environments for precipitation of these solutes are (a) contact with rocks/minerals that promote chemical change in alkalinity (pH), or (b) by an increase in salinity due to evaporation. An example of the former is the precipitation of “yellow boy” from acid rock discharge (ARD) on limestone substrates. Transient “blooms” of efflorescent minerals are progressively layered from the least soluble species to the most soluble in ponds draining waste dumps (Figures 17, 18, and 19).

The efflorescent minerals form best during prolonged dry periods, when ground water is “wicked up” by capillary action through the vadose zone and reaches the surface. A color change related to weather was noted in the Large Cut Face slopes (Figure 8). Copiapite and halotrichite (Figure 19) were noted in sheltered coves such as beneath the Route 322 overhead bridge. Ettringite was identified in a shallow sludge pond east of the Large Cut Face, and a translucent creamy-white alumina-rich gel was found in Pond J2 inlet in section C-12. The latter contained up to 3.5% Zn (probably from a dissolved culvert).



Figure 19. Efflorescent minerals (IMG 0616) crystallized near the Siebert Pond (Collected 9/12/06 from a flowery bloom near the west-bound bridge abutment of Route 322.)



Figure 20. Copiapite (yellow mineral) in a bridge footing.

Legacy

The official opening of the Skytop section of I-99 on November 17, 2008, highlighted a major engineering accomplishment. The long-term legacy includes maintenance of some deep cuts, probable replacement of cover materials in the distant future, and a small but manageable ARD (see Farmerie and Smith paper, this guidebook). In addition, the development of sinkholes in the A-12 section settling ponds is a perennial problem. The ponds were constructed in upper Coburn limestones and Antes calcareous Black Shales; both units are prone to karst development. A concrete plug installed to block a sinkhole developing in one of the ponds was later circumvented by new solution channels. Because of the proximity to I-99, the bedrock had to be excavated with track-mounted jack hammers, then concrete was used again to plug the hole in July, 2015.

The average drainage from the ERPA is estimated at 4 gallons/minute (M. Klinger, pers. comm., 6/03/2017). This effluent is treated passively by two limestones beds that discharge to a passive wetland, prior to flowing into North Bald Eagle Creek.

References

- Barnes, H.L., and Gold, D.P., 2008. Pilot tests of slurries for *in situ* remediation of pyrite weathering products. *Environmental & Engineering Geosciences*, v. XIV, No. 1, pp. 31-41.
- Gold, D.P., and Doden, A.G., 2005, A Geological Report on the Skytop Roadcuts. PennDOT Engr. Dist 2-0, Clearfield, Pa. 57 p.
- Gold, D P., Doden, A G., Mathur, R., Mutti, L.J., and Sicree, A.A., 2007. The Age, Depth, and Nature of Acid-generating Mineralization along Segments of I-99 on Bald Eagle Ridge. Final Report to Bureau of Planning and Research, Pennsylvania Department of Transport, Harrisburg PA 17120, 59 p.
- Gold, D P., Doden, A G., and Scheetz, B., 2008. The significance of vegetation kills and efflorescent mineral blooms from transient ground water plumes during and from highway construction. Abstract, Northeastern Section Meeting of Geological Society of America, v. 40, No.2, p. 7.
- Gold, D.P., and Doden, A.G., 2008. Remediation Stages at the Skytop Section of Route I-99, Centre County, Pennsylvania. Part 1 and Part 2. Extended Abstract, Pennsylvania Water Resources Symposium. Pa. Council Prof. Geologists, May 7, 2008. Hershey PA.
- Hammarstrom, Jane M., Brady, Keith, and Cravotta, Charles A., III, 2004, Acid-rock drainage at Skytop, Centre County, Pennsylvania, USGS Open-File Report 2005-1148.
- McConchie, D., Clark, M., Hanahan, C., and Fawkes, R., 1999, The use of seawater-neutralized bauxite refinery residues (red mud) in environmental remediation programs. *In* Gaballah, I., Hager, J., and Solozabal., R. (Eds.), *Proceedings of the 1999 Global Symposium on Recycling, Waste Treatment and Clean Technology*, San Sebastian, Spain: The Minerals, Metals, and Materials Society, Warrendale, PA. Vol. 1, pp. 391-400.

MONITORING ENVIRONMENTAL IMPACTS OF THE I-99 CONSTRUCTION PROJECT AT SKYTOP

RANDY L. FARMERIE¹ AND MICHAEL W. SMITH²

¹ Department of Environmental Protection, Environmental Cleanup and Brownfields Program, 208 W. Third Street, Suite 101, Williamsport, PA 17701. ² PA Department of Environmental Protection, Moshannon District Manager, Retired, 1308 Springfield Cir., Boalsburg, PA 16827

History and Environmental Setting

In 2003, highway cuts in Patton and Huston Townships, Centre County, Pennsylvania were completed as part of the construction of Interstate Highway 99 (I-99), a north-south interstate through central Pennsylvania. The new section of highway connects Port Matilda and State College at a location where Route 322 crosses the Bald Eagle Ridge, known locally as Skytop (Figure 1). The project is located in the Ridge and Valley Physiographic Province consisting primarily of folded and faulted sedimentary rocks. The highway cuts extend from the State College side of Bald Eagle Ridge, in the Buffalo Run drainage, a tributary of Spring Creek, to the Port Matilda side of the ridge in the North Bald Eagle Creek drainage (referred to as Bald Eagle Creek in the rest of this paper).



Figure 1. I-99 at Skytop

Bedrock geology is also different in the two drainages. Except for the headwaters, most bedrock is limestone with karst development on the Buffalo Run drainage side. The Bald Eagle Creek side of the project is in clastic sedimentary rock. These roadcuts resulted from removal of over one million cubic yards of bedrock, exposing unweathered Tuscarora (quartzite) and Bald Eagle (sandstone) formations. Sections of these formations contained sulfide mineral veins, primarily pyrite (see discussion of the geology elsewhere in this field guide and Hammarstrom et al., 2004). Sulfide mineralization was more extensive in the Bald Eagle Formation. The highway construction was a cut

and fill operation. Rock from the cuts was used in various places in the highway project as fill. At least 11 locations where pyritic fill material was placed for the highway project were identified. These were in addition to exposed pyritic rock in the roadcuts. Soon after placement of excavated rock, acidic discharges were noted at both cut and fill locations where pyritic rock was present.

Acid Rock Drainage Generation

Production of acid mine drainage (AMD) has been a long-standing issue in Pennsylvania coal mining. Acid Rock Drainage (ARD) is a more generic term that refers to production of acid drainage from rock, whether mine related or not. ARD outside the coal mining setting has not been as well studied. In the last 15 to 20 years, it has become an issue with multiple highway projects in Pennsylvania and other location. The Pennsylvania Geologic Survey has mapped the location and potential occurrence of ARD-generating material in Pennsylvania (PA Geologic Survey, 2005). AMD and ARD are formed by the reaction of naturally occurring sulfide minerals with oxygen in air and water. The most common sulfide mineral involved in AMD and ARD generation is pyrite (FeS₂). The reaction is expressed by the equation



Acid Mine Drainage Treatment

In 1964, the Pennsylvania Clean Streams Law classified acid mine discharges as industrial waste. Since then, a National Pollutant Discharge Elimination System (NPDES) permit is required of each designated acid mine drainage. The drainage must be treated to applicable effluent limits of the NPDES permit. This treatment usually involves neutralization with an alkaline chemical followed by aeration and precipitation of metals. This is a very expensive and high-maintenance operation which can continue for decades or even centuries before pyrite oxidation has diminished enough to discontinue treatment. More recently, less expensive passive treatment technologies are employed where mine-drainage chemistry is sufficiently mild. These passive treatment technologies usually employ limestone beds for pH adjustment and a series of ponds for precipitation of metals. They may also include organic substrates for oxygen removal and/or sulfate reduction. Passive treatment technologies are more expensive to construct, but up-front costs are more than offset by lower operation and maintenance costs.

Since the early 1980's, PADEP has worked to prevent acid-drainage rather than approve projects that need long-term treatment. Overburden analysis, chiefly as acid-base accounting, is one of several tools used to predict post-mining water quality. New mining permit applications are only approved if they are expected to produce neutral or alkaline drainage. Following a series of ARD-producing road construction projects, PADOT has adopted a similar policy emphasizing avoidance and prevention over long-term treatment (PennDOT, 2015).

ARD at Skytop

At the Skytop location, sulfide minerals are primarily pyrite and marcasite (FeS₂) (Hammarstrom et al, 2004). Oxidative weathering of pyrite and marcasite, together generically referred to as pyrite in this paper, accounts for the low pH and elevated iron and sulfate concentrations in the leachate. Pyrite oxidizes faster than other sulfide minerals at Skytop. It promotes acidic weathering of

associated sulfide minerals such as galena (PbS), sphalerite (ZnS), and chalcopyrite (CuFeS₂) (other papers in this field book, Hammarstrom *et al.*, 2004). Acid generated from the reaction mobilizes metals present in the environment such as aluminum and manganese. Figure 2 shows a typical example of chemistry of the drainage produced by the fills at Skytop.

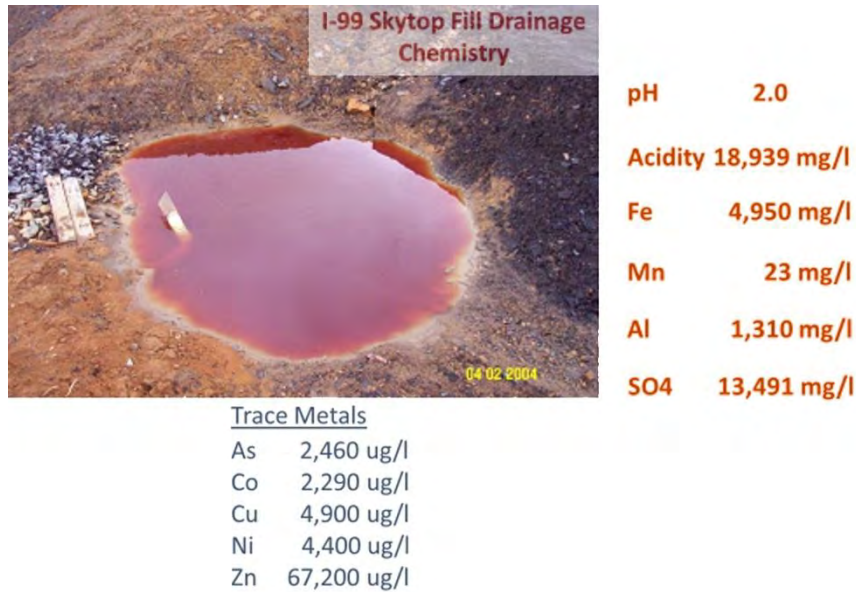


Figure 2. Skytop fill drainage chemistry

Environmental Impacts

The Pennsylvania Department of Environmental Protection (PADEP), the Pennsylvania Department of Transportation (PADOT) and PADOT’s consultant, Skelly and Loy, worked cooperatively to design and implement the investigation and remediation of ARD impacts generated by I-99 construction. Two components of environmental impacts were examined as part of the project. The components included 1) examining environmental impacts from construction of cuts and areas where pyritic material was placed, and 2) how these impacts could be mitigated and excavated rock safely managed while minimizing future environmental problems.

To evaluate environmental impacts, a multi-pronged monitoring scheme was developed for groundwater and surface water in vicinity the of the construction project. First the source of the problem and extent of impacts was defined. For groundwater, monitoring wells were installed. These and residential drinking water wells were sampled. A limited number of preconstruction samples were previously collected from residential wells near the construction project. These wells were primarily sampled to establish background conditions prior to blasting and were in the immediate area of the roadcuts. To evaluate ARD impacts, the following were monitored: groundwater sources within one-half mile of encountered pyritic Bald Eagle Sandstone or Tuscarora Quartzite, or where pyritic rock from those formations was

placed as part of the highway construction. Groundwater sources were primarily residential wells. However, a few springs used as drinking water sources, business wells, and community water-supply wells were also sampled. A total of 82 groundwater sources met this criterion and an additional 52 locations outside the half-mile radius were sampled at least once, usually because of a request from the residents. In total, over 5,400 water samples have been collected to date from residential groundwater sources. Initially, a full suite of anions and cations were analyzed in the water samples. However, based on the analytical results, the primary parameters of concern with respect to drinking water were aluminum, iron, lead, manganese, sodium, sulfate and pH. Subsequent sampling was limited to these parameters. Although sodium is not associated with ARD, it is a constituent of chemical compounds such as sodium hydroxide and soda ash (sodium carbonate) that were used for pH adjustment of impacted water. This residential groundwater monitoring network was designed to look for human exposure to contaminants of concern from the project. The Statewide Health Standards (SHS) for groundwater in Act 2, the Land Recycling and Environmental Remediation Standards Act, were used to evaluate any exposure to the residents. Of the contaminants of concern, only lead and manganese have a health-based standard. Sulfate, iron, aluminum, and manganese have secondary Maximum Contaminant Levels (MCLs). Secondary MCLs are based on taste, odor and staining, and not on a health-based standard.

Because it is not as sensitive to pH changes and other environmental conditions, sulfate is the best indicator of whether ARD had impacted a water supply. Background sulfate concentrations were less than 30 mg/l (parts per million PPM)). These were determined from sampling unimpacted wells. The SHS for sulfate is 250 mg/L. Background metals concentrations in residential wells varied significantly. Some of these wells were installed in pyritic Bald Eagle strata while others were in non-pyritic rock, including limestone. Although residential wells in pyritic Bald Eagle strata had metals concentrations (iron, aluminum, lead, and manganese) above their respective SHS, sulfate concentrations were, none-the-less, low and were usually below 30 mg/L (Fig. 2). Therefore, metal concentrations above the SHS were not sufficient to determine if a well had been impacted. Instead, sulfate concentrations above background levels were a more reliable indicator.

If a drinking-water standard – the SHS - was exceeded due to ARD impacts, alternate water sources were provided. There were five impacted residential wells/springs that exceeded drinking water standards. Chemical analyses showed sulfate concentrations above the drinking-water standard or a combination of sulfate above background level and metals concentrations exceeding a drinking-water standard. These five locations were provided bottled water or a home water-treatment system. Residents qualifying for alternate water sources were located near major roadcuts or large fills. In addition, there were 25+ residential wells that were impacted with sulfate concentrations above background, but no drinking-water standard was exceeded. Sample results for individual wells were evaluated to determine if any trends were present in the data. Following completion of remedial activity, there were no upward trends in groundwater data and most groundwater sample data displayed a downward trend (Figure 3).

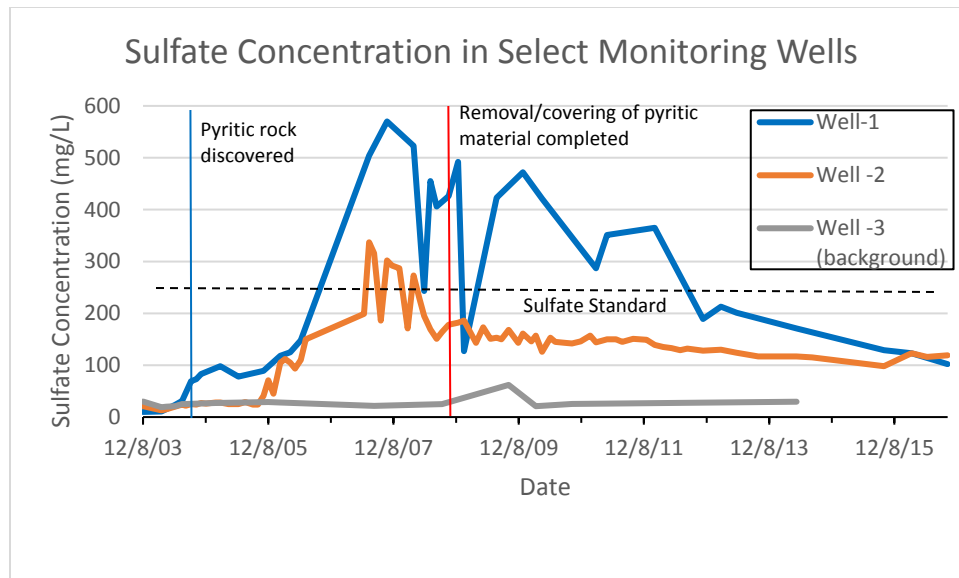


Figure 3. Sulfate concentration in monitoring wells at the Skytop ARD project. Data from Skelly and Loy, 2017a.

The background residential well [Well 3] in Figure 3 was completed in pyritic Bald Eagle sandstone. Despite high levels of metals in the well water, the sulfate concentration remained at background levels. This well was upgradient of construction and ARD from the project did not impact it.

Groundwater sampling of residential wells near Buffalo Run, a limestone area, showed impacts from ARD even though wells closer to the project along the same groundwater flow path did not. This is believed to be evidence of impacted surface water recharging the groundwater in these locations.

As previously mentioned, the second part of the groundwater monitoring program was drilling and sampling monitoring wells around major areas of concern. Monitoring wells were placed upgradient and downgradient of roadcuts and major fills. Over 85 monitoring wells were drilled specifically for this project and 97 wells, including other pre-existing wells not used for water supplies, were sampled for this part of the monitoring program. Well logs were also used to define the extent of pyritic rock in the subsurface and to determine locations where nearby roadcuts might generate ARD. The wells were logged as they were drilled and drill-cutting samples collected for overburden analysis (OBA) to help determine if pyritic material was present in the bedrock. Testing for the overburden analysis consisted of analyzing the percent sulfur of the rock and its neutralization potential (NP). Rock with a percent sulfur content greater than 0.5% has significant potential to create acid drainage. Neutralization potential measures buffering capacity of the rock. Positive net neutralization potential (NNP) indicates the potential to neutralize acid generated from pyrite weathering (Perry, 1998). NPs less than 30 parts per thousand are generally considered insignificant.

In general, monitoring wells near cut faces and large fills had the highest concentrations of the relevant chemical parameters associated with ARD, and the lowest pH levels, as would be expected. These monitoring wells show much greater impacts than any of the residential wells (Table 1).

Table 1. Groundwater quality in an impacted monitoring well and impacted residential well at the Skytop ARD project. Data from Skelly and Loy, 2017a.

	Impacted Monitoring well	Impacted Residential Water Supply Well	Statewide Health Standard (SHS)
pH	3.5	6.64	
Fe	839	0.5	0.3
Mn	7.79	1.45	0.05
Al	580	<0.05	0.2
SO ₄	7191	566	250
Zn	21.9	NA	2

All units in mg/L except pH
 NA -Not analyzed

Monitoring wells in impacted areas had a pH of less than 4.0, along with elevated concentrations of sulfate and metals when compared to background water quality data. Much like the residential wells, these wells showed a decline in concentration following remediation (Table 2). Despite a continued low pH; iron, manganese, aluminum, zinc, and sulfate substantially decreased. Based on experience and long-term observations at reclaimed surface coal mines, the expectation is that water quality returning to background levels will not happen in the near future.

Table 2. Groundwater in impacted monitoring wells before and after remediation at the Skytop ARD project. Data from Skelly and Loy, 2017a.

	Skytop monitoring well water quality before remediation		Post remediation water quality of same Skytop monitoring well in 2016	
	Well 1	Well 2	Well 1	Well 2
pH	3.5	2.3	4.2	3.8
Fe	839	5230	123	372
Mn	7.79	13.1	1.31	4.55
Al	580	3088	57	95.1
SO ₄	7191	32166	1079	1630
Zn	21.9	49.9	3.65	9.5

All units in mg/L except pH

Groundwater monitoring has helped to determine sources, pathways, and areal extent of contamination from ARD, and direct corrective measures and water supply treatment or replacement.

Surface Water

Water quality of the surface water draining from the I-99 Skytop ARD areas was monitored through a network of approximately 40 stream/outfall monitoring points on surface waters draining to both Bald Eagle Creek and Buffalo Run from Skytop. The two drainage areas are markedly different in character. Buffalo Run drainage contains springs and well developed surface-drainage features. Bald Eagle Creek drainage contains less well developed surface-water features that may not be visible beneath the Tuscarora boulder colluvium on this side of Bald Eagle Ridge. The only monitoring location for the project which had pre-project surface water chemistry and benthic data available (semi-annual sampling beginning in 1998) was located about 1.0 mile below Skytop on Buffalo Run. Collection of all other surface water-quality data began in or after November 2003 when PADEP first became involved with the I-99 ARD project.

Surface water degradation occurred in both the unnamed tributary to Buffalo Run that crosses through the project and Buffalo Run. Comparison of sample results collected upstream and downstream of the project in an unnamed tributary to Buffalo Run in May 2004 showed increased dissolved aluminum, iron, and manganese concentrations along with increased acidity and significant decrease in pH. In addition, at that time, Buffalo Run immediately below Skytop showed elevated sulfates and a visible coating of the stream substrate with precipitated iron.

Water-quality at the most downstream monitoring station on Buffalo Run had circum-neutral pH, and non-detect dissolved metals. Sulfate and sodium concentrations at this station were elevated over pre-project levels. The former reflects release of oxidized sulfur compounds from weathered pyritic rock and the latter are from sodium hydroxide treatment for pH adjustment of the discharge while temporary treatment of ARD was ongoing.

Although the watershed does receive some acidic runoff/groundwater from the project, no ARD impacts were observed to Bald Eagle Creek. Unlike the Buffalo Run side, there are few permanent surface-water features on the Bald Eagle Creek side of the project until Bald Eagle Creek. The ARD impacted groundwater discharge from the project to Bald Eagle Creek would be minimal when compared to the flow of Bald Eagle Creek. Since discharges on the Buffalo Run side occur in headwaters of that stream, there is significantly less flow and thus, less dilution on the Buffalo Run drainage area impacted by the project.

Benthic macroinvertebrate studies were conducted throughout the project at the pre-established monitoring point on Buffalo Run approximately one mile below the I-99 construction project. Post remediation benthic macroinvertebrate studies did not demonstrate any long-term impacts to Buffalo Run at the monitoring location (Skelly and Loy, 2013).

Remediation

Remediation of Exposed Rock Cuts

Highway right-of-way cuts through acid rock formations cannot be moved. The only viable remedial option for Skytop roadcuts was an in-place remedy. As previously discussed, reaction of oxygen, water, and sulfur generates ARD from sulfide deposits. The remedy selected for these rock cuts was to cover them and construct a leachate collection system. There were two cuts that needed to be covered: a large cut (LCF) through the Bald Eagle strata where exposed sandstone needed to be

addressed on both sides of, and under, the highway and a smaller cut (SCF) in Tuscarora and Juniata strata. The covers were designed to limit exposed pyritic rocks contact with water and thus reduce ARD generation. Contact with water could be reduced but not eliminated as there is atmospheric moisture and groundwater moving through the bedrock. By reducing contact with water, the volume of leachate generated was greatly reduced. To install and hold the covers in place on the steep cuts, a



Figure 4. GeoWeb covering of the Buttress/Bifurcation Fill

geotextile and GeoWeb system was installed, and held in place by cables tied into concrete posts set into the bedrock (see accompanying paper on Environmental Geology). The latter has a honeycomb-like geometry to hold #57 limestone aggregate (Figure 4). Completion of capping the exposed cut resulted in marked improvement of groundwater quality in the monitoring wells (Figure 5).

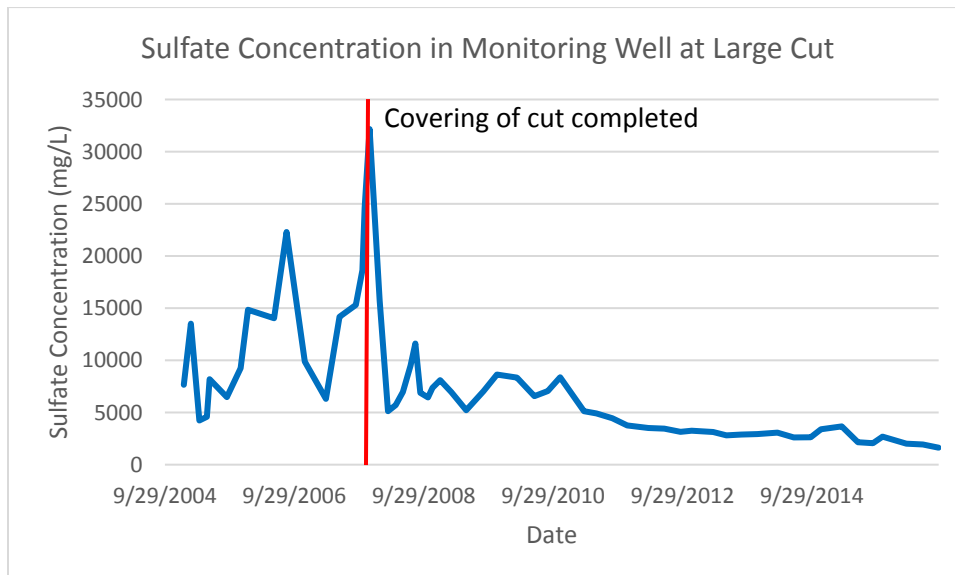


Figure 5. Sulfate concentration in monitoring well monitoring the large cut face. Data from Skelly and Loy, 2017a.

Remediation of the Fill Areas

Initially, major fill areas were capped with plastic to reduce contact with rainwater. This was an interim step while a permanent solution for the areas was developed. The remediation project addressed pyritic-fill areas in two different ways. Some fills needed to remain for structural reasons. For example, the fill area called the Buttress/Bifurcation (Figure 4) was designed to stabilize a hill slope that had previously failed during construction. Fills that could not be removed were handled the same way as the roadcuts – they were capped in place and the leachate collection system collected discharges from the fills.

For those areas where fill could be safely excavated, pyritic material was excavated and removed to the engineered rock placement area (ERPA) constructed specifically for the project. Details of the ERPA are in a subsequent section of this paper. Over 1.275 million cubic yards of rock were taken to the ERPA (Skelly and Loy, 2010). Soil samples were collected at the areas where fill was removed to ensure no ARD sources remained. Much like the covering of exposed bedrock, removal of pyritic fill resulted in marked groundwater quality improvement (Figure 6).

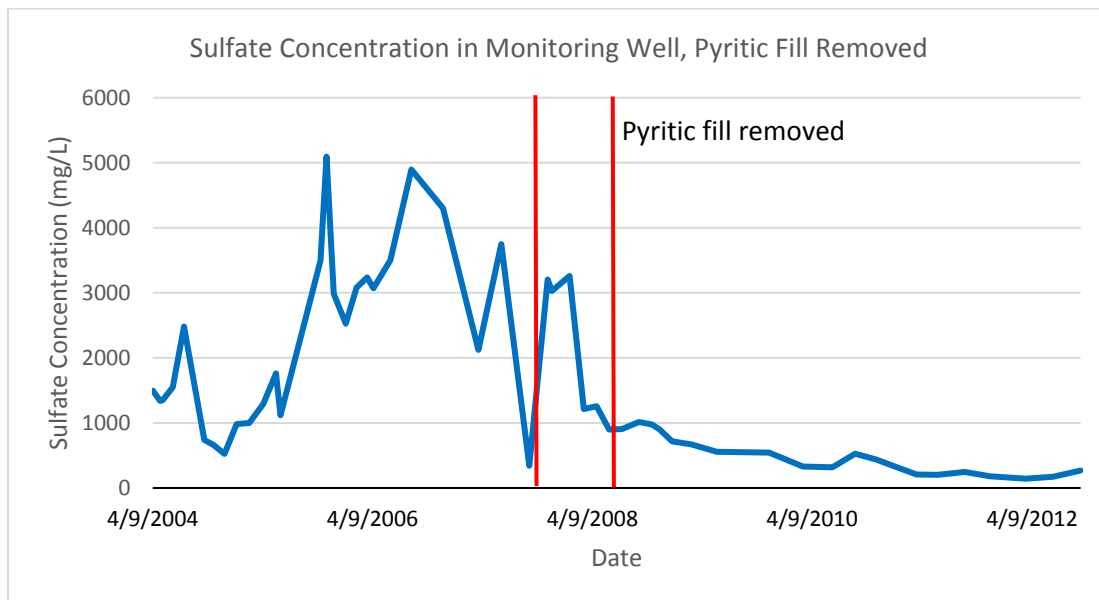


Figure 6. Sulfate concentration in well monitoring the Siebert Fill where pyritic waste rock had been removed. Data from Skelly and Loy, 2017a.

Remediation of Discharges and Streams

Pollution effects from ARD vary, but primary pollutants of concern for streams and freshwater ecosystems are elevated levels of metals, primarily iron, aluminum, manganese, and zinc that are soluble at low pH. Oxidation of these metals in a less acidic stream environment results in the formation of metal precipitates on the stream bottom and rock and gravel substrates.

Surface water and ARD collection were a major portion of the remediation efforts both before and during the covering and removal of pyritic material, and ARD collection continues to this day. One of the first steps early in the remediation was to try to separate ARD discharges from unimpacted surface water, so that transport of ARD constituents could be limited and the water treatment volume

minimized. To achieve this, an unnamed tributary to Buffalo Run was hard-piped past several of the fills before returning to its channel downstream of the construction activities. Leachate that was discharging to the channel where the tributary had formerly flowed was collected and pumped to a central treatment area (Figure 7). Initially, an interim treatment system was established where sodium hydroxide was used for pH adjustment in a former storm-water basin (PADEP, 2015).



Figure 7. Photo of temporary surface water-treatment ponds

pH adjustment removed metals from the discharge but did not remove sulfates. This discharge, along with all the other impacted discharges, was authorized by NPDES permits PADEP issued. These discharges were monitored and the results reported monthly.

As part of the final project remedy, a permanent leachate treatment facility was constructed. The final leachate treatment system was permitted in 2015. The system begins at the Buttress/Bifurcation and collects leachate from highway cuts and fills that could not be moved, including the LCF, and pumps leachate to a centralized location for treatment. This treatment facility is located below the Buttress/Bifurcation in the Bald Eagle Creek drainage, just off old US 322, adjacent to erosion and sedimentation control pond J2. Between August 2012 and December 2013, the average daily flow to the system was 39,500 gallons per day (gpd) with a maximum flow of 149,800 gpd (Skelly and Loy, 2015). The system treats the discharge with pH adjustment and polymer flocculants to achieve NDPEs permit effluent limits. Following completion of the permanent treatment project, the unnamed tributary was returned to its channel and impacted sections of the stream were restored. Chemical water quality also showed significant improvement in comparison to water quality during the construction phase (Figure 8). Biological assessment of the stream after the remediation was completed did not find any prolonged biological impairment (Skelly and Loy, 2013).

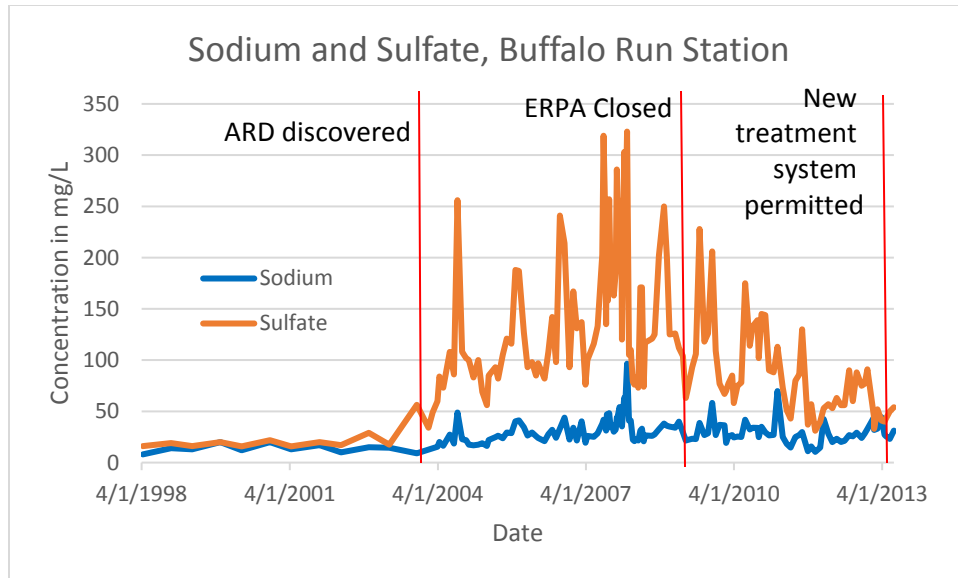


Figure 8. Sodium and Sulfate concentrations in long term monitoring point on Buffalo Run. Data from Skelly and Loy, 2013.

ERPA

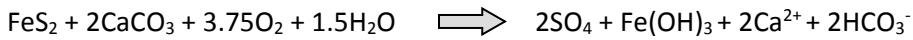
The Engineered Rock Placement Area (ERPA) was a facility built along the highway for the specific purpose of sequestering pyritic rock that had been removed from pyritic fills. The ERPA was constructed to standards required of a residual waste landfill: a leachate collection-system, a double liner with a leachate detection zone under the liner, cap, and monitoring wells. An early phase of the ERPA construction is shown in Figure 9.



Figure 9. ERPA under construction

The pyritic rock was neutralized as it was placed in the ERPA. The neutralization is expressed by the formula:

Acid Neutralization by Carbonate



Experience in surface coal mine reclamation shows that a NNP of greater than 12 will control most acid discharges (Smith and Brady, 1998). Calculation performed for this project with a goal of an NNP of 12 indicated that addition of 400 pounds of waste lime per cubic yard of pyritic rock was required. Using ABA analysis, the amount of lime needed to neutralize ARD generated from pyrite weathering is calculated using the following steps:

1. (Avg. percent S x 3.125 x weight rock/volume) = weight CaCO₃ needed to neutralize sulfur in rock assuming all sulfur is available, for example 2.7% S X 3.125 x 3200 lbs./cu. yd. = 270 lbs. CaCO₃/cu. yd. of rock
2. (Weight per volume rock + Weight per volume CaCO₃ to neutralize rock) X .012 (NNP of 12) = amount of CaCO₃ needed to assure net alkaline discharge, using same example 3470 lbs./cu. yd. x 0.012 = 42 lbs./cu. yd.
3. Total CaCO₃ (Amount CaCO₃ to neutralize + Amount CaCO₃ needed to assure alkaline discharge) x purity of CaCO₃ = amount waste lime added ((270 lbs./cu. yd. +42 lbs./cu. yd.) / 80% = 390 lbs./cu. yd.

A critical aspect of adding alkaline material is that it must be thoroughly mixed with pyrite-bearing rock, replicating a fill of naturally alkaline rock. Previous alkaline material projects placing limestone or other alkaline materials on the surface or base of the fill, or in layers or pods, usually failed to achieve desired goals. Also, not all alkaline materials have proven successful. Waste lime fines are most commonly used in Pennsylvania due to their availability and successful results when used for treatment.

The calculation worked out to adding approximately two front-end loader buckets per truckload of pyritic rock. A total of approximately 1.5 million cubic yards of material, pyritic rock and waste lime were taken to the ERPA. The monitoring wells at the ERPA have shown no impacts after the placement of the pyritic rock (Table 3).

ERPA Leachate and Monitoring Well Chemistry

Chemistry of leachate collected at the ERPA shows lime addition has provided sufficient alkalinity (Figure 10) to neutralize acidity generated by the pyritic rock. Metals concentrations are also reduced sufficient to meet NPDES limits without active treatment (Figure 11). Sulfate concentrations are still elevated (Table 3, Figure 11) but are significantly less than the untreated leachate (Figure 2). This indicates a much-reduced pyrite oxidation rate at near neutral pH. While pyrite oxidation continues, a near-neutral pH slows pyrite oxidation.

Table 3. ERPA Leachate and Monitoring well results from 2016. *Data from Skelly and Loy, 2017b.*

	ERPA Leachate Sampling results	ERPA Monitoring Well Sampling results
	total	dissolved
pH	7.3	7.8
Fe	0.035	0.54
Mn	0.38	0.13
Al	0.29	<0.05
SO ₄	698	24
Alkalinity	98	174

Units are in mg/L except pH

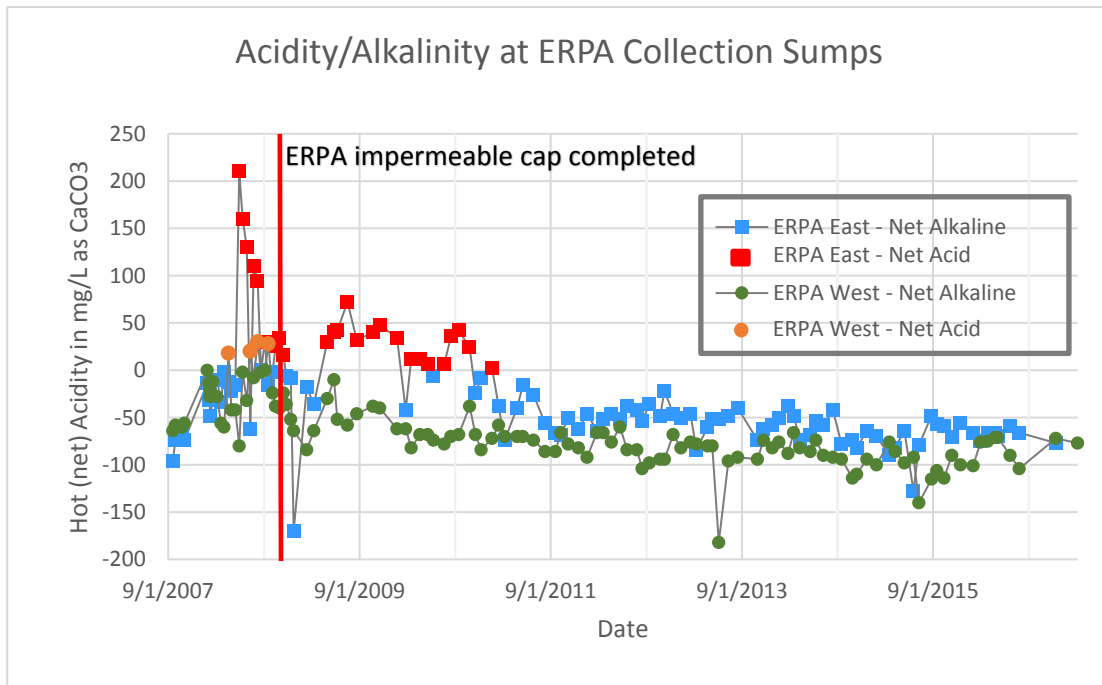


Figure 10. Acidity at the ERPA leachate collection sumps. *Data from Skelly and Loy, 2017b.*

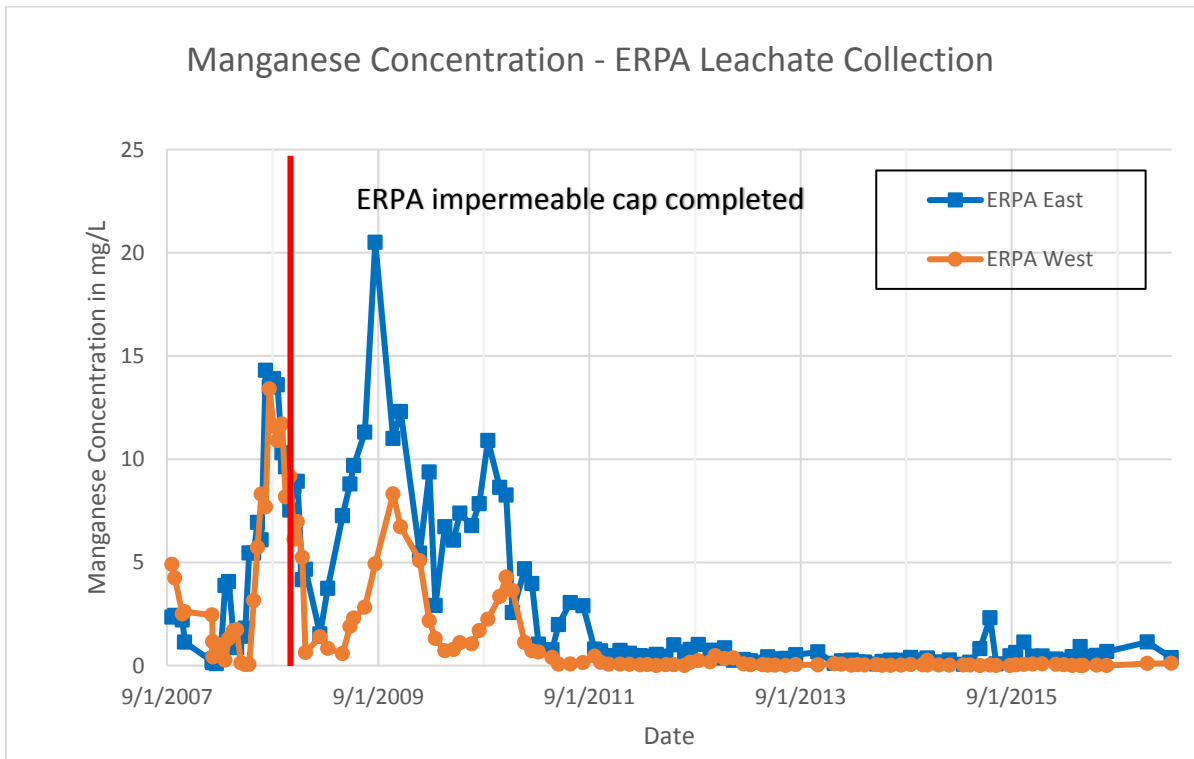
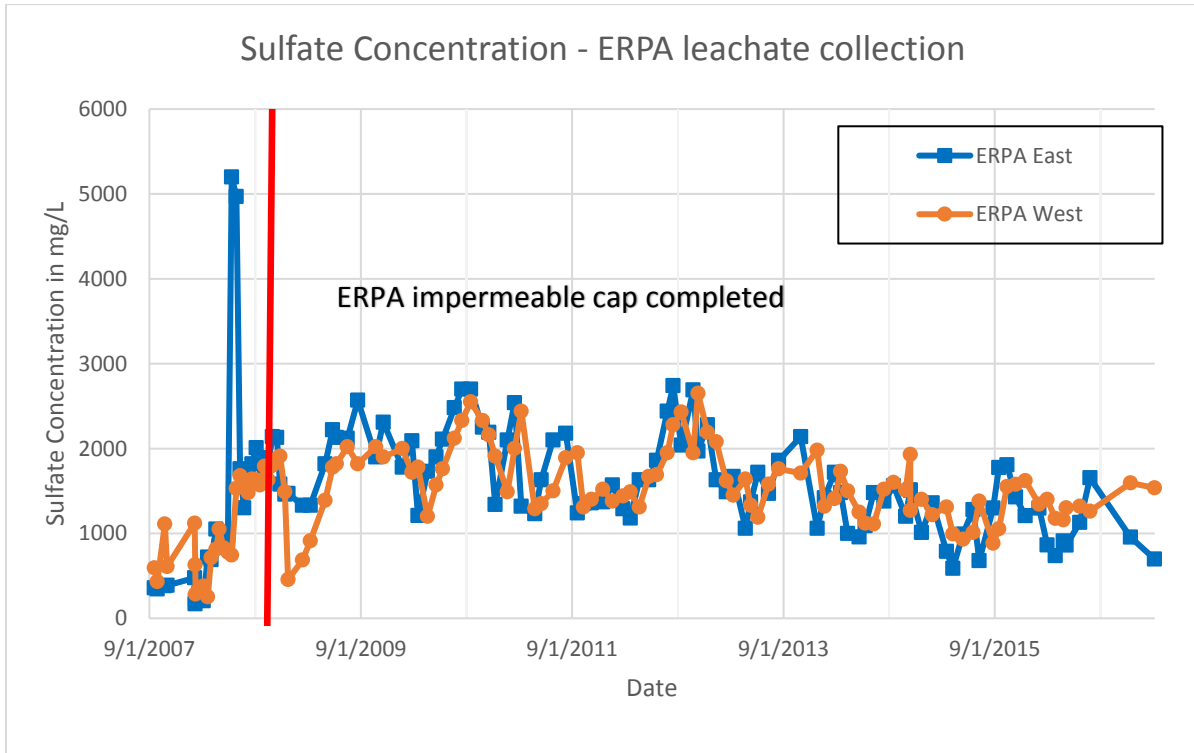


Figure 11. Sulfate and Manganese at the ERPA Leachate Collection Sumps. Data from Skelly and Loy, 2017b

The ERPA leachate quality will continue to be monitored and collected. Collected leachate is not acidic and is treated using a passive-treatment train that includes a sulfate reducing bioreactor, a limestone polish, and aerobic settling ponds (PADEP, 2012). As of 2016, the ERPA generated less than 300 gallons of leachate per day (Skelly and Loy, 2017b).

Conclusions

I-99 construction at Skytop presented numerous environmental challenges in addressing ARD discharges to both surface water and groundwater. As a result of this project, the following are some lessons learned.

- A quality geologic investigation that includes preconstruction well samples is essential **before beginning** construction.
- Take steps to reduce the area of pyritic material disturbed and, if possible, limit its exposure to air and water.
- Analyze drill cuttings to allow for calculation of a lime-addition rate that results in an NNP >12.
- Plan for handling-material up front as part of construction and permitting of the highway projects.

References

- Brady, K. B.C., 1998, Groundwater Chemistry from Previously Mined Areas as a Mine Drainage Prediction Tool in Coal Mine Drainage Prediction and Pollution Prevention in Pennsylvania, PA Department of Environmental Protection, Harrisburg, PA, p. 9-1 to 9-21.
- Hammarstrom, J.M. Brady, K.B.C., and Cravotta III, C. A., 2004, Acid-rock drainage at Skytop, Centre County, Pennsylvania, USGS Open-File Report 2005-1148.
- Pennsylvania Geological Survey, 2005, Geologic units containing potentially significant acid-producing sulfide minerals: Pennsylvania Geological Survey, 4th ser., Open-File Report OFMI 05-01.1.
- PADEP, 2012, NPDES Permit PA0234010 I-99 ERPA Leachate Treatment Facility Permit.
- PADEP, 2015 NPDES Permit 1415201 Interstate 99 J2 Acid Rock Drainage Treatment Facility Permit.

82nd Annual Field Conference of Pennsylvania Geologists

PADOT, 2015. Publication 293 Geotechnical Engineering Manual, Chapter 10- Acid Bearing Rock, May 2015.

Perry, E. F., 1998, Interpretation of Acid-base Accounting in Coal Mine Drainage in Coal Mine Drainage Prediction and Pollution Prevention in Pennsylvania, PA Department of Environmental Protection, Harrisburg, PA, p. 11-1 to 11-18

Skelly and Loy, 2010, I-99 ARD Removal and Verification Documentation,

Skelly and Loy, 2013, U.S. Route 220 Improvement Project Centre/Blair Counties, Pennsylvania; Buffalo Run Station K Water Quality and Benthic Macroinvertebrate Assessment,

Skelly and Loy, 2015, Water Quality Management Permit Application and Design Engineers Report for the I-99 ARD Treatment Facility,

Skelly and Loy, 2017a, I-99 groundwater data table, unpublished communication

Skelly and Loy, 2017b, ERPA data table, unpublished communication,

Smith, M. W. and Brady, K. B.C., 1998, Alkaline addition in Coal Mine Drainage Prediction and Pollution Prevention in Pennsylvania, PA Department of Environmental Protection, Harrisburg, PA, p. 13-1 to 13-13

ARCHAEOLOGICAL LITHIC MATERIALS IN CENTRE COUNTY PENNSYLVANIA

BARRY E. SCHEETZ¹, ROBERT J. ALTAMURA², PAUL RABER³, MARY ALICE GRAETZER⁴ AND SHERMAN STOLTZFUS⁵

¹ PH.D., RETIRED PROFESSOR OF CIVIL ENGINEERING, PENN STATE UNIVERSITY, 810 MULBERRY LANE, LEMONT, PA 16851, ²DISTANCE LEARNING, GREAT FALLS COLLEGE, MONTANA STATE UNIVERSITY, 2100 16TH AVENUE SOUTH, GREAT FALLS, MT 59405, ³VP, DIRECTOR OF ARCHAEOLOGICAL SERVICES, HEBERLING ASSOCIATES, 904 MAIN STREET, ALEXANDRIA, PA, 16611, ⁴464 WESTGATE DRIVE, STATE COLLEGE, PA 16803, ⁵10 WHITEHALL ST., BELLEVILLE, PA 17004

Roadlog

<u>Segment</u>	<u>Cumulative</u>	<u>Road log description</u>
0 mi.	0 mi.	Depart Ramada, turn right onto South Atherton Street.
0.1	0.1	At traffic light, turn left onto University Drive.
1.3	1.4	At light exit right onto East College Avenue. [Rt. 26].
0.8	2.2	At Puddintown Road turn left [Room Doctor business at intersection on left].
0.4	2.6	Follow Puddintown Road past Millbrook Marsh nature center; turn left onto Orchard Road.
0.5	3.1	Follow Puddintown Road past the substation and park in pasture on left.



Plate 1. Jasper blocks recovered for PSU farm field adjacent to the Hatch Quarry Site in the Ordovician Nittany Formation, Centre County, PA.

Stop 1. Hatch Jasper Quarry

0.5	3.6	Re-enter Orchard Road, turn right and return to Puddintown Road.
0.5	4.1	Turn left along Puddintown Road to Quonset hut on right, park here.

Stop 2. Shovel Testing

0.6	4.7	Exit Quonset hut parking lot, turn right on to Puddintown Road and follow to stop sign in Houserville.
-----	-----	--

82nd Annual Field Conference of Pennsylvania Geologists

0.6	5.3	At the stop sign, turn right on to Houseville road and follow to the traffic light intersection of Rt. 26.
0.6	5.9	Proceed through the intersection onto Pike Street and follow it to the next traffic light intersection.
1.9	7.8	At the traffic light, follow Pike St [now East Branch Road.] to the next traffic light intersection with South Atherton Street.
0.1	7.9	At the traffic light turn left and makes an immediate right turn onto West Branch Road.
0.7	8.6	Follow this winding road to the next stop. Park in field on your left.

Stop 3. Esper Farm Jasper Quarry

0.6	9.2	Exit the field parking and retrace your route to the traffic light on South Atherton Street.
0.1	9.3	At the traffic signal exit left onto South Atherton Street and immediately exit right onto East Branch Road.
2.6	11.9	Follow East Branch Road until it turns into Pike Street in Lemont and continue to the traffic light at Rt. 26. At Rt. 26 turn right and follow it toward Bellefonte. At the Nittany Mall, on your right, the Rt. becomes 151. Follow it past Rock View State Prison on the right.
3.9	15.8	Opposite the old brick building on the left is Penntech Road, the entrance to Centre County industrial park.
0.4	16.2	Exit right onto the Industrial Park Road and follow it to the end.
0.1	16.3	Turn right to parking.

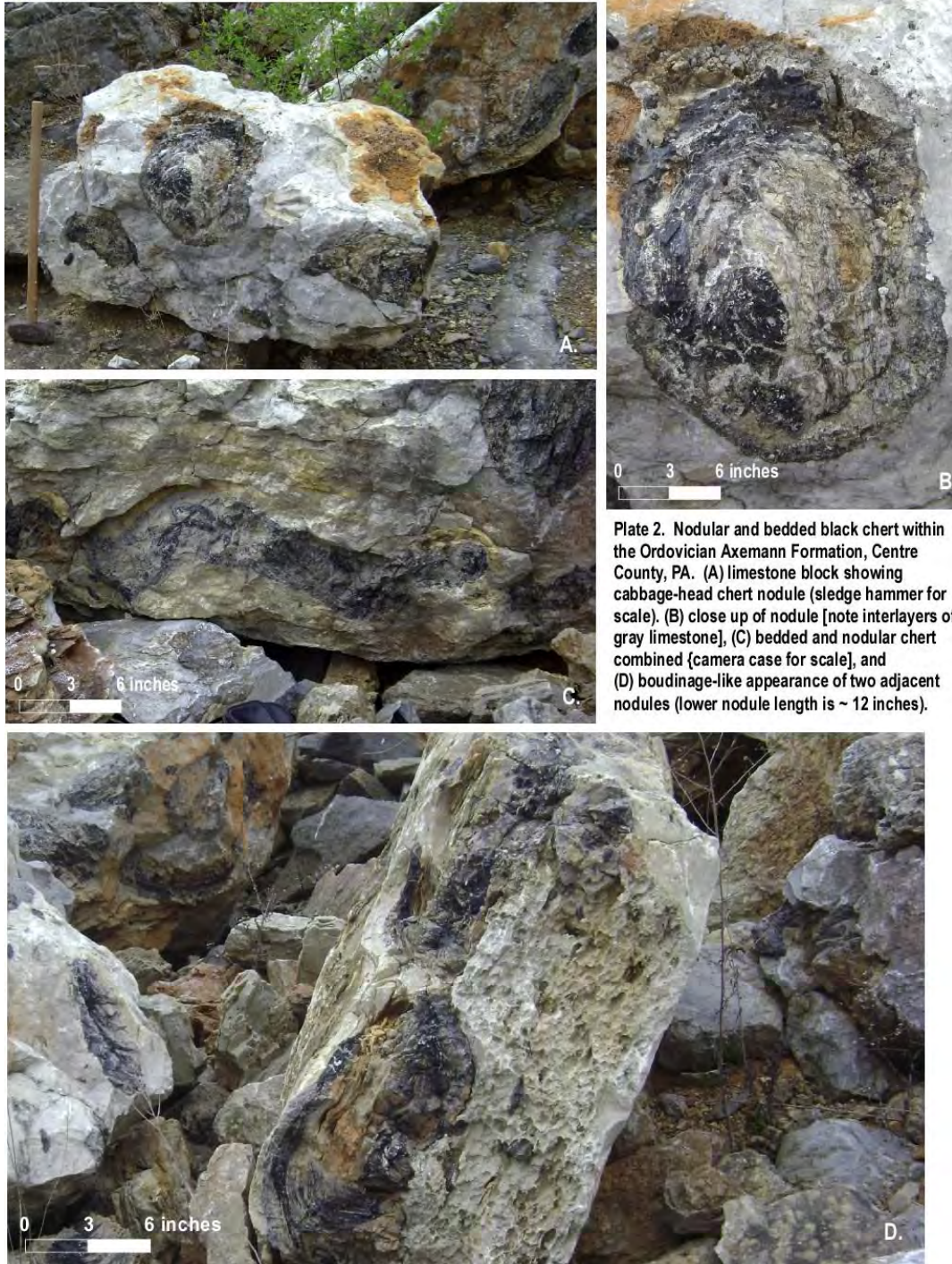
Stop 4. Early Ordovician Chert Borrow Pit (see Plate 2)

5.3	21.6	Retrace you route from the last 4 steps to the traffic light in the village of Lemont.
2	23.6	At the traffic light turn left onto Old Boalsburg Road and follow it to Oak Hall.
2.2	25.8	At the intersection with Rt. 322 turn left onto Linden Hall Road, past an old stone farm house on left; follow this winding road into Linden Hall.
0.3	26.1	In Linden Hall turn left onto Rock Hill Road and follow it to Lower Brush Valley Road.

Stop 5. Campbell Farm Chert Quarry (see Plate 3)

3.2	29.3	Retrace your route [last 3 turns] to Oak Hall and enter I-99 toward State College. Take the State College by-pass [Rt. 322] and exit on College Ave. [Rt. 26]. Turn left on the East College Ave and proceed to an exit onto University Dr. Make a left turn on University Dr. and follow it to South Atherton St. The Ramada Inn will be on the left side of South Atherton as you exit to your right.
3.2	32.5	Return to Ramada, follow Lower Brush Valley road to Old Boalsburg Rd.
2.9	35.4	Turn left and drive to Rt. 322 then turn right and follow to Ramada Inn.

Total mileage



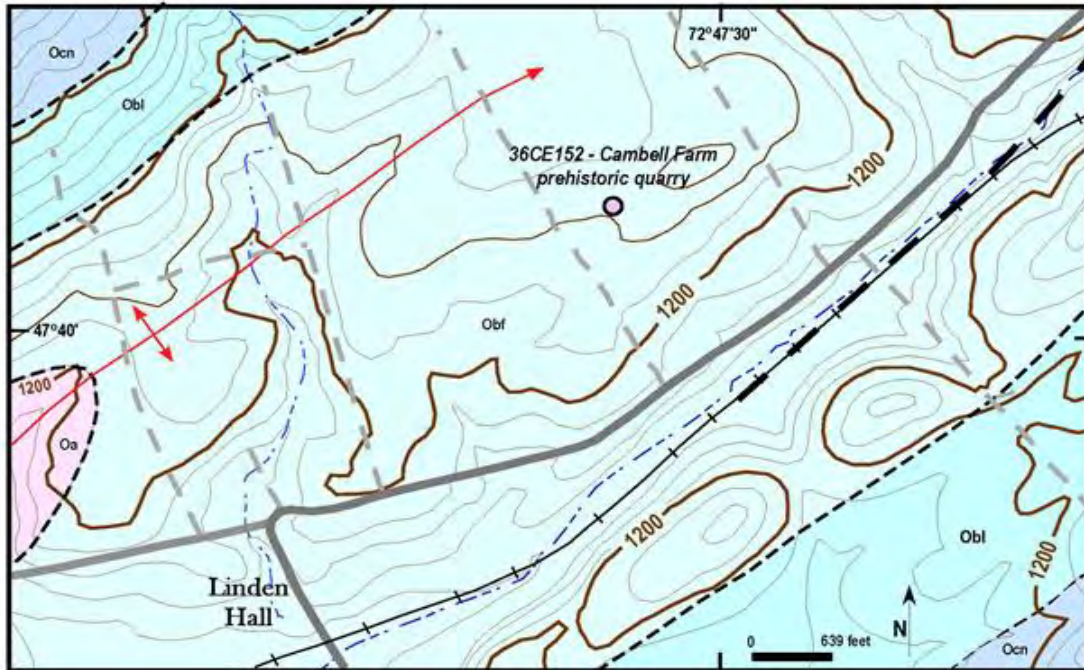


Plate 3. Bedrock geological map showing the location of the Cambell Farm quarry site (circle symbol) near the village of Linden Hall, Pennsylvania. Pennsylvania Archaeological Site Survey (PASS) code is provided. The site is located on soil developed above bedrock of the Ordovician Bellefonte Formation (Obf).

Geological explanation: Obl = Benner through Loysburg carbonate units; Oa = Axemann Limestone, and Ocn = Coburn through Nealmont formations. Red solid line denotes the fold axis of a plunging anticline and the dashed thick black line represents a fault. (Geology from Hoskins and Root, 1976; Hoskins, 1976).

ARCHAEOLOGICAL LITHIC MATERIALS IN CENTRE COUNTY PENNSYLVANIA

BARRY E. SCHEETZ¹, ROBERT J. ALTAMURA², PAUL RABER³, MARY ALICE GRAETZER⁴ AND SHERMAN STOLTZFUS⁵

¹ PH.D., RETIRED PROFESSOR OF CIVIL ENGINEERING, PENN STATE UNIVERSITY, 810 MULBERRY LANE, LEMONT, PA 16851, ²DISTANCE LEARNING, GREAT FALLS COLLEGE, MONTANA STATE UNIVERSITY, 2100 16TH AVENUE SOUTH, GREAT FALLS, MT 59405, ³VP, DIRECTOR OF ARCHAEOLOGICAL SERVICES, HEBERLING ASSOCIATES, 904 MAIN STREET, ALEXANDRIA, PA, 16611, ⁴464 WESTGATE DRIVE, STATE COLLEGE, PA 16803, ⁵10 WHITEHALL ST., BELLEVILLE, PA 17004

Abstract

North American aboriginal inhabitants relied almost entirely upon stone tools to survive. They were skilled knappers who chose the best lithic materials to make their tools. The “best lithic” materials consisted of homogeneous, dense silica-base stone that, when chipped, broke uniformly with conchoidal fractures resulting in formation of sharp cutting edges. From the archaeological record, it is clear these peoples traveled great distances, up to 250 to 300 km to acquire these materials. Centre County has two deposits that would qualify as “good” lithic materials: early Ordovician black cherts and brown Bald Eagle Jasper [a.k.a. Houserville Jasper]. The jasper was the most widely exploited resource in the area and was utilized for perhaps 12,000 years from Clovis times but was most heavily exploited during the Transitional Period between 4300 BC and 2700 BC.

Introduction

When modern man first moved into unoccupied North America between 34,000 and 12,000 years ago, they possessed advanced knowledge of working lithic materials [Collins, 1999] to produce extremely fine-quality stone-tipped tools for hunting. The use of the finest lithic materials and sophisticated knapping techniques are typical of these early peoples, who traveled as much as 250 km to sources of the finest cherts. As time progressed and mankind became less dependent upon hunting for survival, the quality of lithic materials chosen decreased and inferior-quality materials derived from local sources were used. During the Middle Archaic, this behavior predominated and lasted until the

Paleo Period	16,500--10,000 BP
Paleo [Clovis] Period	11,200 – 10,900 BP
Archaic Period	10,000 – 4300 BP
Transitional Period	4300 – 2700 BP
Woodland Period	2700 – 450 BP
Contact Period	450 – 250 BP

Transitional Period when there was a return to a strong lithic preference for jasper, meta-rhyolite and argillite. Following the Transitional Period, there was again a return to locally derived materials [PHMC, Jan 2011]. The utilization of one type of lithic material is not confined to any one spatial or temporal period but controlled by the availability of the lithic material and social demands of those who exploited the materials.

Most lithic procurement occurred by recovery of large surface blocks of materials, while other sources were exposed by digging small shallow pits typically eight feet in diameter and four feet deep. In the most extreme efforts to expose Hardystone Jaspers in Berks and Lehigh counties, pits 80 feet in diameter and as much as 40 feet deep have been identified.

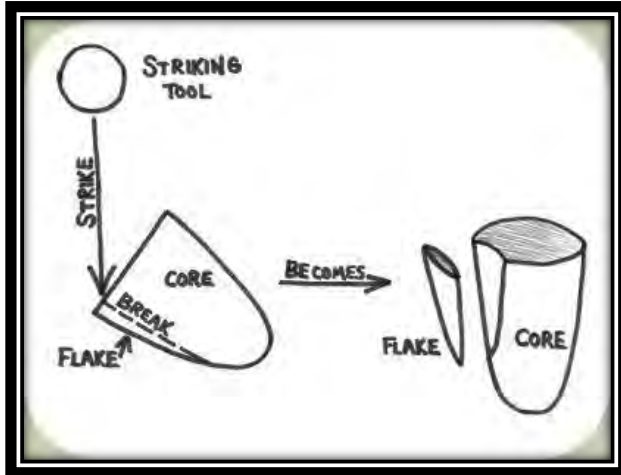


Figure 1. Schematic diagram portraying percussion flaking (retrieved from Google, no date).

Studies have been done by modern “knappers” in which all flakes removed from a cobble were collected, measured for size and mass, and counted. From this study, five categories of flakes were found describing the scope of flake removal during stone-tool production. These ranged from large crude flakes used to shape the cobble into a preform of the final tool down to small, delicate flakes intended to impart a cutting edge. With this understanding of the geometry of the debitage, specimens of debitage being analyzed could be matched to the reduction stage. Thus, specific activities at a particular archaeological site could be determined. For example, at the Hatch quarry site, near the State College hospital, only initial stages of mass removal are observed at the quarry, thus helping to define the activities at this site. The preformed stone core was carried away to the Houserville Historical Complex, where further reduction of the core took place as characterized by the smaller, more delicate debitage.

Lithic materials

Both professional and amateur authors have attempted to categorize the lithic source materials in Pennsylvania. In the early 1980’s, amateur archaeologist Gary Fogelman published a series of pamphlets entitled *The Pennsylvania Artifact Series* [Fogelman, 1983]. Bulletin No. 34 focuses on lithic uses the author identified in his state-wide survey. This was not a useful resource because all gray and black chert, the most common lithic material used across the state, sources are incorrectly lumped into the same geological formation. Subsequently, Holland (2003) established a scientific

Stone tools were manufactured utilizing two methods to reduce the size of the original cobble and to remove flakes in its final form. The first method illustrated here (Figure 1) is “percussion” in which the cobble was directly impacted with another stone to remove flakes.

Pressure flaking was generally accomplished using an antler or bone [modern flint knappers use copper rods] where force could be applied directly to a stone cobble in a localized area (Figure 2).

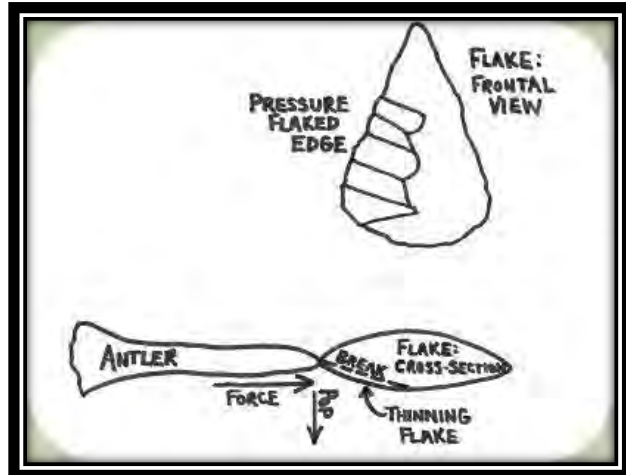
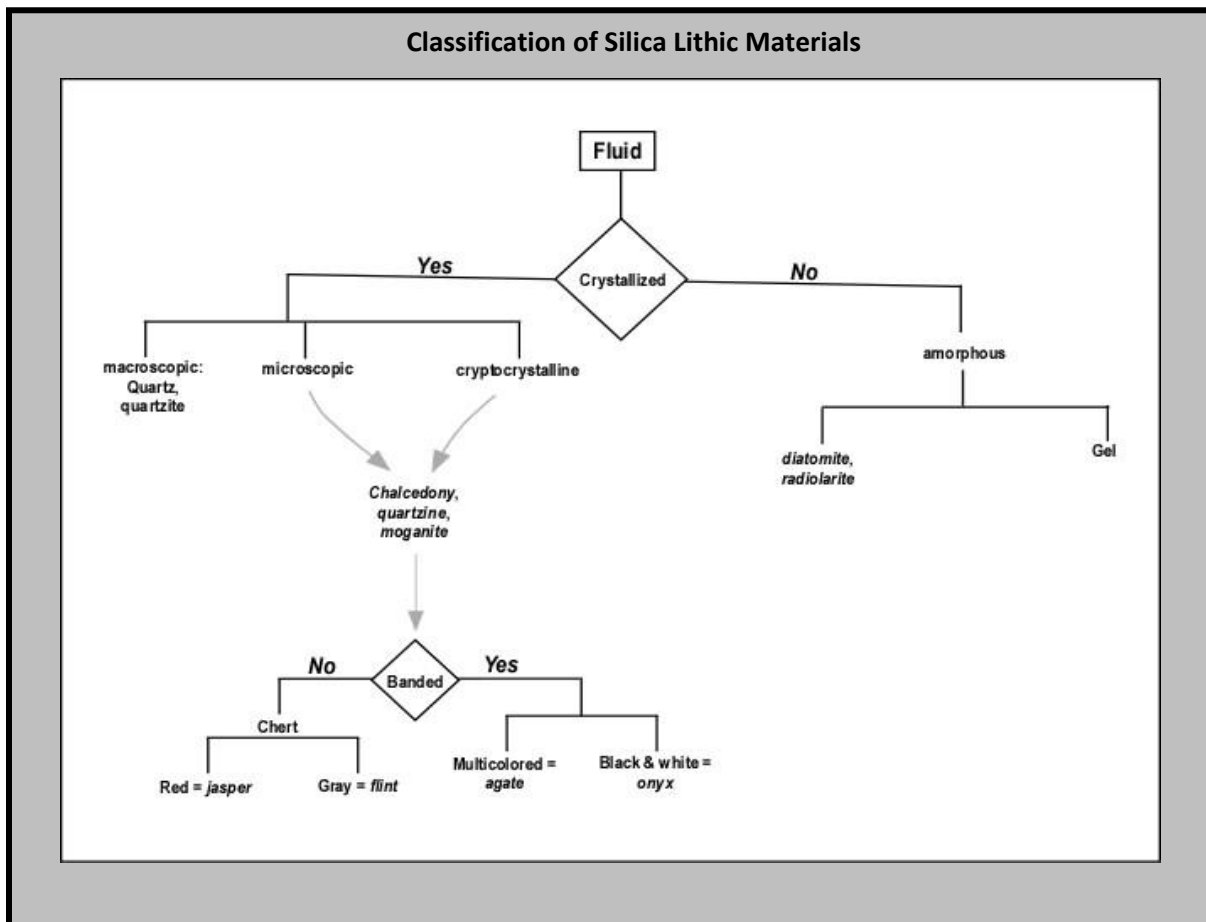


Figure 2. Schematic diagram portraying of pressure flaking (retrieved from Google, no date).

basis for provenance and usage. These studies avoid confusion for assigning multiple common names of the same geological formation.

Neither of these Pennsylvania-specific references addresses the issues of source identification of seemingly nondescript gray/black chert - the single widest-used lithic material in the Commonwealth (PHMC, Feb 2014). Whereas many different lithic materials in the State can be discerned in hand specimen, some rely upon instrumental/analytical methods for discriminating signatures.



Pennsylvania’s Archaeological Site Survey [PASS] consists of over 23,000 sites or approximately 1 for every 1.95 square miles. However, only in 48% of these sites is the lithic content identified. A summary of lithic materials from the PASS files [PHMC, Feb 2014] indicates the most common lithic material is a black or bluish chert. Flint knappers consider this a common material of varying quality and not among the exotic flints [viz., Onondaga, Coxackie, Keepkill, Normanskill or Coshocton]. Jasper is the second most common lithic material found in Pennsylvania and is the subject of our local field trip. There are three major locations for jasper in the State: the Hatch Quarry Site, Reading Prong, and Iron Hill on the border between Delaware and Pennsylvania. Figure 3 places the Hatch quarry site in context with other major known jasper locations within the Mid-Atlantic Region along the East Coast.

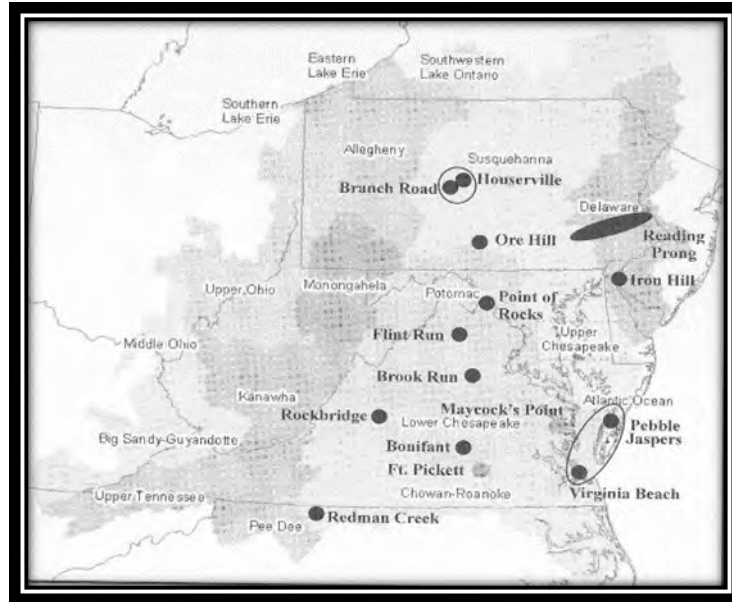


Figure 3. Location of major jasper quarries in the Mid-Atlantic Region of Eastern United States.

The materials from the Vera Cruz area are gemmy with a waxy luster and knap well. Because of these qualities, this material was widely traded along the Eastern Seaboard. With the resurrection in

Lithic Materials in order of frequency in PASS files	
Black/bluish chert	1 st
Jasper	2 nd
Quartz	3 rd
Quartzite (sugar quartz)	4 th
Meta-rhyolite	5 th
Onondaga chert	6 th
Chalcedony	7 th
Argillite	8 th

the desire to use the finest-quality materials during the Transitional Period, these sources were extensively exploited. Quartz and quartzite [sugar quartz] represent the third and fourth most-common lithic materials type. Quartz is very common in Lancaster and York Counties and large quartzite quarries are located in Berks County. These are considered of lesser quality to knappers, and looking at their distribution within the Commonwealth, they did not move far from the source locations. Meta-rhyolite is the 5th most-common lithic material, occurring in the Precambrian Catoclin Formation in Adam and Franklin counties at South Mountain. Meta-rhyolite

was exploited and traded widely during the Transitional Period, moving along the Susquehanna and Juniata river drainages throughout Pennsylvania, New York, and Ohio. Devonian Onondaga chert from the Niagara escarpment, chalcedony, and argillite from the Triassic Lockatong Formation are the 6th, 7th, and 8th most-common lithic material, respectively. The Lockatong Formation extends into New Jersey and Delaware but has found little use outside of Pennsylvania's Upper Piedmont. The PASS files also record the less-common source materials such as diabase, diorite, granite, greenstone, hornfels, ironstone, limestone, meta-sandstone and orthoquartzites.

Local Lithic Materials: Bald Eagle JASPER [a.k.a. Hooverville Jasper]

The Bald Eagle Jasper, also referred to as Houserville Jasper, occurs in the Nittany Formation, an Ordovician-age dolomite. Holland [2003] comments that "...large residuum blocks of jasper occur on the Penn State University campus with pebbles and cobbles occurring in and along Slab Cabin Creek, [near Houserville] Centre County, PA..." Jasper was highly prized for toolmaking and, hence, widely

used within the State and widely traded from North Carolina to Maine [PHMC, 2011]. Figure 4 summarizes the PASS files and reflects the distribution of jasper usage in Pennsylvania. The physical character of the jasper is generally grainy and not the gemmy form often encountered at Vera Cruz, Pennsylvania. The mineralogy of the Bald Eagle jasper is composed of crystalline alpha-quartz and goethite that this author has characterized by quantitative x-ray diffraction. King *et al* (1997) report the iron-containing phase as lepidocrocite; either phases impart

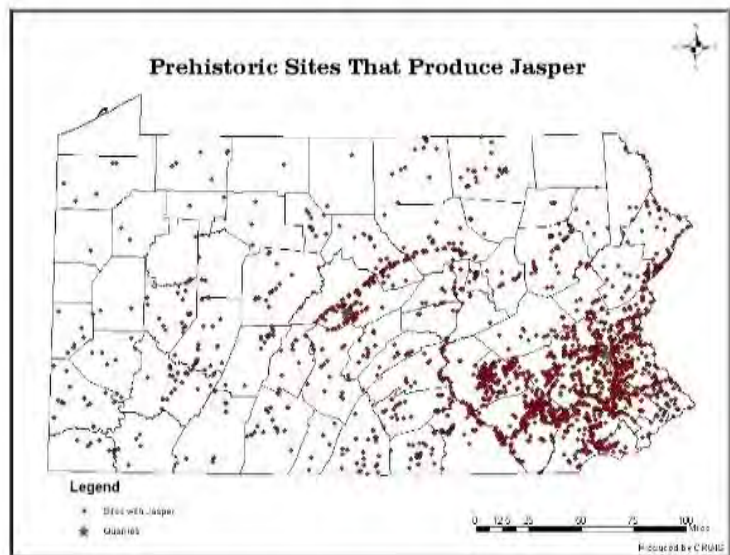


Figure 4. Distribution of archaeological sites in PA which report jasper in the lithic assemblage.

the typical light-brown-to-yellowish color to the jasper. Compositionally, the Bald Eagle Jasper is unique in the relative high iron oxide content that it possesses, ranging between 5 and 25 weight percent with modest amounts of MnO (approaching 1000 ppm). Another jasper source on West Branch Road has a similar mineralogical and chemical signature. A third local jasper locality, at the Continental Trailer Court off Rt. 550, lacks detailed characterization. Gold (1994) reports a fourth jasper locality south of Roaring Spring in Bedford County. This locality off Old Orchard Road in Roaring Springs has been characterized by x-ray diffraction as indistinguishable from the Hatch/Houserville and the West Branch Road jaspers. Although the age for the usage of the Hatch Quarry site on the Penn State campus is dated to the Middle Archaic at least two fluted projectile points have been noted in local collections by personnel associated with the Pennsylvania Association for Archaeology, Chapter 24. Further, King *et al* (1997) references several jasper samples from the State Museum's Witthoft Collection. Sample 93-52, recovered from the Shoop paleo site [36DA20], is from the Bald Eagle Jasper quarry, significantly extending the procurement time from this quarry. The significance of the Shoop Site near Halifax, PA is that it was the first Paleo-period site located on the east coast.

Also, two jasper adzes from Shoop site, Shertzer collection described by Kurt Carr, the State Archaeologist, as "...made from a rough jasper that is more (sic) similar to the Houserville source in Centre County than to the Hardyston quarries in eastern Pennsylvania..." (Adovasio *et al.*, 2008).

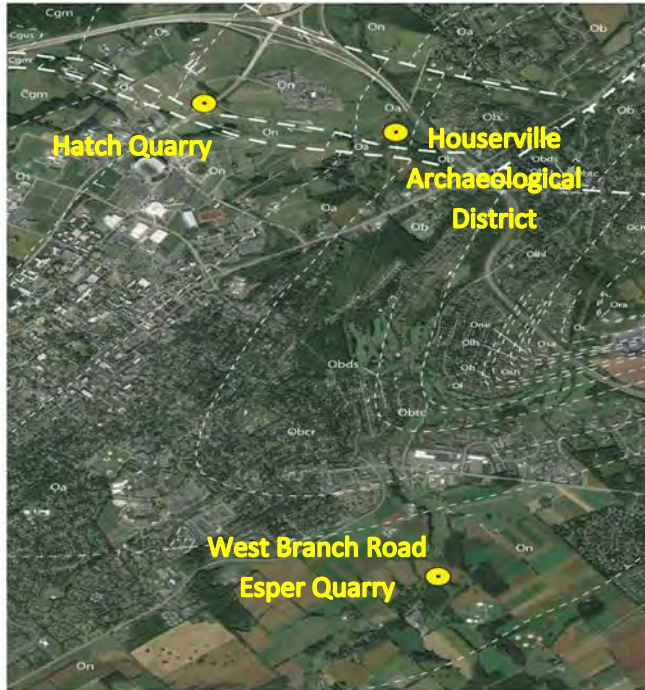


Figure 5. Approximate location of the jasper quarry along Orchard Rd. and Park Ave. [upper yellow dot], the West Branch Rd. location [lower yellow dot] and the Houserville Historical Complex [upper-center yellow dot].

Figure 5 locates both jasper quarry sites north of the University campus. Yellow circles in the figure's upper portion identify the location of the Hatch quarry site as adjacent – to – beneath the intersection of Park Avenue and Orchard Road, in a graben-like depression.

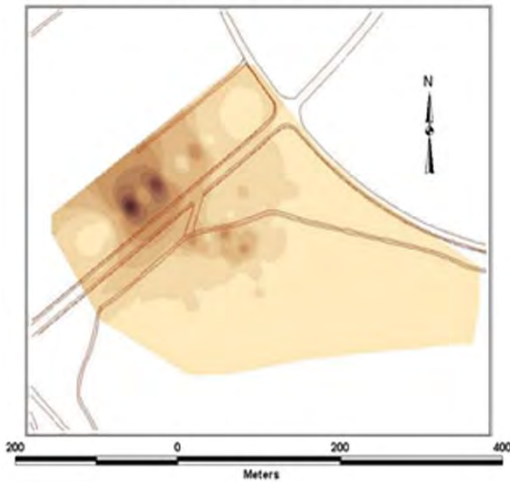
The other yellow marker identifies the foci of the Houserville Historic Complex, composed of approximately 19 locations, which are interpreted as individual camp sites occupied during the lithic procurement activities. Here, jasper from the quarry at the head of Orchard Road was carried to the stream side and processed. Figure 6 details the location of the second jasper quarry located by the yellow dot at the bottom of Figure 5.



Figure 6. Detailed location of the Esper Jasper Quarry along West Branch Road.

Surface collection of debitage were made during recent excavations of the Hatch site to provide a spatial representation of the activities (Scheetz and Murtha, 2017; Andrews *et al.*, 2004). Most the debitage was identified in a localized area adjacent to the quarry (Figure 7).

Total Diagnostic Distribution



Debitage recovered for the site clearly demonstrated thermal treatment of the jasper was conducted at the quarry to achieve an initial size reduction. The spatial distribution of the yellow unaltered jasper, (Figure 8a), and the red jasper, heat treated, (Figure 8b), coincides with the quarry.

Figure 7. Distribution of debitage on Hatch site. Contour map portraying distribution of the total of both yellow and red artifacts found. Exact contour intervals are not provided, however darker shades show higher values.

Total Yellow Pieces

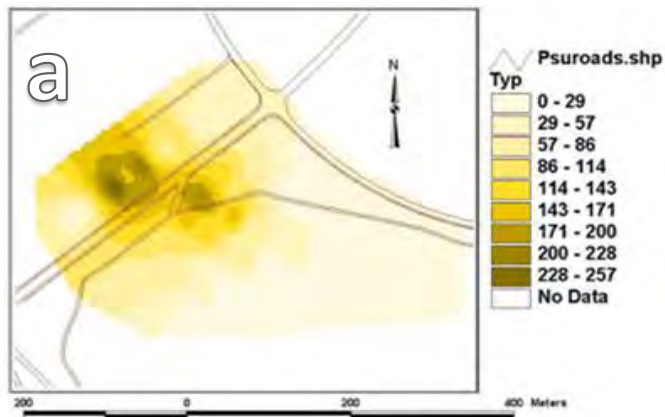
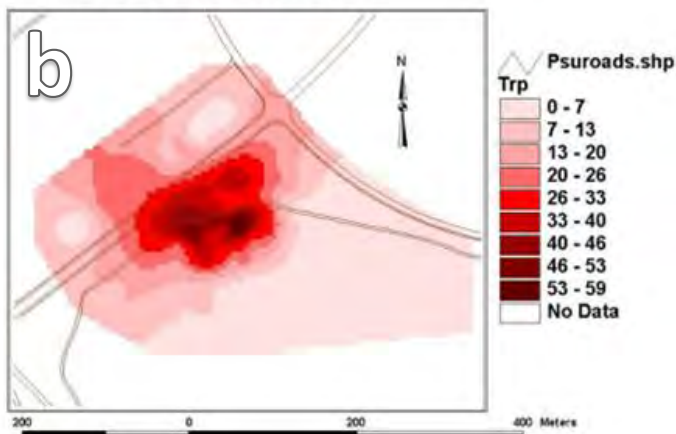


Figure 8 .

a) Spatial distribution of as-recovered jasper debitage and

Total Red Pieces



b) spatial distribution of thermally-treated red jasper.

The bulk of heat-treated samples came from a location southeast of the quarry, adjacent to where fire pits were unearthed.

Blackman (1974) used atomic absorption and flame-emission spectrophotometry to quantify the minor elements (Mg, Cr, Fe, Cu, Ni, Co and Zn)-and trace elements (Na, Li, Ca, Sr, Rb, Ba, and Mn). Of these, he found that only K, Cr, Ni, Co, Fe and Rb were none overlapping and useful for discrimination between these two sources. Iron Hill jaspers mineralogically contain chromite spinel crystals sufficiently large to be recognized with the naked eye and, hence, clearly discriminate based on Cr, Ni, Co and Fe content.

Miller (1982) and Hatch and Miller (1985) used neutron activation analysis to develop the quantitative chemical composition of the jaspers. Stevenson *et al.* (1990, 1992)-used X-ray fluorescence to establish a set of trace elements that could be statistically queried so artifacts could be assigned to their respective quarry locations. One problem with discrimination analyses is the creation of false-positive reports based on a lack of a complete set of sources that contributed to the wide distribution of jasper artifacts.

Stevenson *et al.* (1992) and King *et al.* (1997)-demonstrated that artifacts can be classified by source materials and linked to physiographic provinces in Pennsylvania, Delaware, Maryland and Virginia. However, they were unsuccessful in establishing patterns that could be attributed to individual quarries within these regions. The lack of an ability to establish discrimination characteristic for individual quarries within a given physiological province was attributed to an event which drew upon a homogeneous epithermal fluid source and was emplaced into a regionally homogeneous lithic formation, thus not providing any chemical characteristics upon which a clear differentiation could occur. Because of the mode of formation, it would be the exception rather than the rule to be able to isolate a specific quarry amongst those in that region. Furthermore, it was observed that the known jasper deposits that were included in Stevenson *et al.* (1990) and later in King *et al.* (1997) all occur at the boundaries between the physiological provinces.

Impact Origin of Jasper

In general, the clear majority of jasper deposits are represented by surface-float occurrences, with less than half a dozen *in situ* sites known to this senior author. These include Vera Cruz, [Lehigh Co., PA] Lobachsville [Berks Co., PA] and possibly the Old Orchard Road site in Roaring Springs in Pennsylvania and Brook Run in Virginia. Another *in situ* jasper deposit was reported in Sommersville, NJ by Herman (personal communication, 2017) but at this point there is no evidence that it was exploited by aboriginal peoples. Herman [personal communication, 2017] has expressed his opinion that this deposit was a direct consequence of an impact event. Detailed studies show that the Hatch quarry site and the West Branch Road site can be correlated to lineaments and/or faults. Lovering (1972) further supports the theory that the Hatch and West Branch Road quarries are associated with lineaments or faults.

The existence of well-crystallized α -quartz, which does not reflect any line broadening in the X-ray diffraction pattern, suggests the jasper was emplaced as an epithermal fluid. Figure 9 is an example of the distal end of a jasper emplacement that cooled sufficiently not to metamorphose the included limestone. The hot, acidic aqueous fluids dissolved silica from the rock as the fluids passes to the surface. As these silica-rich, hot and acidic fluids begin to interact with the carbonates of the Lower Ordovician, an acid/base reaction occurred and the iron in the carbonate was incorporated into the silica solution as it was neutralized. The iron oxidized to goethite although some authors have reported lepidocrosite (King *et al.*, 1997).



Figure 9. Distal end of a jasper flow which incorporates limestone breccia. The limestone does not appear to be thermally decomposed in contact with the jasper. Sample location, Iron Mountain approximately 60 miles west of Lewiston, Montana.

A few unanswered questions arise for this scenario are (a) source of the fluids, (b) event triggering their movement, and (c) mechanism of emplacement? There is no active volcanic activity of record around any of the East Coast jasper sites. It has, therefore, been postulated by the senior author that the epithermal fluids were forced to the surface from depth through faults or lineaments. Herman and Ferguson (2015) and Scheetz *et al.* (2009) suggest mantle fluids were forced to the surface as a result of the Chesapeake Bay bolide impact 35 million years ago.

Local Lithic Materials: Early Ordovician Carbonate Sequence [Stonehenge (aka. Larke), Nittany, Axemann and Bellefonte formations]

A common archaeological lithic in the Center region is “cabbage-head” chert nodules and chert beds that occur in the Early Ordovician carbonate stratigraphic sequence including the Nittany, Axemann and Bellefonte formations. These units make up the Beekmantown Group and are estimated to be approximately 3,900 feet in total thickness (Kauffman, 1999).

“Bellefonte Chert” occurs in the Bellefonte “dolomite” Formation throughout the Nittany valley, in cellular “cabbage-head” balls (Figure 10) as well as irregular potato-shaped nodules. It was quarried by prehistoric peoples by digging small “sink-hole” like pits to recover nodules of the material. In hand specimen, the nodules appear as brownish/black material with a translucent appearance on thin edges. It commonly is found as highly-fractured but coherent nodules and although the materials are of very good quality for knapping, the small size of coherent non-fractured pieces limited its use to smaller projectile points. The frequency with which the material appears in local collections suggests it was exploited in the late Woodland Period, although the senior author has seen two fluted points collected near Hecla Gap (near Walker Township, PA) in the Jack Holland collection (personal communication, 1990) that represent significantly larger coherent examples.



Figure 10. Cabbage-head chert nodule from Early Ordovician Axemann Formation near Pleasant Gap, PA. (camera case for scale)

The Bellefonte chert occurs widely at archaeological sites in central Pennsylvania. The best-known sources lie along the base of Nittany Mountain near the village of Linden Hall in Penns Valley. Preliminary archaeological testing occurred during the Central Pennsylvania Archaeological research program (Hatch, 1980) at two of these quarry sites, the Campbell Farm quarry site (36CE152) and the Linden Hall quarry site (36CE151). Hay (1980) notes that the 1978 survey recorded over 40 local sites where the Bellefonte chert was used. Intensive excavations were conducted at one such site, 36CE523 (Raber, 2010), documenting quarry-related activity during the Late Middle and Late Archaic periods, ca. 4100-2000 BC. That study also compared activity at 36CE523 to that at several local sites and proposed a model of local chert procurement. Another quarry-related lithic processing site with deposits ranging from the later Middle Archaic through the Late Woodland Periods was studied at 36CE530 (Raber and Stiteler, 2012). Both Bellefonte chert and local sources of Houserville Jasper were used there.

Fritz (2004, 2006) has noted other sources of the Bellefonte chert in central Pennsylvania, specifically along the Kishacoquillas Creek near Belleville, and others to the southwest near Williamsburg. It is likely that many other unrecorded sources exist.

Geological origin of chert with an emphasis on Centre County

These carbonate units are comprised of limestone and dolostone and formed as marine sediments along the eastern margin of the Proto-North American continent within the Appalachian basin, a large elongate depocenter that paralleled the eastern edge of the continent. During the Ordovician Period the Appalachian basin extended from the carbonate shelf sequence in the west to deeper water deposits (shales) to the east that were the western part of the ancient Iapetus Ocean.

Surface sea water through time is usually considered to be very strongly depleted in silica, so deposition other than biological would appear to be not probable. However, there is no consensus on origin of the chert, and hydrothermal siliceous springs and silica super-saturation of sea water by aeolian dust sources have been proposed. Pettijohn (1975) favored a post-depositional origin and therefore a replacement process to form nodular cherts via diagenetic differentiation. The concentric layers and open vugs in some cabbage-head chert nodules suggest replacement of fossils such as sponges, stromatolites and stromatolites.

Chert (including jasper variety)

Chert is a hard, waxy to grainy, generally microcrystalline sedimentary rock that consists of largely or entirely of silica [quartz, chalcedony, and/or opal] (Raymond, 1995). Most chert is relatively pure silica although trace to minor impurities can be present. This relative purity in composition is consistent with other chemically formed sedimentary rocks such as evaporates and chemical limestones. In geological environments where chemical sedimentary rocks form there typically is relatively little input of detrital sediments that might introduce impurities. Centre County chert nodules tend to be black to shades of gray. Impurities of organic material or metallic sulfides may be the cause of such coloration.

Jasper is a variety of chert containing iron oxide impurities (*e.g.*, hematite or goethite) that can give it various colors, characteristically red, but also brown, yellow, green, grayish blue, and even black (Neuendorf *et al.*, 2005). Jasper commonly is associated with iron ores. Any red chert or chalcedony irrespective of an association with iron ores has had the term jasper applied.

Textures and structures of cherts

Cherts dominated by opal are amorphous, lacking crystal structure. Crystalline varieties of chert include both fibrous (chalcedony) and granular (quartz) forms. Chalcedony has radial or comb-like textures. The most common texture in chert may be the equigranular texture (*e.g.*, Folk and Weaver, 1952). Quartz crystals in chert typically are 5-20 μm , however cherts may consist of finer or coarser crystals (Blatt and Tracy, 1996; Heaney and Davis, 1995).

Occurrences

World-wide, chert generally occurs in three different geological settings: (1) as nodules and layers in carbonate rocks, (2) bedded chert near tectonically active plate margins, (3) hypersaline lake deposits (Blatt and Tracy, 1996), but in addition chert can occur along fractures and hot springs.

Nodular chert

Chert nodules tend to be irregularly shaped masses of microcrystalline and cryptocrystalline quartz and occur most commonly in carbonate rocks but also have been reported in shales and sandstones (Blatt and Tracy, 1996). Some descriptions of chert nodules have originally-calcareous fossils that are replaced by silica as well as preserved original silica fossils. But the dominance of silica of a replacement origin versus silica of an *in situ* origin for chert formation remains debated and is not thoroughly understood.

According to Blatt and Tracy (1996) nodular chert tends to occur in limestones of micritic facies (barely visible calcite grains). However in Centre County nodules also occur in dolostones (Bellefonte and Nittany formations). Blatt and Tracy (1996) envision that the source of the silica for chert nodules

in marine deposits was siliceous organisms such as sponge spicules, radiolaria or diatoms. However since diatoms did not evolve until the Jurassic, they would be excluded from Ordovician carbonates as a silica source.

Chert nodules cover a broad size range, from near silt-size to several meters in length. Nodular chert tends to be concentrated along bedding perhaps suggesting a process of accumulation of siliceous fossils and the subsequent migration of dissolved silica from those fossils along pathways of greatest permeability (bedding or in some cases cross-bedding features such as burrows).

In the Centre County region chert found as nodules in carbonate rocks will be one focus during our Field Trip. Chert nodules have been reported from the Axeman, Nittany and Bellefonte formations. The Stonehenge and Axeman units are dominantly limestone, and the Nittany and Bellefonte units are dominantly dolostone. Nodules range from well-formed ellipsoids, typically flattened in the plane of bedding, to irregular bodies often with bulbous protrusions, see plate #2 in the accompanying road log.

Fracture-related jasper

Such silica deposits occur along a few mapped faults in Centre County (See Hoskins and Root, 1976; (Gold and Doden, unpublished map). While the colors of jasper can range from yellow to green, grayish blue, brown, and even black, Centre County jasper associated with faults tends to range from yellow to brown, see plate #1 in accompanying road log.

Sources of silica

The source of silica comprising sedimentary chert has been debated by geologists but has generally been considered to be from one of the following processes: (a) biochemical extraction of silica from seawater, (b) silica from the dissolution of volcanic ash, (c) silica exhalations from volcanic vents, or (d) silica deposited by post-burial fluid flow along porous strata (*e.g.*, coquina or karst layers) or faults (including breccias).

Most sedimentary cherts are in marine formations and therefore considered to be of marine origin, but other origins such as lacustrine and hydrothermal origins are recognized. Recently Cecil (2015) has proposed a hypothesis where sedimentary chert throughout geological time originated from silica dust from desert areas adjacent to coasts was carried by wind far out into the ocean (*i.e.*, aeolian processes).

An alternative model was suggested by Knauth (1979) for the origin of nodular cherts in limestone calls upon the mixing of meteoric and marine waters in coastal systems. In this model the dissolution of biogenic opal and mixing of marine and fresh waters can produce waters highly supersaturated with respect to quartz and undersaturated with respect to calcite and aragonite.

Typical sea water concentration of silica are (~10 ppm), so deposition of silica in the sea by a process other than biogenesis to result in such large quantities of chert would appear improbable. Living organisms can extract minute concentrations of silica not possible by inorganic chemical processes. The reason that living organisms can do this was considered by Blatt and Tracy (1996) when they wrote: "...living organisms have an energy supply, ultimately obtained from the Sun via photosynthesis, and can use this energy to counter the

inorganic thermodynamic gradient against precipitation. While they are alive, the silica-secreting organisms in the sea extract the minute amounts of silica from undersaturated seawater, bind it within their organic matrix as opal, and keep it from re-dissolving into the sea...”

When such silica organisms die, gravity pulls their remains to the seafloor. The amount of skeleton silica that makes it to the seafloor will vary depending on depth of descent, because skeletal fragments dissolve during descent. Blatt and Tracy (1996) estimated that only a small portion of such biogenic silica makes it into the stratigraphic record as opal which potentially would crystallize to chert after burial to temperatures ranging from 50° – 75°C. Although this process may seem logical for the origin of sedimentary cherts, it is speculative. Ocean drilling of relatively recent strata has shown that all bedded chert sampled are replacement of carbonate oozes; not *in situ* crystallized siliceous deposits or oozes (Blatt and Tracy, 1996).

For chert nodules in carbonate units it seems that a post-depositional and replacement origin via diagenesis is most likely (*e.g.*, Pettijohn, 1975). Chert nodules such as those that occur in the carbonates units of Centre County seem to have formed by replacement, at least in part, on the basis of what appear to be invertebrate fossil remains within nodules, however the ultimate source of the silica is a mystery.

Biogenically precipitated silica forms as amorphous opal, or opal A. Opal A comprises the marine organisms: radiolaria, diatoms and sponge spicules. Upon recrystallization or diagenesis opal A converts to opal-CT, a variety of opal that includes the polymorphs of quartz known as cristobalite and tridymite, or converts directly to low-temperature quartz [alpha quartz] (Greenwood, 1973).

Cherts resulting from biochemical precipitation would form by a two-stage process in which there is an accumulation of organic (opal) tests. Because the resultant chert is so fine-grained (cryptocrystalline) it is thought that the amorphous opal skeletons of such organisms would recrystallize and might explain why fossil evidence for a biological origin has not been observed in Centre County chert.

In carbonate and other environments where the number of opaline skeletons per unit volume is relatively low, crystallization would be expected to result in scattered nodules of chert following the process of diagenesis. At sites where the number of silica skeletons in deposits is relatively large, crystallization can result in more closely spaced nodules or beds of chert that can be hundreds of meters thick (Blatt and Tracy, 1996).

The replacement process

A replacement process for chert deposition involves silica substitution of minerals in the parent rock by silica-bearing aqueous solutions. In the case of chert nodules in Centre County carbonates, either calcite or dolomite would've been replaced. Silica-bearing solutions might have obtained dissolved silica from either radiolaria, stromatolites, or sponge spicules. Such replacement cherts may form through a multistage process in which inorganic opal precipitates from aqueous solutions and is later altered/replaced by granular or chalcedonic (fibrous) quartz (Folk and Pittman, 1971; Raymond, 1995).

Best evidence for this process would be preservation of originally calcareous fossils within a nodule or silica bed. We have not found such evidence. However oolitic chert of the underlying Mines member of the Cambrian Gatesburg Formation has been interpreted to be of carbonate origin and replaced by silica with preservation of carbonate within some ooids (Choquette, 1954, Folk and Pittman, 1971, Pettijohn, 1975).

Summary of geological origins of chert

Chert may form from: a) biochemical precipitation, b) precipitation by evaporation of sea water, c) hydrothermal precipitation, d) replacement, and e) erosion, transportation, and deposition of previously formed siliceous materials. Silica concentrations may be increased by a process of diagenesis. Processes 1 through 4 involve precipitation of silica from solution, and diagenesis involves remobilization of previously deposited silica.

Cherts can form in several ways that include:

1. deposits in deep to shallow marine environments
2. silica deposits in certain lakes
3. fracture- or cavity-fillings precipitated from hydrothermal solutions
4. diagenetic replacement of pre-existing rock by local or regional aqueous solutions

References cited

- Adovasio, J.M., Carr K.W. and Vento F.J., 2008, A Report on the 2008 Field Investigations at the Shoop Site (36DA20), In the Eastern Fluted Point Tradition, 75-103.
- Andrews, B.W., Murtha, T. M., and Scheetz, B. E., 2004, Approaching the Hatch Jasper Quarry from a technological perspective: A study of prehistoric stone tool production in Central Pennsylvania: *Midcontinental Journal of Archaeology*, v. 29, no. 2, pp. 57-101.
- Blackman, M.J., 1974, An analysis of jasper artifacts and source materials by atomic absorption and flame photometry: *Letter of Lithic Technology*, v. 3, no. 40.
- Blatt, H. and Tracy, R.J., 1996, *Petrology – igneous, sedimentary, and metamorphic*, 2nd ed.: W.H. Freeman and Company, New York, 529 p.
- Carr, K.W., Adovasio, J.M., and Vento, F.J., 2013, Report on the 2008 Field Investigations at the Shoop Site (36DA20): *In The Eastern Fluted Point Tradition*, edited by J. A. M. Gingerich, The University of Utah Press, Salt Lake City, UT, p. 75-103.
- Cecil, C.B., 2015, Paleoclimate and the origin of Paleozoic chert: Time to re-examine the origins of chert in the rock record: *The Sedimentary Record*, pp.410, accessed from <https://www.sepm.org/CM_Files/SedimentaryRecord/SedRecord13-3-Final.pdf> on January 31, 2017.
- Choquette, P.W., 1954, A petrographic study of the "State College" siliceous oolite: *Journal of Geology*, v. 63, pp. 337-347.
- Collins, M. B., 1999, *Clovis blade technology*: University of Texas Press, Austin, TX, ___p.
- Doden, A.G., Gold, D.P., Mathur, R., and Jensen, L.A., 2011 in progress. *Bedrock Geology of the State College Quadrangle, Centre County, Pennsylvania*. DCNR, Open File Report.
- Fogelman, G. L., 1983, *Lithic Book: The Pennsylvania Artifacts Series*, No. 34, Fogelman Publishing Company, Turbotville, Pennsylvania.
- Folk, R.L. and Pittman, J.S., .1971, Length-slow chalcedony; a new testament for vanished evaporites: *Journal of Sedimentary Research*, v. 41, no. 4., DOI: 10.1306/74D723F1-2B21-11D7-8648000102C1865D

- Folk, R.L. and Weaver, C.E., 1952, A study of the texture and composition of chert: *American Journal of Science*, v. 250, Issue 7, pp. 498-510.
- Fritz, B. L., 2004, Appendix A: Lithic source studies: *In Phase III Archaeological Data Recovery Investigations, Sites 36Ju104 and 36Mi92*. S. R. 0022, Sections A09 and A11, Lewistown Narrows, Juniata and Mifflin Counties, Pennsylvania (Two volumes), by P. A. Raber, J.A. Burns, P.L. Byra, B.A. Carr, N. C. Minnichbach, B.L. Fritz, and F.J. Vento, Report prepared for the Pennsylvania Department of Transportation, District 2-0, and the Federal Highway Administration. Heberling Associates, Inc., Alexandria, Pennsylvania. ER No. 97-8013-042.
- Fritz, B. L., 2006, Appendix B: Canoe Creek Raw Lithic Source Survey, Blair County, Pennsylvania: *In Phase III Archaeological Data Recovery Investigations, Sites 36BL60 and 36BL62*. S. R. 0022, Section 010, Canoe Creek Improvements, Frankstown Township, Blair County, Pennsylvania, by P.A. Raber, J.A. Burns, N. C. Minnichbach, B.L. Fritz, and F.J. Vento, Report prepared for the Pennsylvania Department of Transportation, District 9-0, and the Federal Highway Administration, Heberling Associates, Inc., Alexandria, Pennsylvania, ER No. 1993-2438-013
- Gold, D.P. (1994). mapping of Roaring Springs quadrangle.
- Google, (no date provided), Percussion flaking reduction sequence:
<https://www.google.com/search?q=percussion+flaking+reduction+sequence&tbs=isch&tbs=ring&cad=h>
 [accessed March 8, 2017].
- Google, (no date provided), Pressure flaking reduction sequence:
www.google.com/search?q=percussion+flaking+reduction+sequence&source=lnms&tbs=isch&sa=X&ved=0ahUKewjng_HzibbRAhWM4CYKH4AIEQ_AUICSGC&biw=1523&bih=702#q=percussion+flaking+reduction+sequence&tbs=isch&tbs=ring: [accessed March 8, 2017].
- Greenwood, R., 1973, Cristobalite; its relationship to chert formation in selected samples from the Deep Sea Drilling Project: *Journal of Sedimentary Petrology*, v. 43, Issue 3, pp. 337-347.
- Hatch, J. W. (editor), 1980, *The Fisher Farm Site: A Late Woodland hamlet in context*: Department of Anthropology, The Pennsylvania State University, Occasional Papers in Anthropology, No. 12, University Park, PA.
- Hatch, J.W., 1993, Research into the prehistoric jasper quarries of Bucks, Lehigh and Berks counties Pennsylvania: Report submitted to the Pennsylvania Historical and Museum Commission, Harrisburg, PA.
- Hatch, J.W. and Miller, P.E., 1985, Procurement, tool production, and sourcing research at the Vera Cruz Jasper quarry in Pennsylvania: *Journal of Field Archaeology*, v. 12, pp. 219-230.
- Hay, C. A., 1980, An analysis of the Chipped Stone Assemblage from the National Register Survey—1978: *In The Fisher Farm Site: A Late Woodland Hamlet in Context*, edited by J.W. Hatch, Department of Anthropology, The Pennsylvania State University, Occasional Papers in Anthropology, No. 12, University Park, Pennsylvania, pp. 65-82.
- Heaney, P. J. and Davis, A. M., 1995, Observation and origin of self-organized textures in agates: *Science*, v. 269, no. 5230, pp. 1562-1565.
- Herman, G. and Ferguson, S.M., 2015, Neotectonics of the New York Recess: Meeting Proceedings and Field Guide for the 2015 Conference of the Geological Association of New Jersey, Lafayette College, Easton, PA.
- Holland, J. D., 2003, A guide to Pennsylvania lithic types: *Journal of Middle Atlantic Archeology*, v. 19, pp. 129-150.
- Hoskins, D.M. and Root, S.I., 1976, Bedrock geologic map of the State College 7.5' quadrangle, PA: *In Atlas of Preliminary Geologic Quadrangle Maps of Pennsylvania (Map 61)*, Pennsylvania Geological Survey Fourth Series, Harrisburg, PA, 1:62,500 scale.
- Hoskins, D.M., 1976, Bedrock geologic map of the Centre Hall 7.5' quadrangle, PA: *in Atlas of Preliminary Geologic Quadrangle Maps of Pennsylvania (Map 61)*, Pennsylvania Geological Survey Fourth Series, Harrisburg, PA, 1:62,500 scale.
- Kauffman, M. F., 1999, Ecocambrian, Cambrian and transition to Ordovician, chapter 4 of Shultz, C.H., ed., *The geology of Pennsylvania*: Pennsylvania Geological Survey, 4th ser., Special Publication 1, p. 59-73. [Co-published with Pittsburgh Geological Society]

- King, A., Hatch, J.W., and Scheetz, B.E., 1997, The chemical composition of jasper artefacts from New England and the Middle Atlantic: Implications for the prehistoric exchange of "Pennsylvania Jasper": *Journal of Archaeological Science*, v. 24, no. 9, pp. 793-812
- Knauth, P.L., 1979, A model for the origin of chert in limestone: *Geology*, v. 7, pp 274-277.
- Lovering, T.G., 1972, Jasperoid in the United States - its characteristics, origin, and economic significance: U.S. Geological Survey Professional Paper 710, U.S. Government Printing Office, Washington, 164 p.
- Miller, P.E. 1982, Prehistoric lithic procurement: A chemical analysis of Eastern U.S. jasper sources and a consideration of archeological research design: University Park, PA, The Pennsylvania State University, M.A. thesis.
- Neuendorf, K.K.E., Mehl, J.F., and Jackson, J.A. (Eds.), 2005, *Glossary of Geology*: American Geological Institute, Alexandria, Virginia, 779.
- PHMC (Pennsylvania Historical & Museum Commission), January 28, 2011, Prehistoric lithic quarries in Pennsylvania: *In This Week in Pennsylvania Archaeology (TWIPA)*, http://twipa.blogspot.com/2011_01_01_archive.html [accessed January 2017]
- PHMC (Pennsylvania Historical & Museum Commission), February 21, 2014, Our journey through Pennsylvania: *In This Week in Pennsylvania Archaeology (TWIPA)*, http://twipa.blogspot.com/2014_02_01_archive.html [accessed January 2017]
- PHMC (Pennsylvania Historical & Museum Commission), 2015, Time periods: *Pennsylvania Archaeology*, <http://www.phmc.state.pa.us/portal/communities/archaeology/native-american/time-periods.html> [accessed March 8, 2017].
- Petraglia, M., Knepper, D., Rutherford, J., LaPorta, P., Puseman, K., Schuldenrein, and Tuross, N., 1998, Jasper characterization: *In The prehistory of Lums Pond: the formation of an archaeological site in Delaware, Volume II, Technical analyses and appendices*, Delaware Department of Transportation Archaeology Series No. 155, pp. 479-518, accessed from http://www.deldot.gov/archaeology/lums_pond/pdf/vol2/lums_vol2_jasper.pdf [accessed on March 8, 2017].
- Pettijohn, F.J, 1975, *Sedimentary rocks*: 3rd edition, Harper & Row, Publishers, New York, 628 p.
- Raber, P. A., 2010, Chert use and local settlement in central Pennsylvania: Investigations at 36Ce523.: *Journal of Middle Atlantic Archaeology*, v. 26, pp. 115-140.
- Raber, P. A. and Stiteler, J.M., 2012, Phase I/II Archaeological Investigations, Kissinger Meadow Wetlands Expansion Project, College Township, Centre County, Pennsylvania: Report prepared for the University Area Joint Authority by Heberling Associates, Inc, Alexandria, Pennsylvania, ER No. 2011-1366-027.
- Raymond, L.A., 1995, *Petrology – The study of igneous, sedimentary, metamorphic rocks*: Wm. C. Brown Publishers, Boston, MA, 742 p.
- Scheetz, B.E. and Murtha, T.M, 2017 (in press), Sourcing and studying the source: Bald Eagle jasper quarries and the Houserville Habitation Complex: *In Lithic Quarries in Pennsylvania: The Archaeology of Tool Stone Procurement*, edited by K. W. Carr and P.A. Raber., The Pennsylvania State University Press, University Park, PA.
- Scheetz, B.E., Gold, D.P., Ellsworth, C.J., and Mathur, R., 2009, Chesapeake Bay Bolide Impact on regional mineralization in Pennsylvania: Unpublished manuscript in possession of the authors.
- Stevenson, C.M., Maria Klimkiewicz, M., and Scheetz, B.E., 1990, X-ray fluorescence analysis of jaspers from the Woodland Site (36CH374), the Kasowski Site (36CD161) and selected Eastern United States jasper quarries: *Journal of Middle Atlantic Archaeology*, v. 6, pp. 43-54.
- Stevenson, C.M, Scheetz, B.E., and Klimkiewicz, M., 1992, The chemical characterization of Pennsylvania jasper using X-ray fluorescence analysis: Report submitted to the Pennsylvania Historic and Museum Commission, Harrisburg, PA.

SINKING VALLEY, PENNSYLVANIA

AUSTIN BEYER

Geologic Setting

Nestled comfortably within the Ridge and Valley province of South Central Pennsylvania, Sinking Valley offers unique geologic features to Pennsylvania’s residents. Primarily within the Coburn and Bellefonte formations, Sinking Valley is composed mostly of carbonate limestones, CaCO_3 , and dolostones, $\text{Ca,Mg}(\text{CO}_3)_2$. These carbonate layers are more susceptible to chemical weathering than their siliclastic sandstone counterparts that form the ridges surrounding the valley (Figure 1). Because of the chemical makeup of the rock, many of the waterways within the sinking valley area will travel directly through units of limestone.

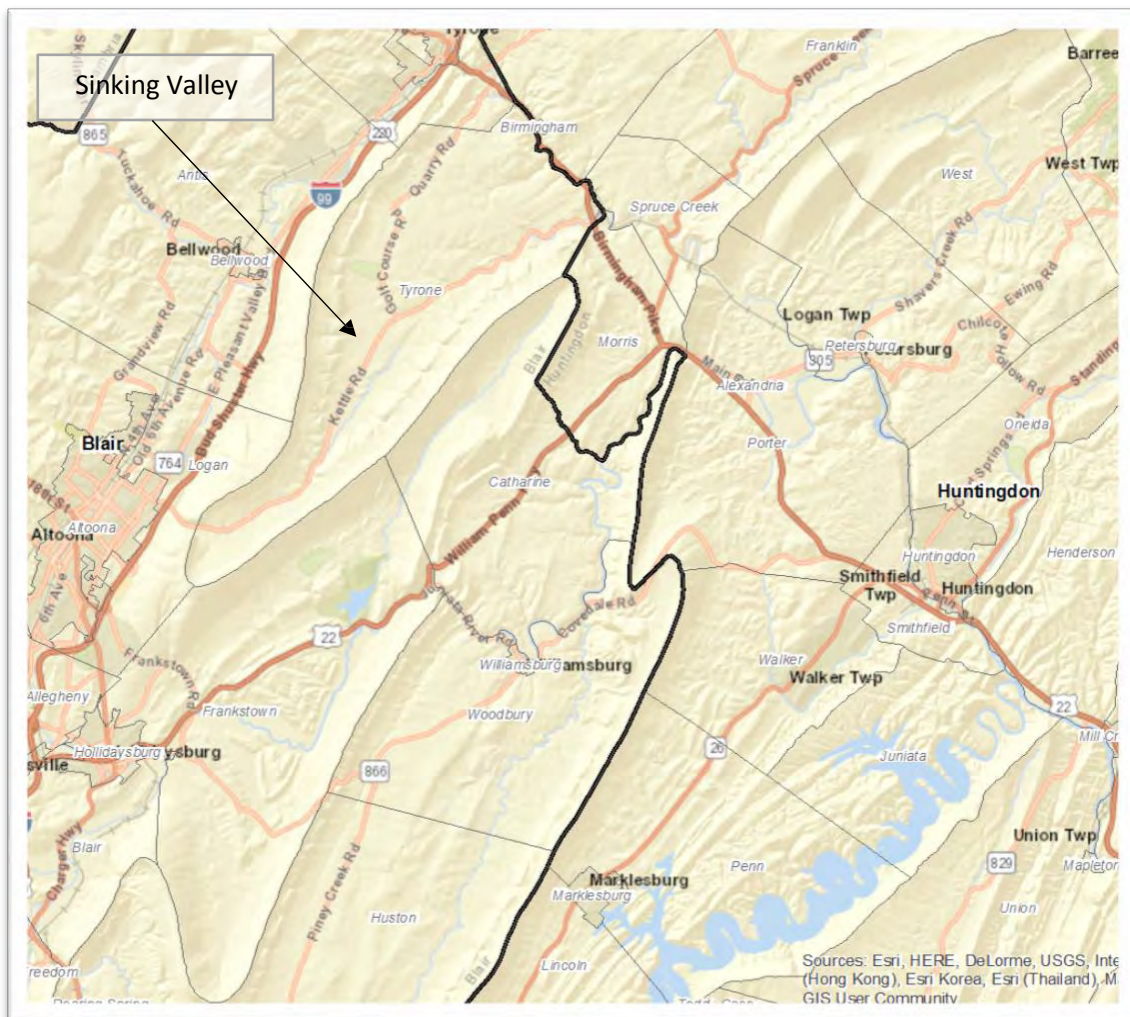


Figure 1. Sinking Valley location

Water and air forming carbonic acid

- $\text{H}_2\text{O} + \text{CO}_2 \rightarrow \text{H}_2\text{CO}_3$

Chemical weathering of limestone via carbonic acid

- CaCO_3 (Limestone) + H_2CO_3 (Carbonic Acid) \rightarrow $\text{Ca}(\text{HCO}_3)_2$ (aq) (Calcium Bicarbonate)

As water moves through rock units, more of the rock is dissolved, which over time produces caves and sinkholes.

Geologic Features

The two most prominent features in this area are Arch Spring and Tytoona Cave. Arch Spring can only be viewed from the roadside, since it is located on private property.

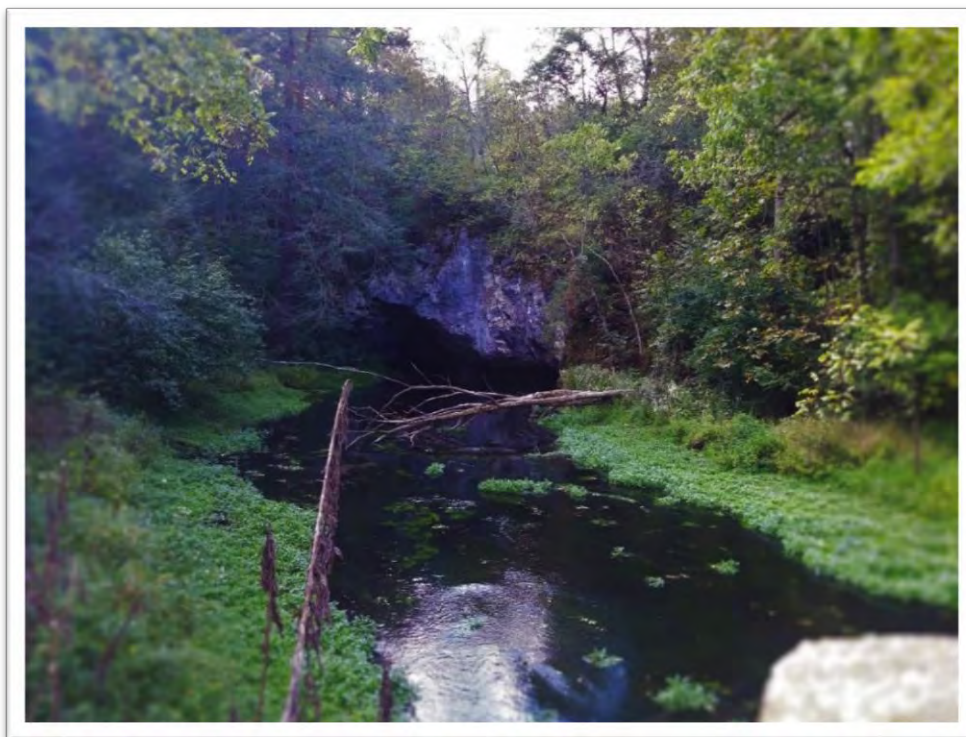


Figure 2. Arch Springs Viewed from the Roadside

Fortunately, Tytoona Cave is open to the public to explore (Figures 3 & 4). Tytoona is formed after two streams converge roughly 50 feet away from the cave's entrance, one tributary seems to bubble directly from its respective rock face, while the other travels along a narrow valley produced by collapsed sinkholes. The mouth of Tytoona Cave is where the stream reenters the bedrock. A large portion of the cave's roof is a single, steeply dipping limestone layer, this provides a beautifully flat surface with many types of stalactites. Stalactites form as the dissolved limestone recrystallizes from water.

Calcite precipitation and deposition as stalactites

- $\text{Ca} + 2(\text{HCO}_3) \rightarrow \text{H}_2\text{CO}_3 + \text{CaCO}_3$

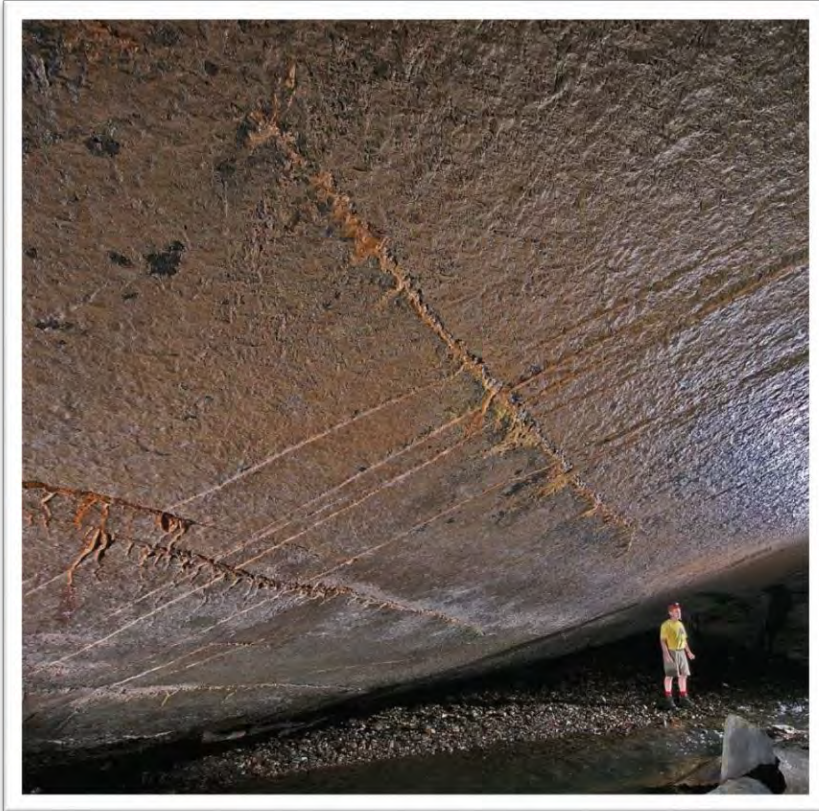


Figure 3. Inside of Tytoona Cave.
Notice the flat, steeply dipping roof.

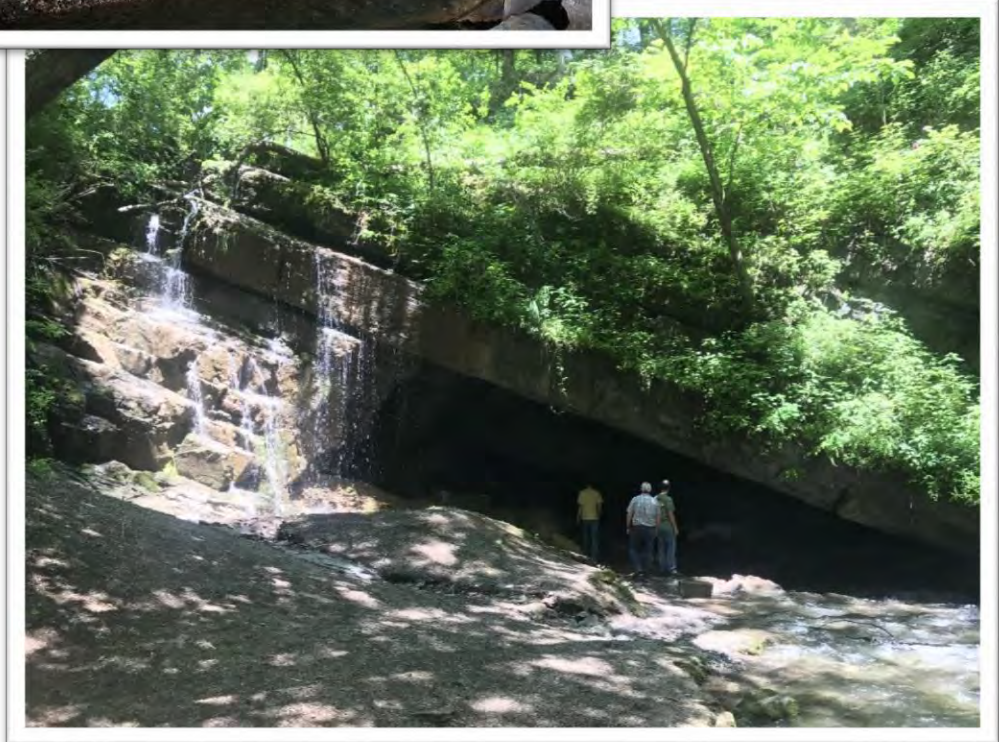


Figure 4. Mouth of Tytoona Cave

82nd Annual Field Conference of Pennsylvania Geologists

The type of stalactite formed in the cave is considered a speleothem, which is specifically the deposition of minerals from water. Speleothems can form many different shapes, like straws or even bacon.

It is possible to travel roughly 900 feet into the cave, but there is a log jam halfway through making the second half of the cave relatively hard to access (but not impossible). Tytoona Cave and surrounding property is owned by the National Speleological Society.

For more information visit <http://caves.org/region/mar/tytoona.htm>

A SPECIAL THANK YOU TO OUR MANY SPONSORS!

Ackerman John (Twin Oaks Consulting LLC)*	Jenkins, Andy
Avary, Katharine Lee	Jones, Michal
Ball, Gary	Kribbs, Gary *
Baughman, Samuel	Lee, Joseph *
Harrisburg Area Geological Society (HAGS))	Leitel, John
Bill, Steven	Littlefield, Kent *
Bowling, G. Patrick	Markowski, Toni
Bragonier, William	Marschak, Fred
Bruck, William	Martino, Paul
Carter, Kris (Veronica Reynolds Scholarship)	Mason, John
Charles, Emmanuel *	Meiser, Edgar *
Clark, Steven	Mooney, David
Clarke, John	Neubaum, John
Coleman, Neil	Newcomb, Sally
Cornell, Sean	O'Hara, Aaron *
DeBarber, Peter (Delta Phase Electronics)	Payne, Walter *
Dodge, Cliff *	Pazzaglia, Frank
Drahuschak, Joseph	Phillips, Beverly
Duerr, Christopher	Rudnick, Barbara
Dunst, Brian	Saunders, Dawna
Eby, James	Shank, Steve
Fehrs, Ellen *	Sheasley, Jason (Wilkes Scholarship)
Fradel, Joel	Shocker, Heather (Wilkes Scholarship)
Fridirici, Tom *	Skema, Vik
Frishkorn, Andrew	Stefl, John
Gelinas, Morgan *	Stephens, Bill
Hall, Frank *	Swann, Jacob (Signet Analysis)
Halperin, Alan *	Swift, Mark
Hanes, Barbara *	Urbanik, Stephen
Harper, John *	Winter, Jay
Hockenberry, Jacqueline	Zofchak, Edward
Hoskins, Donald	
Ioos, Mark *	
Jeffries, Rose	

**Denotes an individual who donated to both the Scholarship Fund and the General Fund*



2016
SOTE



81ST FCOPG GROUP PHOTO